UNIVERSITY OF CATANIA

INTERNATIONAL PhD IN CHEMICAL SCIENCES

XXX CYCLE

CURRICULUM: ORGANIC CHEMISTRY

Luana Pulvirenti

NATURAL OR BIO-INSPIRED POLYPHENOLS IN THE SYNTHESIS OF POTENTIAL CHEMOTHERAPEUTIC AGENTS

Final report of research activity

Tutor: Prof. CORRADO TRINGALI

Coordinator: Prof. SALVATORE SORTINO

ACADEMIC YEAR 2016 – 2017

This thesis is dedicated to the memory of Prof. Carmela Spatafora, a special and talented scientist who has been my teacher in the science and in life.

ABBREVIATIONS

AbL	*Agaricus bisporus* Laccase
BXL	Benzoxanthene
CAL	*Candida antarctica* Lipase
C NMR	Carbon Nuclear Magnetic Resonance
gCOSY	Gradient Correlation Spectroscop
CD	Circular Dichroism
DMC	Dimethylcarbonate
DMAP	4-Dimetilamminopiridina;
DCC	Dicyclohexylcarbodiimide
DMSO	Dimethylsulfoxide
EDCCI:HCl	N-(3-Dimethylaminopropyl)-N′-ethylcarbodiimide hydrochloride
EtOAc	Ethyl acetate
EtOH	Ethanol
EP	Petroleum ether
gHSQCAD	Gradient Heteronuclear Single Quantum Coherence Adiabatic
gHMBCAD	Gradient Heteronuclear Multiple-Bond Correlation Adiabatic
G-Q	G-quadruplex
HHDP	hexahydroxydiphenoyl
H NMR	Proton Nuclear Magnetic Resonance
HPLC	High Performance Liquid Chromatography
HRP	Horseadish Peroxidase
IDA	iodobenzene diacetate
MeOH	Methanol

NHTP	nonahydroxyterphenoyl
ODN	Oligodeoxyribonucleotide
PE	Petroleum ether
PoL	*Pleurotus ostreatus* Laccase
PcL	*Pseudomonas cepacea* lipase
rt	Room Temperature
SIBX	Stabilized 1-hydroxy-1-oxo-3H-1λ^5,2-benziodaoxol-3-one
SPR	Surface Plasmon Resonance
TBAF	tetra-n-butylammonium fluoride
TBSCl	tert-Butyldimethylsilyl chloride
TLC	Thin Layer Chromatography
t_R	Time of retention
TvL	*Trametes versicolor* Laccase

ABSTRACT

My doctoral research activity was focused mainly on natural or bioinspired polyphenols, aimed to the synthesis of new bioinspired compounds and to their evaluation as potential chemotherapeutic agents. More specifically, my research activity was devoted to lignans and neolignans, synthetized by chemical and/or enzimatic methodology. Hence, in particular, two polyphenol groups were studied, namely benzoxanthene lignans, their related phenazines and bisphenol neolignans; furthermore during the synthesis of magnolol-inspired neolignans, an unexpected dihydrobenzofuran neolignan was also obtained and characterized. The products have been studied in collaboration with others research team for the interaction with G-quadruplex DNA, as α-glucosidase inhibitors, as ABCG2 inhibitors, as agonist/antagonist of the Bile X receptors FXR and LXRα/β, antioxidant and antimicrobial agents. Further goal of this work was an inverse virtual screening focused on magnolol analogues, carried out during my short internship in the lab of prof. G. Bifulco (University of Salerno). In addition, the last part of my work was carried out at the University of Bordeaux, under the guidance of Prof. Stéphane Quideau, and was devoted to synthetic work on ellagitannins, an important subgroup of tannin family. In this context I gave a contribution to the total synthesis of vescalin and a vescalagin conjugate.

CHAPTER 1

1. INTRODUCTION

The use of extracts from plants or other organisms for the treatment of diseases is as old as human history, but only in relatively recent times the active ingredients present in these natural remedies have been isolated and identified. After decades of research on the isolation and structural characterization of biologically active natural compounds, now we know the structure of more than 200,000 metabolites, and in the future this number could raise to more than 500,000.[1] In recent years there has been a renewed attention to bioactive natural products,[2] and one of the reasons is the observation that the structural diversity (also called 'chemodiversity') of natural products is far superior to that of the compounds that can be obtained by synthetic methods, including combinatorial synthesis.[3] One further reason is the awareness that many natural products may be considered as 'lead compounds' selected through millions of years of evolution; in fact, natural products have given an 'evolutionary advantage' to plants and other living organisms that produce them. These organisms have evolved in parallel with other species incorporating 'biological targets' for the products of their metabolism,[4] e.g. some alkaloids produced by plants are very toxic to herbivorous predators because the biosynthesis of these substances has evolved in parallel to that of the proteins 'target' of predators.[5] On the other hand, many antibiotics produced by fungi or other microorganisms are probably chemical defense systems against other competing microorganisms. The development of these 'natural leads' was exploited in drug discovery: in fact, modifying and optimizing key features of selected natural compounds it is possible to improve their biological activity,

bioavailability, the mode of administration, etc. A variety of examples can be cited in this regard. Probably the most popular semi-synthetic derivative of a naturally occurring compound is acetylsalicylic acid (**1**) or aspirin®, the first of the non-steroidal anti-inflammatory drugs (NSAIDs), synthesized by chemists at Bayer more than a century ago with a simple modification of salicylic acid, itself a product of oxidation of salicin (**2**), the natural metabolite found in willow (*Salix alba* var. *tristis*) extracts.[6]

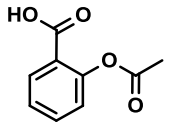

1

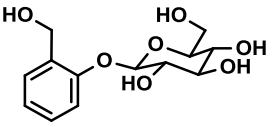

2

Although the efficacy of willow extract as antipyretic is reported in the Ebers Papyrus (1550 BC), and aspirin has now been used by more than 100 years as an antipyretic and anti-inflammatory agent, only recently its mechanism of action has been defined. This molecule acts as an inhibitor of cyclooxygenase (COX-1 and COX-2), the key enzymes in the biosynthesis of pro-inflammatory prostaglandins but also of thromboxanes, which facilitate the coagulation of the blood. As a matter of fact, today aspirin is also used to prevent cardiovascular diseases, such as myocardial infarction. Many compounds with antitumor properties have been derived from bioactive natural products: eg. flavopiridol (**3**), an inhibitor of cyclin-dependent kinases (CDKs) is a semisynthetic derivative marketed under the name of alvocibid® and undergoing clinical evaluation for some forms of leukemia,[7] which has been developed from the natural alkaloid rohitukin (**4**), isolated from the bark of *Amoora rohituka*.

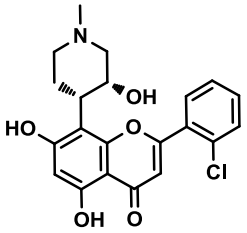

3

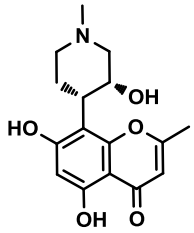

4

The anticancer drug etoposide phosphate (**5**) (etopophos®) has been selected through the synthesis of hundreds of compounds derived from podophyllotoxin (**6**), a lignan isolated from the rhizomes of *Podophyllum peltatum*. Interestingly, molecular modeling studies and experimental evidence has established that podophyllotoxin acts as an inhibitor of tubulin polymerization,[8] while etoposide is a topoisomerase II inhibitor.

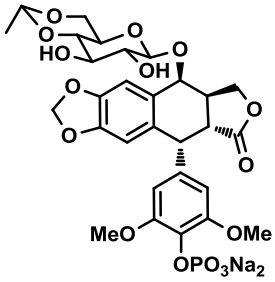

5

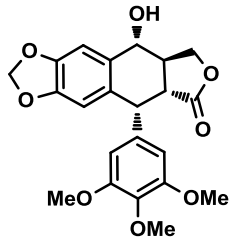

6

1.1 Polyphenols

Among the various families of natural products, phenolic compounds (and in particular plant polyphenols) have recently received increasing attention from researchers working in different fields: in fact, many polyphenols found in edible fruits, herbs, vegetables, as well as in foods and beverages derived from them, have been the subject of studies

indicating their role in the chemoprevention of degenerative diseases, such as cardiovascular diseases, cancer or Alzheimer's disease. Some of these polyphenols are called 'nutraceuticals', because they are constituents of foods and beverages able to play a 'functional' role in the body. In many cases, these natural polyphenols are very effective antioxidants (radical scavengers) and many studies support the hypothesis that they are also able to counteract pathologies such as inflammation, carcinogenesis or neurodegenerative disorders. Phenolic compounds are widespread mainly in the Plant Kingdom and include more than 8000 known compounds. Their role in the plant is presumably defensive but they may also have other biological activities in interspecies relationships. This group of compounds is one of the most studied worldwide and many publications report beneficial effects of polyphenols on various aspects of human health and well-being.[9]

The growing interest in (poly)phenolic compounds and their exploitation in the fields of agro-food, cosmetic and drug industry has led to a broader (and sometimes inappropriate) use of the term ‘polyphenols’ with respect to the original definition of ‘plant polyphenols’, later expanded by E. Haslam,[10] and recently by S. Quideau.[11] Originally, the ‘plant polyphenols’ were substantially equivalent to ‘vegetable tannins’, with reference to the tanning action of some plant extracts that had been employed for centuries in the leather-making process. However, this definition has subsequently been broadened in the common use to include low-molecular weight phenolic molecules as well, not necessarily water-soluble or exerting a ‘tanning’ action. Consequently, the common feature of polyphenols has been reconfigured with regard to their biosynthetic origin, thus including phenolic metabolites biosynthetically derived through the shikimate and/or the acetate/malonate pathways. The

Scheme 1 summarizes very shortly the biosynthesis of phenolic compounds, mainly through the shikimate pathway (**Scheme 1**).[12]

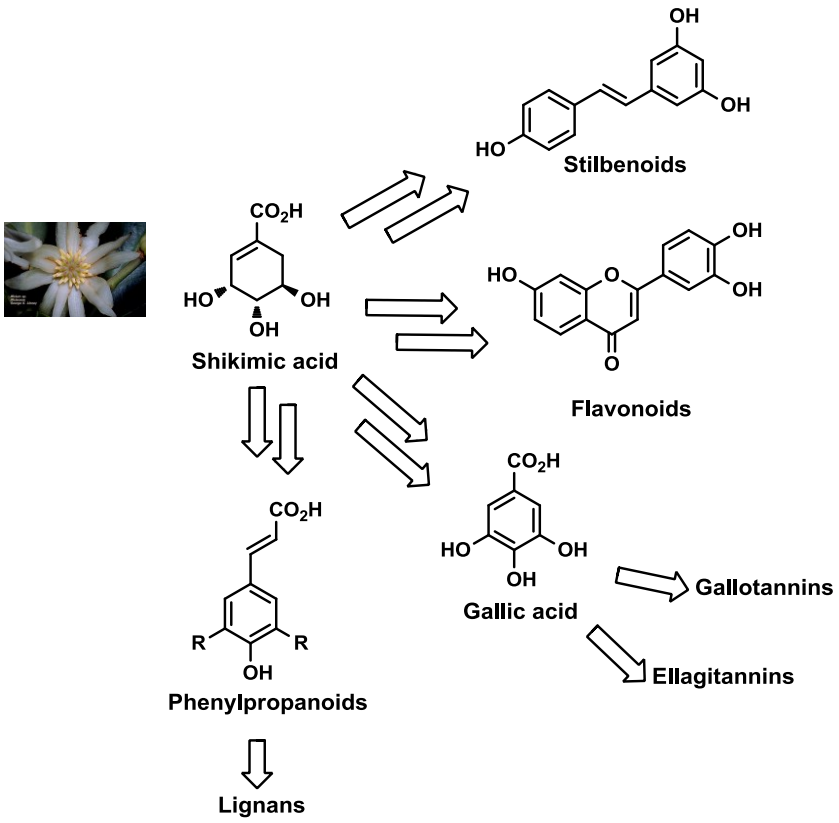

Scheme 1: shikimic acid secondary metabolism

Some examples of bioactive polyphenols are reported below. Probably the best know polyphenol is resveratrol (**7**), present in grapes and red wine, considered cardioprotective and anticarcinogenic, which has become very popular due to the so-called 'French paradox' (ie, the lower risk of the French people towards cardiovascular diseases, attributed to their consumption of red wine). A recent review by J. Pezzuto cites 512 references on its cancer chemopreventive properties.[13] A further well-known phenolic compound is curcumin (**8**), the golden yellow pigment of turmeric, which is cited in hundreds of scientific

papers for a variety of biological properties including neuroprotective and anticarcinogenic activity. Genistein (**9**) is an isoflavone present in soybean (*Glycine soja*) and considered a phytoestrogen able to relieve menopause symptoms and prevent some estrogen-dependent cancers, such as breast cancer.[14] Ellagic acid (**10**), found in many fruits and pomegranate juice is a powerful antioxidant and is considered a preventive agent for prostate cancer.[15]

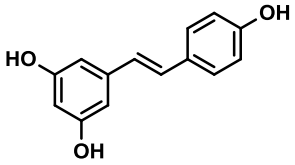

7

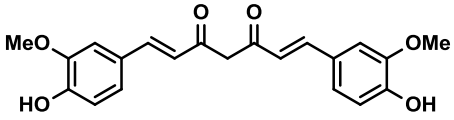

8

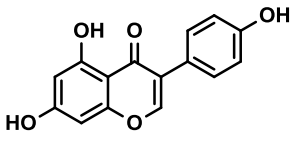

9

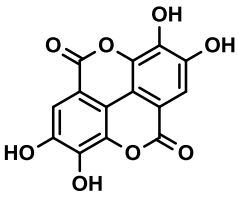

10

Many polyphenols are esters or amides of phenolic acids: for instance, cynarin (1,3-O-dicaffeoyil quinic acid, **11**), present in artichoke (*Cynara scolymus*), was recently reported as inhibitor of P-glycoprotein (P-gp), a membrane transporter involved in 'multidrug resistance'.[16] CAPE (caffeic acid phenethyl ester, **12**), found in propolis, a substance produced by bees, is known as a potent antioxidant and antitumor compound;[17] many scientific reports are dedicated to CAPE. A very recent work reports that **12** built on nanoparticles could be a promising candidate in the chemotherapy of cancer with anti-metastatic activity of tumor cell lines of colorectal CT26.[18]

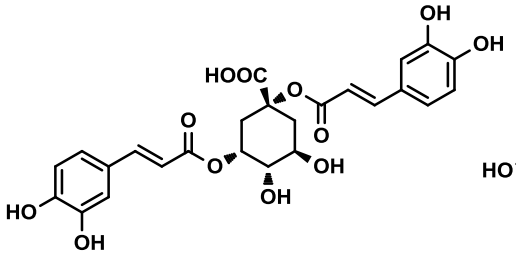

11

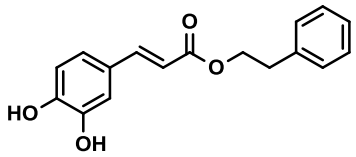

12

An epidemiological study showed a lower incidence of estrogen-dependent tumors, monitoring the different eating habits of people who adopt a diet rich in polyphenols, especially rich plant lignin, compared with people who adopt a diet low in polyphenols. This study was corroborated by the observation that protection may result from the presence in biological fluids, of the so-called 'mammalian lignans', namely enterolactone (**13**) and enterodiol (**14**). These are actually products of metabolic transformations in charge of intestinal microflora, of plant lignans taken with food; these compounds show a considerable anti-estrogenic activity,[19] which prompted some research groups to their evaluation for treatment of breast cancer.

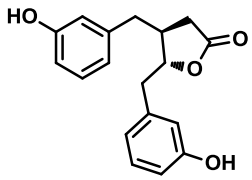

13

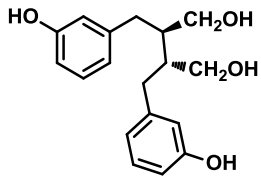

14

The above reported examples give an idea of the promising properties of many natural phenolic compounds; nevertheless, poor bioavailability and fast metabolic conversion are frequently observed for natural polyphenols. Thus many research groups have carried out studies aimed at obtaining bioactive compounds derived or inspired from natural

polyphenols, although showing a higher metabolic stability and possibly enhanced biological activity. A number of semisynthetic analogues of natural polyphenols have been prepared, in particular with antitumor properties.[20] The preparation of libraries of analogues may also support structure-activity relationship (SAR) studies and allow a better understanding of the molecular mechanisms of action of the natural polyphenols. In addition, optimized analogues may possess improved activity even through a different, more effective, mechanism of action; consequently, the phenolic compounds can be used as building blocks in the synthesis of more complex molecules with promising biological activity. Some of these researches were devoted to the synthesis of bioinspired polyphenol analogues, obtained starting from simple phenolic compounds; many of these products belong to the family of lignans and neolignans (see Section 1.1.2) and were obtained through biomimetic methodologies.

1.1.1 Natural polyphenols as antioxidative agents

It is well known that many phenolic compounds, some of which mentioned above for their chemopreventive properties, are powerful antioxidants. Actually there is a precise relationship between antioxidant activity and chemoprevention of degenerative diseases. Antioxidants are good ‘radical scavengers’ and consequently can 'capture' some highly reactive radical species which may be dangerous for the cells and living organisms, namely reactive oxygen species (ROS, and in particular $OH^{\bullet}$ hydroxyl, alkoxy $RO^{\bullet}$, $ROO^{\bullet}$ peroxyl and superoxide $^{\bullet}O2^{-}$) but also reactive nitrogen species (RNS). These reactive radicals can damage cells by reacting with the DNA, proteins or cell membrane constituents.[21] In particular, damage towards DNA or enzymes able to repair damaged

DNA may cause the process of 'initiation' of a cell that subsequently, through the 'promotion', may convert into a neoplastic cell capable of proliferating in an uncontrolled manner.[22] Recently, antioxidative phytochemicals have been seriously considered also as supplements for animal nutrition. Phytochemicals have been shown to exert their positive antioxidant benefits towards animals in terms of favored performance, production quality, and enhanced endogenous antioxidant system.[23] Polyphenols are an important group of natural antioxidants because they are good donors of a hydrogen atom, and are able to replace ROS or RNS with phenoxy radicals that are much less reactive and consequently less dangerous for the cell (**Scheme 2, A**). The main reason of the low reactivity of phenoxy radicals is the stabilizing effect of resonance. In particular, catecholic polyphenols bearing two hydroxyl groups in ortho, are very effective antioxidants because they benefit of a further effect of stabilization of the phenoxy radical, due to intramolecular hydrogen bonding, as illustrated in **Scheme 2, B**. The better antioxidative properties of *ortho*-diphenols have also been corroborated through theoretical studies.[24]

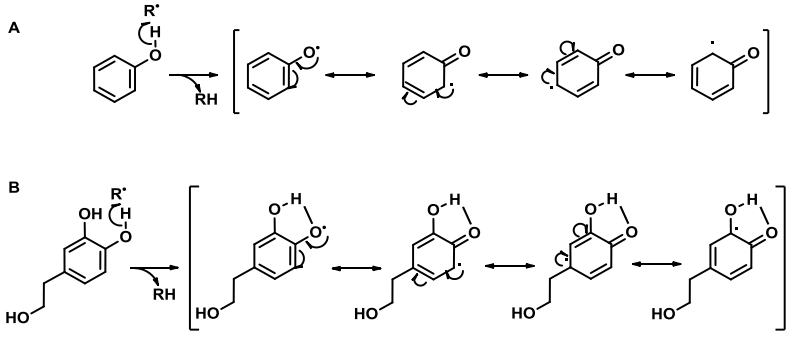

Scheme 2

Just to name a few of the best known catecholic antioxidants we have to mention chlorogenic acid (**15**), piceatannol (**16**), quercetin (**17**)

and hydroxytyrosol (**18**). Chlorogenic acid (**15**), (an ester of caffeic acid with quinic acid), found in many plants including the coffee (*Coffea arabica*)[25] and the artichoke (*Cynara scolymus*), has widely been studied as antioxidative agents and there are evidences that it may decrease the risk of prostate cancer (up to 60%) for the habitual coffee drinkers compared to non-drinkers.[26] Piceatannol (**16**) a naturally occurring hydroxylated analogue of resveratrol, is less studied than resveratrol but displays a wide spectrum of biological activities. It has been found in various plants, including grapes, passion fruit, white tea, and Japanese knotweed. In addition to antioxidant activity, piceatannol (**16**) blocks proliferation of a wide variety of tumor cells, including leukemia, lymphoma, cancers of the breast, prostate, colon and melanoma.[27] Also the well-known antioxidant quercetin (**17**) was reported as antitumor agent. It is reported that **17** triggers apoptosis in various tumor cells.[28] Data in literature indicate the potent '*in vitro*' antioxidant activity of hydroxytyrosol (**18**);[29] in addition, **18** prevents oxidative damage in human erythrocytes[30] and is also considered an important cancer chemopreventive component of extra-virgin olive oil.[31] Antioxidant polyphenols are also reputed able to prevent neurodegenerative diseases[32] or diabetes.[33]

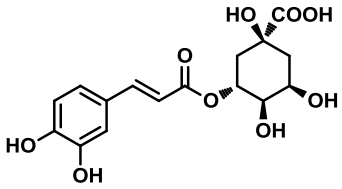

15

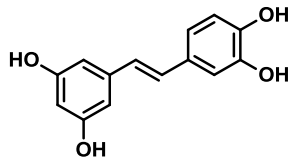

16

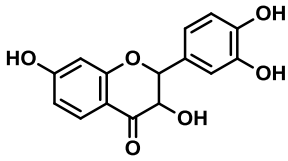

17

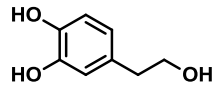

18

1.1.2 Lignans and neolignans

Lignans and the related neolignans represent an important group of polyphenols frequently found in vascular plants and in particular in some toxic or not edible plants. These compounds are probably produced by the plant as chemical defense agents and are known for interesting biological activities, such as cytotoxic,[34] antiangiogenic,[35] antioxidant, hepatoprotective and antiviral activity.[36] These dimeric or oligomeric compounds present a large structural variety, although their molecular backbone consists normally of simple phenylpropane (C_6C_3) building blocks: structural differences are mainly due to their biosynthetic mechanism, based on radical oxidative coupling reactions mediated in nature by peroxidases or laccases; these enzymes have different action mechanisms, and bear different metal cations in their active site, Fe^{3+} in the former and Cu^{2+} in the latter. According to the 2000 IUPAC recommendations, lignans are the dimers in which the new primary C-C bond is formed between the C-8 (or C-β) of one and the C-8' (or C-β') of the other monomer.[37] Lignans originated by monomer connect through a bond other than the 8-8' (or β-β') bond are called neolignans. Neolignans

in which the two monomers are connected through a primary *C*-*O* bond are specifically named 'oxyneolignans'. Therefore there are different combinations of these radicals which lead to different regioisomeric dimers. The most frequently found structures in lignans are based on 8-8', 8-5' and 8-*O*-4' coupling. Coupling at position 5 is only possible when this position is unoccupied. On the other hand, coupling between *O* atoms or between *C* atoms both in position 1 (1-1' coupling) have not been observed in lignans because in the former case it would create a highly unstable peroxy dimer, whereas in the latter case it could not be effected due to steric hindrance because both monomers bear a propanoid side chain in position 1.[38]

The biosynthetic pathway leading to lignans by coupling of phenylpropanoid units has been largely studied and is exemplified by the biosynthesis of (+)-pinoresinol (**19**) by 8-8' (or β-β') coupling of two conyferil alcohol (**20**) units in the presence of a peroxidase enzyme, generating the radical species (**Scheme 3**). A reactive quinone–methide intermediate undergoes intramolecular cyclization, thus affording (+)-pinoresinol (**19**), interestingly, it has been showed that a protein called 'Dirigent Protein' (DP, **Figure 1**), and not the enzyme, controls the stereochemistry of the reaction; in the absence of this protein, racemic mixtures are obtained.[39] The DP hosts two coniferyl radicals in binding site '*si*-face to *si*-face' in order to determine the stereochemical asset of the quinone-methide intermediate and consequently, the stereogenic centres of final product, as in (+)-pinoresinol (**19**) biosynthesis.

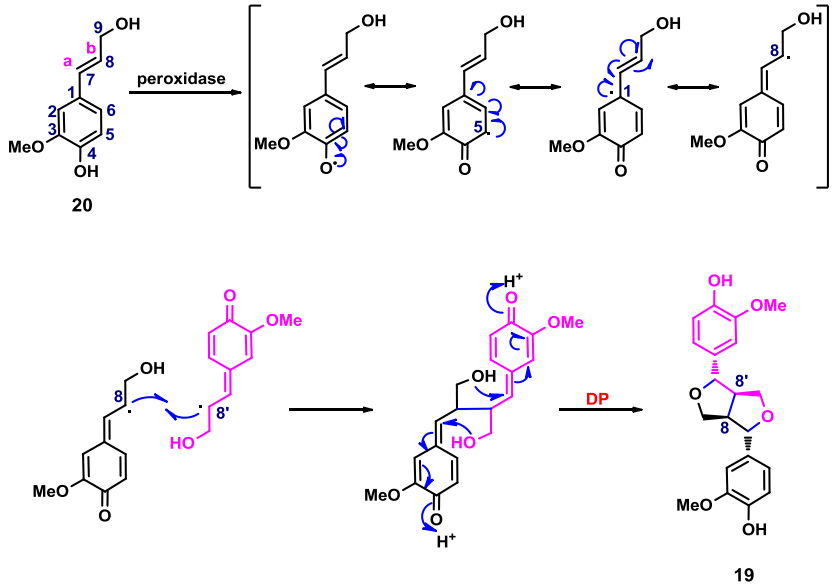

Scheme 3

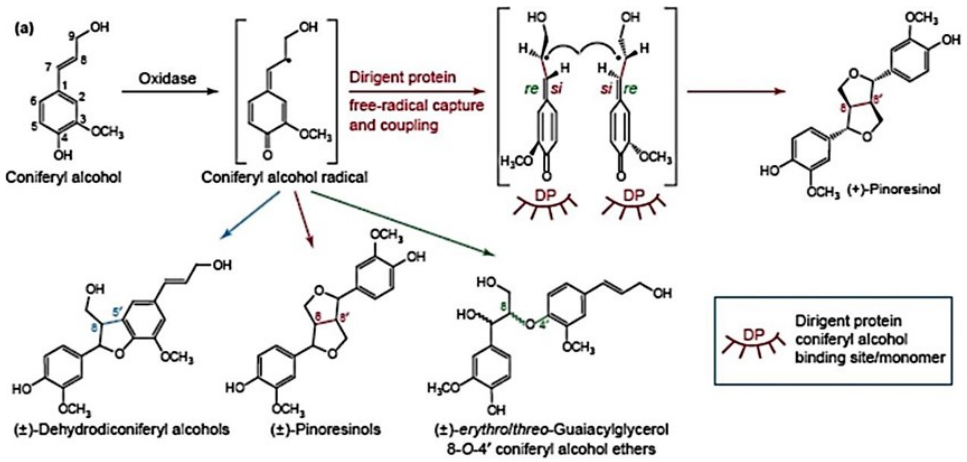

Figure 1: stereochemical control through Dirigent protein - Adapted from: *Science,* 1997, 275, 362-366

One of the most studied bioactive lignans is podophyllotoxin (**6**); the optimization of this natural lead, obtained through the synthesis of hundreds of analogues, has afforded anticancer drugs such as etoposide (**21**), teniposide (**22**), and etopophos (**5**).[40]

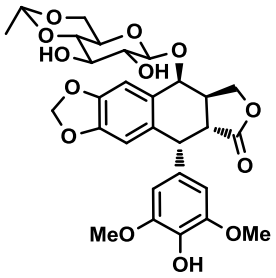

21

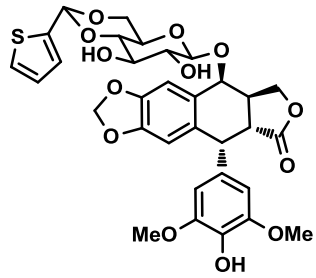

22

Among the neolignans, those with a dihydrobenzofuran core are worthy of particular attention for the wide range of their biological activities, including antioxidant,[41] antibacterial,[42] anti-inflammatory,[43] cardiovascular,[44] and cytotoxic effects.[45] The 8-5' coupling originates neolignans with this structural core, as reported below for the biosynthesis of (+)-dehydroconiferyl alcohol (**23**), (**Scheme 4**).

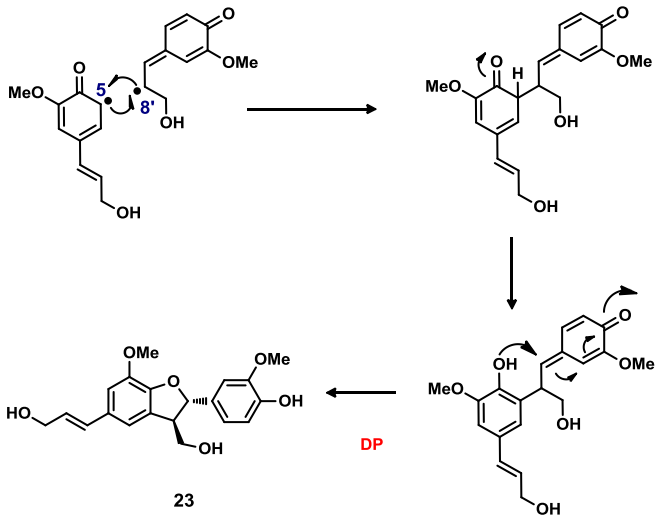

23

Scheme 4

Frequently cited examples of bioactive dihydrobenzofuran neolignans are bohemenan H (**24**) and bohemenan K (**25**), strong cytotoxic agents against HeLa, Hep-2 and A-549 cell lines.[46]

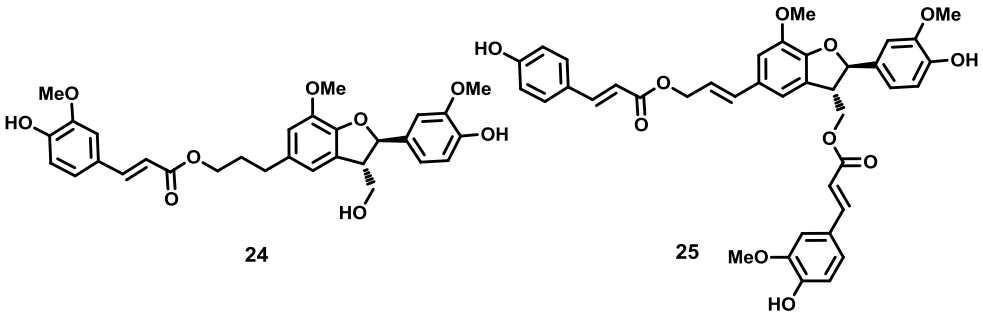

The promising biological activities of dihydrobenzofuran neolignans have prompted many research groups to develop efficient methodologies for their synthesis to obtain not only natural products, but also their synthetic analogues and hybrids with other small molecules. With regard to the preparation of synthetic analogues of natural dimeric polyphenol, worth noting are the 'biomimetic' syntheses, mediated by metals or enzymes, and mimicking the biosynthetic coupling pathway. These synthetic methodologies are often carried out on natural precursors with the aim to obtain their correspondents analogues, which yet retain a natural basic skeleton, and possibly have a profile of bioactivity similar to, or better than the natural precursor. It is worth highlighting that this dimerization, even in enzyme-mediated reactions, occurs with regio- and diastereoselectivity, but not enantioselectivity, and consequently affords *trans*-substituted racemic mixtures. When eco-friendly syntheses are planned, these kind of reactions should be mediated by oxidase enzymes, instead metal-based oxidative reagents.[47] The most common enzymes employed in reactions of oxidative dimerization are laccases, which are able to convert atmospheric oxygen (as an oxidizing agent) into water,[48] or peroxidases, which oxidize aromatic substrates in the presence of hydrogen peroxide, converting it, also in this case, in water.[49]

The structure of the enzymatic site and the mechanism of reaction today is well known and reported below in **Figure 2** and in **Figure 3**.

Precisely, laccase catalyzes the one-electron oxidation of four reducing-substrate molecules with the concomitant four-electron reduction of molecular oxygen to water (**Figure 2**), resulting in a green cycle.[50]

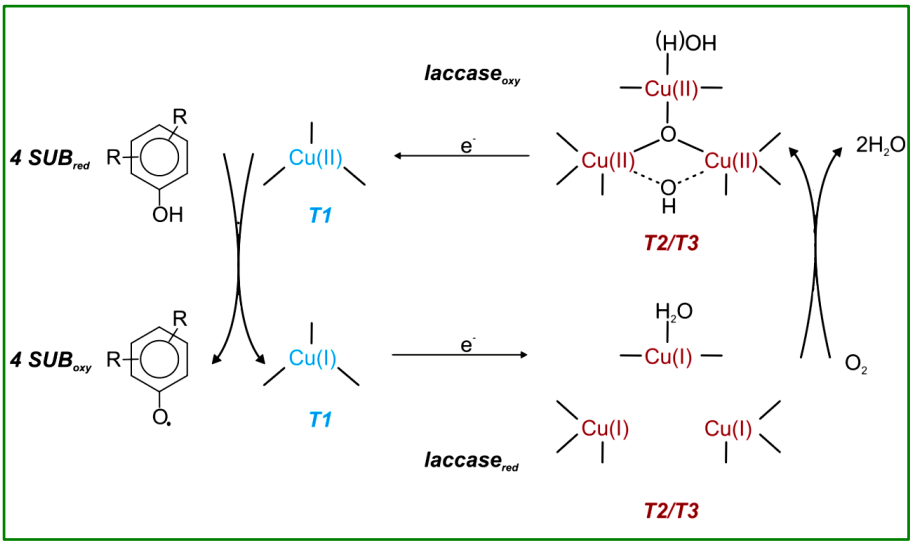

Figure 2: Schematic representation of a fungal laccase catalytic cycle. Two molecules of water result from the reduction of molecular oxygen (at T2/T3) and the concomitant oxidation (at the T1 copper site) of four substrate molecules to the corresponding radicals.

Peroxydases are eme-protein working through the formation of a phenoxy radical and concomitant reduction of hydrogen peroxide (H_2O_2) to water (**Figure 3**).[51] The application of enzyme-mediated reactions is common to various fields, including synthetic and analytical purposes,[52] environmental purpose for the wastewater treatment,[53] and biotechnology purpose for must and wine stabilization.[54] Also these enzymes have been used for biomimetic synthesis of dihydrobenzofurans.[49]

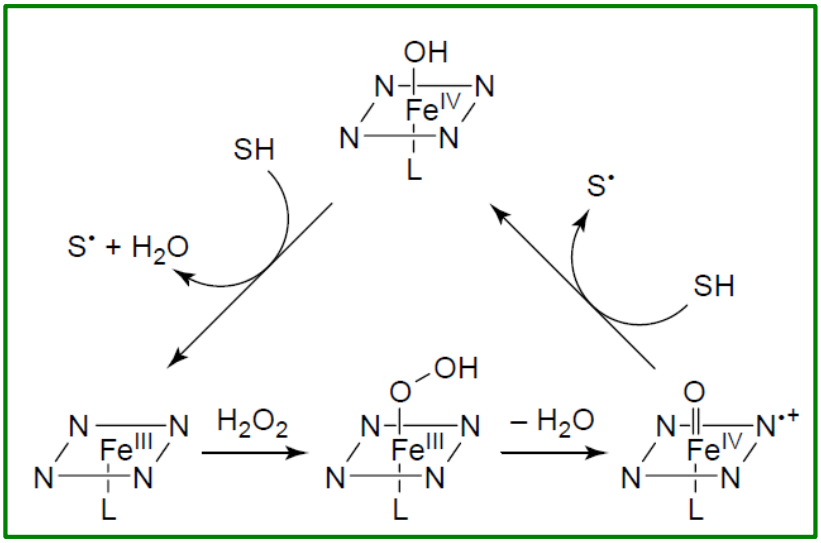

Figure 3: Schematic representation of Horseradish Peroxidase (HRP) catalytic cycle. Abbreviations: SH = substrate, S• = radical substrate.

A representative example is the synthetic dimer **26**, that it was tested as anticancer agent following the protocol of the National Cancer Institute (NCI) and showed a GI_{50} average of 3 μM on 60 cancer cell lines and nanomolar scale values towards three breast cancer cell lines and some lines of leukemia. Further studies indicated that the antiproliferative activity of **26** was due to the inhibition of tubulin polymerization. In a study of a series of lipophilic analogues of **26**, the synthetic neolignan **27** showed a strong activity towards *Plasmodium falciparum* (antimalaric) and *Leishmania donovani* (anti-leishmaniasis).[55]

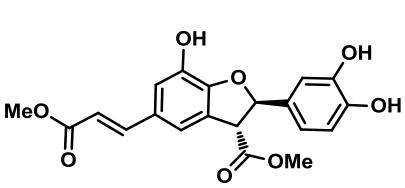

26

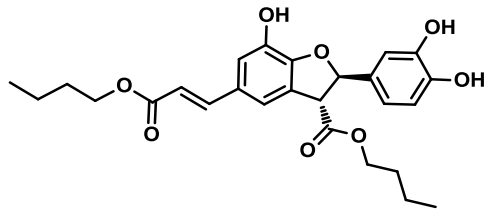

27

In particular, a simple preparation of the neolignan **28** (8-5' coupled diethyl diferulate), with HRP/H_2O_2, gave a better yield (50%) than the previously used Ag_2O-promoted reaction (30%).[56] Another work, on the use of laccase in a biphasic system, showed a rapid formation of the racemic bis-lactone on lignan **29** (from ferulic acid) and **30** (from synapic acid).[57] These reports are only a few examples of the many papers devoted to dihydrobenzofuran neolignans which thus appear as an attractive target for chemical synthesis or modification.

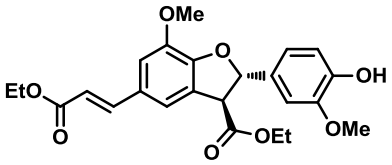

28

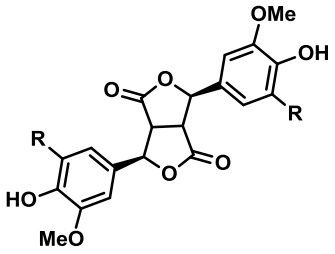

29 R = H
30 R = OMe

1.1.3 Benzoxanthenes lignans

A part of my PhD research activity has been focused on benzo[*k,l*]xanthene lignans (in the following, simply 'BXL'), a subgroup of lignans scarcely reported in the literature, because of their rarity in nature. Only five natural BXLs have been reported in the literature until recent times, namely: mongolicumin A (**31**), rufescidride (**32**), yunnaneic acid (**33**), chiliantin D (**34**), and dodegranoside (**35**) respectively isolated from the following species: *Taraxacum mongolicum*,[58] *Cordia rufescens*,[59] *Salvia yunnanensis*,[60] *Rhoiptelea chilianta*,[61] e *Dodecadenia grandifora*.[62] A simple derivative of mongolicumin A, **36**, previously synthesized by the research team guided by Prof. C. Tringali,

has been recently identified as a new natural product isolated from plant belonging to the family of *Orobanchaceae*.[63]

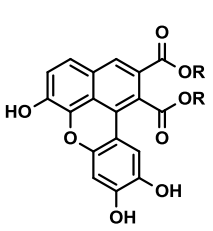

31 R=H
36 R=Me

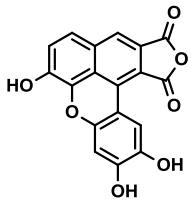

32

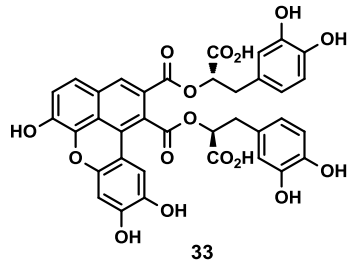

33

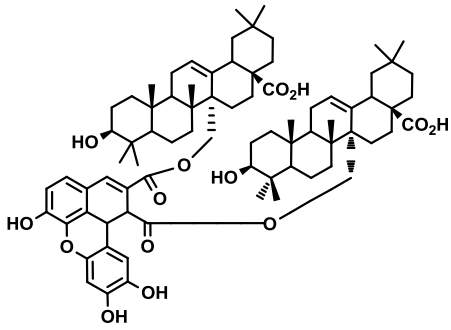

34

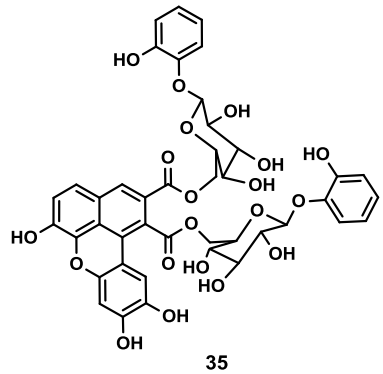

35

These compounds have been isolated with low yields and long extraction procedures; due to their rare diffusion in nature and the poor availability, they have not been subjected to any evaluation of biological activity. Only for the compound **32** a patent referring to its antimicrobial activity is reported.[64] In a recent study, the above cited research group[47] developed a method of biomimetic synthesis (dimerization by oxidative coupling) to obtain BXLs from esters of caffeic acid. A mechanism for the formation of these dimers has been proposed and corroborated by experimental data and calculations. It is worth noting here that an "orientation" effect towards 8–8' coupling was observed in the presence of $Mn(OAc)_3$. This mechanism favours the oxidative coupling 8-8' between the caffeate radicals, followed by intramolecular cyclization processes and oxidative additional steps (**Scheme 5**).

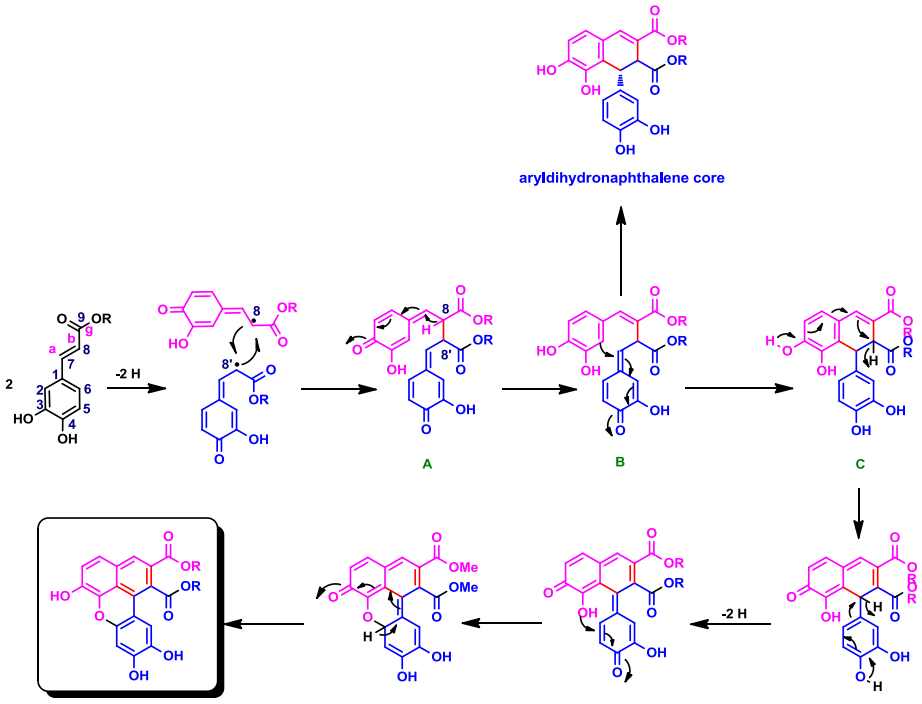

Scheme 5

The reaction affords essentially two products: the benzoxanthene lignan as main product and a lignan with an aryldihydronaphthalene core as minor product. It is worth noting that the formation of the aryldihydronaphthalene derivative is a strong indication of the biomimetic nature of the synthesis; in fact, the natural BXL **33** was isolated along with the related aryldihydronaphthalene lignan rabdosiin (**37**) from the same plant *Salvia yunnanensis* and this supports the hypothesis that these natural products are formed in nature through a mechanism that is very similar to that proposed here. So the "unnatural" BXLs are mimetic of known natural products and, in principle, may be biogenetically "natural" products and not yet discovered in nature, as confirmed by the recent isolation of compound **36**

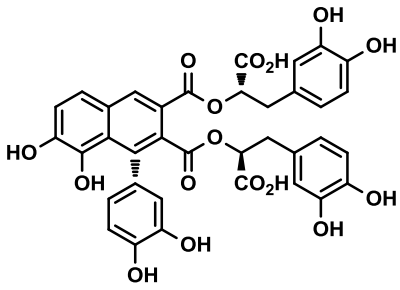

37

In the above cited work the BXLs **36**, **38** and **39** and subsequently series of their analogs (**40** - **43**) were obtained with this biomimetic procedure.

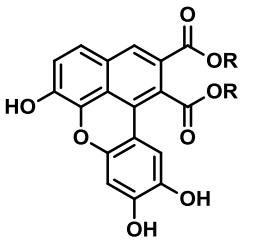

36 = CH_3
38 = CH_2CH_2Ph
39 = $CH_2CH_2CH_2CH_3$

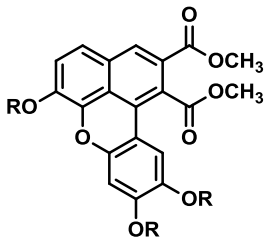

40 R = $COCH_3$
41 R = CH_3

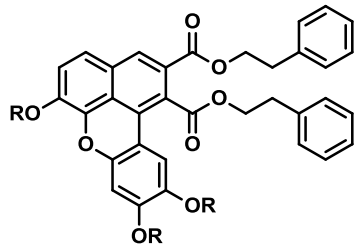

42 R = $COCH_3$
43 R = CH_3

In the frame of a collaboration of Prof. Tringali's team with that of Prof. G. Bifulco at the University of Salerno these synthetic benzoxanthenes were evaluated in a study on the interaction with DNA, based on STD-NMR experiments and molecular docking calculations (**Figura 4**);[65] a parallel study of their antiproliferative activity was carried out in collaboration with Prof. Latruffe at the University of Burgundi (Dijon, France). The compounds were evaluated in vitro on two different cell lines of human cancer namely SW 480 (human colon carcinoma) and HepG2 (human hepatoblastoma). Compound **38** resulted

the most potent, with a GI_{50} = 2.57 μM on SW 480 e GI_{50} = 4.76 μM on HepG2. A three-dimensional model of the ligand-DNA complex was built which made it possible to shed light on the structural elements important for the interaction with the biological target. The results obtained from the STD-NMR measures are compatible with the calculations of molecular docking. In fact, both studies confirmed that the parallel planar structure of benzoxantenes intercalates between the bases of DNA, by establishing a series of π-π interactions, but also the pendants ester contribute to the binding, establishing interactions through Van der Waals forces and hydrogen bonds with the minor groove. This also highlighted the important role of phenolic OH, in the interaction with DNA. In fact, the methylated derivatives showed a lower affinity for the biological target and turned out to be inactive against tumor cells.

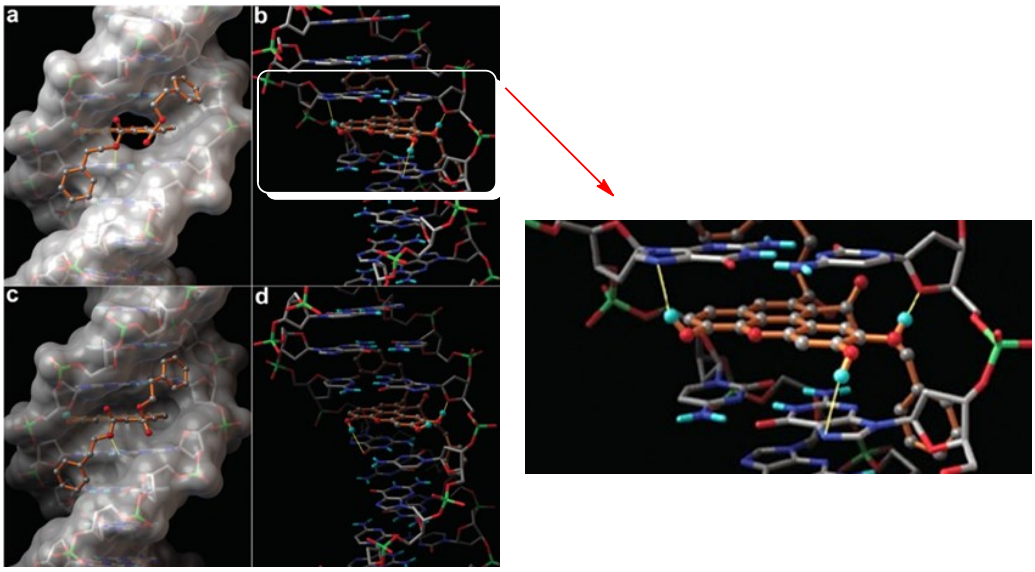

Figura 4: Molecular modeling (docking) of complex **38** - DNA

Further work on BXLs as potential anticancer agents was carried out by collaboration with Prof. D. F. Condorelli (University of Catania); a

small library of BXLs with different pendant chains were synthetized and evaluated towards a panel of cancer cell lines, namely HT29 (Caucasian colon adenocarcinoma grade II), Caco-2 (Caucasian colon adenocarcinoma), HCT-116 (human colon tumor), H226 (lung squamous carcinoma) and A549 (lung carcinoma). The antiproliferative activity data and lipophilicity measurements showed that the most active compounds are also those more lipophilic.[66] The CAPE-derived benzoxanthene **38** again resulted the most potent, and was also the most lipophilic. This benzoxanthene was also the subject of studies on its anticancer properties[67, 68] in collaboration with Dr. G. Srinivas (Cancer Research Program, Rajiv Gandhi Centre for Biotechnology, Thiruvananthapuram, India). BXLs were also studied, in collaboration with Prof. R. Amorati (University of Bologna) as a new class of antioxidant polyphenols, able to effectively react with peroxyl radicals.[69] These studies revealed benzoxanthene lignans as a new class of bioactive natural products, and for this reason we planned, as part of this PhD project, to expand the biological studies on BXLs, as will be detailed below.

1.1.4 Bisphenol neolignans

Diaryl motifs are featured in numerous natural and synthetic compounds used, inter alia, as drugs, agrochemical agents, polymeric materials, and various material additives.[70] In particular, natural C-C or C-*O* bisphenol neolignans have normally monomeric phenolic precursors, and their biosynthesis is thus viewed to rely on oxidative coupling processes (**Scheme 6**).

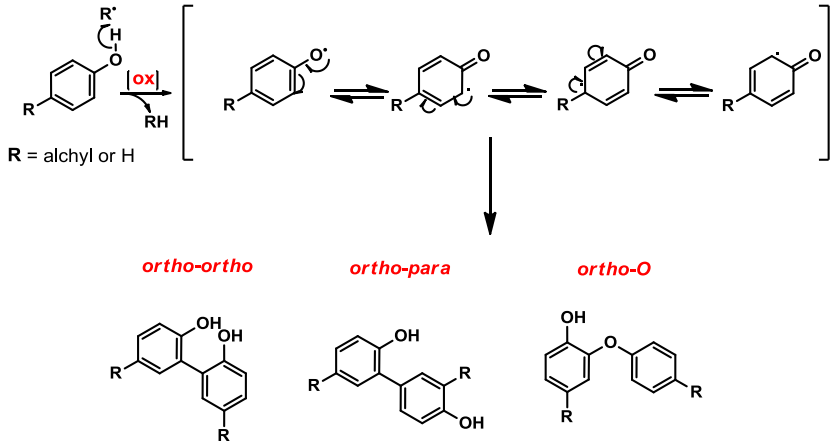

Scheme 6: bisphenol biosynthesis through oxidative coupling

Among the biarylic neolignans, in recent years two simple dimeric compounds, magnolol (**44**) and honokiol (**45**) gained growing attention by researchers, and a literature search on these compounds affords today more than 2000 results. Both are natural products originally isolated from the bark of *Magnolia officinalis*,[71] a plant used in Japanese and Chinese traditional medicine for various diseases such as gastrointestinal disorders, anxiety and allergic diseases; *M. officinalis* bark is reported for a number of biological activities including anti-cancer, anti-inflammatory, anti-depressant and anti-platelet activity.[72]

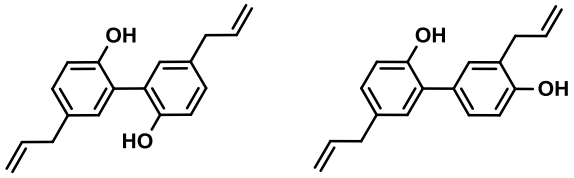

44 **45**

Magnolol (**44**) is probably the most cited among *M. officinalis* constituents, and a non-exhaustive list of its properties includes antitumor,[73] anti-inflammatory,[74] anti-angiogenic,[75] antimicrobial,[76] antiviral[77] and antioxidant[78] activity, as well as prevention of

inflammation-induced tumorigenesis,[79] inhibition of osteoclast differentiation,[80] reduction of multidrug resistance through P-glycoprotein modulation[81] and protection against cerebral ischaemic injury.[82] A comparable variety of biological properties has also been reported for honokiol. These properties prompted a number of researchers to synthetize magnolol and honokiol analogs and evaluate their biological properties: this afforded new bisphenol neolignans and derivatives with antimicrobial/antiproliferative,[83, 84] neuroprotective,[85] anti-inflammatory[86] and antioxidant activity, cytotoxicity against cancer cell lines,[87, 88] modulation of GABA receptors[89] and insecticidal activity.[90] Interestingly, only one report deals with inhibition of α-glucosidase by honokiol derivatives (namely, dimers and trimers),[91] notwithstanding that a potent inhibitory activity has been reported for honokiol and especially magnolol isolated from *Trichilia cannaroides*.[92] In view of the diverse pharmacological activities of magnolol scaffold we felt the need for further structural manipulations towards development of improved structures derived from **44**, and in particular given the activity of magnolol (**44**) on α-glucosidase, we were interested to study the potential activity as α-glucosidase inhibitors, of its synthetic analogues.

1.1.4.1 Magnolol analogues as α-glucosidase inhibitors

The search for new and effective α-glucosidase inhibitors is rapidly growing in the last decade, in view of the epidemic diffusion of diabetes and consequently of the efforts devoted to the discovery of potent glucosidase inhibitors able to retard glucose absorption and reduce blood glucose levels.[93] Diabetes mellitus is a chronic metabolic disease associated with disorders of carbohydrate metabolism and characterized by hyperglycemia. The control of postprandial blood glucose excursions

has come to the fore of the treatment of diabetes. One of the therapeutic approaches to reduce postprandial hyperglycemia is to retard digestion and absorption of dietary carbohydrates by inhibiting digesting enzymes, such as α-glucosidase and α-amylase, in the digestive organs.[94] Infact, inhibition of intestinal α-glucosidases delays the digestion of starch and sucrose, flattens the postprandial blood glucose excursions, and thus mimics the effects of dieting on hyperglycaemia, hyperinsulinaemia and hypertriglyceridaemia. Therefore, the mechanism of α-glucosidase inhibition represents the pharmacological optimization of the dietary principle of delayed carbohydrate absorption. Furthermore, the treatment with α-glucosidase inhibitors does not only could improve the metabolic state but it has also the potential to delay, or possibly prevent, the development of diabetic complications (**Figure 5**).[95]

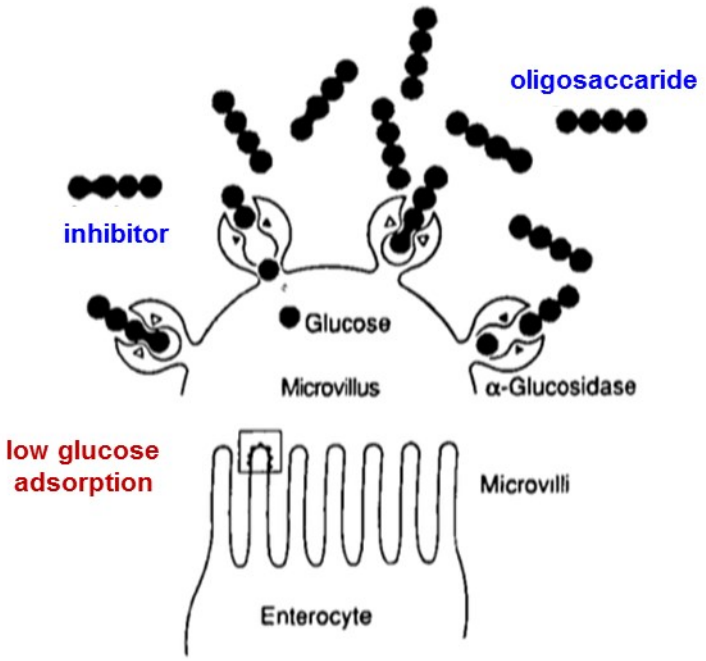

Figure 5: Schematic diagram of enzymatic hydrolysis of oligosaccharides and competitive inhibition of intestinal brush-border α-glucosidases. Adapted from H. Bischoff, Act Endokr Stoffw 1991;12:25-32.

Since the 1960s, considerable efforts have been devoted to the studies of glucosidase inhibition, aiming at the discovery of potent glucosidase inhibitors for the treatment of diabetes through the retardation of glucose absorption and lowering of blood glucose levels. Various types of glucosidase inhibitors, have been extensively studied and reviewed in the past few decades, and among these acarbose (Glicobasey, **46**), miglitol (Glyset, **47**) or voglibose (Prandial, **48**) have been successfully commercialized as anti-glucosidase drugs against type-2 diabetes. However, the effectiveness of these drugs is compromised by their deleterious side effects.[96]

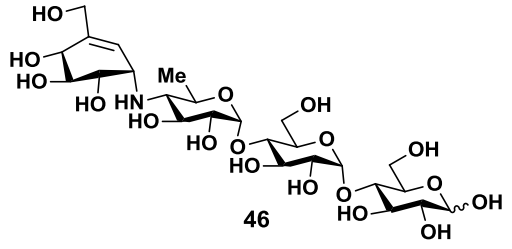

46

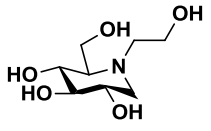

47

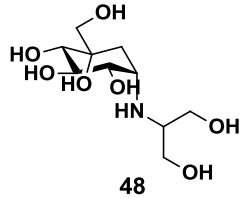

48

As a new class of α-glucosidase inhibitors, polyphenols are attracting great interest for understanding the mechanisms of action of glucosidase inhibition, and for developing alternative drugs to prevent and treat diabetes and obesity.[97] Recently some efforts have been devoted from the research group guided by Prof. C. Tringali to investigate resveratrol-related synthetic glycosides[98] and natural polyphenols[99] as inhibitors of yeast α-glucosidase, the enzyme most frequently employed in the preliminary steps of the search for new antidiabetic drugs. On the

basis of the above, as further goal of my research activity and as a continuation of the studies to develop new α-glucosidase inhibitors, we planned here the chemo-enzymatic synthesis of a series of bisphenols (or related compounds) inspired by magnolol (**44**) and their evaluation as yeast α-glucosidase inhibitors.

1.1.5 Ellagitannins: bioactive plant polyphenols

Ellagitannins belong to the hydrolyzable tannins family, a subclass of the group of tannin molecules. Research interest in these plant polyphenols initially emerged from the discovery of their occurrence in numerous herbal remedies used in oriental traditional medicine and the remarkable biological activities related to their antioxidant,[100] antiviral,[101] and host-mediated anti-tumor properties.[102] In particular, several reports of Quideau's group showed an interesting targeting ability of some wine ellagitannins toward the human topoisomerase II, a nuclear enzyme involved in DNA processes such as replication, transcription, chromosome condensation and segregation, suggesting a potential anti-proliferative activity and potential use of these molecules as new anti-cancer drugs.[103] Furthermore, the same group discovered that vescalagin (**49**) is capable to inhibit the activity of certain cells (endothelial and smooth muscle cells) by dismantling their actin cytoskeleton, opening the way towards a potential novel therapy against osteoporosis.[104] To date, after more than 50 years of investigations, more than 1000 members of this subclass of hydrolyzable tannins have been isolated from various plant sources and fully characterized, thus constituting by far the largest group of known tannin molecules.[11, 105, 106] The ellagitannin chemical structures are basically composed of a central sugar core, typically D-glucopyranose, to which are esterified gallic acid units that are further

connected together through C–C biaryl and C–O diaryl bonds as a result of intra- and intermolecular oxidative coupling processes. The biosynthetic pathway (**Scheme 7**) starts from a common penta-*O*-galloyl-α-D-glucopyranosidic (β-PGG) precursor, which generates the so-called hexahydroxydiphenoyl (HHDP) moiety through an intramolecolar oxidative C-C coupling of appropriately juxtaposed galloyl groups, as proposed by Schimdt and Mayers.[107] The HHDP biaryl unit is a structural determinant to define ellagitannins 'hydrolyzable tannins': in fact, hydrolytic release of HHDP units from ellagitannins causes their simple conversion into the bis-lactone ellagic acid (**10**). Representative compounds of the ellagitannin's family are peduncalagin (**50**), stachyurin (**51**), castalagin (**52**), vescalagin (**49**), castalin (**53**), vescalin (**54**), grandinin (**55**) and roburin E (**56**) in which D-glucose could be in open or closed form. The HHDP and NHTP (nonahydroxyterphenoyl) units possess an axial chirality (atropisomerism) giving the possible production of different stereoisomeric forms.

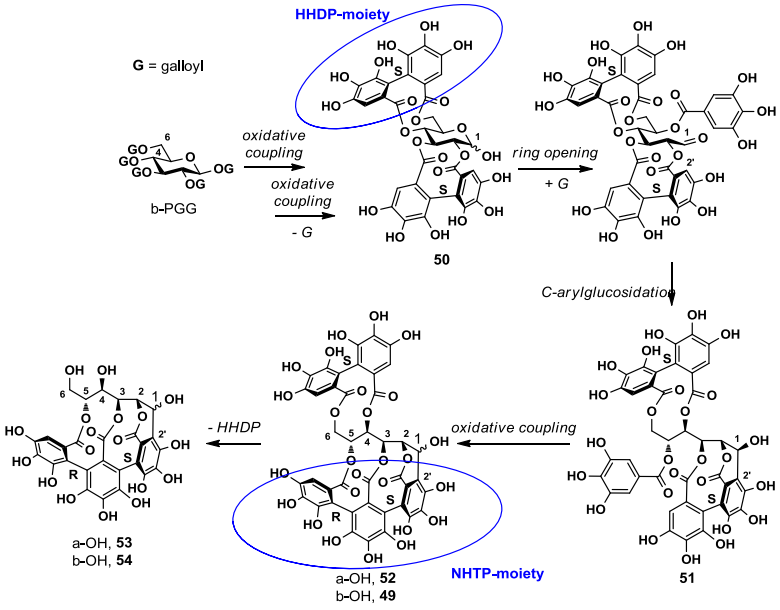

Scheme 7: Biosynthetic pathway

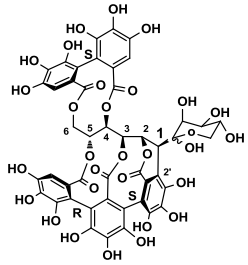

55

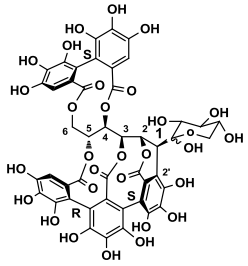

56

1.1.5.1 Stereochemical consideration on ellagitannins

When a molecule has a biaryl bond, it is possible to observe an axial chirality or atropisomerism, and for each biaryl bond, there are two possible atropisomers, distinguished as *S* and *R*.[108] Vescalagin (**49**), its C-1 epimer, castalagin (**52**), and their hydrolysis derivatives, castalin (**53**) and vescalin (**54**), were first isolated in 1967 from the same oak specimen *Quercus Sesselijlora* from Mayer et al.[109] Molecular structure of these compounds was elucidated using hydrolytic studies combined with spectroscopic analytical methods.[110] In most of the books and papers, reported in literature, the NHTP-atropisomer of vescalagin (**49**) was defined as (2*S*,3*S*)-isomer, together to others ellagitannins correlated with its structure.[11, 105, 111] However, in 1995, a revised study concerning a conformational analysis was published by N. Vivas[112] team; the results of this study, based on molecular mechanics calculations (MM2 force field), showed that the most stable atropoisomer of vescalagin (**49**) and castalagin (**52**) is (2*S*, 3*R*)-isomer. This axial stereochemistry concerning only one of the two biaryl bonds of the terphenoyl group has been reinvestigated also by the group of T. Tanaka[113] using computational methods (**Figure 6**). This structure revision is based on the comparative study between a simulation of the circular dichroism spectra of each possible atropoisomer (by TDDFT) and the experimental results (by

ECD) obtained from the natural vescalin (**54**) isolated by extraction process (**Figure 7**). A comparison between calculated and experimental data shows a much better agreement of the experimental data with those calculated for the revised atropoisomer (2*S*,3*R*) than with those calculated for the original (2*S*,3*S*) structure.

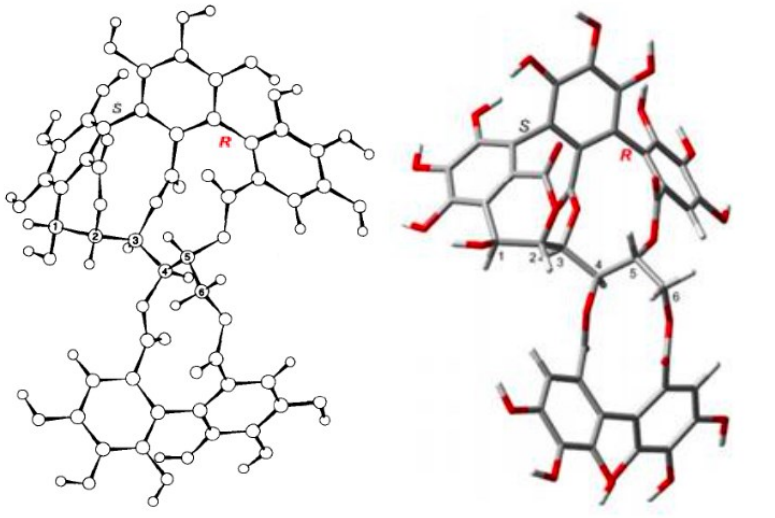

Figure 6: 3D structures of vescalagin (**49**) proposed by N. Vivas (on the left) and T. Tanaka (on the right)

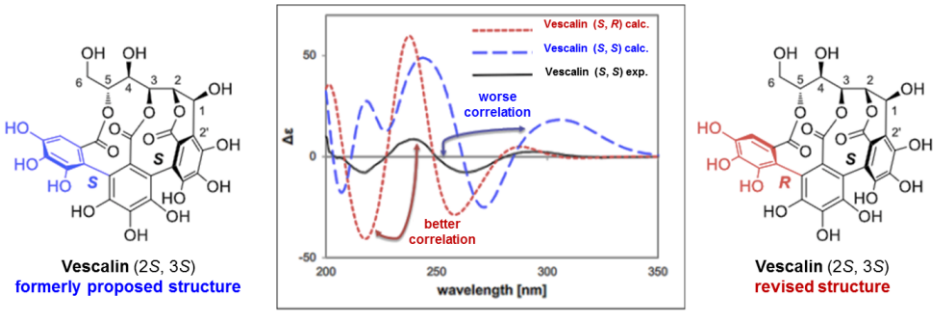

Figure 7: Experimental and calculated ECD spectra of vescalin (**54**); adapted from Org. Lett. 2015, 17, 46−49.

The ambiguity about the atropisomerism of triphenoyl moiety of all the ellagitannins isolated until now, prompted a number of researchers

in the challenge of the total synthesis of these compounds, and in the synthesis of ellagitannin-bearing devices in proteomics with the aim to study them by crystallography. Part of my Doctorate research activity during the third year was focused on that goal; this part of my work was carried out during my stay at the University of Bordeaux, France (January – July, 2017), under the supervision of Prof. Stéphane Quideau.

1.1.7 Aims of the PhD research activity

On the basis of the above, the main goal of the present research project was to obtain new potential chemotherapeutic agents starting from natural or bio-inspired polyphenols. This objective has been pursued following two parallel, although distinct, strategies:

a) modification of natural polyphenols to obtain optimized analogues with promising bioactivity, for possible use as chemotherapeutic agents.

b) synthesis of new potential chemotherapeutic agents through a chemo-enzymatic approach.

In both cases, chemical and/or enzymatic methodologies have been employed. The compounds obtained have been characterised by spectral analysis and, through collaboration with other laboratories, they have been evaluated for properties of biomedical interest, namely antioxidant, α-glucosidase inhibitor, antiproliferative, antiviral and antibacterial activity. Molecular modelling and structure-activity relationship (SAR) studies have been carried out in selected cases. Further goals of this work were an inverse virtual screening focused on magnolol analogues, and a contribution to the total synthesis of vescalin (**54**) and a vescalagine probe carried out at the laboratory of Prof.

Stéphane Quideau (University of Bordeaux, France). In the following, the results of my work are discussed in detail.

CHAPTER 2

2. RESULTS AND DISCUSSION

2.1 Synthesis and biological evaluation of bioinspired benzo[*k,l*]xanthene lignans and related phenazines

On the basis of what we have reported in the Introduction on benzo*[k,l]*xanthene lignans (BXLs) (Section 1.1.3), part of my research activity has been devoted to different studies aimed to highlight new properties of BXLs of potential pharmacological interest. To this purpose we planned the biomimetic synthesis of selected BXLs and related phenazines. The compounds obtained were purified and spectroscopically characterized. Subsequently, by collaboration with other laboratories, BXLs and their analogues were evaluated as:

- potential G-quadruplex DNA ligands;
- agonist/antagonist of FXR and LXR receptors;
- antimicrobial agents.

In some cases, the biochemical or biological assays were limited to the compounds available at the moment of the experiments, so not all compounds were subjected to the same assays.

2.1.1 Biomimetic synthesis of benzo[*k,l*]xanthene lignans

In order to evaluate new biological properties of BXLs, the synthesis of new and previously reported benzoxanthene has been planned. The synthesis of BXLs (**36**, **38**, **39**, **60**, **63**, **65** and **67**) was carried out employing the Mn-mediated biomimetic methodology, summarized in **Scheme 8**. In the general procedure, the synthesis of a

suitable caffeic ester was carried out as first step, using a Fisher esterification or in selected cases the Steglich esterification. Then we employed the methodology previously reported by the group where I carried out my PhD project and based on biomimetic oxidative coupling of caffeic esters, mediated by Mn^{3+}.[47] In the following, the details are discussed.

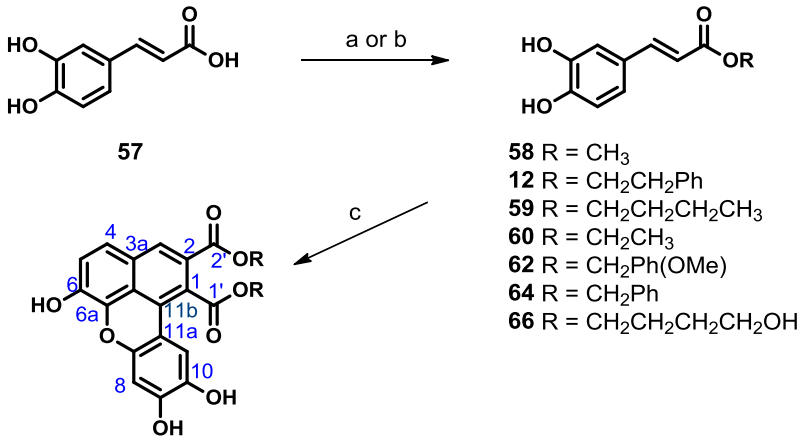

Scheme 8: (**a**) ROH, H_2SO_4, reflux temperature, 24 h; (**b**) ROH, DCC, dry THF , 24 h; (**c**) $Mn(OAc)_3$, CH_3Cl.

*2.1.1.1 Synthesis of dimethyl 6,9,10-trihydroxybenzo-[k,l-]xanthene-1,2-dicarboxylate (**36**)*

As reported in **Scheme 8**, the caffeic methyl ester **58** was obtained through Fischer esterification using caffeic acid (**57**) and methanol in the presence of concentrated H_2SO_4 as catalyst. The purified product showed NMR data in perfect agreement with those reported in literature.[114] Compound **58** was submitted to dimerization in presence of an excess of

$Mn(OAc)_3$ in $CHCl_3$. The yellow-brown residue obtained, was chromatographically purified to recover the compound **36**. The ^1H and ^{13}C NMR spectra are respectively reported in **Figures 1S** and **2S** (**Appendix A**); the spectroscopic data, compared with the data previously obtained and reported in the literature,[47] confirmed the structure of the benzo[*k,l*]xanthene lignan **36**.

*2.1.1.2 Synthesis of diphenethyl 6,9,10-trihydroxy-benzo-[k,l-]xanthene-1,2-dicarboxylate (**38**) and its methylated derivative (**43**)*

The procedure for the preparation of compound **38** (**Scheme 8**) is similar to the previous, with the only difference that CAPE (**12**, caffeic acid phenethyl ester), the substrate of this reaction, was not synthesized because it is a commercially available. Thus, compound **12**, in presence of $Mn(OAc)_3$ afforded the expected benzoxanthene **38**. After purification, this latter was subjected to ^1H and ^{13}C NMR spectral analysis; NMR spectra are reported in **Figures 3S** and **S4** (see **Appendix A**) and are in agreement with those previously reported in the literature,[47] confirming the structure of the compound **38**. This compound was treated with treated with dimethyl sulphate, as previously reported in literature,[65] to prepare its permethylated **43**, in order to check the possible role of a free/blocked catechol group for antimicrobial activity (**Scheme 9**, see below for biological evaluation).

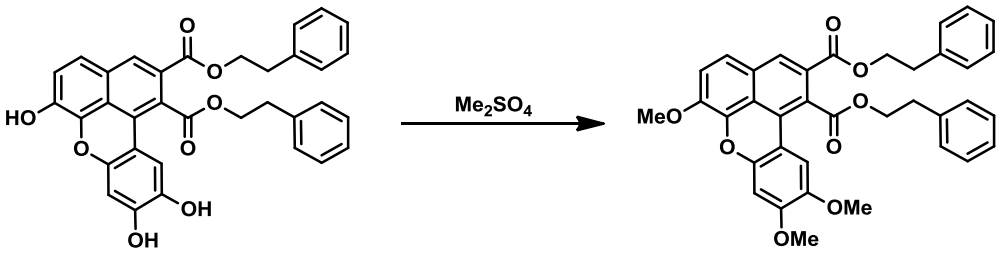

38 43

Scheme 9

*2.1.1.3 Synthesis of dibutyl 6,9,10-trihydroxybenzo-[k,l]-xanthene-1,2-dicarboxylate (**39**)*

Caffeic acid (**57**) was treated with butanol in presence of concentrated H_2SO_4 to obtain the caffeic acid butyl ester **59** (**Scheme 8**). The NMR data are in perfect agreement with those reported in the literature.[115] The ester **59** was employed for the dimerization reaction with $Mn(OAc)_3$. After purification, afforded the pure compound **39**. The ^1H and ^{13}C NMR spectra of **39** was respectively reported in **Figures 5S** and **6S** (see **Appendix A**). The NMR data are in agreement with those reported in literature and confirmed the structure of compound **39**.[66]

*2.1.1.4 Synthesis of diethyl 6,9,10-trihydroxybenzo-[k,l]-xanthene-1,2-dicarboxylate (**61**)*

The synthesis of benzoxanthene **61** is reported in **Scheme 8**. Briefly, caffeic ethyl ester (**60**) was obtained through Fischer esterification reaction starting from caffeic acid (**57**). The NMR data of the product are in perfect agreement with those reported in literature.[115] The monomer **60** was treated with $Mn(OAc)_3$ in $CHCl_3$ and after reaction, the purification afforded the pure compound **61**. The ^1H-NMR and ^{13}C-NMR spectra are respectively reported in **Figures 7S** and **8S** (see

Appendix A); these data confirmed the structure of the benzo[*k,l*]xanthene lignan **61**, and are in perfect agreement with those reported in the literature.[66]

*2.1.1.5 bis(4-methoxybenzyl)6,9,10-trihydroxybenzo-[kl]-xanthene-1,2-dicarboxylate (**63**)*

To expand the structural variety of BXLs we planned to synthetize two new analogues of the above cited benzoxanthenes. These syntheses are reported here.

To a solution of caffeic acid (**57**) in THF, was added N,N'-dicyclohexylcarbodiimide (DCC) in presence of the commercial 4-metoxybenzyl alcohol to obtain the 4-metoxybenzyl caffeate **62** (**Scheme 8**). The NMR data are in perfect agreement with those reported in the literature.[116] The ester **62** was employed for the dimerization reaction with $Mn(OAc)_3$. The new benzoxanthene **63**, recovered after purification, was fully characterized by 1D and 2D NMR spectroscopy; in **Figures 9S** and **10S** (see **Appendix A**) the ^{1}H and ^{13}C NMR spectra of **63** are reported.

The ^{1}H NMR and ^{13}C spectra of **63** showed the typical signals for the benzoxanthene core: three singlets at 8.17, 7.34 8 and 6.70 ppm at for H-3, H-8 and H-11 respectively in the ^{1}H NMR spectrum and, the resonances at 129.8, 112.4 and 104.9 ppm for C-3, C-8 and C-11 in the ^{13}C NMR spectrum; two doublets at 7.49 and 7.30 ppm mutually coupled (J = 8.5 Hz; see COSY spectrum) for H-4 and H-5 respectively, and the corresponding ^{13}C resonaces at 122.3 and 120.7 ppm. Also the resonances for aromatic chains were detected: two doublets at 7.44 and 6.96 ppm mutually coupled (J = 8.7 Hz) for H-2^{IV}/6^{IV} and H-3^{IV}/5^{IV} respectively and the corresponding ^{13}C resonances at 131.27, 114.8 ppm; two doublets at 7.32 and 6.88 ppm mutually coupled (J = 8.7 Hz) for H-2^{VI}/6^{VI} and H-

$3^{VI}/5^{VI}$ and the corresponding ^{13}C resonances at 131.22 and 114.7 ppm. These resonances are unambiguously assigned studying HMBC correlations. In the upper fields region (5.27 – 3.77 ppm) of ^{1}H NMR spectrum the resonances for alkyl chains were detected: two differently shielded singlets for the α-methylene protons (respect to ester functions) at 5.26 (67.5 ppm, C-1''), and 5.27 ppm (68.3 ppm, C-1''') for H-1'' and H-1''' respectively; finally, two singlets integrating for three protons, namely for the two –OMe in $4^{IV}/4^{V}$-CH_3 3.81 (55.6 ppm, -OMe^{IV}-4), and 3.77 ppm (55.5 ppm, -OMe^{V}-4) ppm.

All resonances were assigned through the study of HSQC correlations . All the NMR data are in agreement confirmed the structure of compound **63**.

*2.1.1.6 bis(benzyl)6,9,10-trihydroxybenzo-[kl]-xanthene-1,2-dicarboxylate (**65**)*

To a solution of caffeic acid (**57**) in THF, was added N,N'-dicyclohexylcarbodiimide (DCC) in the presence of the commercial benzyl alcohol to obtain the benzyl caffeate **64** (**Scheme 8**). The NMR data are in perfect agreement with those reported in the literature.[117] The ester **64** was employed for the dimerization reaction with $Mn(OAc)_3$. After purification, the pure compound **65** was obtained. The new benzoxanthene was fully characterized by 1D NMR spectroscopy (see **11S** – **12S** in **Appendix A**). All the NMR data confirmed the structure of compound **65**. The structure of **65** differs than **63** only for the aromatic pendants which they do not present the para-methoxy groups.

*2.1.1.7 Synthesis of bis(4-hydroxybutyl) 6,9,10-trihydroxybenzo-[kl]-xanthene-1,2-dicarboxylate (**67**)*

1,4-Butanediol and caffeic acid (**57**) reacted through the Fisher esterification and the intermediate **66** was obtained with 95% yield. The NMR data are in perfect agreement with those reported in literature.[118] The ester **66** was employed for the dimerization reaction with $Mn(OAc)_3$. After purification, the pure compound **67** was isolated and spectroscopically characterized. The ^{1}H and ^{13}C NMR spectra of **67** was respectively reported in **Figures 13S** and **14S** (see **Appendix A**). The NMR data are in agreement with those reported in literature and confirmed the structure of compound **67**.[118]

2.1.2 Synthesis of phenazine derivatives of benzoxanthene lignans

In order to extend our library of compounds inspired by natural BXLs, the synthesis of new phenazine derivatives has been planned, as detailed in the following.

Phenazines are generally prepared starting from catechol compounds, by reaction with 1,2-phenylenediamine (**Scheme 10**).[119] The key step in this reaction is the formation of *o*-benzoquinone, which is normally achieved by catechol oxidation. Many reagents have been reported to convert catechol to *o*-benzoquinone, these include $NaIO_4$,[120] tetrachloro-1,2-benzoquinone,[121] $NaNO_2$,[121] PbO_2,[122] Ag_2O,[119] and Ag_2CO_3/ Celite.[123]

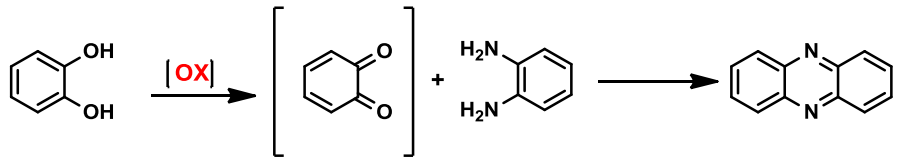

Scheme 10: phenazine formation from a phenol

The benzoxanthene **39** was submitted in a preliminary screening to develop the synthetic method for the synthesis of 8,9-benzoxanthene quinone.

2.1.2.1 Preliminary screenings: benzo[k,l]xanthene oxidation

Compound **39**, whose HPLC profile at different wavelengths is reported in **Figure 8** (a) 254 nm b) 360 nm c) 390 nm d) 420 nm), was subjected to preliminary oxidative reactions employing both enzymatic and chemical methods. Three different oxidases, namely *Trametes versicolor* Laccase (TvL), *Pleurotus ostreatus* Laccase (PoL), *Agaricus*

bisporus Laccase (AbL), and two chemical oxidants, namely Ag_2O and $Mn(OAc)_3$ were tested. All reactions were monitored by TLC and HPLC (see Experimental section for details). As reference, the HPLC profile of the substrate **39** (t_R = 8.75), has been recorded (**Figure 8**).

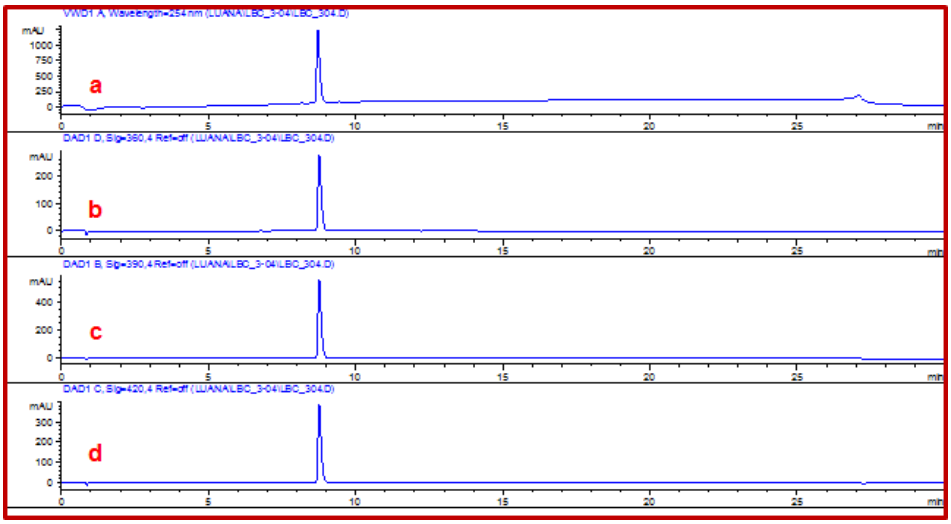

Figure 8: HPLC- profiles of **39**: Column Luna C-18, 250 x 4.6 mm, 5 μm, ϕ = 1 ml/min, from 50% CH_3CN/H^+ in H_2O/H^+ to 100% CH_3CN/H^+; a) 254 nm; b) 360 nm; c) 390 nm; d) 420 nm.

2.1.2.2 Enzymatic methods

Three samples of compound **39** were dissolved in EtOAc and each solution was stirred with acetate buffer solution of the above cited enzymes. The reactions were carried out under atmospheric O_2 and were monitored both by TLC and HPLC. In **Figure 9** the chromatographic profiles at 360 nm of: **a**) **39**; **b**) **39** and *Trametes versicolor* Laccase (TvL); **c**) **39** and *Pleurotus ostreatus* Laccase (PoL); **d**) **39** and *Agaricus bisporus* Laccase (AbL). As seen, any product was obtained employing enzymatic methods.

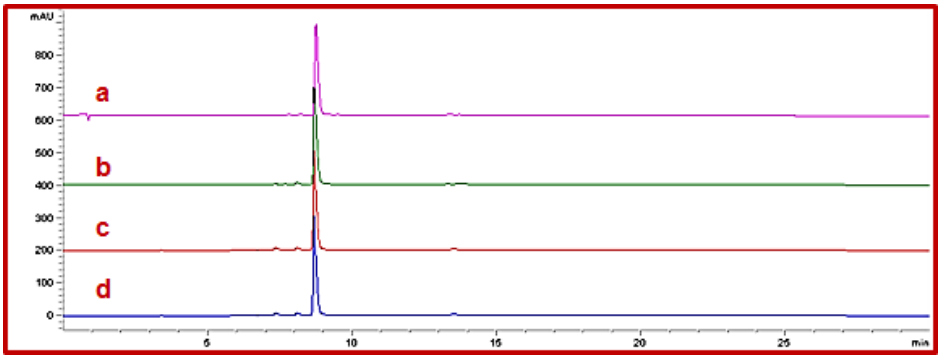

Figure 9: HPLC-profiles: Column Luna C-18, 250 x 4.6 mm, 5µm, ϕ = 1 ml/min, from 50% CH_3CN/H^+ in H_2O/H^+ to 100% CH_3CN/H^+; ʎ = 360 nm. a) **39**, b) TvL, c) PoL, d) AbL.

2.1.2.3 Chemical methods

Two separate aliquots of compound **39** were dissolved in CH_2Cl_2 and additioned respectively of $Mn(OAc)_3$ and Ag_2O. The reactions were stirred at room temperature and monitored both by TLC (6% MeOH-CH_2Cl_2) and HPLC at regular time intervals. In **figure 10** we report the chromatographic profiles at 360 nm of: **a**) **39**; **b**) **39** and $Mn(OAc)_3$; **c**) **39** and Ag_2O. The reaction with $Mn(OAc)_3$ does not shows effective substrate conversion, whereas the reaction mediated by Ag_2O shows an almost complete conversion of the substrate and the formation of a less polar product (peak at t_R = 12.3 min) presumably the expected *ortho*-quinone derivative. On this basis we decided to proceed on preparative scale using Ag_2O as an oxidizing agent. However, despite our best efforts it was not possible to isolate the intermediate quinone of this reaction, because it was largely degraded during the extraction and purification procedure. This observation was also confirmed by literature data.[124] Thus, we carried out the synthesis of the phenazine derivatives without isolation of the intermediate quinone.

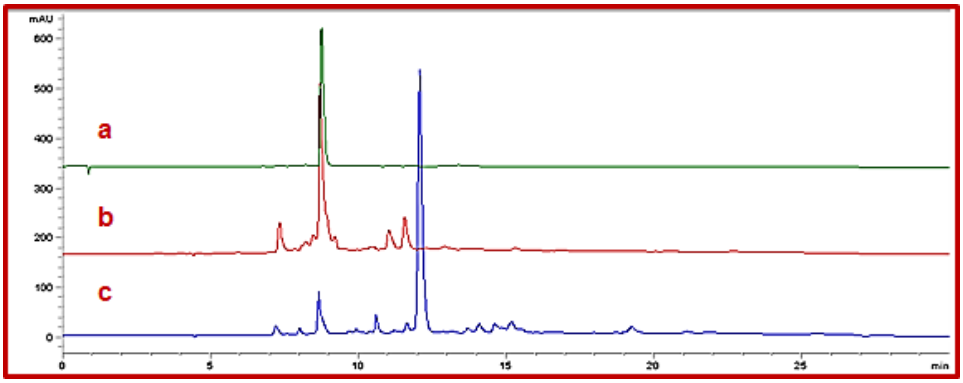

Figure 10: HPLC-profiles: Column Luna C-18, 250 x 4.6 mm, 5µm, ϕ = 1 ml/min, from 50% CH_3CN/H^+ in H_2O/H^+ to 100% CH_3CN/H^+; ƛ = 360 nm. **a**) **39 b**) $Mn(OAc)_3$ **c**) Ag_2O.

On the basis of the preliminary screening to obtain the BXL-quinone I planned the synthesis of phenazines **69**, **71**, **73**, **74** and **75** employing the procedure summarized in **Scheme 11**. In the general procedure, the synthesis of BXL quinone was carried out as first step, using Ag_2O-mediated oxidation of the catechol moiety. In this manner a convenient and simple procedures for the synthesis of phenazine derivatives were developed via a reaction of *o*-phenylenediamines and 1,2-dicarbonyl compounds by condensation reaction in presence of acetic acid in catalytic amount, at reflux temperature in dry CH_3CN as solvent. In the subsequently sections, the details are discussed.

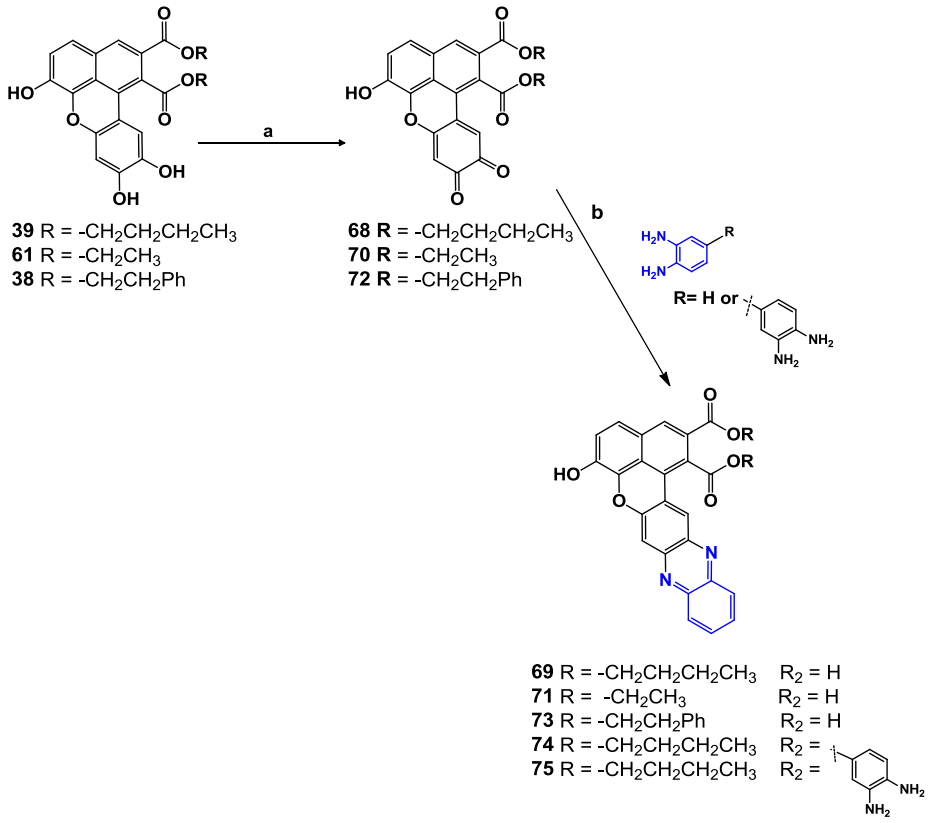

Scheme 11: general procedure for the synthesis of phenazines: (**a**) Ag_2O, CH_2Cl_2, rt; (**b**) *ortho*-phenylenediamine, acetic acid, dry CH_3CN.

*2.1.2.4 Synthesis of dibutyl 6-hydroxybenzo[4,5]chromeno[2,3-b]phenazine-1,2-dicarboxylate (**69**)*

Compound **39** was dissolved in CH_2Cl_2 and to this solution Ag_2O was added. The reaction mixture was stirred at room temperature and monitored by TLC for 6 h (**Scheme 11**). The crude mixture containing **68** was dissolved in dry CH_3CN and *o*-phenylenediamine and acetic acid were added to this solution (**Scheme 11**). The reaction mixture was stirred at room temperature and monitored by TLC for 24 h. After column purification, a red pigment of benzo[*k,l*]xanthene phenazine **69** (yield: 19%) was obtained. This compound was fully characterized by MS

spectrometry and 1D and 2D NMR spectroscopy and all spectra are reported in **Appendix B**.

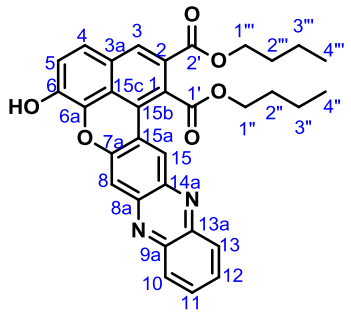

The ESI-MS spectrum of **69** (see **Figure 15S** in the supporting material section) showed a main peak at 537.5 *m/z,* imputable to molecular ion $[M+H]^+$, which confirmed the formation of the product. The ^1H and ^{13}C NMR spectra are reported in **Figure 16S** and **17S** (see **Appendix B**); the assignments of all the found signals were aided by the analysis of gCOSY, gHSQCAD and gHMBCAD correlations, which spectra are reported in **Figures 18S, 19S** and **20S** respectively. All the data obtained from spectroscopic analysis were listed in the experimental section. The ^1H NMR spectrum (**Figure 16S**) showed the typical signals of benzoxanthene moiety at lower fields: namely the singlets at 8.66, 8.36 and 7.65 ppm were assigned to the protons H-15, H-3 and H-8 respectively; analogously the two mutually coupled doublets at 7.44 and 7.28 ppm (J = 8.7 Hz), as evidenced by gCOSY spectrum (**Figure 18S**), were assigned to H-4 and H-5 protons. In the region at lower fields it can be observed also the characteristic signals of phenazine ring protons: two doublets at 7.97 (J = 6.5 Hz) and 8.14 ppm (J = 6.5 Hz) were assigned to the protons H-10 and H-13 and the double doublets at 7.72 ppm (J = 6.5, 3.2 Hz) which it integrates for two protons, was assigned to H-11 and H-12. The key COSY correlations are reported in **Figure 11**. The last

signals discussed, are characteristics a phenazine ring moiety, suggesting the formation of the expected phenazine derivative **69**. At upper fields the aliphatic proton signals of ester chains were found and on the basis of COSY correlations the two triplets at 4,70 and 4.40 ppm were assigned to H-1″ and H-1‴respectively; the two pentets at 1.89 and 1.84 ppm to H-2″ and H-2‴, the two sextets at 1.46 and 1.54 ppm to the H-3″ and H-3‴, the two triplets at 0.94 and 1.04 ppm were assigned to the H-4″ and H-4‴.

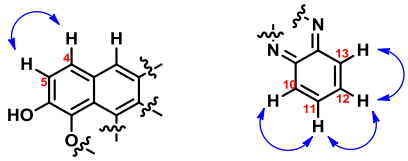

Figure 11: selected gCOSY correlations.

The analysis of the ^{13}C-NMR (**Figure 17S**) spectrum resonances and the study of gHSQCAD and gHMBCAD correlations, which allowed the unambiguous assignment of all ^{13}C resonances, corroborated the formation of compound **69**. For example, the two typical signals for a sp^2 quaternary carbons of esters at 170 and 165 ppm were discriminated trough gHMBCAD correlations. Namely, the correlation of the signal at 165.5 ppm with the proton signal at 8.36 ppm (H-3) allowed to assign the resonance at 165.5 as C-2′, as well as the correlation of the same signal with the proton signal at 4.40 ppm (H-1″) allowed to distinguish between the two butyl side chains. In addition, the signals at 111.72 and 127.75 ppm (C-8 and C-15 respectively), were shift to lower fields if compared with those present in the spectrum of the substrate **39** (104 and 112.06 ppm respectively); confirming the extension of the aromatic skeleton. Other key signals indicating the formation of expected compound, are those of phenazine moiety: two new signals forsp^2 quaternary carbons at

143.63 and 143.77 ppm were unambiguously assigned to C-9a and C-13a respectively, trough gHMBCAD correlation between the signal at 143.63 ppm with the proton signal at 7.97 ppm (namely H-10), and between the signal at 143.77 ppm with the proton signal at 8.14 ppm (namely H-13). Furthermore the four signals of -CH sp^2 signals at 128.87, 129.63, 131.10 and 130.05 ppm were assigned to C-10, C-11, C-12 and C-13 respectively on the basis of the gHMBCAD correlations reported in **Figure 12**. Thus, the signal at 128.87 ppm showed a correlation with the proton signal at 7.72 ppm (namely H-11); at the carbon signal at 129.63 ppm with the proton signals at 7.97 and 7.72 ppm (namely H-10 and H-12 respectively); the signal at 131.10 with 7.72 and 8.14 ppm (namely H-9 and H-11 respectively); and finally the resonance at 130.05 with the proton signal at 7.72 ppm (namely H-12).

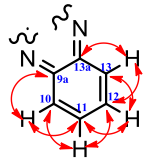

Figure 12: gHMBCAD correlations of phenazine nucleus.

*2.1.2.5 Synthesis of diethyl 6-hydroxybenzo[4,5]chromeno[2,3-b]phenazine-1,2-dicarboxylate (**71**)*

The benzoxanthene **61** was employed for the synthesis of the proper phenazine **71** via the formation of the quinone **70** as described in **Scheme 11**. Briefly, the intermediate **70** was obtained by oxidation of benzoxanthene **61** in presence of Ag_2O and, after workup, the mixture was dissolved in dry CH_3CN and *o*-phenylenediamine and acetic acid were added. The reaction mixture were stirred at room temperature and it

was monitored through TLC for 24 h. Finally, the purification afforded the benzo[*k,l*]xanthene phenazine **71** (yield: 19%) as red residue. This compound was completely characterized through MS spectrometry and 1D and 2D NMR spectroscopy; all spectroscopic data are reported in the supporting material section.

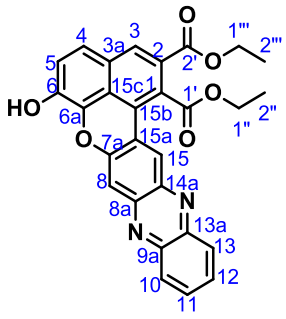

The ESI-MS spectrum of **71** (**Figure 21S**) showed a main peak at 481.3 *m/z,* imputable to molecular ion $[M+H]^+$, which suggested the formation of the expected product. The ^1H and ^{13}C NMR spectra are reported in **Figures 22S** and **23S;** the assignments of all the found signals were aided through the analysis of gCOSY, gHSQCAD and gHMBCAD correlations, which spectra are reported in **Figures 24S**, **25S** and **26S** (see **Appendix B**) respectively. All the data obtained from analysis were listed in the experimental section. The lower fields region of ^1H NMR spectrum (**Figure 22S**) showed the typical signals of benzoxanthene moiety, namely three singlets at 8.61, 8.39 and 7.82 ppm (H-15, H-3 and H-8 respectively) and two mutually coupled doublets at 7.50 and 7.32 ppm (H-4 and H-5). In the same region of the spectrum, also the characteristic signals of phenazinic ring protons were observed: the two doublets at 8.07 and 8.15 ppm were assigned to the protons H-10 and H-13 while the two triplets at 7.73 and 7.79 ppm to H-11 and H-12 respectively. The assignment was aided by the analysis of COSY correlations (See **Figure**

12).The presence of the characteristic signals for phenazine ring moiety suggested the formation of derivative **71**. Finally in the upper fields region of ^{1}H NMR spectrum the aliphatic proton signals of ester chains were clearly assigned: the two quadruplets at 4.65 and 4.36 ppm to the H-1″ and H-1‴ protons respectively; the two partially overlapped triplets at 1.39 ppm (integrating for 6 protons) to H-2″ and H-2‴ methyl protons. In the same way, the ^{13}C NMR spectrum (**Figure 23S**) showed the expected resonances for the formation of phenazine **71** and most of them were unambiguously assigned thanks to HSQC and HMBC correlations. For example the two typical signals for a sp^2 quaternary carbons of esters at 170.68 and 166.07 ppm with the proton signal at 8.39 ppm (namely H-3). Indeed in the ^{13}C NMR spectrum of **71** there were two new signals for sp^2 quaternary carbons at 144.90 and 142.80 ppm respect to that of **61**; these signals can be assigned unambiguously to C-9a and C-13a respectively of phenazine moiety which are the key signals indicating the formation of expected compound: aided by HMBC correlations between the signal at 144.90 ppm with the proton signal at 8.07 ppm (namely H-10), and between the signal at 142.80 ppm with the proton signal at 8.15 ppm (namely H-13). Analogously, the four signals of -CH sp^2 at 127.34, 130.29, 133.23 and 132.67 ppm were assigned to C-10, C-11, C-12 and C-13 respectively of phenazine moiety, trough HMBC correlations as reported in **Figure 13**.

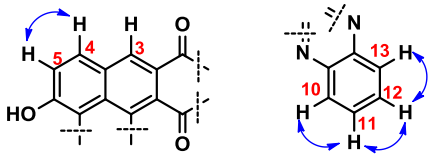

Figure 12: selected gCOSY correlations of **71**.

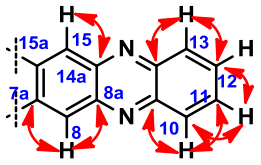

Figure 13: gHMBCAD correlations of phenazine nucleus of **71**

2.1.2.6 Synthesis of diphenethyl 6-hydroxybenzo-[4,5]chromeno- [2,3-b]-phenazine-1,2-dicarboxylate (73)

The benzoxanthene **38** was employed for the synthesis of the proper phenazine **73** via the formation of the quinone **72** as described in **Scheme 11**. Briefly, the intermediate **72** was obtained by oxidation of benzoxanthene **38** in presence of Ag_2O and, after workup, the mixture was dissolved in dry CH_3CN and *o*-phenylenediamine and acetic acid were added. Benzo[*k,l*]xanthene quinone **72** was dissolved in dry CH_3CN; *o*-phenylenediamine and acetic acid were added at this solution (**Scheme 11**). The reaction mixture were stirred at room temperature and was monitored by TLC for 24 h. After column purification, the benzo[*k,l*]xanthene phenazine **73** (yield: 38.6%) was obtained as red residue. This compound was completely characterized using MS spectrometry and 1D and 2D NMR spectroscopy; all spectroscopic data are reported in the supporting material section.

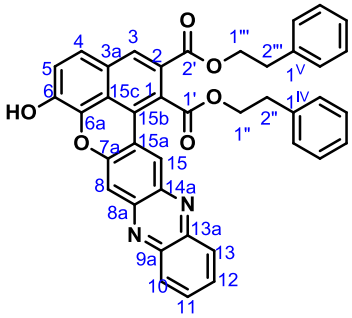

The ESI-MS spectrum of **73** (**Figure 27S**) showed a main peak at 633.4 *m/z,* imputable to molecular ion $[M+H]^+$, which suggested the formation of the expected product. The ^1H and ^{13}C NMR spectra are reported in **Figure 28S** and **29S** (see **Appendix B**); the assignments of all the found signals were aided by the analysis of gCOSY, gHSQCAD and gHMBCAD correlations, which spectra were reported in **Figures 30S**, **31S** and **32S** (see **Appendix B**) respectively. All the data obtained from analysis were listed in the experimental section. In the ^1H NMR spectrum (**Figure 28S**) the signals of benzoxanthene moiety were clearly identified: namely the three singlets at 8.54, 8.27 and 7.69 ppm for H-15, H-3 and H-8 protons respectively; and the two doublets 7.41 and 7.30 ppm (overlapped with other signals), for H-4 and H-5. In the same region the characteristic signals expected for of phenazine ring protons were detected suggesting the formation of **73**. Thus, the two doublets at 8.01 and 8.12 were assigned to the protons H-10 (J = 6.5 Hz) and H-13 (J = 6.7 Hz) and the double doublets at 7.72 (J = 6.7, 2.0 Hz; integrating for two protons),were assigned to H-11 and H-12 respectively.Indeed, in the region at lower fields it can be observed some signals attributable to two non-equivalent aromatic moieties of phenethyl residues: the multiplet from 7.38 to 7.28 ppm which can be assigned to the proton H-2^V, H-3^V, H-4^V, H-5^V, H-6^V (integrate for six protons); while the signals at 6.86,

6.95 and 7.18 ppm can be assigned to the protons H-2^{IV}, H-3^{IV}, H-4^{IV}, H-5^{IV}, H-6^{IV}. Finally, at 4.84, 4.55 and 3.11 ppm were identified the mehilene and methyl proton signals of ethyl chains phenethyl residues which were assigned as reported in the experimental section. The analysis of the ^{13}C-NMR (**Figure 29S**) spectrum signals and the study of heteronuclear correlation through the gHSQCAD (**Figure 31S**) and gHMBCAD (**Figure 32S**) spectra, confirmed the formation of compound **73**. The ^{13}C NMR spectrum showed two typical signals for a sp^2 quaternary carbons of esters at 171.17 and 165.55 ppm; which were discriminated on the basis of the gHMBCAD correlation of 165.55 ppm with the proton signal at 8.27 ppm (namely H-3) and assigned as C-1′ (171.17) and C-2′ (165.55). The signals at 110.59 and 126.81 ppm attributable to C-8 and C-15 respectively, were shift to lower field respect to those present in the spectrum of the substrate **38** (104 and 112.06 ppm respectively); this shift confirmed the extension of the aromatic skeleton of the molecule. The most significant resonances of ^{13}C NMR spectrum for the formation of expected compound, were those of phenazine nucleus. Precisely, two sp^2 quaternary carbon signals at 130.63 and 130.43 ppm, assigned unambiguously to C-9a and C-13a respectively, trough gHMBCAD correlation between the signal at 130.63 ppm with the proton signal at 8.01 ppm (namely H-10), and between the signal at 130.43 ppm with the proton signal at 8.12 ppm (namely H-13). In the same way, three -CH sp^2 signals at 127.88, 128.62 and 128.86 ppm were assigned to C-10, C-11/C-12 and C-13. In this case the signal at 128.62 ppm for isochronous C-11 and C-12 was confirmed by the gHMBCAD correlations of this resonance with the proton signals at 8.01 ppm (namely H-10) and 8.12 ppm (namely H-13). Indeed, further typical aromatic resonances were also detected in the ^{13}C NMR spectrum attributable to

two non-equivalent phenethyl moieties: namely, the signals at 138.48, 129.84, 127.97 and 126.87 ppm assigned to the carbons C-1^{V}, C-2-6^{V}, C-3-5^{V}, and C-4^{V} respectively; and the signals at 136.63, 129.77, 127.91 and 126.96 ppm for the C-1^{IV}, C-2-6^{IV}, C-3-5^{IV} and C-4^{IV} respectively.

2.1.2.7 Synthesis of dibutyl 12-(3,4-diaminophenyl)-6-hydroxybenzo[4,5]chromeno[2,3-b]phenazine-1,2-dicarboxylate (74 and 75)

The benzoxanthene **39** was also employed for the synthesis of the fhenazine derivatives **75** and **75** via the formation of quinone **68** as described in **Scheme 11**. Briefly the oxidative reaction with Ag_2O gave the intermediate **68**, which was employed in the second step of reaction, after workup, in presence of 3,3′-diaminobenzidine and of acetic acid. The purification afforded two main red compounds with 10.6 and 7.8% yield, presumably the expected isomeric phenazines **74** and **75**. One of these compounds was completely characterized by MS spectrometry and 1D and 2D NMR spectroscopy. The ESI-MS spectrum (**Figure 33S**) showed a main peak at 643.3 *m/z,* imputable to molecular ion $[M+H]^+$, which was in agreement with the formation of the phenazine product; of course the MS spectrum did not allow to distinguish between the two isomers. The ^{1}H and ^{13}C NMR spectra are reported in **Figures 34S** and **35S** (see **Appendix B**); the assignments of all the found signals were aided by the analysis of gCOSY, gHSQCAD and gHMBCAD spectra, reported in **Figures 36S**, **37S** and **38S** (see **Appendix B**) respectively. All the data obtained from this analysis were listed in experimental section.

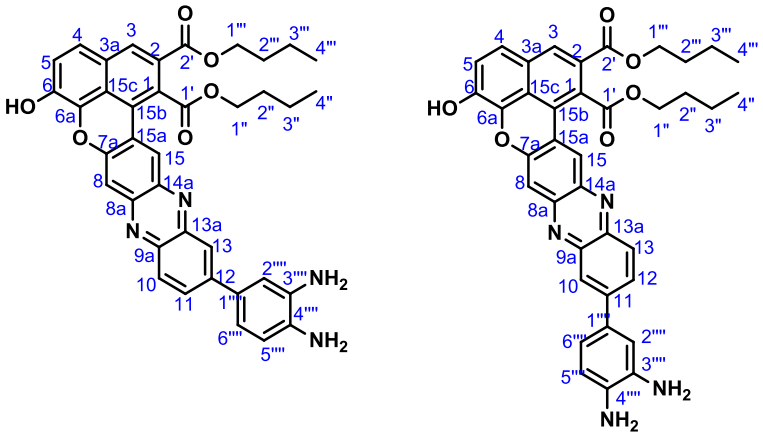

Proposed interchangeable structures for compounds **74** and **75**

The lower fields region of ^{1}H NMR spectrum (**Figure 34S**) showed the typical signals of benzoxanthene moiety, namely three singlets at 8.44, 8.34 and 7.71 ppm (H-15, H-3 and H-8 respectively) and two mutually coupled doublets at 7.51 and 7.32 ppm (H-4 and H-5). In the same region of the spectrum, also the characteristic signals of phenazinic ring protons were observed: the two doublets at 7.93 and 7.82 ppm and the singlet at 8.10 were assigned to H-10, H-11 and H-13 protons respectively of benzidine moiety. Whereas, the singlet at 7.17 and the two doublets at 6.69 and 7.10 ppm were assigned to the protons at H-2"", H-5"" and H-6"" respectively of benzidine. The presence of these latter signals suggested the formation of derivative **74** or **75**. Of course, in the upper fields region of ^{1}H NMR spectrum the aliphatic proton signals of ester chains were clearly identified: the two triplets at 4.64 and 4.35 ppm to the H-1″ and H-1‴ protons respectively; the two overlapped triplets at 1.80 ppm (integrating for 4 protons) to H-2″ and H-2‴; two multiplets at 1.51 and 1.42 ppm (integrating for 2 protons respectively) to H-3″ and H-3‴; finally two triplets at 1.02 and 0.87 ppm (integrating for 3 protons respectively) to H-3″ and H-3‴. In the same way, the ^{13}C NMR

spectrum (**Figure 35S**) showed the expected resonances for the formation of phenazine **74** (or **75**) and most of them were unambiguously assigned thanks to HSQC and HMBC correlations. For example the typical signal for a sp^2 quaternary carbon of ester at 167.01 ppm showed an HMBC correlation with the proton signal at 8.34 ppm (namely H-3) and it was unambiguously assigned as C-2′. Indeed in the ^{13}C NMR spectrum there were two new signals for sp^2 quaternary carbons at 149.69 and 130.42 ppm respect to that of benzoxanthene **39**; these signals can be assigned to C-9a and C-13a respectively of phenazine moiety and are the key signals for the formation of expected compound. The analysis of NMR spectra acquired for the main recovered product confirmed the formation of a fenazine derivative of **39**; these data were compared with those of ^{1}H NMR spectra calculated (ACD Labs 11.0) for the two isomers **74** and **75**. Nevertheless, this comparison and data analysis did not allow an unambiguous assignment to one of the two isomeric structures.

2.1.3 Study of the interaction of benzoxanthenes with DNA G-quadruplex

Recently the interest towards molecules able to interact with DNA, and in particular with unusual secondary structures as G-Quadruplex, has been growing rapidly because they have a role on gene expression, apoptosis and activation or repression of several *proto*-oncogenes (e.g. *c*-Myc, *c*-Kit, *k*-Ras); consequently, molecules able to interact with G-quadruplex both as stabilizing or destabilizing agents, could act as modulator of gene regulation mechanism. Hence, several studies have been devoted to develop novel G-quadruplex ligands. G-quadruplex DNA structures were firstly observed in the single-stranded 3′ overhang of human telomeres.[125] More recently, G-quadruplexes were found to form in the proximal promoter regions of human oncogenes to regulate gene transcription. Hurley and co-workers[126] provided the direct evidence for a G-quadruplex structure formation in a promoter region of *c*-MYC and its stabilization with several small molecules, resulting in the repression of *c*-MYC transcription. These findings suggest that G-quadruplex formation may be related to a general mechanism for gene regulation, and that the modulation of gene expression could be achieved by targeting these structures. A number of researches have shown that telomerase is reactivated and overexpressed in most tumor cells; in fact, high telomerase activity correlates with the degree of malignancy and the likelihood of tumor progression. The inhibition of telomerase activity selectively induce apoptosis in tumor cells. Thus stabilization of telomeric G-quadruplexes often leads to tumor cell apoptosis, through the block of telomerase activity because ligands that selectively bind to and stabilize telomeric G-quadruplex structures could act as indirect telomerase inhibitors.. For this reason G-Quadruplex has

become a new target in development of new anticancer drugs. Based on the data reported in Section 1.1.3, it has been speculated that BXLs, possessing an extensively conjugated planar core, and reported as DNA duplex intercalating agents, could stabilize the G-quadruplex DNA structure, and therefore could have a crucial role in the inhibition of telomerase activity leading to apoptosis in cancer cells. Thus, as a first goal of this research, we planned to resynthesize four BXLs, selected on the basis of their binding with duplex DNA, to be employed in a preliminary study about their interaction with G-Quadruplex DNA structures. As discussed in the following Section, we planned also to obtain and evaluate some phenazine derivatives of the above cited BXLs. This study was carried out through a collaboration with the laboratory of Professor G. Piccialli (University of Naples). The BXLs **36**, **38**, **39**, **61**, and the related phenazines **69**, **71**, **73**, **74** and **75** were sent to the laboratory of prof. G. Piccialli at the University of Naples (Department of Chemistry of Natural Substances, "Federico II" University, Naples) to study the possible interaction of our compounds with G-quadruplex DNA. More specifically, the compounds under study were evaluated through spectroscopic techniques for their capability to recognize and specifically bind G-quadruplex DNA structures. Compounds **36**, **38**, **39**, and **61** were firstly evaluated, in a preliminary spectroscopic evaluation of their capability to recognize and specifically bind G-Quadruplex. The possible conformational change of the G4 structure induced by the interaction with these compounds was examined by CD spectroscopy in the presence of K^+ buffer (**Figure 14**). The profiles show a strong positive band around 264 nm and a negative peak at 240 nm, even in the presence of the ligands. However, a reduction of the intensity was observed at 264

nm, after the addition of increasing amounts of BXLs **36**, **38**, **39** and **61** suggesting a destabilization of the G-Q structure.

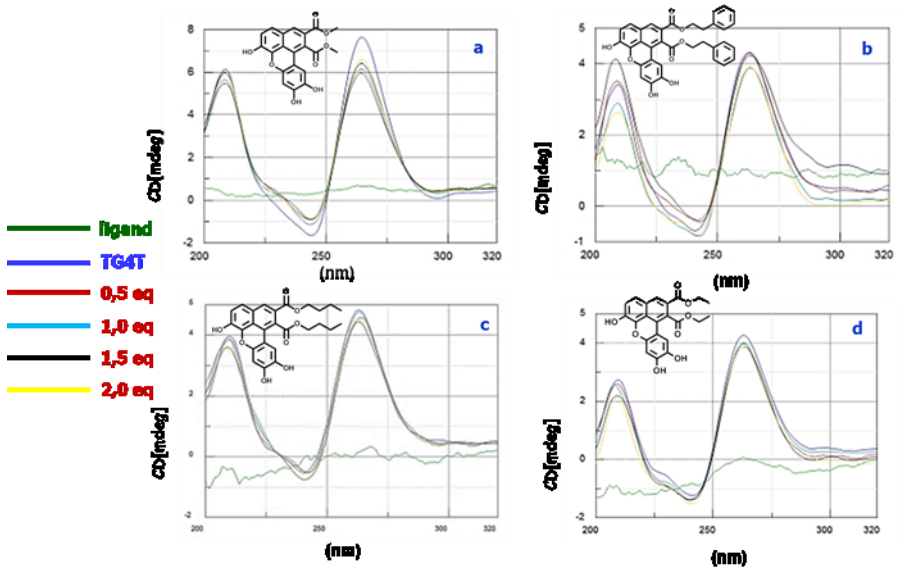

Figure 14*:* CD titration of d($^{5'}$TGGGGT$^{3'}$)$_4$ in the presence of **36** (**a**), **38** (**b**), **39** (**c**), **61** (**d**)

Subsequently, the same compounds were evaluated in the G-quadruplex denaturation experiments. The CD melting spectra, of d($^{5'}$TGGGGT$^{3'}$)$_4$ + 1:2 of each evaluated compound, are reported in **Figure 15** (respectively **a** (**36**), **b** (**38**), **c** (**39**) and **d** (**61**)), show a clear sigmoidal curve at 264 nm, suggesting a destabilization of G-Q[127] and consequently confirming the above esperiments. Nevertheless, no denaturation is observed for d($^{5'}$TGGGGT$^{3'}$)$_4$ in the presence of 2 equivalents of **36** (**Figure 15a**), and this result suggests an interaction with G-quadruplex structures.

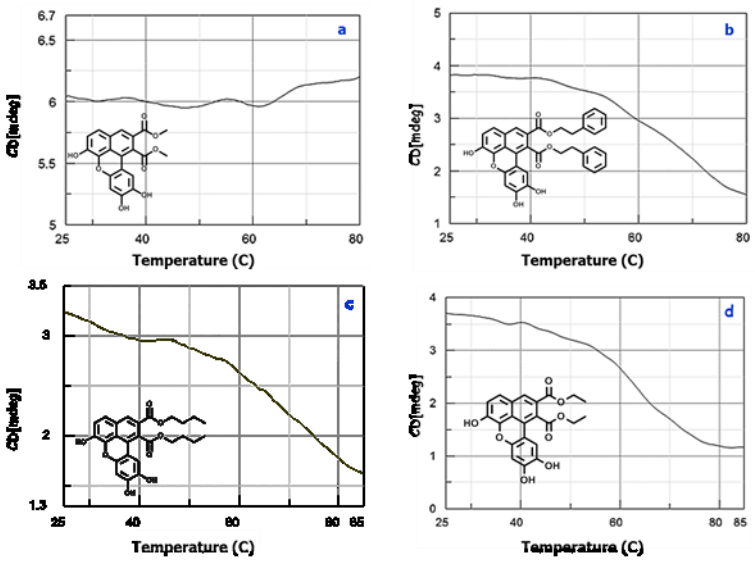

Figure 15: CD-melting curves of d($^{5'}$TGGGGT$^{3'}$)$_4$ + **36** 2 equiv. (**a**), **38** 2 equiv. (**b**), **39** 2 equiv. (**c**), **61** 2 equiv.(**d**).

Finally the fluorescence experiments show an increase of the intensity for both **36** and **61** (**Figure 16**), in presence of the TG4T; the observed results may be ascribed to a different kind of interaction, for example groove ligand/G4 structure. Furthermore these results suggest that when the ligands interact with the G-quadruplexes, proton transfer can occur easily.[128]

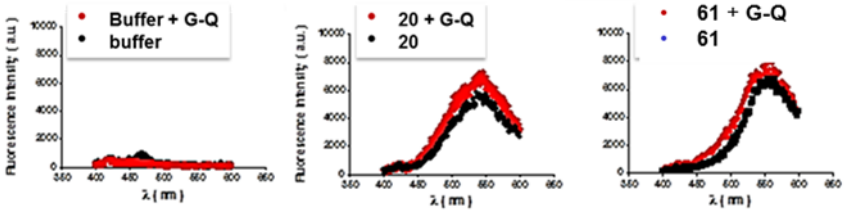

Figure 16: fluorescence emission spectra of d($^{5'}$TGGGGT$^{3'}$)$_4$ alone, d($^{5'}$TGGGGT$^{3'}$)$_4$ + **36**, d($^{5'}$TGGGGT$^{3'}$)$_4$ + **61**.

Based on these partly encouraging results, we planned as second step of this study to evaluate the binding abilities of the benzoxanthene phenazines in comparison with the parent lignans **36**, **38**, **39** and **61**. Thus,

also these compounds were evaluated from Prof. Piccialli, for their interaction with G-quadruplex. Our compounds were subjected to a spectroscopic evaluation of their capability to recognize G-quadruplex and the possible conformational change of the G4 structure induced by the interaction with **69**, **71**, **73**, **74** and **75**; the experiments were carried out in the same conditions used for the first group of ligand: CD titration of d(5'TGGGGT3')4 in the presence of each compounds (**Figure 17**), and their CD melting experiments (**Figure 18**).

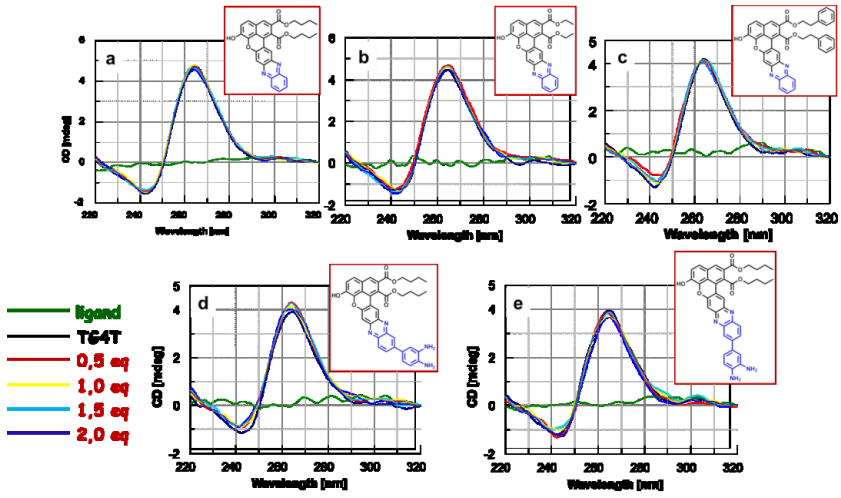

Figure 17: CD titration of d(5'TGGGGT3')4 in the presence of **69** (**a**), **71** (**b**), **73** (**c**), **74** (**d**), **75** (**e**).

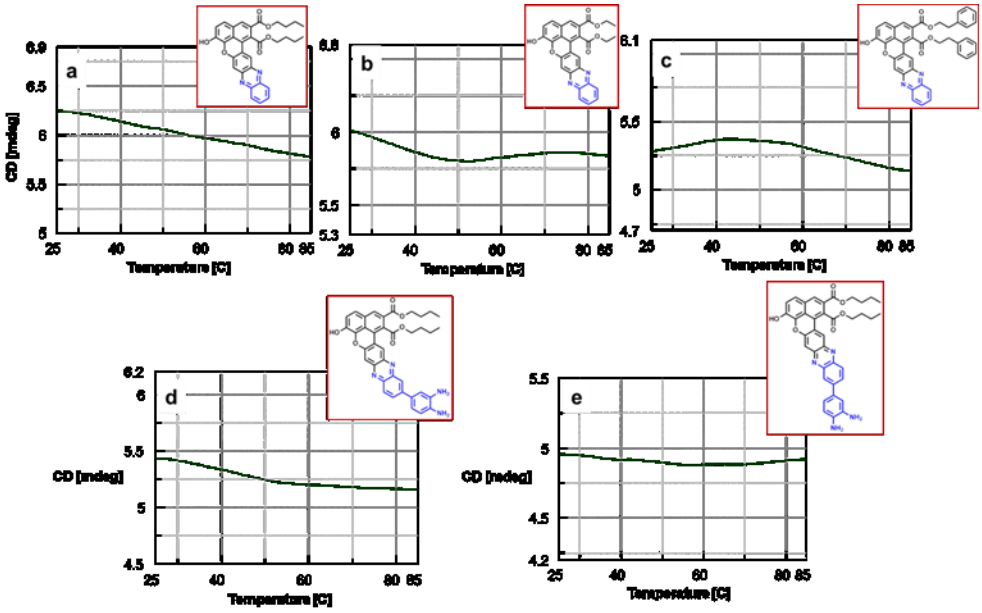

Figure 18: CD melting of d(5'TGGGGT3')4 in the presence of **69** (**a**), **71** (**b**), **73** (**c**), **74** (**d**), **75** (**e**).

Unfortunately, these experiments show that the phenazine derivatives of benzoxanthene lignans are not able to interact with G-quadruplex structures. A possible explanantion of this result is that, despite their extended planar moiety and asymmetric structure, benzoxanthene phenazines lack of basic functional groups that can increase interaction with DNA, how suggested by the literature.[129] Furthermore this result confirms that, as highlighted in previous studies on DNA interaction,[65] the catechol moiety of benzoxanthene lignans is important for the interaction with G-Q.

In conclusion, this preliminary study strongly suggests that the catechol portion of the unmodified benzoxanthene lignans (**36**, **38**, **39** and **61**) is very important for the recognition of G-Quadruplex. In this regard, as a possible continuation of this study could be interesting to plan the synthesis of new benzoxanthene lignans decorated with flexible pendants

at C-1' and C-2' bearing basic functional groups, with the aim to obtain a selective interaction with G-Q, possibly involving the groove/loop interactions.

2.1.4 Study of the interaction of benzoxanthenes with Bile receptors

The scarce number of data reported in literature about the potential biological activity of the rare benzoxanthene lignans, prompted us to evaluate them also as potential agonist/antagonist of bile receptors (BAR), a family of nuclear receptors involved in regulation of several metabolic processes, including cholesterol metabolism, that have recently been indicated as targets for development of new drugs for the treatment of chronic liver disease, hepatocellular cancer and extrahepatic inflammatory and metabolic diseases.[130] In particular, many research studies point to discover new selective ligands for the intracellular nuclear receptor farnesoid X receptor (FXR).[131] FXR is more expressed in the liver, and the natural ligand are bile acids, in particular the primary bile acids and their conjugate like chenodeoxycholic acid (CDCA) that is obtained from the cholesterol catabolism. Several studies have demonstrated an important role of FXR in the regulation of bile acids absorption, synthesis, and secretion in the intestine, liver, and kidney; for this reason it is considered a promising target in cholestasis, a liver disorder that occurs primarily in the context of genetic mutation of basolateral or apical membrane transporters in hepatocytes and that is the main biochemical feature of primary biliary cirrhosis and and sclerosing cholangitis.[132] It is known that FXR can be activated by a number of compounds not structurally related to bile acids.[130] Thus, we planned to test BXLs as potential FXR ligands. We started with a preliminary investigation on the benzoxanthenes **36**, **61**, **67** and the BXL-related phenazines **69**, **71** and **73**, in collaboration with Prof. A. Zampella (University of Naples) and Prof. S. Fiorucci (University of Perugia). The above cited compounds were tested on FXR and on LXRa/b, in a

luciferase reporter assay using HepG2 cells, which were previously transfected with responsive elements for FXR and LXRα/β, respectively, cloned upstream to the luciferase gene. CDCA (10 mM) and GW3965 (10 μM) were used as positive controls for FXR and LXRs transactivation, respectively.

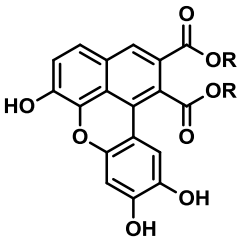

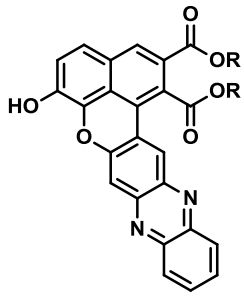

36 = CH_3
61 = CH_2CH_3
70 = $CH_2CH_2CH_2CH_2OH$

69 = $CH_2CH_2CH_2CH_3$
71 = CH_2CH_3
73 = $CH_2CH_2CH_2Ph$

Figures 19 and **20** report the results of FXR and LXRs assays. Unfortunately, none of the compounds were able to transactivate FXR and LXRs on HepG2 cells. Of interest, compounds **73** and **69**, when administered in presence of 10 μM CDCA (**Figure 19**, panel b), showed inhibitory activity against FXR transactivation induced by its endogenous ligand CDCA. Both compounds are phenazines, and are related to the most lipophilic BXLs (see Section 1.1.3). These data are encouraging, and we have already planned to test further compounds; in particular, the assay on BXL **38** (related to **73**) should confirm that the phenazine portion is an important structural determinant for the antagonist action.

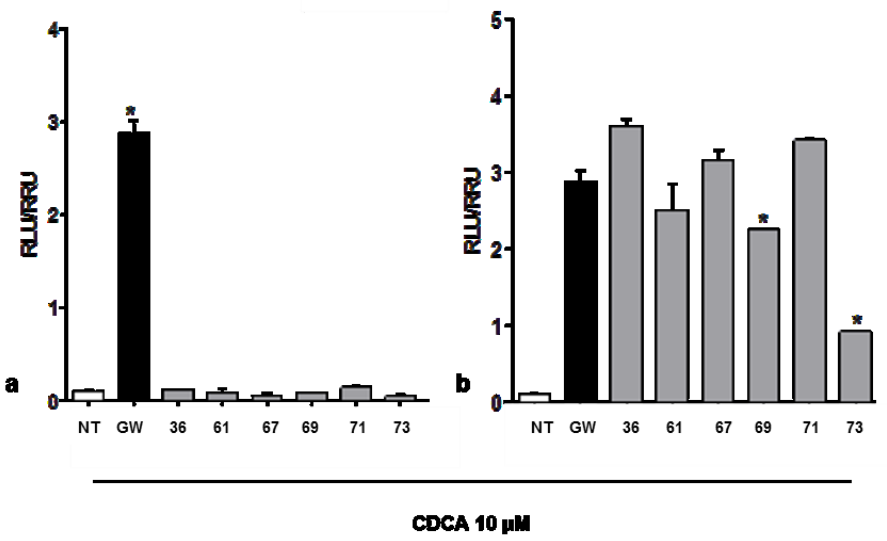

Figure 19: **Transactivation assays on FXR**. A) HepG2 cells were transfected with pSG5-FXR, pSG5-RXR, pCMV-βgal, and p(hsp27)TKLUC vectors. Cells were stimulated with compounds **36**, **60**, **67**, **69**, **71**, **73** (10 µM). CDCA (1, 10 µM) was used as a positive control. Results are expressed as mean ± standard error; *p <0.05 versus not treated cells (NT). B) HepG2 cells were stimulated with 10 µM CDCA alone or in combination with 50 µM compounds **36**, **61**, **67**, **69**, **71**, **73**. *p<0.05 *versus* CDCA stimulated cells.

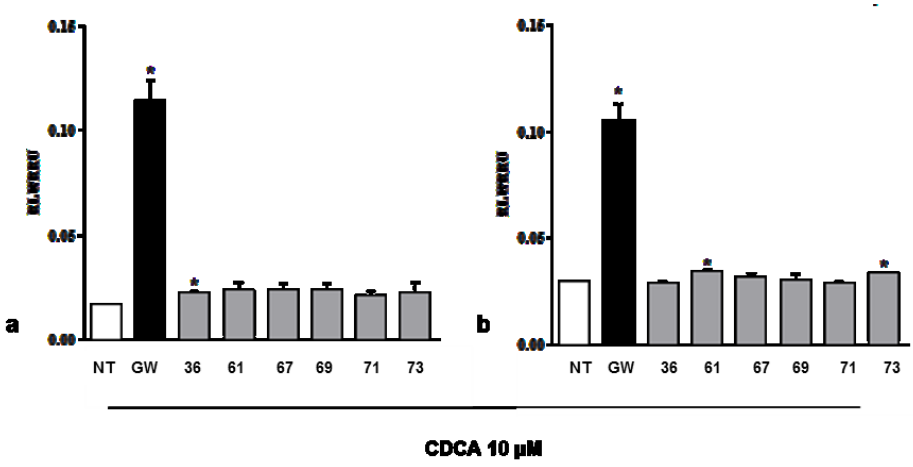

Figure 20: **Transactivation assays on LXRs.** HepG2 cells were co-transfected with the Gal4 luciferase reporter vector and with a chimera in which the Gal4 DNA binding domain is fused to the LBD of LXRα (panel A) or LXRβ (Panel B), and stimulated 18 h with GW3965 (10 µM), a LXR agonist, or with compounds **36, 61, 67, 69, 71, 73** 10 µM. Results are expressed as mean ± standard error; *p <0.05 versus not treated cells (NT).

2.1.5 Study of the antimicrobial properties of benzoxanthenes

Recently, there is an urgent need to develop new classes of antimicrobial agent to contrast the microbial resistance towards the most commonly used drugs.[133] It's well known that plants have an immune system able to prevent their infection from most of microorganisms including oomycetes and fungi.[134] This potential self-defense includes the production of secondary metabolites with antimicrobial activity, biosynthesized mainly in response to biotic or abiotic stresses.[135] For these reasons, there is a growing trend in the search for new antimicrobial drugs, and many research groups are studying the potential activity of natural compounds and their synthetic analogues with the aim to develop new antimicrobial agents. Benzoxanthenes lignans are good candidates for this kind of study because of the scarcity of literature data on this class of rare natural products, and specially on their antimicrobial activity, the only exception being a citation on the natural lignan rufescidride.[64] Thus, as a continuation of our investigation of compounds inspired by natural polyphenols, we started a collaboration with Prof. G. Tempera (University of Catania) aimed to the evaluation of a series of benzo[*k,l*]xanthene lignans, namely the compounds **38**, **43**, **61**, **63**, **65** (these latter two synthetized for the first time within this project), **67** and the above cited phenazine **69** as potential antimicrobial agents; namely, these compounds were assayed against eight gram-positive and eight gram-negative bacteria and twenty different *Candida* spp. strains (namely, 13 *C. albicans* strains and 7 *C. non-albicans* strains), isolated in a nosocomial environment.

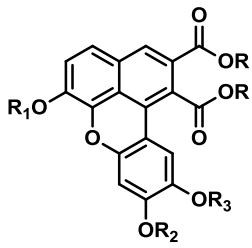

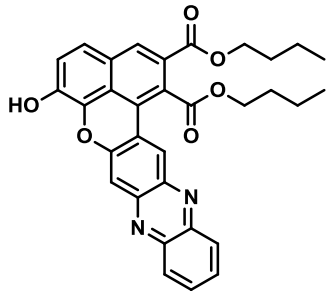

69

38 = CH_2CH_2Ph R_1= H R_2 = H R_3 = H
43 = CH_2CH_2Ph R_1= Me R_2 = Me R_3 = Me
61 = CH_2CH_3 R_1= H R_2 = H R_3 = H
63 = $CH_2Ph(OMe)$ R_1= H R_2 = H R_3 = H
65 = CH_2Ph R_1= H R_2 = H R_3 = H
67 = $CH_2CH_2CH_2CH_2OH$ R_1= H R_2 = H R_3 = H

Preliminary antibacterial assays were carried out on compounds **61**, **67**, and **69**; unfortunately all the tested compounds were only very poorly active, showing MIC (minimum concentration inhibiting the 50% growth) values respectively higher than 85.5 μM (**60**), 94.3 μM (**67**), and 42.4 μM (**69**); thus, BXLs were not further evaluated as antibacterial agents.

The data on antimycotic activity are more interesting: in **Table 1** the MIC values for benzoxanthenes **38**, **43**, **61**, **63**, **65**, **67** and the phenazine **69** are reported using fluconazole (**FLU**), a well-known antifungal drug as positive reference compound. Usually, the MIC value for fluconazole is defined as the minimum concentration inhibiting the 50% of fungal growth, and the measurements observed for the tested compounds are compared with that of the control. This antimicotic assay is based on a spectrophotometric determination of fungal growth at 490 nm. It is worth noting here that a number of *Candida* strains were resistant to fluconazole drug in the concentration range employed, consequently no MIC value is reported in **Table 1** (entries 2, 4, 5, 13, 15 and 19).

Two compounds, **38** and **67**, show promising antimycotic activity being able to inhibit the fungal growth of the majority of *Candida* fungal strains with MIC values in the range 4.6 - 19.2 μM and 26.0 - 104.3 μM respectively for **38** and **67**. In three cases (see entries 3 and 17 for **38** and 12 for **67**) the MIC values were lower than those obtained for fluconazole; in two further cases (entries 2 and 4) **38** (MIC = 19.2 μM) and **67** (MIC = 52.1 μM) were active at least on one resistant strain.

Table 1: MIC of **38**, **43**, **60**, **63**, **65**, **67** and **69** towards *Candida* fungal strains

		MIC (μM)							
Entry	**strain**	**38**	**43**	**61**	**63**	**65**	**67**	**69**	**FLU**
1	*C. albicans*	19.2	-	-	-	-	104.3	-	1.6
2	*C. non-albicans*	19.2	-	-	11.7	-	52.1	-	-
3	*C. non-albicans*	9.5	-	48.7	5.8	2.8	104.3	1.3	13.0
4	*C. non-albicans*	19.2	-	-	11.7	-	-	-	-
5	*C. albicans*	-	-	-	-	-	-	-	-
6	*C. albicans*	-	-	-	-	-	-	-	0.81
7	*C. albicans*	19.2	-	-	-	-	104.3	-	6.5
8	*C. non-albicans*	-	-	-	-	-	-	-	52.2
9	*C. albicans*	-	-	-	-	-	-	-	1.6
10	*C. albicans*	-	-	97.5	-	-	104.3	-	3.2
11	*C. albicans*	-	-	-	-	-	-	-	6.5
12	*C. non-albicans*	-	-	-	-	-	52.1	-	52.2
13	*C. albicans*	-	-	-	-	-	-	-	-
14	*C. albicans*	-	-	-	-	-	-	-	6.5
15	*C. non-albicans*	-	-	-	-	-	-	-	-
16	*C. albicans*	9.5	-	-	-	-	52.1	-	3.2
17	*C. albicans*	4.7	-	12.9	5.8	5.6	26.1	-	6.5
18	*C. albicans*	9.5	-	-	-	-	104.3	-	6.5
19	*C. non-albicans*	-	-	-	-	-	-	-	-
20	*C. albicans*	19.2	-	-	-	-	104.3	-	3.2

The other compounds, in the concentration range tested, were inactive or selectively active only towards a few strains. However, especially worth noting is that compounds **63**, **65** and **69** showed MIC values lower than that of fluconazole. In particular, **63** , is active against four strains (entries 2, 3, 4 and 17), including two resistant strains, and showed MIC values in the range 5.8 - 11.7 μM; **65** is active only against two strains (entries 3 and 17), showing MIC values of 5.6 μM on *C.*

albicans and 2.8 μM on *C. non-albicans*; finally, **69**, although active only towards one strain (entry 3) was one order of magnitude more potent (MIC = 1.3 μM) than fluconazole (MIC = 13.0 μM) Although on the basis of the present data it is not possible to establish general structural determinants for the antimycotic activity of BXLs, it is worth noting that the comparison between **38** (mostly active) and its methylated analogue **43** (inactive) suggests that the catechol moiety is important for growth inhibition of *Candida* Considering the difficulty to find new and effective antimycotic agents, these results are promising and suggest to extend this study on further BXLs models, in particular related to the very potent phenazine **69**.

2.2 Biomimetic synthesis of dimeric neolignans inspired by magnolol and their biological activities

Based on the data reported in the Introduction (1.1.4), about the biological properties of magnolol (**44**) and its analogs, one of my research goal was the chemo-enzymatic synthesis of a series of bisphenols inspired by magnolol (**44**). Magnolol itself was used as substrate, and I report here, for the first time, the IBX-mediated *ortho*-selective hydroxylation of **44**; subsequently, this method was applied to other bisphenols obtained through enzymatic dimerization of simple natural phenols, in order to obtain the corresponding catechol derivatives. All the compounds here reported were purified and spectroscopically characterized. Although these compounds were synthetized to be evaluated firstly as potential yeast α-glucosidase inhibitors; by collaboration with other laboratories magnolol related compounds were also evaluated as:

- Chain-breaking antioxidant
- Inverse Virtual Screening and related biological evaluations
- ABCG2 inhibitors (MDR)

In the following, the details are discussed.

2.2.1 Chemoenzymatic synthesis and selective hydroxylation of dimeric neolignans inspired by magnolol

Natural or natural-derived catechols are frequently reported as promising bioactive compounds, and in particular their antioxidant activity is higher than that of their monohydroxylated or *meta*-dihydroxylated analogues;[136] hence, we planned to get bisphenols both with monohydroxylated aromatic moieties and with catechol substructures. As starting material we used, in addition to magnolol (**44**), other natural monomeric phenols, namely eugenol (**76**), an allylphenol isolated from *Eugenia aromatica* and other plants,[137] tyrosol (**77**), a phenol found in a variety of plants and in olive oil,[138] and the dopamine metabolite, homovanillic alcohol (**78**).[139] As detailed in the subsequently sections, in this first study on magnolol-derived neolignans we also converted tyrosol (**77**) and homovanillic alcohol (**78**) into their alcoholic acetates **79** and **80**, employed as substrates for dimerization reactions; these acetylated dimers could be treated with IBX without possible oxidation of the $-CH_2OH$ group, as suggested by literature reports.[140]

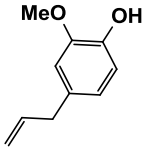

76

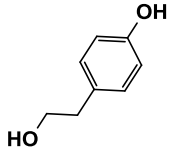

77

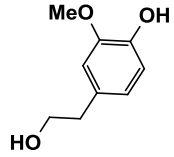

78

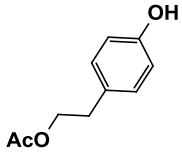

79

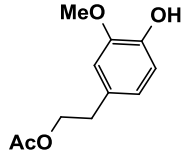

80

To obtain magnolol related compounds, I employed a two-step methodology, namely enzymatic dimerization of monomeric

phenylpropanoids (C6C3) followed by IBX-mediated regioselective hydroxylation of magnolol (**44**) and the related dimers, as reported in detail in the subsequently sections. As discussed in the introduction (1.1.2), the enzymatic dimerization of phenolic compounds through oxidative coupling is currently employed in biomimetic, eco-friendly synthesis of lignans and neolignans, and this methodology has previously been employed to obtain bioactive dimeric compounds related to resveratrol,[141] as well as to *p*-coumaric, ferulic and caffeic acid.[142, 143] 2-Iodoxybenzoic acid (1-hydroxy-1oxo-1*H*-1λ^5-benz[d][1,2]iodoxol-3-one, in the following, simply IBX) is a versatile and environmentally benign[144] reagent of hypervalent iodine, with an increasing number of applications in recent years,[145] firstly prepared by Hartmann and Mayer[146] and then by Santagostino et al. with a safe procedure;[147] when combined with an *in situ* reduction of the products, IBX allows regioselective *ortho* hydroxylation[148] of phenols with free *ortho* position and the selective *ortho* demethylation of phenolic methyl aryl ethers (**Scheme 12**). Thus IBX has been employed fruitfully to rapidly obtain *ortho*-dihydroxylated analogues, with a selectivity similar to that mediated by enzymes in nature.[149] This procedure is generally more convenient than alternative methods requiring the use of metal oxidants environmentally unsafe, hard reaction conditions and affording unsatisfactory yields of products.[150]

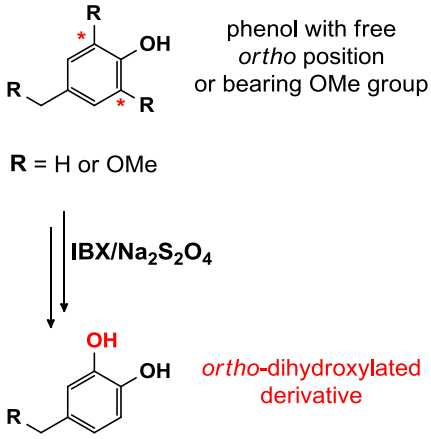

Scheme 12

2.2.1.1 IBX in the simple synthesis of catechol compounds

As above discussed, I planned to employ IBX (1-hydroxy-1-oxo-3H-1λ^5,2-benziodaoxol-3-one), a reagent reported as potentially explosive; actually, it was later found that one sample, cited in the literature, was contaminated with residual bromine which is likely to have contributed significantly to this negative feature.[151] It has also been shown that the oxidative hydroxylation mediated by IBX is regioselective for the *ortho*-position of phenols; in fact phenols with *ortho* position free may be easily converted into the corresponding *ortho*-quinones that under conditions of reductive reaction allow easy access to the catechol group. This reagent through a phenolic '*umpolung*' allows to convert a nucleophilic phenol in an electrophilic species; this allows the delocalization of a positive charge in the *ortho* and *para* position to the phenol, so these positions become susceptible to the attack of a nucleophilic species (**Scheme 13**).[152]

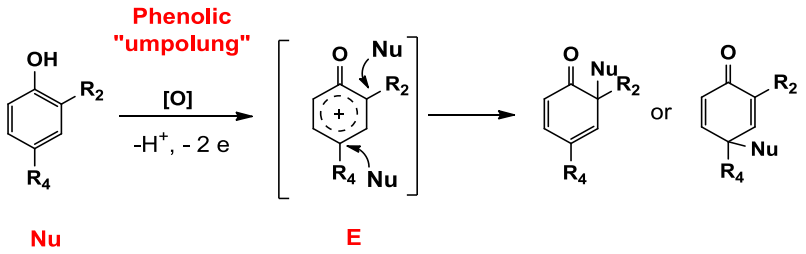

Scheme 13

Some aspects of the proposed reaction mechanism are still not fully understood. In this regard it is very important the work of Pettus and co-workers;[148] as reported in **Scheme 14**, in which the proposed mechanism provides an initial ligand-exchange between IBX (electrophile) and the *O* of the phenol (nucleophile) with simultaneous elimination of a molecule of H_2O, to give as product a phenyloxy-Λ^5-iodanil (**A**). This species undergoes a sigmatropic rearrangement, which enables the formation of a new carbon-oxygen bond in the *ortho* position, with simultaneous reduction of iodine (V) to iodine (III).

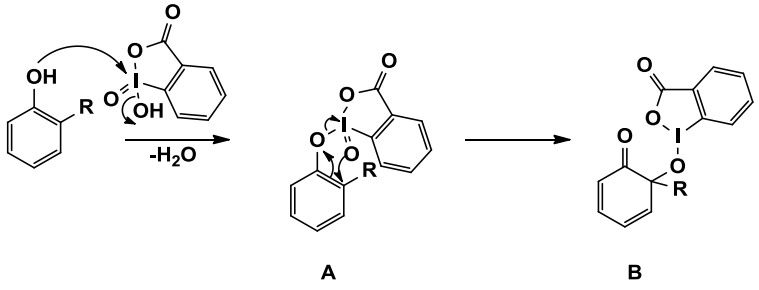

Scheme 14

The intermediate (**B**) evolves in a different way depending on the substitution pattern of the original substrate. In fact, if the *ortho*-position is not substituted, an *ortho*-quinone is obtained; generally this quinone undergoes an *in situ* reduction to afford a catechol product (**Scheme 15**).

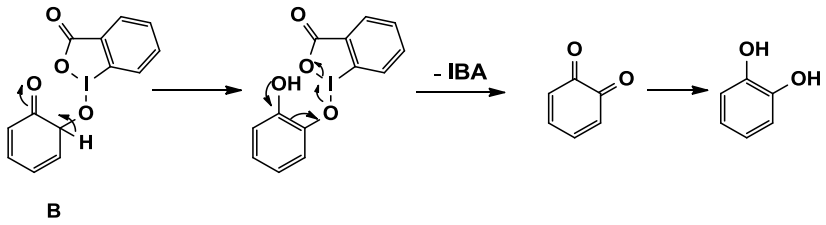

Scheme 15

If an *ortho*-methoxy group is present with respect to the free hydroxyl, the reaction with IBX/SIBX evolves with a different mechanism and afford a demethylated *ortho*-dihydroxy product (**Scheme 16**).

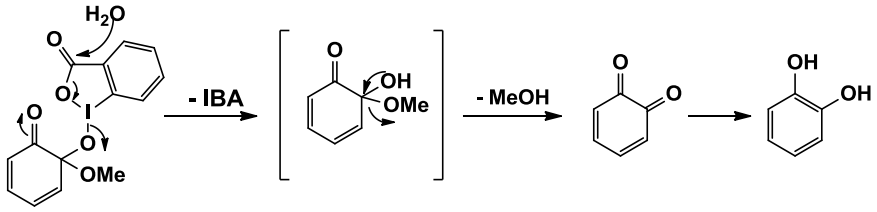

Scheme 16

*2.2.1.2 Selective hydroxylation of magnolol (**44**) mediated by IBX*

Firstly we employed magnolol (**44**) as substrate for a preliminary study of the regioselective hydroxylation procedure mediated by IBX, followed by *in situ* reduction with $Na_2S_2O_4$, according to the methods reported in the literature[153] (**Scheme 17**). This reaction could afford, in principle, both the mono- and the dihydroxylated products, respectively **81** and **82**.

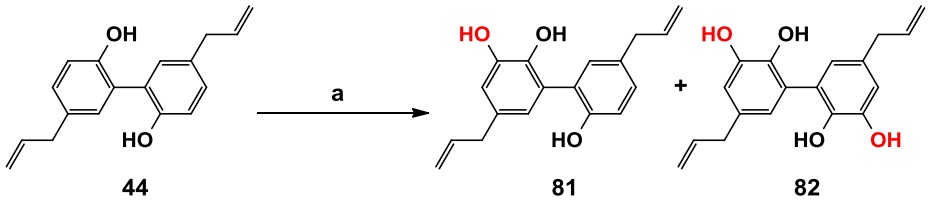

Scheme 17: conditions: (a) MeOH, IBX (1.2 eq.), 0 °C, 30 min; $Na_2S_2O_4$ solution (H_2O), rt, 10 min.

The plausible mechanism for the oxidative conversion of magnolol (**44**) mediated by IBX through iodine (V) is reported in **Scheme 18**. According to the above illustrated mechanism, magnolol (**44**) adds to the iodine (V) center of IBX to form a λ^5-iodanil intermediate (**A**) with elimination of H_2O, then an intramolecular (and regioselective) delivery of an oxygen from the λ^5-iodanyl moiety leads to a more stable λ^3-iodanil intermediate (**B**) which undergoes tautomerization and oxidatively collapses to produce an *ortho*-quinone derivative (**83**) and 2-iodobenzoic acid (**IBA**), the only by-product of this reaction. The reaction proceeds with the same mechanism also on the other ring. The catecholic moieties are finally obtained after the *in situ* reductive step by treatment with $Na_2S_2O_4$, thus affording the products **81** and **82**.

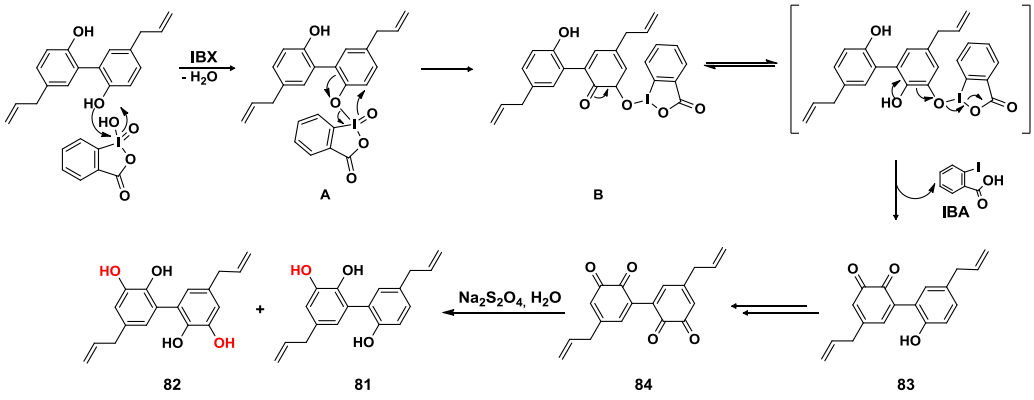

Scheme 18

We performed a preliminary screening of selective hydroxylation of **44** with IBX, employing different reaction conditions, that is varying solvent, concentration of substrate, reaction time and temperature as reported in **Table 2**.

Table 2: Optimization of the *ortho*-selective hydroxylation of **44**

Entry	equiv. IBX	Solvent	*T* (°C)	Time	% of 81[a]	% of 82[a]
1[b]	1.2	DMSO	rt	2 h	<1	<1
2[b]	1.5	DMSO	rt	4 h	<1	0[d]
3[b]	2.1	DMSO	rt	2 h	<1	0[d]
4[b]	1.5	DMF	rt	4 h	1.1	2.1
5[b]	2.1	DMF	rt	2 h	<1	<1
6[c]	1.2	MeOH	rt	40 min	7.1	6.9
7[c]	1.2	MeOH	0	30 min	14.3	11.3
8[c]	2.1	MeOH	0	30 min	2.5	8.1

[a]The yield was determined by HPLC-UV. [b] [**44**] = 0.1 M; [c] [**44**] = 0.2 M; [d]not obtained.

The two main products are here indicated as **81** and **82**, as confirmed by their isolation and spectral analysis, reported below for a preparative scale reaction. The experiments carried out in DMSO (entries 1-3) and DMF (entries 4 and 5) gave unsatisfactory results, and despite showing a high conversion of the substrate a mixture of low-yield products was obtained, even working with excess of IBX (1.5 and 2.1 equiv) or at 80°C. The reaction was then carried out in methanol (MeOH) at room temperature, employing 1.2 equiv of IBX (entry 6): after 40 min two main products, more polar than **44**, and subsequently characterized as **81** and **82**, were formed. Further reactions were carried out, in the same solvent, at 0 °C with 1.2 (entry 7) or 2.1 (entry 8) equiv of IBX. The former conditions allowed a high conversion rate (>95%), and the two main products, **81** and **82**, were obtained with 14.3% and 11.3% yield, respectively, whereas a greater amount of IBX significantly lowered their yields. Furthermore, on prolonging the reaction time up to 1 h, no

improvement of the yields was observed; thus 30 min was confirmed as the best reaction time. In **Figure 21** the HPLC profiles of reactions carried out at different time intervals in MeOH at 0 °C are reported. Through these experiments, we found that 30 min at 0 °C were the best conditions, giving an almost complete conversion of the substrate and the higher yields of the two main products.

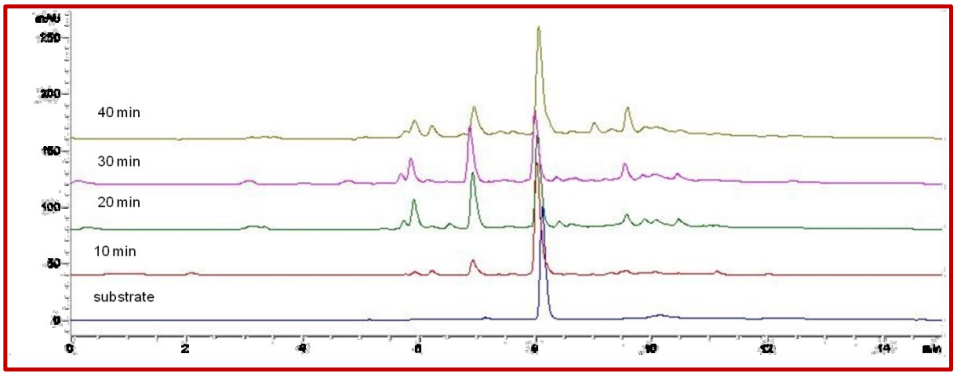

Figure 21: HPLC profiles of reaction of [**44**] = 0.2 M, with IBX (1.2 equiv,) in MeOH at 0 °C at different time intervals.

Based on the above results, we proceeded in *macro* scale using these conditions as detailed in the following.

*2.2.1.2.1 Synthesis of compounds **81** and **82***

Magnolol (**44**) was treated with IBX in MeOH according to **Scheme 17** and maintained at 0°C for 30 min. After the *in situ* reduction with $Na_2S_2O_4$, a reaction mixture showing two main products on TLC was obtained; after purification on DIOL Silica-gel, this afforded two main products **81** and **82**, more polar than the substrate, obtained respectively with 18.5% and 14.4% yields. These products were subjected to spectral analysis. The ESIMS spectrum (**Figure 39S**, in **Appendix C**) of the least polar product **81,** gave an $[M-H]^-$ peak at *m/z* 281.1, 16 amu higher than the mw of **44**, suggesting a monohydroxylation of magnolol. The ^1H and

^{13}C NMR spectra of **81**, reported respectively in **Figures 40S** and **41S**, in comparison with those of magnolol (**44**), show doubled ^{1}H and ^{13}C NMR signals, clearly due to the loss of symmetry. In detail, the ^{13}C NMR spectrum (**Figure 41S**) showed two sp^3 methylene signals (39.7, 39.4 ppm), two sp^2 methylene signals (115.9, 115.9 ppm) seven sp^2 methyne signals (137.7, 137.5 ppm) and seven signals attributable to quaternary carbons (150.4, 145.2, 138.8, 134.0, 133.6, 125.1, 124.5 ppm), three of which are in the range 150.4 – 138.8 ppm typical for oxygenated carbons. In the 500 MHz ^{1}H NMR spectrum (**Figure 40S**), two *meta*-coupled signals at 6.66 (1H, d, J = 2.0 Hz) and 6.80 (1H, d, J = 2.0 Hz) ppm were assigned respectively to H-4 and H-6 of the dihydroxylated ring A. The proton signals of one allyl chain were observed at 3.32 (H_2-7), 5.97(H-8) and 5.06 (H_2-9) ppm, and assigned through analysis of gCOSY, gHSQCAD and gHMBCAD spectra (**Figures 42S**, **43S** and **44S**). Key HMBC correlations are reported in **Figure 22**, allowing to unambiguously assign all the quaternary carbon resonances, and to discriminate the signals related to the different chains. In particular, the heteronuclear correlation of C-5 with H-6 and H-7 allowed to identify the chain linked to C-5 as the ring A pendant. The remaining signals in the spectrum of **81** were clearly resembling those of magnolol (**44**), namely an AMX system was observed at 6.91 (d, J = 8.5 Hz, H-3'), 7.10 (dd, J = 8.5, 2.0 Hz, H-4') and 7.13 ppm (d, J = 2.0 Hz, H-6') clearly due to the monohydroxylated ring B, and assignments of the ring B pendant at 3.37 (H_2-7'), 5.96 (H-8') and 5.06 (H_2-9') ppm were confirmed by two-dimensional NMR spectra. The complete list of NMR assignment is reported in the Experimental section.

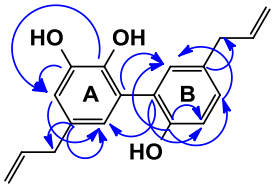

51

Figure 22: Key HMBC correlations

ESI-MS of the most polar compound **82** gave an [M−H]− peak at *m/z* 297.1, suggesting a dihydroxylation of **44**. Unlike from **81**, the ^{1}H and ^{13}C NMR spectra of **82** respectively reported in **Figures 45S** and **46S** (see **Appendix C**), indicated that the symmetry of magnolol has been maintained; a literature search confirmed the structure of 3,3'-dihydroxymagnolol through the perfect agreement of ^{1}H and ^{13}C NMR data, with those previously reported for **82**.[83]

2.2.1.3 Preliminary study of the synthetic route to magnolol-inspired compounds

Based on the above encouraging results on magnolol (**48**), we firstly considered two alternative methodologies to obtain a small library of magnolol-inspired bisphenols: the first is based on the treatment of the monomeric phenolic compound (**A**) with IBX/$Na_2S_2O_4$, followed by an enzyme-mediated oxidative coupling of the catechol **Ba** to afford the tetrahydroxylated dimer **C** (**Scheme 15a**); the second involves an initial enzymatic coupling of phenol **A** to give the intermediate dimer **Bb**, followed by the reaction with IBX/$Na_2S_2O_4$, providing the dimer **C** (**Scheme 15b**).

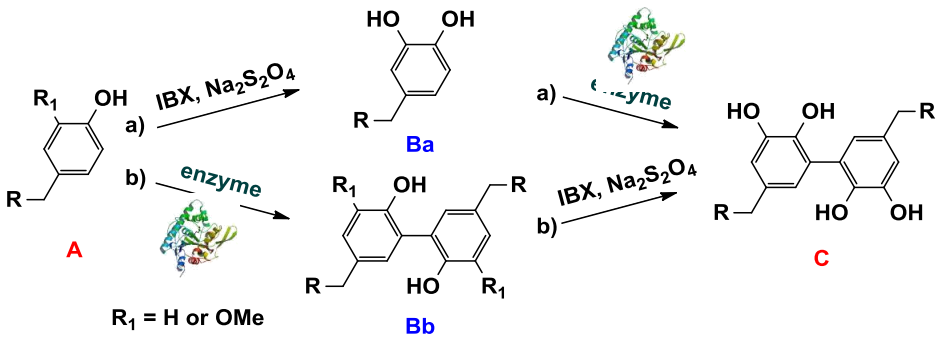

Scheme 19

2.2.1.3.1 Preliminary study on synthetic route a

We employed eugenol (**76**), a commercially avaible natural phenol, as substrate for the first experiments. In agreement with the general **Scheme 19a**, in a first step **76** was subjected to a preparative demethylation reaction with IBX followed by reduction with $Na_2S_2O_4$ (**Scheme 20**). After purification, the main product **83** was obtained with a good yield (70%); its ESI-MS and ^{1}H NMR data were identical to those previously reported for hydroxyeugenol.[153]

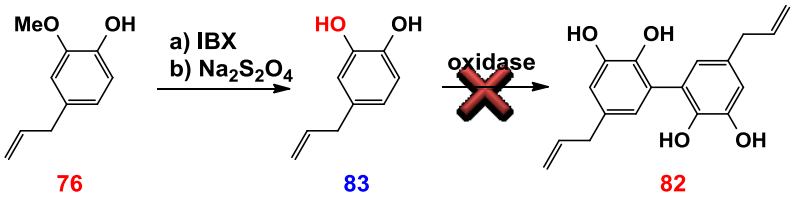

Scheme 20: conditions:(**a**) THF, IBX (1.5 eq.),rt,3 h; $Na_2S_2O_4$ solution (H_2O), rt, 10 min. (**b**) MeOH, HRP (acetate buffer, 0.1 M, PH 5.0), H_2O_2, rt,2 h;

In a second step, the catechol **83** was used as substrate for a preliminary screening of the dimerization reaction carried out employing different enzymes, namely horseradish peroxidase (HRP) and laccases from the basidiomycetes *Agaricus bisphorus* (AbL), *Pleurotus ostreatus* (PoL), and *Trametes versicolor* (TvL). The reactions were carried out at

rt; a set of experiments was carried out in a biphasic system using acetate buffer (where the enzyme was solubilised), and ethyl acetate or dichloromethane as co-solvents, while a further set of reactions was done in monophasic system consisting of acetone or MeOH in acetate buffer (**Table 3**).

Table 3: Enzymatic reaction of **76**[a]

Entry[a]	Enzyme	Solvent	Conversion (%)[b]	% of 82[b]
1	TvL	acetone	91.1	5.6
2	TvL	MeOH	87,0	3.3
3	TvL	CH_2Cl_2	89.0	6.4
4	TvL	AcOEt	92.7	3.7
5	PoL	acetone	94.8	6.6
6	PoL	MeOH	79.7	6.7
7	PoL	CH_2Cl_2	97.5	9.7
8	PoL	AcOEt	85.0	9.3
9	AbL	acetone	98.7	9.6
10	AbL	MeOH	87.7	6.7
11	AbL	CH_2Cl_2	46.1	8.4
12	AbL	AcOEt	23.6	6.3
13	HRP	acetone	97.1	8.9
14	HRP	MeOH	96.1	2.1
15	HRP	CH_2Cl_2	61.1	7.3
16	HRP	AcOEt	68.3	9.3

[a] All experiments were carried out with 26 U/mL of each enzyme, [b] Based on quantitative analysis by HPLC-UV of reactions stopped at 4 h.

Notwithstanding the high conversion of **76**, expecially in the presence of TvL and PoL, a number of low-yield products was obtained in all these reactions, an the main product, later identified as **82**, was obtained with low or very low yield (< 10%).

*2.2.1.3.2 Preliminary study on synthetic route b and synthesis of the neolignans **84** and **85***

These unsatisfactory results, described in the previous paragraph, prompted us to try the general method summarized in **Scheme 19b**. Thus, in a first step **76** was used as substrate for a preparative HRP-

mediated dimerization (**Scheme 21**); this reaction has been previously reported in the literature,[88] and was then carried out accordingly, employing HRP/H_2O_2 in methanol/acetate buffer. After purification on DIOL Silica-gel, the reaction mixture afforded one major product (45% yield), subjected to spectroscopic analysis: ^{1}H and ^{13}C NMR (**Figures 47S** and **48S** in the **Appendix C**) data were in perfect agreement with those reported in the literature for the symmetric 1,1'-dieugenol **84**.[154] In a second step, the bisphenol **84** was used as substrate for an IBX-mediated *ortho*–selective demetylation; also for this substrate, we carried out a preliminary screening varying solvent, temperature, reaction time and equivalents of IBX. After *in situ* reduction with $Na_2S_2O_4$, The reactions were monitored by HPLC-UV on a C18 reversed-phase silica gel column and results are summarized in **Table 4**. The reactions carried out in MeOH (entry 1), DMSO (entry 2) and DMF (entry 3), gave a high conversion of substrate **84**, but no significant amount of the expected compounds was detected. When the reaction was carried out in tetrahydrofuran (THF) for 3 h (entry 4), two main products, more polar than the substrate, were formed and subsequently identified as **85** (18.7%) and **82** (10.0%).

Table 4: Optimization of *ortho*-Selective Demethylation of **84**[a]

Entry	IBX (equiv.)	Solvent	*T* (°C)	Time	82(%)b	85 (%)b
1	1.5	MeOH	rt	3 h	<1	<1
2	1.5	DMSO	rt	3 h	1.0	<1
3	1.5	DMF	rt	3 h	1.8	2.1
4	1.5	THF	rt	3 h	10.0	18.7
5	1.5	THF	0	3 h	4.5	9.8
6	1.2	THF	rt	3 h	5.9	12.2

[a] All the reactions were carried out using 0.06 M solution of **84**. [b] The yield was determined by HPLC-UV.

The reaction in THF was monitored at regular time intervals up to 16 h and the quantitative analysis confirmed 3 h as the best reaction time. Further experiments carried out at 0 °C with 1.5 equiv. of IBX (entry 5) and at rt with 1.2 equiv. of IBX (entry 6), afforded **85** and **82** with lower yields. Thus, a preparative reaction of **84** with IBX was carried out in THF at rt for 3 h, followed by in situ reduction with $Na_2S_2O_4$ (**Scheme 21**).

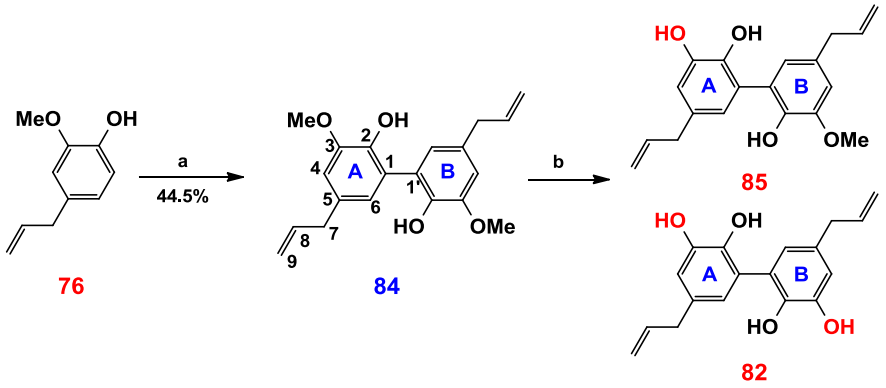

Scheme 21: conditions:(**a**) MeOH, HRP (acetate buffer, 0.1 M, PH 5.0), H_2O_2, rt,2 h; (**b**) THF, IBX (1.5 eq.),rt,3 h; $Na_2S_2O_4$ solution (H_2O), rt, 10 min.

The reaction mixture was chromatographed and the products were purified and subjected to spectral analysis. The least polar product **85** (18,2% yield) showed an ESIMS $[M-H]^-$ peak at *m/z* 311.1, suggesting that only one methyl group had been removed from **84**. Both ^1H and ^{13}C NMR (**Figures 49S** and **50S** in the **Appendix C**) spectra indicated an unsymmetrical structure, and resulted in perfect agreement with those previously reported for 3-demethyl-1,1'-dieugenol **85**.[83] All ^1H and ^{13}C resonances, previously not assigned are reported in the Experimental section. The other main product (14% yield), neatly more polar than **85**, showed ESIMS and NMR data identical to those of 3,3'-dihydroxymagnolol (**82**), as expected for the product of an IBX-mediated

double demethylation reaction. These satisfactory results and the advantage of obtain mono- or dihydroxylation products, thus increasing the structural variety of the projected library prompted us to choose the method summarized in **Scheme 19b** for the synthesis of a series of magnolol-inspired bisphenols. Thus, we carried out firstly the dimerization reactions of the natural phenols **76** - **80** and subsequently the selective hydroxylation/demethylation of these dimeric products, as detailed below in the subsequently section.

*2.2.1.4 Chemoenzymatic synthesis of bis-phenol neolignans **86 - 93***

The chemoenzymatic synthesis of a series of bisphenol neolignans **86** – **93** was carried out according to the general **Scheme 19b**. All reactions discussed in the subsequently sections, are summarized in **Scheme 22**.

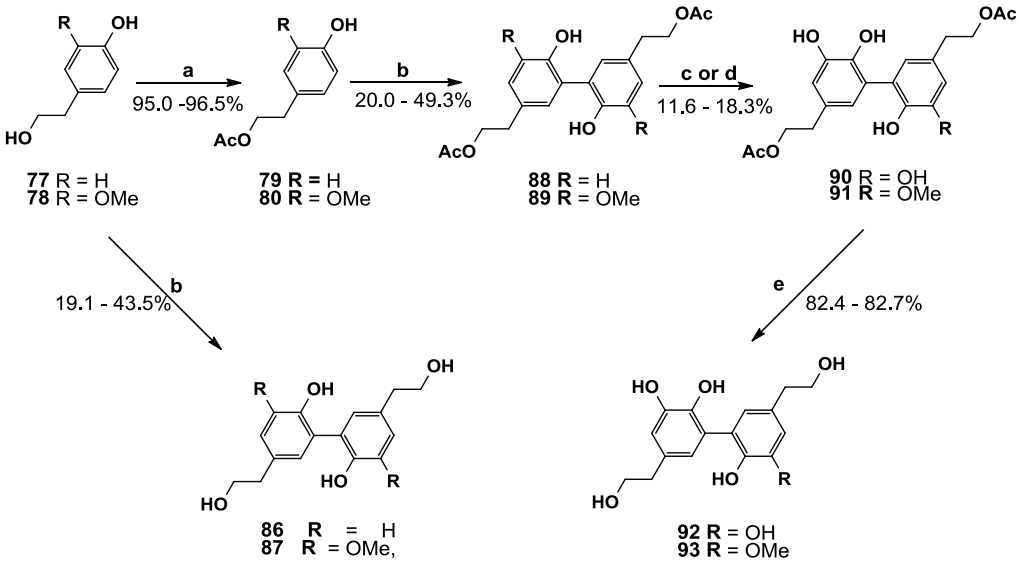

Scheme 22: Condition: (**a**) CaL, vinyl acetate, MTBE, 40 °C, 1 h; (**b**) acetone, HRP solution (acetate buffer, 0.1 M, pH 5.0), H_2O_2, rt, 4 h; (**c**) MeOH, IBX (1.2 eq.), 0 °C, 30 min; $Na_2S_2O_4$ solution (H_2O), rt, 10 min; (**d**) THF, IBX (1.5 eq.), rt, 3 h; $Na_2S_2O_4$ solution (H_2O), rt, 10 min; (**e**) CaL, *n*-butanol, MTBE, 40 °C, 92 h.

*2.2.1.4.1 Biomimetic synthesis of bis-phenol neolignans **86 - 89***

Tyrosol (**77**) was dissolved in acetone and to this solution HRP in acetate buffer and H_2O_2 were added. The reaction mixture was stirred at rt and monitored by TLC for 6 h. Notwithstanding an unsatisfactory conversion of the substrate and the formation of a mixture of products, the main product **86** was obtained with 19.1% yield after purification on DIOL Silica-gel (**Scheme 22**).

This compound was fully characterized by MS spectrometry and 1D and 2D NMR spectroscopy. ESIMS shows a $[M-H]^-$ peak at *m/z* 273.1 which confirmed the formation of a dimeric product. The assignments of all signals in both ^1H and ^{13}C NMR spectra (**Figures 52S** and **53S** in **Appendix C**) were aided by the analysis of, gCOSY and gHSQCAD NMR experiments (**Figures 54S** and **55S**). Both ^1H and ^{13}C NMR spectra indicated a symmetrical structure, in agreement with the formation of symmetric 1.1'-dityrosol **86**. The ^1H NMR spectrum showed the typical AMX system at lower fields, namely the singlets at 7.13, 7.06 and 6.86 ppm were assigned to the protons H-6/6', H-4/4' and H-3/3' respectively; analogously, at upper fields the aliphatic proton signals due to the two triplets at 3.70 and 2.74 ppm (J = 7.0 Hz), were assigned to H-8/8' and H-7/7' protons and resulted mutually coupled by analysis of gCOSY spectrum. The analysis of the ^{13}C-NMR spectrum and the study of gHSQCAD correlations corroborated the structure **86** and allowed the unambiguous assignment of all ^{13}C resonances. The complete list of NMR assignment is reported in the Experimental section.

Analogously to tyrosol, homovanillic alcohol (**78**) was subjected to a dimerization reaction with HRP/H_2O_2 in acetone/acetate buffer (**Scheme 22**). The reaction mixture was stirred at rt and monitored by TLC for 6 h. A better conversion was observed for this substrate than **77**,

and purification of the reaction mixture on on DIOL Silica-gel afford the main product **87** with 43.5% yield. This compound was fully characterized by MS spectrometry and 1D and 2D NMR spectroscopy. ESIMS shows a $[M-H]^-$ peak at *m/z* 333.20 coherent with the formation of a dimer; this was confirmed by both ^1H and ^{13}C NMR spectra, respectively reported in **Figure 57S** and **58S**, indicating the structure of a symmetrical bisphenol, confirmed as 1,1'-dihomovanillic alcohol (**87**) by careful analysis of mono- and two-dimensional NMR spectra. The main differences in ^1H NMR and ^{13}C NMR spectra with respect to those of **86** were the signals of a methoxy groups (^1H NMR: 3.89 ppm; ^{13}C NMR: 58.03 ppm), the presence of two *meta*-coupled protons (^1H NMR: 6.86 ppm and 6.74 ppm, H-4 and H-6, respectively) instead of the AMX system, and the substitution of a sp^2 CH signal with a sp^2 deshielded quaternary carbon signal (^{13}C NMR: 128.2 ppm). The assignments of all the found signals were aided by the analysis of gCOSY and gHSQCAD correlations, which spectra are reported in **Figures 59S** and **60S** respectively. The complete list of NMR assignment is reported in the Experimental section.

2.2.1.4.2 Enzymatic acetylation of 77 and 78

On the basis of literature reports,[140] applying to these dimers the procedure summarized in **Scheme 19b**, the alcoholic group could be oxidatized by IBX. Thus, we planned to convert tyrosol (**77**) and homovanillic alcohol (**78**) into their alcoholic acetates **79** and **80** through a regioselective enzymatic acetylation. Dimerization of these acetates would also allow to obtain more lipophilic dimers, useful for possible SAR studies. To this purpose we exploited the previous expertise of the team to which I joined for my PhD research on the regioselectivity of lipase-catalyzed acetylation carried out in organic solvents.[155]

Therefore, a selective acetylation was carried out on **77**, according to **Scheme 22**. The substrate **77** was treated with vinyl acetate in the presence of *Candida antarctica* Lipase (CAL) (35 min at 40 ◦C) and afforded a single acetylation product, 1-acetyltyrosol (**79**), with 95% yield. The NMR data of the product (**79**) were in perfect agreement with those of the literature.[155] Following an analogous procedure, homovanillic alcohol (**78**) was treated with the above cited acyl donor in the presence of CAL, thus obtaining the corresponding C-1 acetate (**80**). The monoacetate was obtained with 94% yield. The NMR data of the product (**80**) were in perfect agreement with those of the literature.[155]

*2.2.1.4.3 Biomimetic synthesis of bis-phenols **88** and **89***

The synthetic procedure with HRP/H_2O_2 in acetone/acetate buffer at rt was used also for the dimerization of **79** (**Scheme 22**), although only partial conversion of the substrate was observed. After 4h a main product **88** was obtained with 20% yield. After purification on DIOL Silica-gel, **88** was subjected to spectral analysis; its ESIMS spectrum showed a [M-H]$^-$ peak at 357.1 *m/z* indicating the formation of a dimeric product. Its ^{1}H NMR spectrum, reported in **Figure 62S** (see **Appendic C**), suggested a symmetrical structure; in addition to the signals due to the -CH_2CH_2OAc pendants (2.91 ppm, t, J = 7.0 Hz, H_2-7; 4.24 ppm, t, J = 7.0 Hz, H_2-8), an aromatic AMX system was observed at 6.95 (d, J = 8.5 Hz, H-3), 7.15 (dd, J = 2.5, 8.5 Hz, H-4) and 7.21 ppm (d, J = 2.5 Hz, H-6), almost superimposable to that observed for **86**. The ^{13}C NMR spectrum, reported in **Figure 63S**, and the two-dimensional NMR experiments gCOSY and gHSQCAD, reported respectively in **Figures 64S** and **65S**, supported the structure of 1,1'-dityrosol 8,8'-diacetate (**88**), and allowed the assignment of all ^{1}H and ^{13}C NMR resonances (see Experimental section).

The monoacetate of homovanillic alcohol (**80**, 4-Hydroxy-3-methoxyphenetyl acetate) was subjected to HRP-mediated oxidative coupling in acetone/acetate buffer (**Scheme 22**); after 4h, a main product **89** was observed, and it was recovered with 50.1% yield after purification. The DIOL-purified product was subjected to spectral analysis: ESIMS showed an $[M-H]^-$ peak at 417.2 *m/z* confirming the formation of a dimer. The ^1H NMR and ^{13}C NMR spectra of **89**, reported respectively in **Figures 67S** and **68S** (see **Appendix C**), indicated a symmetrical structure. The main differences respect to **86** were the signals of two methoxy groups (^1H NMR: 3.93 ppm; ^{13}C NMR: 55.57 ppm), the presence of the H-4, H-6 *meta*-coupled protons (^1H NMR: 7.10 ppm and 6.89 ppm, respectively) instead of the AMX system, and the substitution of a sp^2 CH signal with a sp^2 deshielded quaternary carbon signal (^{13}C NMR: 125.44 ppm). The OH signal was observed as a *bs* at 7.45 ppm. Also gCOSY and gHSQCAD 2D NMR spectra, reported respectively in **Figures 69S** and **70S**, confirmed **89** as dihomovanillic alcohol 8,8'-diacetate. Only neolignans **88** and **89**, whose $-CH_2OH$ groups were preventively protected (as acetates), have been subjected to the IBX-mediated hydroxylation/demethylation reactions.

*2.2.1.4.3.1 selective hydroxylation of **88** and **89***

A preliminary screening of IBX-mediated reactions on **88,** followed by *in situ* reduction showed the formation of a number of products in various solvents; however, in MeOH at 0 °C for 30 min., a satisfactory conversion and the formation of a major, product, significantly more polar than **88**, were observed. The preparative hydroxylation (**Scheme 22**) afforded, after DIOL Silica gel chromatography, the product **90** (12% yield), which was analysed by ESIMS and NMR. An $[M-H]^-$ peak at 389.1 *m/z*, indicated the addition of

two oxygen atoms to **88**; ^{1}H and ^{13}C NMR spectra, respectively reported in **Figures 72S** and **73S** (see **Appendix C**), confirmed a symmetrical structure. Ten ^{13}C NMR signals were observed, including four deshielded sp^2 quaternary carbons; the ^{1}H NMR spectrum showed the aliphatic chain signals at 2.83 (H_2-7/7'), and 4.22 (H_2-8/8') ppm; signals for the H-4/4', H-6/6' *meta*-coupled protons at 6.81 and 6.73 ppm, respectively, and a signal at 8.0 ppm attributable to OH groups. The structure of 3,3'-dihydroxy-1,1'-dityrosol 8,8'-diacetate (**90**) was reinforced by analysis of 2D NMR spectra (**Figures 74S** and **75S**, respectively: gCOSY, gHSQCAD) also allowing complete assignment of ^{1}H and ^{13}C NMR signals (see Experimental section).

Differently from the previous reaction, a preliminary screening of the IBX-mediated demethylation reaction on **89** in various solvents at rt allowed to obtain a good conversion of the substrate and the formation of two main products employing THF for 3 h (**Scheme 22**). A preparative reaction of **89** afforded, after usual work-up and purification, two products more polar than the substrate. The most polar product (17.9% yield) showed ESIMS and NMR data identical to those of compound **90**, as expected for a double demethylation reaction. The least polar product **91** (20% yield) was analysed by ESIMS and NMR; a $[M-H]^-$ peak at 403.1 *m/z* suggested a mono-demethylation of **89**. ^{1}H and ^{13}C NMR spectra, respectively reported in **Figures 77S** and **78S** (see **Appendix C**), indicated the formation of an unsymmetrical bis-phenol, showing two different pairs of *meta*-coupled protons at 6.94 and 6.83 ppm (respectively H-4 and H-6) at 6.78 and 6.70 ppm (respectively H-4' and H-6'). A two-dimensional NMR (**Figures 79S – 81S**, respectively gCOSY, gHSQCAD, gHMBCAD) analysis allowed assigning all ^{1}H and ^{13}C NMR signals. Key HMBC correlations allowing to unambiguously

assign all the quaternary carbon resonances, and to discriminate the signals related to the different chains. In particular, the heteronuclear correlation of C-5 (131.0 ppm) with H-7 (2.91 ppm) allowed to identify the chain linked to C-5 as the ring A pendant. Furthermore the heteronuclear correlation of C-1 (126.3 ppm) with H-6' (6.70 ppm) and C-1' (127.5 ppm) with H-6 (6.83 ppm) confirmed, the 1-1' junction also for this dimer, established as 3-hydroxy,3'-methoxydityrosol diacetate (**91**).The complete list of NMR assignment is reported in the Experimental section.

*2.2.1.4.4 Enzymatic alcoholysis of **90** and **91***

A lipase-mediated alcoholysis procedure was employed for the deprotection of alcoholic functions of **90** and **91** in which the substrate was treated with CaL, using *n*-butyl alcohol as acyl acceptor (**Scheme 22**). From this reaction, the product **92** (3,3'-dihydroxy-1,1'-dityrosol) was obtained with 82.7% yield. The ESI-MS spectrum, with a main $[M-H]^-$ peak at 305.1 *m/z*, gave the expected molecular formula $C_{16}H_{18}O_6$, confirming the removal of two acetyl groups. The main differences in the ^1H and ^{13}C NMR (see **Figures 83S** and **84S** in **Appendix C**) spectra of **92** with respect to those of **91** were the lack of acetate signals. Analogously, **91** was submitted to the CaL-mediated alcoholysis. The product **93** (3-hydroxy-3′-methoxy-1,1′-dityrosol) was obtained with 82.4% yield. The ESI-MS spectrum ($[M-H]^-$ peak at 319.1 *m/z*), as well as the ^1H and ^{13}C NMR (see **Figures 86S** and **87S** in **Appendix C**) spectra of **93** confirmed the removal of two acetyl groups from **91**.

*2.2.1.5 Synthesis of compounds **94 - 96***

A simple methylation of **44** was carried out to obtain the corresponding methylated derivative, in order to study, in selected cases

(see section 2.2.5), the biological relevance of the phenolic OH of this simple natural compound. The reaction was performed in conventional condition as summarized in the **Scheme 23**, using *dry* acetone, K_2CO_3 and CH_3I. After purification both, the monomethylated and the permethylad compounds were recovered with a good yield. The NMR data are in agreement with those previously reported in literature. Then, the compound **94** was treated with IBX in MeOH according to **Scheme 23** and maintained at 0°C for 30 min. After the *in situ* reduction with $Na_2S_2O_4$, a reaction mixture showing one main products on TLC was obtained; after purification on DIOL Silica-gel, this afforded the product **96** more polar than the substrate, obtained with 18.5% yields. This product was subjected to spectral analysis (see **Figures 88S** and **89S** in **Appendix C**), that confirming a selective hydroxylation of **94**. All NMR data are in agreement with those previously reported in literature.[156]

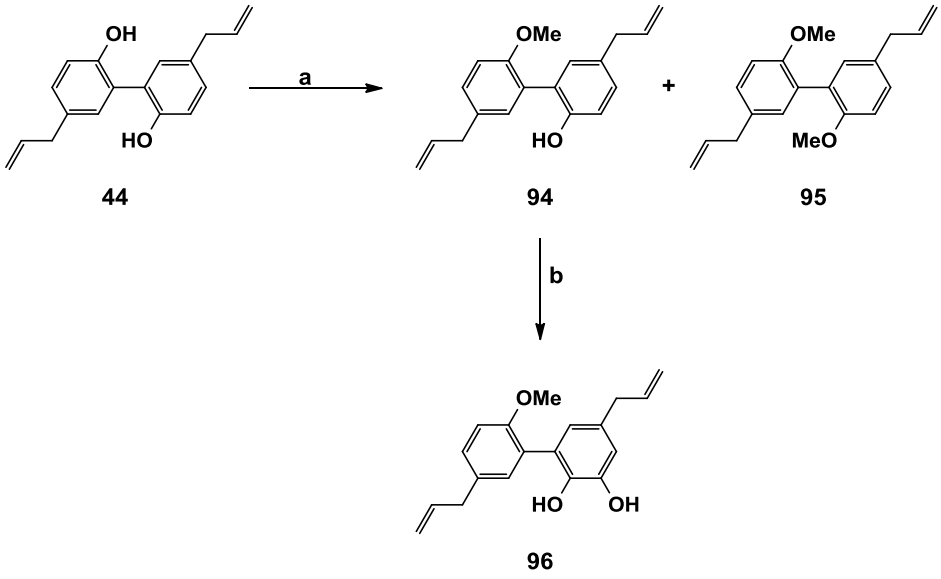

44 **94** **95** **96**

Scheme 23: (**a**) acetone, K_2CO_3 (12 eq.), CH_3I (12 eq), reflux, 48 h;(**b**)) MeOH, IBX (1.2 eq.), 0 °C, 30 min; $Na_2S_2O_4$ solution (H_2O), rt, 10 min.

2.2.2 Biochemical evaluation of magnolol analogues as α-glucosidase inhibitors

Based on the literature data in which magnolol (**44**) is reported as potent α-glucosidase inhibitor,[92] we started a study in which the synthetized magnolol analogues **81**, **82** and **84 - 93** were evaluated as inhibitors of yeast α-glucosidase, in view of their possible optimization as anti-diabetic drugs.

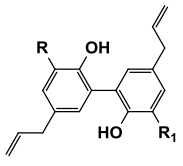

81 R = OH R_1 = H
82 R = OH R_1 = OH
84 R = OMe R_1 = OMe
85 R = OH R_1 = OMe

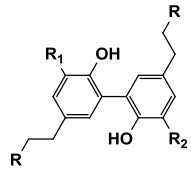

86 R = OH R_1 = H R_2 = H
88 R = OAc R_1 = H R_2 = H
90 R = OAc R_1 = OH R_2 = OH
92 R = OH R_1 = OH R_2 = OH

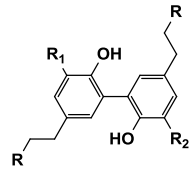

87 R = OH R_1 = OMe R_2 = OMe
89 R = OAc R_1 = OMe R_2 = OMe
91 R = OAc R_1 = OH R_2 = OMe
93 R = OH R_1 = OH R_2 = OMe

A slight modification of the method of Kurihara et al.[157] was used to evaluate the inhibition of the synthesized compounds towards α-glucosidase from *Saccharomyces cerevisiae*. Also magnolol (**44**) and honokiol (**45**) were tested for comparison, and also to confirm previous reports on their inhibitory activity. Quercetin (**17**) and acarbose (**46**) were employed as reference standard.[97] The activity of the enzyme, in presence of the substrate *p*-nitrophenyl α-D-glucopyranoside (*p*NP-α-G) and of compounds **44**, **45**, **81**, **82**, **84** – **93**, was spectrophotometrically determined (see Experimental section).

The % of inhibition at 1.5 μM of each compound and the IC_{50} values are reported in **Table 5**. The corresponding empirical inhibitory constants are also reported and were calculated through the expression *K*i = IC_{50}/ [(1+S)/*K*m][158] (where S is the substrate concentration, *K*m is the experimental Michaelis-Menten constant tabulated for yeast α-glucosidase in presence of pNP-α-Glc at 37 °C and pH 7.0). For the sake

of clarity, a graph is also reported (**Graphic 1**) where $1/IC_{50}$ values are reported as hystograms.

Table 5: Inhibition percentage, IC_{50} and calculated *Ki* values of magnolol analogues on yeast α-glucosidase

compounds	Inhibition (%)[a]	IC_{50} (μM) ± SD[b]	*Ki*[c]
magnolol (44)	29.8	2.04 ± 0.40	1.81
honokiol (45)	3.9	23.0 ± 2.4	21.98
81	97.6	0.49 ± 0.19	0.43
82	36.7	2.11 ± 0.59	1.86
84	46.7	1.95 ± 0.57	1.76
85	98.0	0.50 ± 0.13	0.44
86	76.9	0.86 ± 0.25	0.76
87		n. d.[c]	
88	98.9	0.15 ± 0.09	0.13
89	64.5	1.12 ± 0.41	0.94
90	31.4	2.90 ± 0.33	2.57
91	21.3	3.34 ± 0.91	3.21
92	18.2	4.13 ± 0.84	3.95
93		n. d.[c]	
quercetin (17)	5.3	14.2 ± 2.1	12.9
Acarbose (46)		280.6 ± 34.6	

[a]Inhibition determined at 1.5 μM; [b]results are reported as mean ± SD (n=3); [c]*Ki* values were calculated by the expression *Ki* = IC_{50}/ [(1+S)/Km]; [d]not determined.

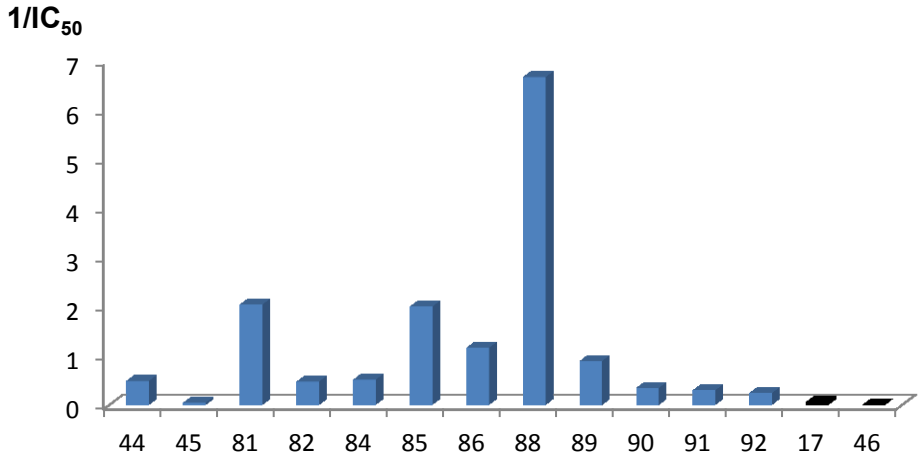

Graphic 1: $1/IC_{50}$ values of magnol analogues

The synthetic analogues of magnolol showed a strong inhibitory activity with IC_{50} values in the range 4.13 – 0.15 μM, much lower than those of quercetin (14.2 μM), acarbose (280.6 μM) and honokiol (23.0 μM). Magnolol was confirmed to be very active with an IC_{50} value of 2.04 μM, not far from that reported in the literature.[111] Most interestingly, a very potent inhibitory activity, with IC_{50} = 0.15 μM, and 98.9% inhibition at 1.5 μM, was observed for 1,1'-dityrosol-8,8'-diacetate (**88**); a comparable inhibitory activity was also showed by bisphenols **81** (0.49 μM), **85** (0.50 μM) and **86** (0.86 μM), with percentage inhibition in the approximate range 77 – 98%. These compounds are, on the basis of literature data, by far more potent than known carbohydrate-related glucosidase inhibitors, such as acarbose.

It is worth noting that **81**, the catechol analogue of magnolol (**44**), is significantly more potent than **44**, and a similar difference is observed for **85** with respect to **84**. Nevertheless both **88** and **86**, lacking of a catechol moiety, show potent inhibition and suggest that also the dityrosol scaffold is specially promising for future optimization of anti-diabetic drugs based on natural models. The markedly lower potency of honokiol (**45**) suggests that an OH group *ortho* to the allyl chain in ring B may be detrimental for the activity. However, other compounds, closely related to those showing a potent inhibitory activity, resulted significantly less potent (IC_{50} values in the range 4.13 – 1.12 μM); thus, further studies are required to establish clear structural determinants for the α-glucosidase inhibitory activity of magnolol-related bisphenols.

To get some insight about the mode of action of these neolignans, we carried out a kinetic study of the inhibitory effect of the most potent compound **88** on yeast α-glucosidase. In the **Figures 23a** and **23b** the kinetic curves and the Lineweaver–Burk plots of α-glucosidase inhibition

at different concentrations of substrate (*p*NP-α-G) and inhibitor **88**, respectively are reported. The results indicated that **88** acts as a competitive inhibitor with Ki value of 0.86 µM.

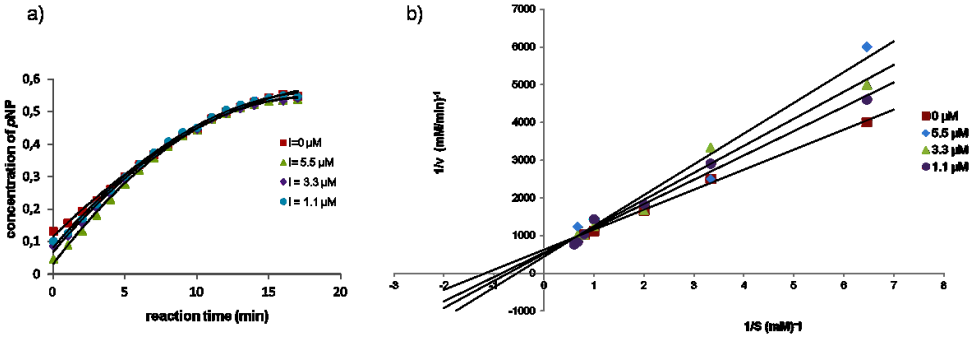

Figure 23: a) Kinetics of yeast α-glucosidase inhibition by compound **88** (0, 1.1., 3.3, and 5.5. µM), *p*NP-α-G was employed as substrate (0.5 mM) and the *p*NP (*p*-nitrophenol) released in time has been reported; b) Lineweaver-Burk plots of α-glucosidase inhibition at different concentrations of substrate and compound **88** (0, 1.1., 3.3, and 5.5. µM). The data points present the average of two experiments.

2.2.3 Chain-breaking antioxidant activity of hydroxylated and methoxylated magnolol derivatives

Based on the literature data in which magnolol (**44**) is reported as good chain-breaking antioxidant,[78] we started a study in collaboration with Prof. R. Amorati (University of Bologna) in which the chain-breaking antioxidant activity of the hydroxylated and methoxylated magnolol derivatives **81**, **82**, **84** and **85** was explored by experimental and computational methods. All compounds evaluated bearing two allylic side chains located in *meta* position with respect to the diphenyl junction, having structural modification with respect to magnolol (**44**) that could increase its radical trapping ability. The dimeric neolignan **81** presents one additional hydroxyl group with respect to **44**, generating a catechol moiety; compound **83** has two catechol moieties; compounds **84** and **85** are structurally related to **82** by substitution respectively of one or two hydroxyl groups with methoxyl groups. Three phenols related to these compounds, namely eugenol (**76**), 4-methylcatechol (**94**), and 4-methylguaiacol (**95**) were also evaluated as monomeric model compounds.

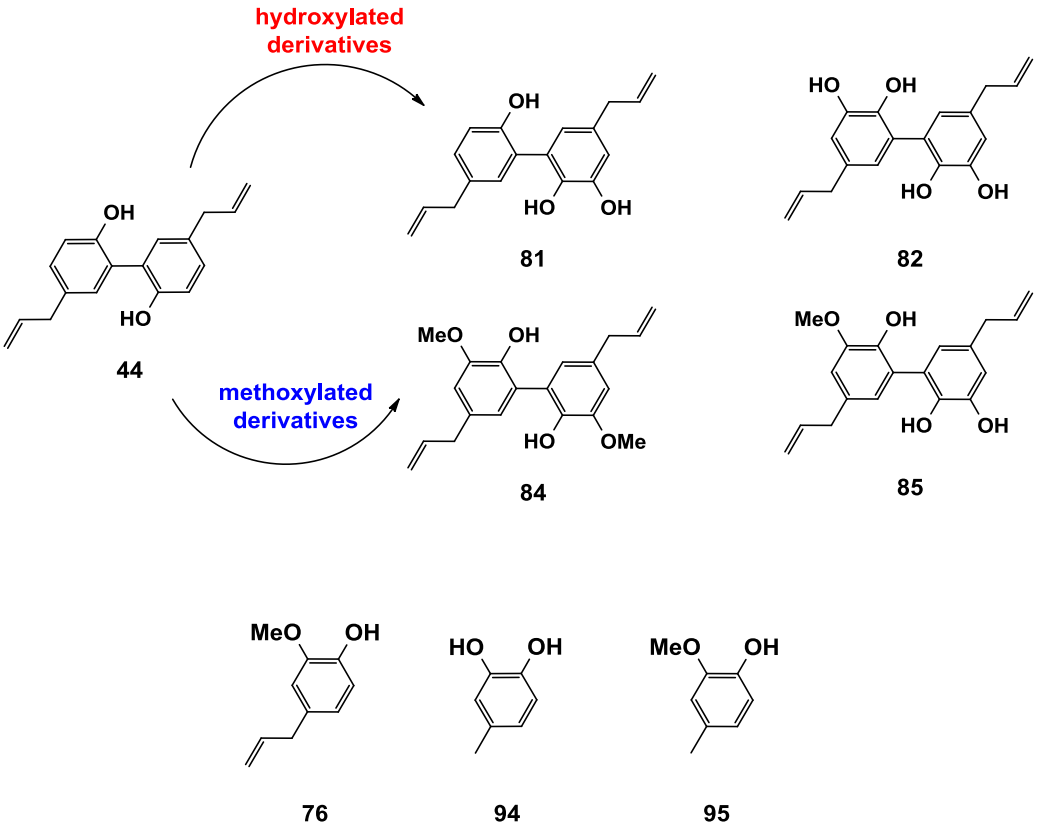

As detailed in the following, the chain-breaking antioxidant behavior of these derivatives has been explored in comparison to that of parent magnolol (**44**), by measuring the rate constant of reaction with peroxyl radicals, that are the responsible for peroxidation in biological systems, and in natural and man-made materials in general.[159, 160] We report the rationalization of the reactivity of **81**, **82**, **84** and **85** by keeping into account their complex multifunctional structure and the major role that non-covalent interactions play on their reactivity.

2.2.3.1 Kinetics and stoichiometry of the reaction with peroxyl radicals

The chain-breaking antioxidant activity was assessed by measuring the rate constant of reaction with $ROO^{\bullet}$ radicals and the number of radicals trapped by each antioxidant molecule. This was achieved by monitoring, under controlled conditions, the oxygen consumption during the inhibited autoxidation of styrene or cumene in chlorobenzene (50% v/v) at 303 K, initiated by the homolytic decomposition of the initiator 2,2'-azobis(isobutyronitrile) (AIBN), in the presence of variable amounts of compounds **81**, **82**, **84** and **85,** and the monomeric model compounds **76**, **94** and **95**. Styrene is typically employed for studying strong antioxidants (i.e with k_{inh}> $1x10^5$ $M^{-1}s^{-1}$), whereas cumene, was suitable for weaker inhibitors. As it is evident from **Figure 24**, styrene autoxidation is efficiently inhibited only by compounds **81** and **82** whereas **84** and **85** provide only a weak retardation. On the contrary, cumene autoxidation was inhibited by all investigated phenols (**Figure 25**).

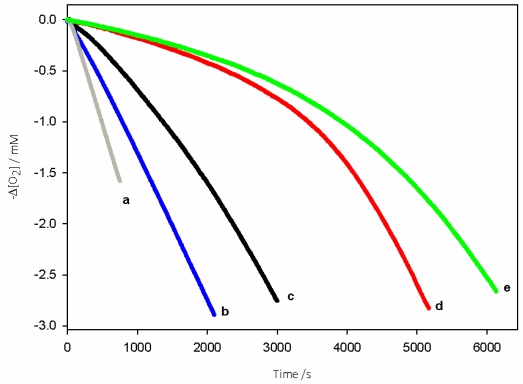

Figure 24: Oxygen consumption during the autoxidation of styrene (4.3 M) initiated by AIBN (0.05 M) in PhCl at 30° C without inhibitors (**a**) or in the presence of antioxidant (1.3×10^{-5} M) **84** (**b**), **85** (**c**), **81** (**d**), **82** (**e**).

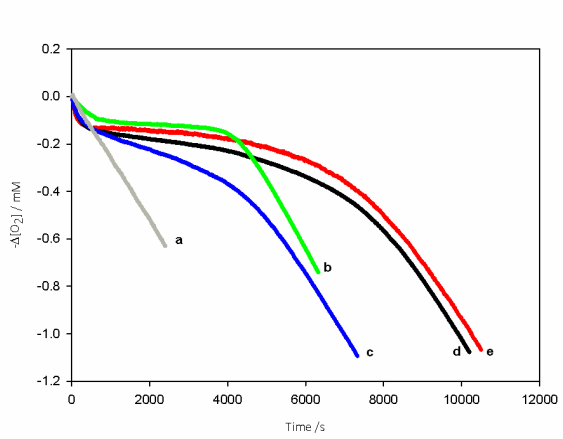

Figure 25: Oxygen consumption during the autoxidation of cumene (3.6 M) initiated by AIBN (0.05 M) in PhCl at 30° C without inhibitors (**a**) or in the presence of antioxidant (1.3×10^{-5} M) **82** (**b**), **84** (**c**), **85** (**d**), **81** (**e**).

The inhibition given by magnolol derivatives **81** and **85** is composed of two parts, a stronger inhibition (lasting for about 4000 s) corresponding to the trapping of two ROO$^{\bullet}$ radicals and a weaker retardation of oxidation which approximately corresponds to the trapping of two additional radicals. In the case of **82** and **84** this residual antioxidant activity is very weak. This behavior can be explained by considering that, after the trapping of the first two ROO$^{\bullet}$ radicals, one of the two phenolic rings is converted into the corresponding dienone (or ortho-benzoquinone, in the case of catechols), which engages a strong H-bond interaction with the second phenolic ring, reducing its reactivity. In the **Table 6** are reported the $\boldsymbol{k_{inh1}}$ (rate constants for the strongly inhibited period), $\boldsymbol{k_{inh2}}$ (rate constants for the weakly inhibited period), and $\boldsymbol{n}$ (stoichiometric coefficient) values, estimated for each compounds.

Table 6: Rate constants for the reaction with peroxyl radicals ($M^{-1}s^{-1}$, 303 K, solvent chlorobenzene) measured for the strongly (k_{inh1}) and the weakly (k_{inh2}) inhibited period, and stoichiometric coefficient (n).[a]

compound	k_{inh1}	k_{inh2}	n[a]
44	6.1×10^{4} [b]	4.3×10^{3} [b]	2.0 (1.7)[b]
76	$(4.8\pm0.2)\times10^{3}$		2.0±0.2
81	$(2.4\pm0.2)\times10^{5}$	$(2.7\pm0.1)\times10^{3}$	1.8±0.2 (1.8±0.2)
82	$(3.3\pm0.2)\times10^{5}$		1.9±0.1
84	$(1.1\pm0.1)\times10^{4}$	$\approx8\times10^{2}$	2.0±0.1 (2[c])
85	$(6.0\pm0.3)\times10^{4}$	$(2.5\pm0.3)\times10^{3}$	2.0±0.2 (1.6±0.3)
94	$(4.2\pm0.2)\times10^{5}$		1.9±0.2
95	$(7.5\pm0.3)\times10^{3}$		2.0±0.2

a) the stoichiometric coefficient of the weakly inhibited period is reported in brackets, b) from reference,[83] c) the stoichiometric coefficient could not be measured because the k_{inh} value is too low, so it was assumed to be equal to 2.

2.2.3.2 FT-IR measures

To rationalize the k_{inh1} reactivity order of evaluated compounds, their intramolecular H-bond pattern was investigated by FT-IR spectroscopy in CCl_4 solution. The frequencies of the phenolic O-H bond stretching are reported in **Figure 26**. The spectra of compounds **81**, **82**, **84** and **85** show that the H-bond patterns of the hydroxylated and methoxylated derivatives are in part different to that of magnolol (**44**). All the investigated compounds showed relatively narrow peaks at about 3550 cm^{-1} and broader ones at about 3400 cm^{-1}, while **44** displays a small peak of free (not H-bonded) OH group that is typically observed between 3600-3610 cm^{-1} and a bigger one at about 3550 cm^{-1}. By comparison to **44** and **81**, **82**, **84** and **85**, the peaks at about 3550 cm^{-1} can be attributed to a broad family of OH groups H-bonded to different kind of acceptors such as: the oxygen atom of an ortho OH or OMe group, (as in case of **81**, **82**, **84** and **85**), the π electron density of an aromatic ring or an oxygen atom of a OH group on the nearby ring (as in **44**). The peak at about 3400 cm^{-1} can be only attributed to OH groups participating to an H-bond array (OH---OH---OR) that strengthen the interaction and shifts the peak towards lower frequencies. This red-shifted peak at about 3400 cm^{-1} is

clear only in the case of **85**, whereas in **81**, **82** and **84** it is relatively weak, suggesting that the conformation characterized by the H-bond array is the minor one. In **81** and **82** the peak at 3400 cm^{-1} should be accompanied by the peak of a free OH group at 3610 cm^{-1}, which would represent the starting OH of the H-bond array, however this peak is very weak and it merges with the background noise.

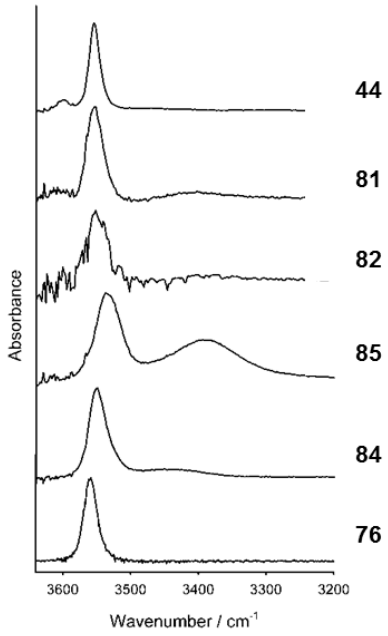

Figure 26: Absorption infrared spectra of phenols **44**, **76**, **81**, **82**, **84** and **85** measured in CCl_4

2.2.3.3 Theoretical Calculations

To rationalize kinetic and spectroscopic results, the preferred conformations, the IR spectra and the dissociation enthalpies of the O-H bonds (BDE-OH) were computed by DFT calculations. To reduce computation time, para-allyl groups were simplified to methyl groups. The most relevant conformations of each phenol and the relative stability are reported in **Figure 27**.

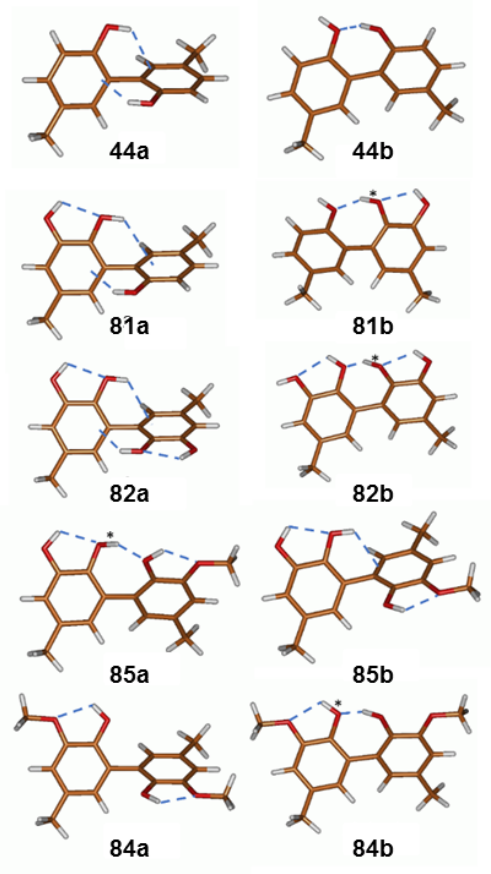

Figure 27: Optimized geometry and free energy difference (kcal mol^{-1}) between the two most stable conformers. Asterisks show OH groups responsible for the red-shifted peak between 3370 and 3440 cm^{-1}.

Calculations confirm the presence of red-shifted signals corresponding to specific OH groups participating in a H-bond array (see OH groups marked by an asterisk in **Figure 27**). The most stable conformation of **44**, **81** and **82** is stabilized by two H-bonds between a OH group and the nearby aromatic ring, while that of **85** is characterized by a H-bond array (**Figure 27**). In compound **84**, the most stable conformation has two H-bonds between the hydroxyl and the ortho methoxy group. In this context the BDE(OH) values were calculated for

both conformers of **81**, **82**, **84** and **85** (see **Figure 27**) and for the reference compounds, and are collected in **Table 7**.

Table 7: Calculated BDE(OH) values (kcal mol^{-1})

compound	conformer a[a]	conformer b[a]
44	89.4	78.4
76	84.9	
81	78.9	77.5
82	79.5	77.7
84	83.9	80.6
85	79.9	77.4
94	76.1	
95	84.6	

BDE(OH) values reported in **Table 7** have been obtained by allowing only minimal geometric variation when passing from the phenol to the phenoxyl radical. In most cases, the geometry considered was only a local minimum on the potential energy surface, which (usually) did not coincide with the most stable conformation. The importance of the fact that the geometry of the phenoxyl radicals is as similar as possible to that of the parent phenol is explained in **Figure 28** for the case of **82**. The BDE(OH) obtained without allowing geometrical relaxation is 79.5 kcal mol^{-1}, while that obtained after rotation of 95 deg about the Ar-Ar single bond is 72.7 kcal mol^{-1}. Thus, allowing the relaxation of the radical geometry lowers the BDE(OH) by 6.8 kcal mol^{-1}. From a mechanistic point of view, this indicates that H-atom transfer gives rise to a phenoxyl radical having the same geometry of the phenol, which only afterward relaxes to the most stable conformation.

Figure 28: Effect of the conformation of the phenoxyl radical on the BDE(OH).

The values of k_{inh1} show that the ortho selective introduction of one or two OH groups to magnolol increases the reactivity towards ROO$^{\bullet}$ radicals of an order of magnitude. This is due to the formation of a catechol unit which has an inhibition constant greater than simple phenols. This is also confirmed by comparing the k_{inh} values of the compounds **81** and **82** with 4-methyl-catechol **95**. The presence of two OMe groups in compound **84** decrease its reactivity compared with magnolol (**44**), as demonstrated by the presence of a methoxy group in *o*-position (and allyl or methyl group in *p*-position) in the monomer models **76** and **95** that have the same reactivity of compound **84**. The BDE(OH) values of the hydroxylated magnolol derivatives **81** and **82** are relatively low, thanks to the presence of at least one catechol moiety. However, their BDE(OH) values are larger than that of 4-methylcatechol, thanks to the formation of OH---Ar H-bond with the nearby aromatic ring.

This work showed that the introduction of hydroxyl groups *ortho* to the phenolic OH in magnolol is a good strategy to obtain new magnolol derivatives which are more active (as chain-breaking antioxidants) than the natural counterpart. The di-methoxylated derivative is less reactive than magnolol, while the insertion of both hydroxyl and methoxyl groups showed no effect. Infrared spectroscopy and DFT calculations allowed a rationalization of these results and pointed out the role of the H-bond

network, which deeply influences the reactivity of magnolol derivatives, compared to the parent mono-phenols. These finding provide the rational basis for the development of novel and possibly pharmacologically active lignans.

2.2.4 Inverse Virtual Screening of magnolol analogues and their biological activities on bromodomain, tankirase and caseinase

Computational methods have been recently shown to be an important complementary tool for the study of the pharmacological activity of natural or bio-inspired compounds.[161] The inverse virtual screening[162] is a new computational approach that could represent a new tool used in facilitating new drug discovery, by overcoming the problem of performing experimental evaluation of a library of compounds on a large number of biological targets; in addition, these methods have a better chance of highlighting their potential activity.[163] This approach is normally based on the molecular docking of a panel of small molecules against a panel of biological targets, ex. receptor sites, in an attempt to find ligands and binding conformations useful to direct experimental assays selected for specific targets. This approach has been applied to the discovery of potential chemotherapeutic agents through the interaction with a number of protein targets involved in different kind of degenerative diseases. The panel of targets is built from the Protein Data Bank (PDB), by the selection of proteins involved in a specific disease; if commercially available, these proteins are used for subsequent biological tests. It is noteworthy that this approach is also potentially applicable to accelerate the analysis and to evaluate structure-activity relationships of a library of different analogues through a virtual method before the experimental study. This method has been used to evaluate magnolol (**44**) and its synthetic analogues **82**, **82** and **84** - **93** on a panel of biological targets, during my visiting-PhD period (July 2016) at the University of Salerno (Fisciano), under the supervision of Prof. G. Bifulco and his collaborators.

2.2.4.1 Inverse Virtual Screening

A small library of compounds, namely magnolol (**44**) and its synthetic analogues **81**, **82** and **84** - **93**, was evaluated with the Inverse Virtual Screening methodology.

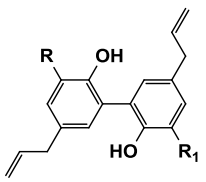

81 R = OH R_1 = H
82 R = OH R_1 = OH
84 R = OMe R_1 = OMe
85 R = OH R_1 = OMe

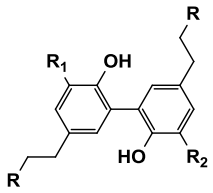

86 R = OH R_1 = H R_2 = H
88 R = OAc R_1 = H R_2 = H
90 R = OAc R_1 = OH R_2 = OH
92 R = OH R_1 = OH R_2 = OH

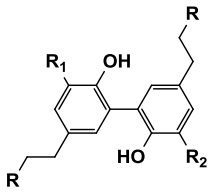

87 R = OH R_1 = OMe R_2 = OMe
89 R = OAc R_1 = OMe R_2 = OMe
91 R = OAc R_1 = OH R_2 = OMe
93 R = OAc R_1 = OH R_2 = OMe

The calculations were carried out through the software Autodock-Vina,[164] using a panel of 307 biological target, involved in the occurrence of cancer. The results of calculations were normalized using the equation reported below [**1**]:

$$V = V_0/V_R \quad [\mathbf{1}]$$

in which '**V**' is the normalized affinity value, '$\mathbf{V_0}$' is the affinity value without normalization and '$\mathbf{V_R}$' is the average affinity values for each considered target. In this manner, only 4 candidates, on a panel of 307, were selected (**Table 8**), and considered the best in terms of interaction with the magnolol-inspired compounds.

Table 8: biological targets selected by inverse virtual screening

entry	Biological targets
1	Tankyrase 2
2	Bromodomain-containing protein 4
3	Bromodomain-containing protein 9
4	Casein Kinase II

We investigated binding of all magnolol analogues **81**, **82** and **84** - **93**, seeking to determine the binding modes within the cavity of each

selected biological targets, and ideally they established favorable interactions for the recognition. As example, we report here the Molecular Docking of compound **88** with the above cited selected targets (**Figure 29** and **30**).

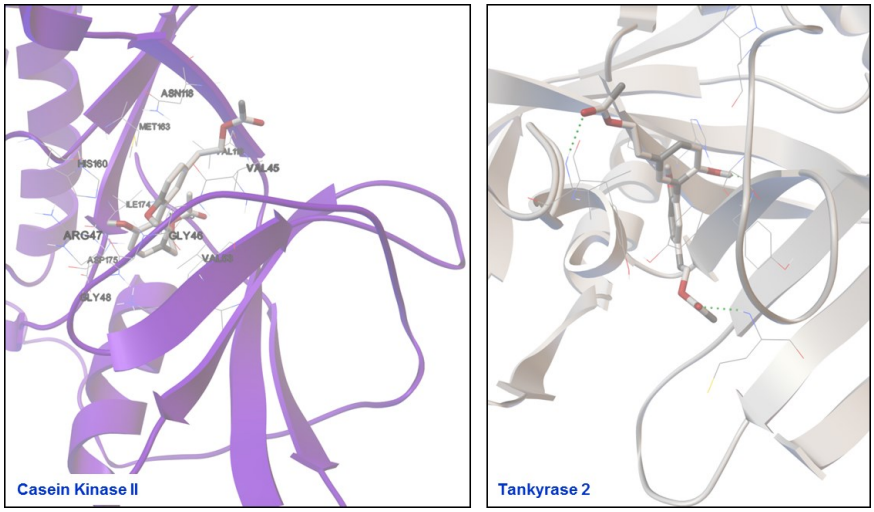

Figure 29: Molecular docking of compounds **88** with Casein Kinase II and Tankyrase 2

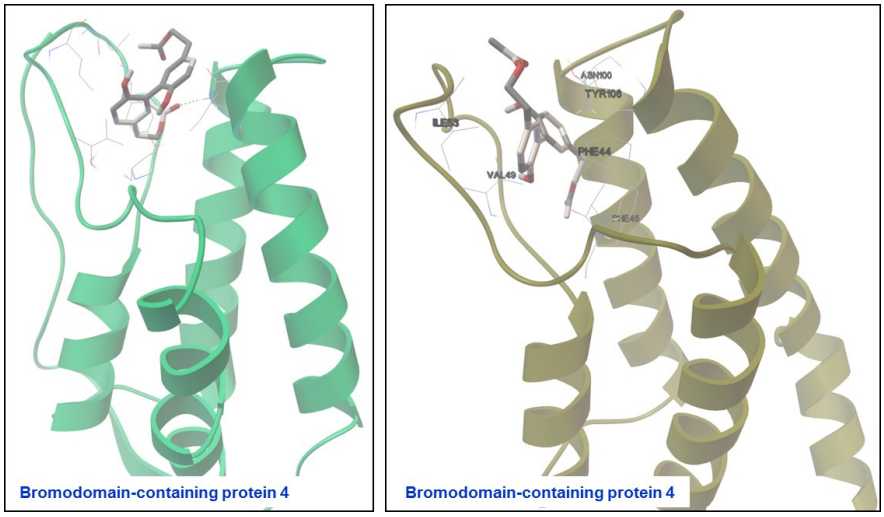

Figure 30: Molecular docking of compounds **88** with Bromodomain-containing protein 4 and 9

On the basis of these results, the experimental assays were planned on Bromodomain-containig protein (in collaboration with Prof. Panagis Filippakopoulos, Oxford University) Tankyrase 2, and Casein Kinase II, (in collaboration with Prof. Ines Bruno, Univesity of Salerno). Only Tankirase 2 gave positive results, whereas assays on the other biological targets did not evidence any kind of interaction.

2.2.4.1.1 Assay on Tankyrase 2

Several studied have been shown that tankyrases have a regulatory function in the centriole elongation and mitotic spindle formation, telomere cohesion, exocytosis of IRAP and GLUT4 containing trans-Golgi vesicles. Tankyrases 1 and 2 are specialized members of the ARTD (ADP-ribosyltransferase) protein family; their inhibition may have therapeutic potential against cancer, metabolic disease, fibrotic disease, fibrotic wound healing and HSV viral infections. Thus, discover and develop new potent and selective tankyrase inhibitor would be an opportunity to find new potent chemotherapeutic agents. In order to simplify the experimental work and also considering the limited amounts of synthetic magnolol analogues, we selected only a limited number of candidates for a preliminary set of bioassays. In particular, based on the results obtained from the Inverse Virtual Screening and by studying the key interactions of each magnolol analogue with Tankyrase 2, we firstly have evaluated five compounds (**81**, **85**, **87** and **89**) and magnolol (**44**) as reference natural product. Surface Plasmon Resonance (SPR) binding analysis methodology and recombinant human Tankyrase 2 (TNKS2) were used to study the molecular interaction. SPR is an optical technique for detecting the interaction of two different molecules in which one is mobile and the other is fixed on a thin gold film. In the work described here, TNKS2s are immobilized by an amine-coupling reaction on a sensor

chip surfaces. For this study different concentration of each compound were used namely 0.250 nM, 1 μM, 10 μM, and 20 μM. Simple interactions were fitted to a single-site bimolecular interaction model, as reported below [**2**], yielding a single K_D using the equation reported below [**3**], and all the K_D values for each compounds are reported in the **Table 9**. Very interestingly, among the evaluated compounds, three (**85**, **87** and **89**) have a K_D in the low nanomolar range (7 – 21.9 nM); the other two compounds, including the natural lead magnolol (**44**) and **81**, did not gave detectable interaction. Although this is a small set of compounds, and further analogues will be evaluated, the reported results are very encouraging and indicate that the chemical modification of magnolol is a structural determinant for interaction with Tankyrase 2.

$$A + B \underset{K_d}{\overset{K_a}{\rightleftharpoons}} AB \qquad [2]$$

$$K_D = K_d / K_a \qquad [3]$$

Table 9: KD values for the compounds **44**, **81**, **85**, **87** and **89**.

compound	K_D * (nM)
81	-
85	21.9
87	18.5
89	6.5
44	-

*Average between three experiments

To further evaluate binding of **81**, **85**, **87** and **89** onto Tankyrase 2, we analyzed the molecular docking previously carried out (**Figure 31** and **32**). Differently from **44** and **81** that interact with tankyrase only through the phenolic OH, the compounds **85**, **87** and **89** exhibit a series of additional interaction. For example one of the alcoholic OH of **87** interact

with one glycine (Gly1074) inside the cavity of TNKS2 by a hydrogen bond; also 89 is able to interact through both acetyl functions with a glycine (Gly107) and a methionine (Met1054) inside the cavity by hydrogen bond.

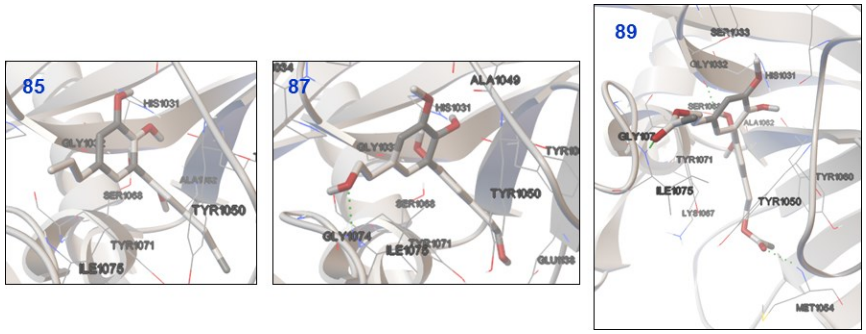

Figure 31: Molecular docking of compounds **85**, **87** and **89** with Tankyrase 2

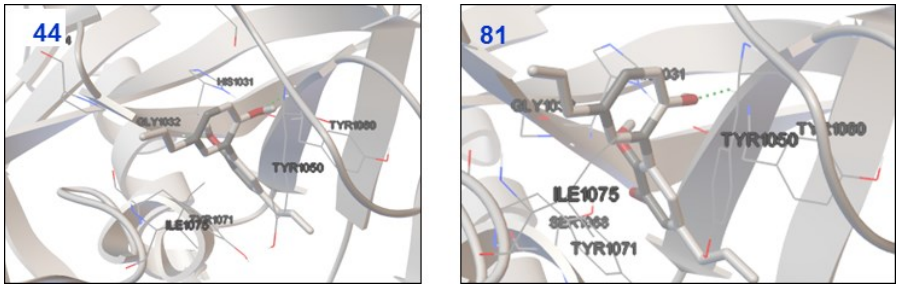

Figure 32: Molecular docking of compounds **44** and **81** with Tankyrase 2

2.2.5 Magnolol derivatives as inhibitors of the human breast cancer resistance protein (BCRP/ABCG2)

Breast cancer resistance protein (BCRP/ABCG2) is one of the major transporters involved in the cell efflux of anticancer compounds, contributing to multidrug resistance (MDR). They belong to the ATP-Binding Cassette (ABC) transporters, one of the largest membrane protein superfamily. Acting as ATP-powered pumps, ABC transporters are able to extrude a wide variety of structurally-unrelated compounds from the cells, and are crucial for cell detoxification and survival, by effluxing exogenous toxic substances outside the cell. Their overexpression in tumor cells contributes to chemo-resistance through the efflux of anticancer drugs. So far the three major ABC proteins, P-glycoprotein (Pgp/ABCB1),[165] multidrug resistance protein 1 (MRP1/ABCC1),[166] and breast cancer resistance protein (BCRP/ABCG2),[167] are recognized to be strongly involved to the multidrug resistance developed by cancer cells against cytotoxic commonly used drugs. Particular interest, in the research of new effective and not toxic MDR, was directed on ABCG2, since its discovery, as a target for the development of new inhibitors to be used in combination with conventional anti-cancer drugs for restoring their efficacy.[168] With the aim to evaluate the potential of magnol derivatives as chemotherapeutic agents, in collaboration with Prof. G. Valdameri of Federal University of Paraná (Brazil) we started a collaboration to study these compounds as inhibitors of ABCG2 and Pgp (ABCB1). In this preliminary evaluation we decided to test only the magnolol analogues **86, 91, 95** and **96**.

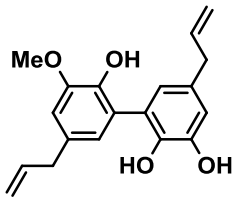

86

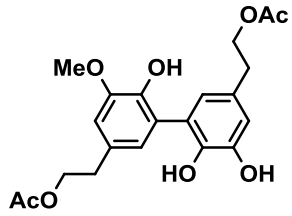

91

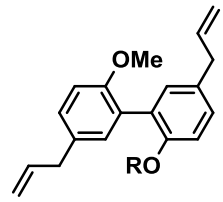

95 R = H
96 R = Me

Preliminary *in vitro* inhibition assays were performed as previously reported from Valdameri et al.,[169] using HEK293-*ABCG2* and HEK293-*ABCB1* cells; the cells were exposed to mitoxantrone (5 μM), rhodamine 123 (5 μM), respectively, and different concentration (10 and 50 μM) of each evaluated compounds. The result, reported respectively in the **Figures 33** and **34**, were expressed as percentage of inhibition, calculated by using the following equation:

$$\% \text{ inhibition} = (C - S)/(I - S) \times 100$$

in which C corresponds to the intracellular fluorescence of cells in the presence of magnolol derivatives (**86, 91, 95** and **96**) and substrate (mitoxantrone or rhodamine 123), and S to the intracellular fluorescence of cells in the presence of only substrate. Here, I is the intracellular fluorescence of cells in the presence of the reference inhibitor Elacridar and substrate.

In **Figure 33** the % inhibition at 10 and 50 μM of each evaluated compound are reported; only compounds **91** and **95** inhibited ABCG2, and clearly the compound **95** is the most potent inhibitor showing a full inihibition (100%) at 50 μM. It is worth of noting that it is quite common to have inhibitors able to inhibit both ABCG2 and ABCG1 (Pgp), but in our case, this class of compounds seems to be selective for ABCG2, because none of the tested compounds inhibited P-gp (**Figure 34**). These promising first results, showed a new class of potent and selective

inhibitors of ABCG2 that could display a very high therapeutic potential in the treatament of cancer; based on those considerations we wanted to extend the evaluation also on the compounds **81**, **85**, **86**, **88**, **89**, **90** and **96** and the experiments are in progress.

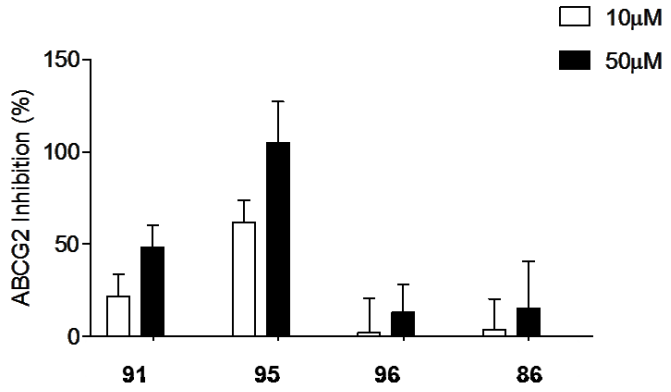

Figure 33: Inhibition of ABCG2 by Magnolol derivatives. Cells HEK293-*ABCG2* were exposed to mitoxantrone (5 μM) and Magnolol derivatives (**91**, **95**, **96** and **86** - 10 and 50 μM). Elacridar (1 μM) was used as a positive control. Intracellular mitoxantrone accumulation was determined by flow cytometry using FL4-H channel. Results were expressed as percent of inhibition (Elacridar corresponds to 100% of inhibition). Data represents mean ± SD of three independent experiments.

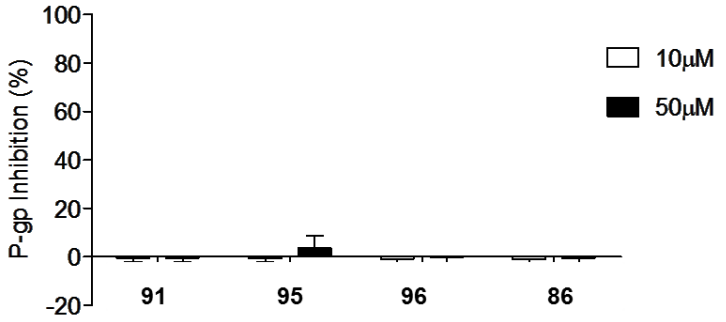

Figure 34: Inhibition of P-glycoprotein (P-gp) by Magnolol derivatives. Cells NIH3T3-*ABCB1* were exposed to rhodamine 123 (5 μM) and Magnolol derivatives (**91**, **95**, **96** and **86** - 10 and 50 μM). Elacridar (0,5 μM) was used as a positive control. Intracellular rhodamine 123 accumulation was determined by flow cytometry using FL1-H channel. Results were expressed as percent of inhibition (Elacridar corresponds to 100% of inhibition). Data represents mean ± SD of three independent experiments.

2.3 IBX-mediated synthesis of a new hydroxylated dihydrobenzofuran neolignan

In this Section I would like to report an unexpected result obtained during the work on magnolol analogues (see Section 2.2.1). More specifically, in the first steps of this part of my research activity, isoeugenol (**97**), that differ than eugenol (**76**) only because has a conjucate chain to the aromatic ring instead an allylic chain, was treated with IBX with the aim to obtain a demethylderivative (**98**), to be dimerized with an oxidase enzyme, according to **Scheme 24**. As reported in Section 2.2.1., this approach was later abandoned in favour of the more convenient dimerization followed by IBX-mediated demethylation/hydroxylation. However, a preliminary NMR analysis of the product obtained treating **97** with IBX in the same conditions employed for eugenol (**76**), showed that an unexpected product **99** was formed. Thus, in parallel with the projected syntheses of magnolol analogues, we purified and examined this product, whose structure was established as detailed below.

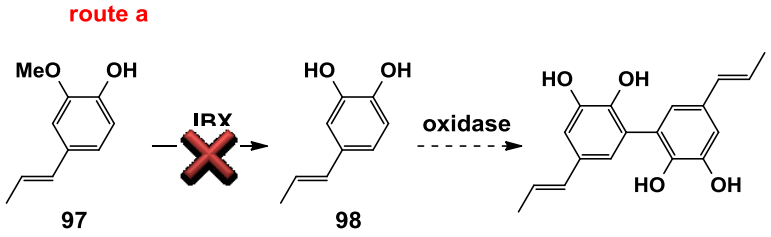

Scheme 24

The ESIMS of **99** (See **Figure 90** in **Appendix C**) showed a main peak at 313.2 *m/z,* imputable to a molecular ion $[M+H]^+$, which suggested the formation of a dimeric product instead of the expected demethylderivative. Nevertheless, a MW of 312 is not compatible with a

simple dimerization of two isoeugenol units, and suggest for the dimer **99** the probable loss of one methyl associated to a 2H addition.

To acquire more data useful to the determination of the structure, a complete NMR analysis was carried out on **99**, including both ^{1}H and ^{13}C NMR spectra and and two-dimensional experiments (COSY, HSQC, HMBC). The ^{1}H and ^{13}C NMR spectra of **99** are reported respectively in **Figure 91S** and **92S** (see **Appendix C**), and show doubled signals with respect to those of **97**, suggesting the formation of an asymmetrical dimer. The signals for only one methoxy group were observed at 3.85 ppm and 60.67 ppm, respectively in the ^{1}H and ^{13}C NMR spectra, thus confirming the demethylation of one of the monomeric isoeugenol units. In the low-field region of the ^{1}H NMR spectrum, the signals of an aromatic AMX system, resembling those observed for the substrate **97,** were observed respectively at 7.11 (d, J = 2.0 Hz), 6.93 (dd, J = 2.0, 8.0 Hz) and 6.86 ppm (d, J = 8.0 Hz). These data, corroborated by analysis of the ^{13}C NMR spectrum and 2D NMR experiments (See **Figure 35** for selected HMBC correlations and the experimental section for ^{1}H and ^{13}C NMR assignments), indicated the presence of one trisubstituted aromatic ring (B in **Figure 35**).

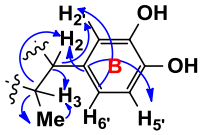

Figure 35: HMBC correlation for B-ring

The presence of two *meta*-coupled protons (6.77 and 6.73 ppm, bs), correlated to the sp^2 CH resonances in the ^{13}C NMR spectrum (respectively at 118.5 and 117.4 ppm), indicated a modified substitution pattern for the second aromatic ring with respect to the isoeugenol

structure. Careful analysis of the 2D NMR experiments (see **Figure 36**) confirmed the presence of a tetrasubstituted aromatic ring (A in **Figure 36**), bearing one propenyl pendant, as demonstrated by the HMBC correlation of the olefinic proton at 6.31 ppm (H-7') with a quaternary sp^2 carbon resonating a 136.4 ppm (C-5) and by the further correlations observed in COSY and HMBC spectra. In particular, the HMBC correlation of the methyl signal at 3.41 ppm with a quaternary sp^2 carbon at 146.1 ppm (C-7) established the location of the methoxy group on ring A.

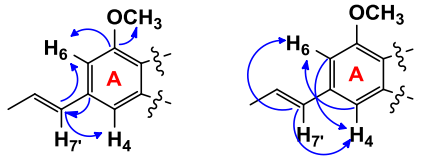

Figure 36: HMBC correlation for A-ring

Finally, the deshielded doublet observed in the ^{1}H NMR spectrum at 5.07 ppm (J = 9.5 Hz, H-2), coupled with a multiplet at 3.41 ppm (J = 9.5 Hz, H-3), in turn correlated to a singlet methyl signal at 1,35 ppm (s, H_3-8) indicated that the second propenyl chain of one eugenol unit has been modified; further analysis of 2D NMR spectra (see **Figures 93S – 95S Appendix C**) demonstrated the formation of a dihydrobenzofuran ring, with resonance values for H-2/C-2 and H-3/C-3 in perfect agreement with literature data.[49, 143] In particular, the HMBC correlation of the methyl at 1,35 ppm with the C-3a aromatic carbon, resonating at 50.75 ppm, confirmed the junction between the two monomers. Furthermore the coupling constant for C-2H and C-3H (J = 9.5 Hz) clearly showed that the adjacent 2-aryl and 3-methyl substituents are trans oriented. The lack of NMR signals due to a second methoxy group, as well as the replacement

of the second propenyl chain with a dihydrobenzofuran ring, are in agreement with the molecular mass found by ESI-MS spectrometry. Analysis of COSY, HSQC and HMBC spectra globally confirmed the structure **99**.

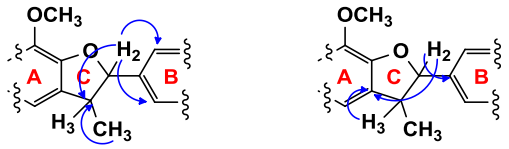

Figure 37: HMBC correlation for C-ring

A subsequent literature search showed that **99** is a previously unreported compounds, although being the demethylderivative of licarin A, a dihydrobenzofuran neolignan found in the wood of *Licaria aritu* and reported as antioxidant,[170] antiviral,[171] cytotoxic,[171] and neuroprotective[172] agent. Spectral data of licarin A are in agreement[173] with those of **99** (3'-*O*-demethyllicarin A). This product is interesting because its formation is not so obvious.

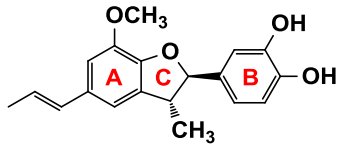

We present here a plausible hypothesis on the mechanism of formation of 3'-*O*-demethyllicarin A (**99**). As known from the literature, the reactions mediated by IBX on phenolic compounds, allow the phenolic 'umpolung' to yield the corresponding phenoxenium ion intermediate (See Section 2.2.1.1). This may be described with hybrid

resonance structures where the positive charge is formally delocalized in various positions as illustrated in **Scheme 25**. According to this hypothesis, the mechanism of IBX-mediated formation of **99** is illustrated in **Scheme 26**. Isoeugenol (**97**) adds to the iodine (V) center of IBX to produce a demethylated *ortho*-quinol derivative **100** and 2-iodobenzoic acid (**IBA**), the only by-product of this reaction. The reaction may proceed as an electronic substitution at *C*-5 of the *ortho*-activated aromatic ring of a second molecule of isoeugenol (**97**), by the *ortho*-quinol **100** bearing a positive charge at *C*-5, to form a the quinone-methide intermediate **101**. Finally an intramolecular cyclization due to a nucleophilic attack of the phenolic group at C-4 to the quinone-methide system may afford the heterodimeric dihydrobenzofuran neolignan **99**. It is worth noting that the reaction proceed with a *trans* diastereoselectivity, as previously observed in the formation of dihydrobenzofuran neolignans with a different dimerization mechanism (ex. enzyme-mediated oxidative coupling)[143] but similar final cyclization of the quinone methide intermediate.[143] To the best of my knowledge, there is no previous report in the literature for this kind of *in situ* hetero-dimerization to obtain dihydrobenzofuran neolignans.

Only one report was found in literature about the dimerization of isoeugenol (**97**) mediated by iodobenzene diacetate (IDA),[173] another reagent belonging to the hypervalent iodine family like IBX. In this paper the reaction occurred with homodimerization in the presence of IDA, and without *in situ* demethylation of the substrate. This reference confirm that demethylation occours before (and not after) the coupling of the two monomeric units and is in favour of our proposal of mechanism. Further experiments could confirm if this reaction is of general applicability to obtain new potentially bioactive dihydrobenzofuran neolignans. To

verify this hypothesis of mechanism a computational study, in collaboration with Prof. A. Rescifina (University of Catania), is in progress.

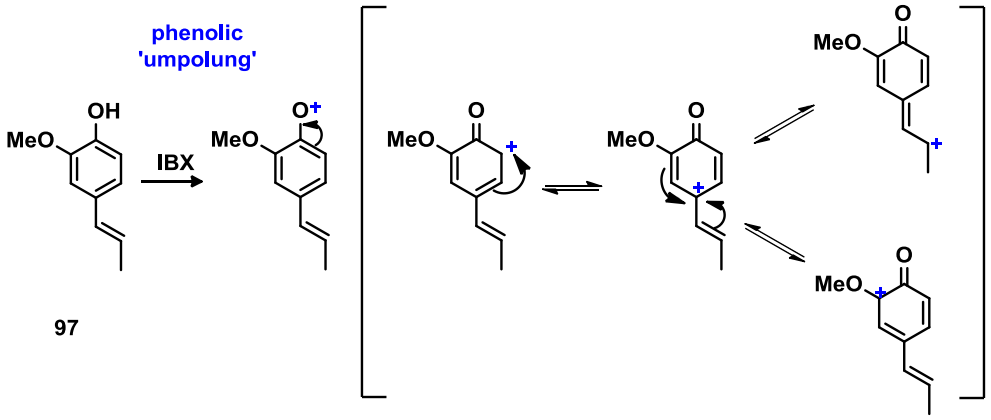

Scheme 25: formation of phenoxenium ion intermediate and its resonance structures

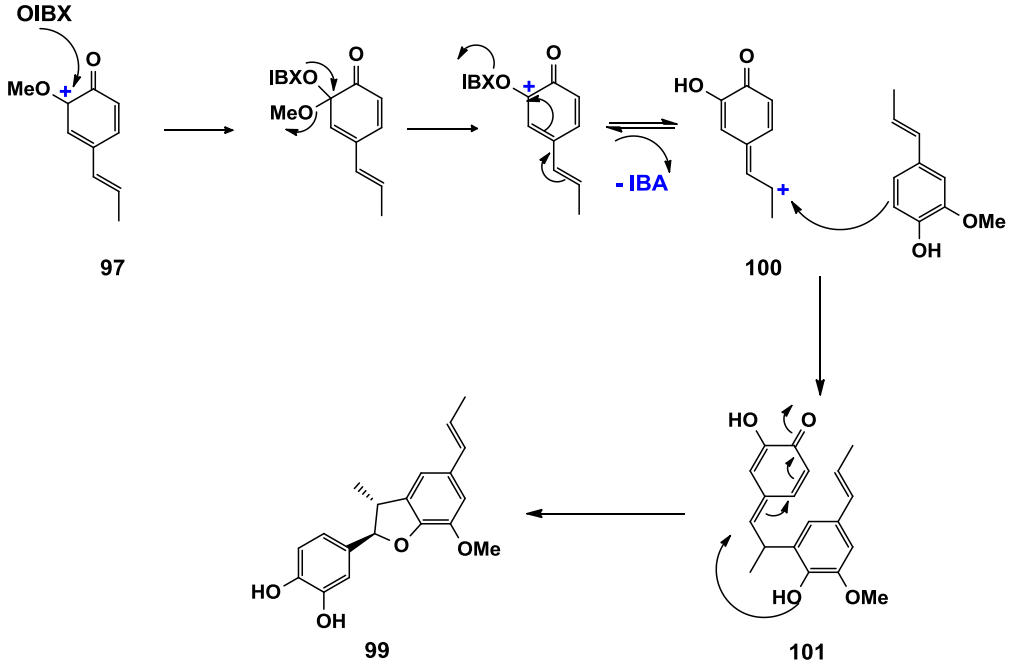

Scheme 26: proposal of the possible mechanism of reaction for the compound **99**

2.4 Contribution on total synthesis of ellagitannins

In the context of my International PhD course, I carried out an internship from January to July 2017 at the 'Institut des Sciences Moléculaires' (ISM, University of Bordeaux, France), in the "Organic synthesis and natural products" group (ORGA-SQ) under the supervision of Prof. Stéphane Quideau. The work research of this group is mostly focused on developing new methods for organic synthesis, applied to natural products total synthesis. A special interest of Prof. Quideau's team is devoted to the synthesis of polyphenols, so I planned to complete my doctoral training with a synthetic work on ellagitannins, a group of polyphenols with complex structure, whose biosynthesis and stereochemical details are reported in Section 1.1.5. The main goal of my internship work was:

- the scale-up of the total synthesis of vescalin (**54**), a compound beloging to the the subclass of the C-arylglucosidic ellagitannins;
- total synthesis of a vescalagin-fucose probe

2.4.1 Vescalin total synthesis

In the context of ellagitannins's chemistry, the total synthesis represents a challenge to better understand their biosynthesis, biological activity and structural features, in particular in terms of the stereochemistry of the NHTP (nonahydroxyterphenoyl) unit. This structural detail shows some ambiguity in literature, and this prompted researchers involved in this field to find a good strategy to establish without ambiguity the stereochemistry of the NHTP unit. The total synthesis of ellagitannins is very often inspired to their biosynthesis, and this offers different and very complex challenges for organic chemists: chemoselectivity, regioselectivity, and stereoselectivity, especially in terms of atroposelectivity related to the galloyl coupling. Thus, planning of an actractive synthetic strategy has to face efficiency and especially all these selectivity issues. To answer to this complex challenges in the specific case of the total synthesis of vescalin (**54**), prof. Quideau's team developed[174] an approach in which the protective groups played positive and negative strategic role in the modulation of the key step, namely the intramolecular biaryl coupling. Obviously, in a multi-step reaction like a total synthesis, the choosen protecting groups have to be compatible with the possibility of simple manipulation of the intermediates and an easy recover of the final product at the end of the synthesis. Then, it was designed a divergent and stereoselective synthetic route[174] to obtain vescalin (**54**) but also others more complex ellagitannins. Initially it was necessary to evaluate a possible retrosynthetic route (**Scheme 27**), inspired by the biosynthetic pathway (see **Scheme 7**). As summarized in **Scheme 27**, the retrosynthetic plan identified the polybenzylated compound **102** as the key immediate precursor of vescalin (**54**); **102** may be obtained trough a 5-*O*-galloylation, a [3,5]-biarylic atroposelective

coupling and an intramolecular *C*-arylglucosidation of an open intermediate, not shown in **Scheme 27**. In the synthetic direction, the sequential esterification of protected glucose with suitably protected galloyl units, followed by the [2,3] intramolecular biaryl coupling provide the ortoghonally protected bis-galloyl intermediate **103**.

Based on this retrosynthetic analysis, the scale-up (scale of grams) of the vescalin total synthesis was organized as follows:

- synthesis of the glucose precursor
- synthesis of the galloyl precursor
- multi-step synthesis of vescalin

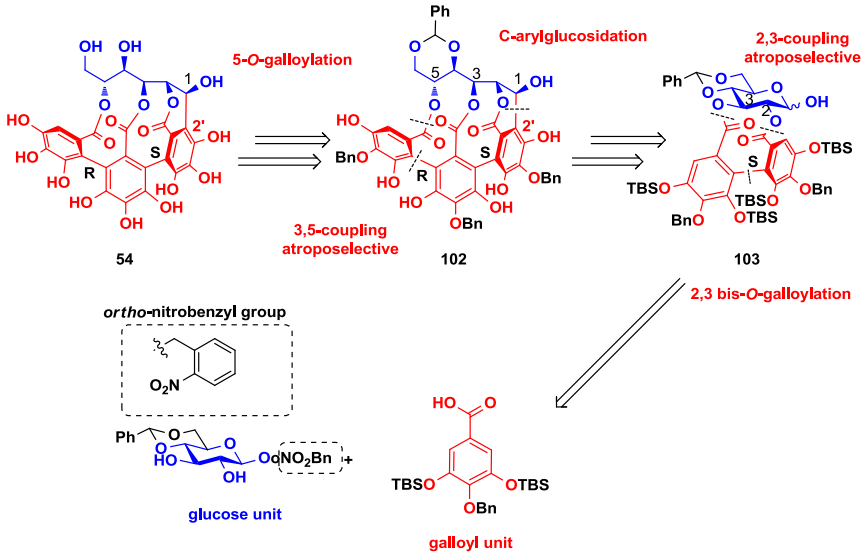

Scheme 27: retrosynthetic pathway

*2.4.1.1 Synthesis of the glucose precursor **108***

My first activity was focused on the preparation of the glucose precursor. The commercially avaible acetobromoglucose (**104**) was employed as starting material to perform the glycosidation reaction according to Knoenigs-Knorr conditions.[175] The *o*-nitrobenzyl alcohol (**104**) was selected as hydroxyl protecting group at the anomeric position;

the advantages of this protection is that the *o*-nitrobenzyl is a photolabile group, easily removable under mild conditions[176] and is a convenient alternative to other conventional protective methods. The *o*-nitrobenzyl unit (*o*NO_2Bn) is stable under many chemical conditions and can be selectively removed by UV irradiation around 300-350 nm. The reaction was carried out on 12.5 g of acetotobromoglucose (**104**), in the presence of *o*-nitrobenzyl alcohol (**105**), Ag_2CO_3 and I_2 as catalyst, in dry dichloromethane as reported in **Scheme 28** (see the Experimental section for further details). The *O*-glycoside **106** was obtained after purification and the NMR data were in perfect agreement with those previously reported in the literature.[177] Then, the deacetylation of *O*-glycoside **106** under conventional conditions (NaOMe in methanol) quantitatively provided the tetrahydroxy sugar **107**. Also in this case the structure was confirmed by NMR analysis.[178, 179] Finally the tetraol **107** was further protected at the *O*-4 and *O*-6 positions by treatment with $ZnCl_2$ and benzaldehyde (**Scheme 28**) to yield the benzylidene derivative **108** with alcoholic functions at *C*-2 and *C*-3. The regioselectivity of this protection was driven by the enhanced nucleophilicity of the primary alcohol at *C*-6 position. The NMR data were in perfect agreement with the formation of this compound.[180] The ^{1}H NMR and ^{13}C NMR spectra of compound **108** are reported in **Figures 96S** and **97S**, respectively (see **Appendix D**).

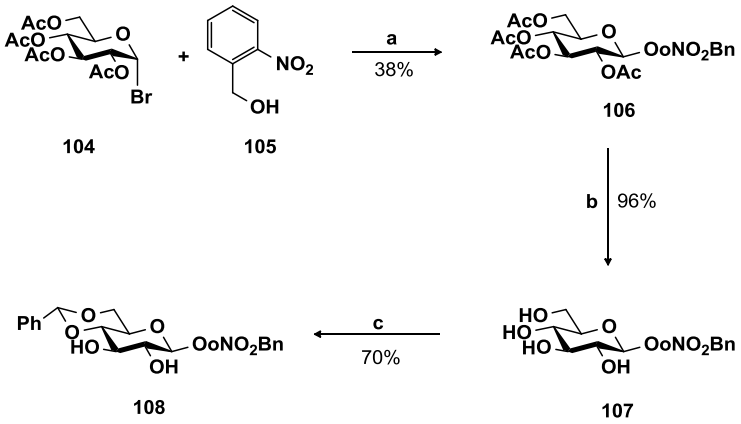

Scheme 28: Conditions:(**a**) Ag_2CO_3 (3 eq.), I_2 (cat), CH_2Cl_2, rt, 16 h; (**b**) NaOMe (1 eq.), MeOH, rt, 30 min.; (**c**) $ZnCl_2$ (5.3 eq.), benzaldeyde, rt, 24 h.

*2.4.1.2 Synthesis of the galloyl precursor **111***

The next step was the synthesis of a galloyl precursor (**Scheme 29**) to be employed for the esterification of glucose intermediate, namely the protection of phenolic functions of the galloyl precursor to avoid the formation of other by-products during the esterification. Furthemore, the *para*-phenolic functions need to be differently protected from the two *meta*-positions, because for the key step of the total synthesis of vescalin (**54**), the coupling developed by H. Yamada for the synthesis of corilagin,[181] was choosen (see **Scheme 30**),[181] and in this conditions, Feldman and co-workers reported the formation of regioisomeric by-products, when the *para*-phenolic function was unprotected.[182] To this aim, the methyl gallate was selectively protected in the *para*-phenolic function with a benzyl group (Bn), and both *meta*-phenolic positions with terbutylmethylsilane group (TBS) as it is summarized in **Scheme 29**. The benzylated derivative **109**, was obtained by a simple peracetylation of the commercially avaible methyl gallate, subsequently benzylation of its *para*-position and deacetylation of both meta-functions[183] (this two steps are not showed). As reported in **Scheme 29, a**, a saponification of compound **109** afforded, after purification, the *para*-benzylated

carboxylic acid **110**; the NMR data were in perfect agreement with that previously reported in the literature for this compound.[184] Then (**Scheme 29**, **b**), a silylation reaction was performed **110**, in the presence of TBSCl and imidazole, affording a product silylated also at the acidic function;, therefore a selective deprotection was performed (**Scheme 29**, **c**) to yield, after purification, the prodcut **111** with free acidic function. The NMR data of this compounds were in agreement with those previously reported in the literature.[185] The ^{1}H NMR and ^{13}C NMR spectra of compound **111** are reported in **Figures 98S** and **99S**, respectively (see **Appendix D**).

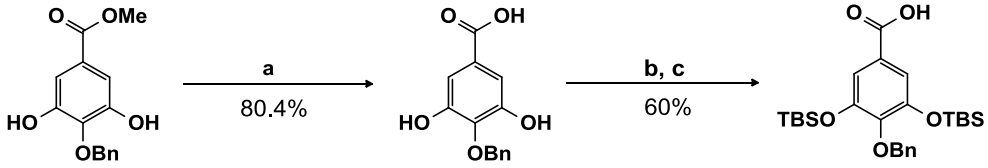

Scheme 29: Conditions:(**a**) NaOH (3.3 eq.), THF/MeOH/H_2O, rt, 2.5 h; (**b**) TBSCl (4.7 eq.), imidazole (10 eq.), DMF, rt, 24 h (**c**) CH_3COOH/H_2O, THF, rt, 18 h.

*2.4.1.3 Multi-step synthesis of vescalin (**54**)*

The esterification of the remaining *C*-2 and *C*-3 diol groups of **108** with the suitably protected gallic acid **111** under modified Steglich's conditions[186] afforded, after purification, the fully protected sugar **112** as summarized in **Scheme 30** (see the Experimental section for details). The reaction was performed in the presence of an acid activating agent, namely the *N*-(3-Dimethylaminopropyl)-*N*′-ethylcarbodiimide hydrochloride (EDCI, 5.0 eq.) and the 4-dimethylaminopyridine (DMAP, 7.0 eq.) and required a slight excess of **112** (about 1.25 - 1.5 eq.) for each alcohol functions. The use of EDCI, instead *N*,*N*′-dicicloesilcarbodiimide (DCC), normally used in in this kind of reactions, has the advantage of simplifying the crude treatment; in fact when DCC is used for the esterification reaction, dicyclohexylurea (DCU) can be formed as by-

product; DCU is difficult to eliminate during treatment and makes purifications often problematic; conversely the secondary product obtained from EDCI during the esterification is an ammonium salt, easily eliminated by partition in acidic conditions.

Subsequently, as reported in **Scheme 30**, the intermediate **112** was submitted to desilylation reaction to obtain a product with free *meta*-phenolic functions of both galloyl units, to be used as substrate for the key intramolecular oxidative coupling. An orthogonal deprotection was carried out using *tetra*-*n*-butylammonium fluoride (TBAF), thus avoiding to use the corresponding hydrofluoric acid (HF) which could remove the benzylidene unit present at position 4 and 6 of the glucosidic core. In these conditions, the compound **113** was quantitatively obtained.

At this point it was decided to proceed directly with the key step, the intramolecular biaryl oxidative coupling mediated by $CuCl_2$ and *n*-butylamine as reported in **Scheme 30** (see the experimental section for details). We employed the conditions reported by Yamada, except for the use of *n*-butylamine, which makes the mixture more homogeneous and thus yields more repeatable. Hence, the coupling was successful, affording with good yield the desired *S*-configured derivative **114** as the only isomer. The structure of this product was confirmed by complete NMR analysis and all resonances were unambiguously assigned (see the Experimental section). The ^{1}H and ^{13}C NMR spectra of **114** are reported in the **Figures 100S** and **101S** (see **Appendix D**).

In conclusion, during my intership in Bordeaux it was reached an important point along the synthesis of vescalin (**54**), by providing access to the advanced intermediate **114**, which features the presence of synthetically challenging [2,3] biaryl bond and orthogonally protected phenol rings. Just for the sake of completeness, I reported in **Scheme 31**

the subsequently steps to obtain the final product vescalin (**54**) starting from this intermediate.

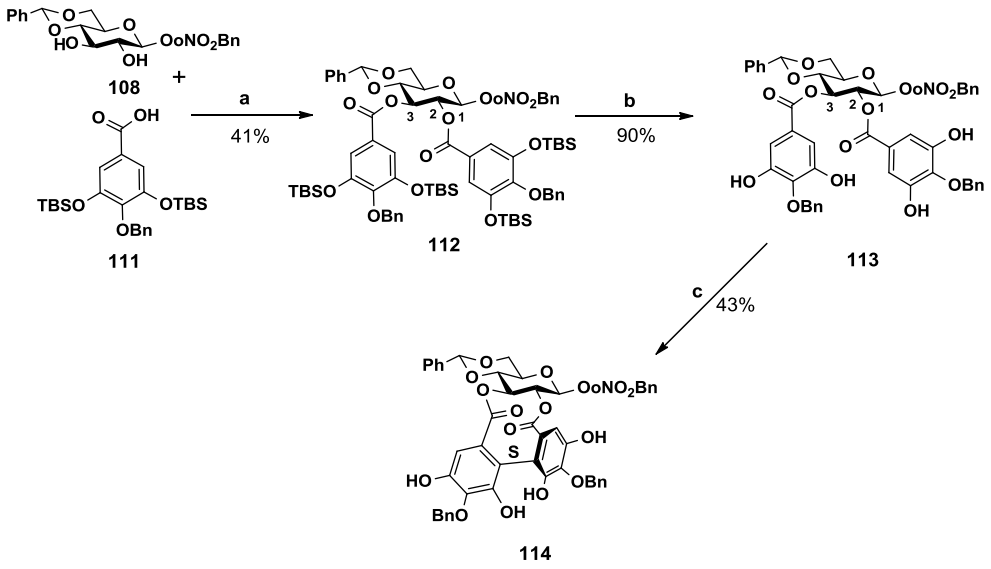

Scheme 30: Conditions:(**a**) DMAP (7.0 eq.), EDCI.HCl (5 eq.), CH_2Cl_2, rt, 18 h; (**b**) TBAF (6.0 eq.), acetic acid (12 eq.), THF, rt, 4 h (**c**) $CuCl_2$ (5 eq.), $nBuNH_2$ (25.0 eq.), MeOH, rt, 30 min.

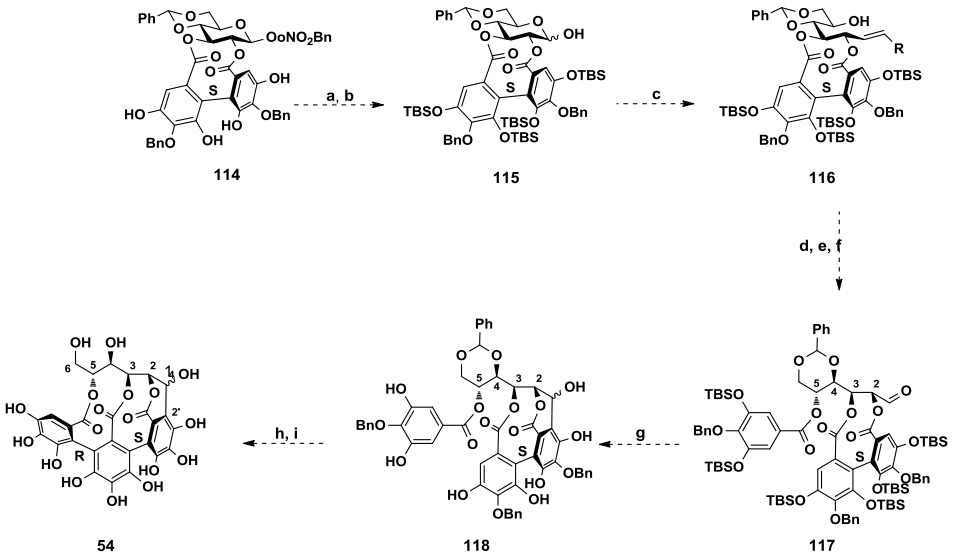

Scheme 31: Conditions:(**a**) TBSOtr (15.0 eq.), DMAP (1.0 eq.), NEt_3 (20.0 eq.); CH_2Cl_2, reflux, 7 h; (**b**) THF/EtOH/H_2O, 350 nm, rt, 48 h (**c**) Ph_3OCHO_2Et, TFE, toluene, 60 °C, 5 h; (**d**) DMAP (7.0 eq.), EDCI.HCl (5 eq.), CH_2Cl_2, rt, 6 h; (**e**) OsO_4 (0.02 eq.), NMO (1.5 eq.), 2,6-lutidine, dioxane/H_2O; (**f**) $Pb(OAc)_4$, $NaHCO_3$, CH_2Cl_2,

rt, 5 min; (**g**) TBAF (6.0 eq.), acetic acid (12 eq.), THF, rt, 4 h; (h) $CuCl_2$ (5 eq.), sperteine, MeOH, rt, 30 min.; (i) H_2, $Pd(OH)_2$, THF; HCl 0.2 N.

2.4.2 Synthesis of a vescalagin-fucose conjugate

As described in the Introduction, the ambiguity about the atropisomerism of the triphenoyl moiety in many ellagitannins prompted a number of researchers in the challenge of the total synthesis of these compounds. Nevertheless, often the absolute configuration of stereocenters was not unambiguously established. A possible alternative route to study the stereochemistry of the NHTP unit of ellagitannins could be to study a cocrystal with a protein of a vescalagin derivative. In fact in a recent work of Reymond,[187] fucosylated conjugate of a series of dendrimers were prepared to obtain a cocrystall with lectin A (Lec-A), a protein able to selectively ricognize fucose (**Figure 38**), and finally these complexes were studied through X-Ray. Based on this paper Quideau and his team planned to use a similar approach for vescalagin (**49**), with the aim to definitively solve the stereochemistry ambiguity of the NHTP unit. Thus, we envisaged that, in order to co-crystallize vescalagin (**49**) with Lec-A, fucose must be covalently bonded to vescalagin (**49**), and on this basis we planned to synthetize a vescalagin-fucose conjugate, that is, more precisely, a molecule with a linker connecting vescalagin with fucose (**119**), in which the linker was an aromatic moiety; in fact, as described in the paper of Reymond, this structural motif could increase the recognition with LecA.

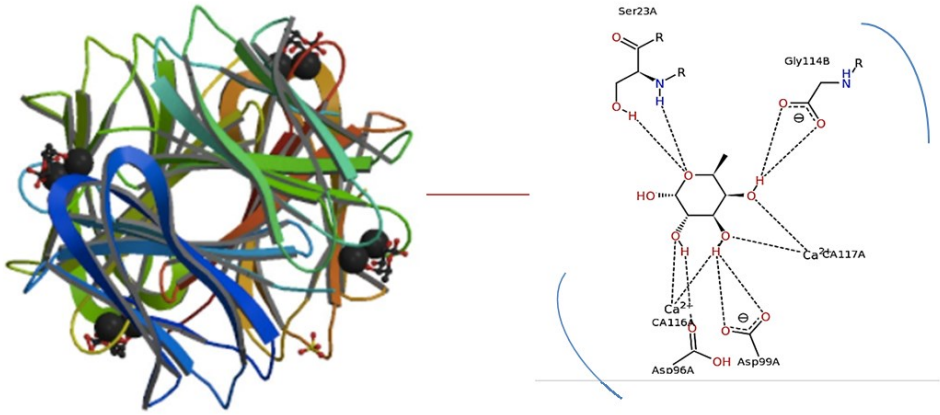

Figure 38:*co*-crystal structure of Lec-A with a molecule of fucose from protein data bank (PDB) 10.2210/pdb1oxc/pdb

Thus, a vescalagin-linker-fucose through a thiol bond was designed, being the thiol a more effective nucleophile than primary and secondary alcohols of fucose, and so more reactive towards the nucleophilic substitution on the anomeric carbon of vescalagin (**49**).

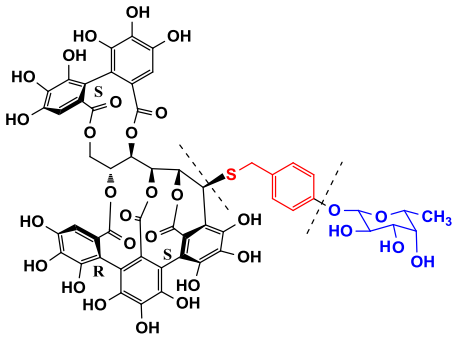

119

As summarized in **Scheme 32**, the retrosynthetic analysis of vescalagin-fucose conjugate showed two main disconnections: the cleavage between the linker conjugated to fucose and vescalagin (**49**), and then the cleavage between the aromatic linker and fucose. This strategy leads to three starting fragments: vescalagin, 4-mercaptomethyl phenol, and finally the acetobromofucose.

Based on this retrosynthetic analysis, the synthesis of the vescalagin-fucose conjugate was organized in:

- synthesis of fucose precursor
- synthesis of aromatic precursor
- synthesis of linker precursor

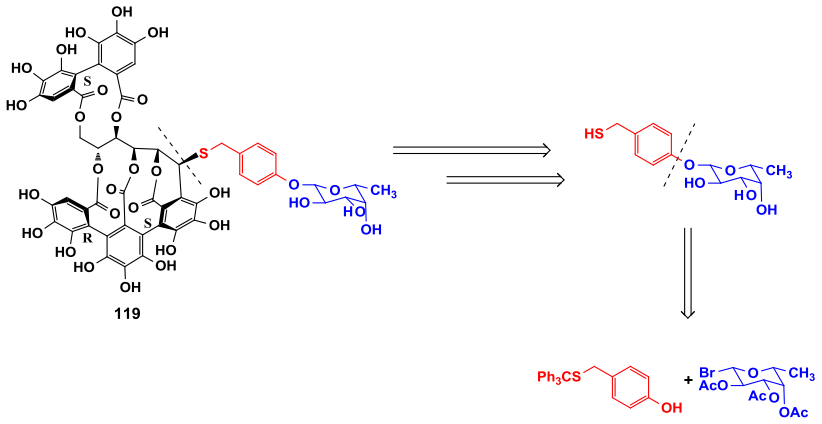

Scheme 32: retrosynthetic pathway

*2.4.2.1 Synthesis of the fucose precursor **122***

As reported in **Scheme 33**, and according to the procedure described in the literature,[187] fucose (**120**) was acetylated in conventional conditions in presence of pyridine and Ac_2O, to obtain a racemic mixture of α-β peracetilated fucose (**121**) in quantitative yield. Then, the acetofucose (**121**) was employed to perform aselective bromination, to give exclusively the β-acetobromofucose (**122**, **Scheme 33**).[188] It is worth of noting that the manipulation of fucose and their derivatives is not simple, because of their instability. The structures of all compounds prepared were confermed by NMR, and all data acquired were in perfect agreement with those previously reported in literature.

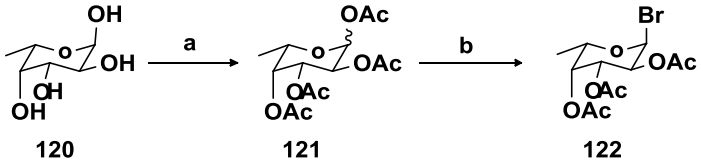

Scheme 33: (**a**) 1:1 pyridine-Ac_2O, reflux, 24 h; (**b**) HBr in 33% CH_3COOH, CH_2Cl_2, rt, 2 h.

*2.4.2.2 Synthesis of the aromatic precursor **127***

The aromatic precursor was prepared in four steps using as starting material the 4-hydroxy benzyl alcohol (**123**) as reported in **Scheme 34**. First, the phenolic function was acetylated in mild conditions to yield the compound **124** with free alcoholic function. A nucleophilic substitution was carried out on **124** in presence of PPh_3 and CBr_4[189] in order to obtain the corresponding brominated derivative **125** (**Scheme 34**). The benzyl bromide **125** was subsequently employed in a nucleophilic substitution with K_2CO_3 and triphenylmethanethiol (TrSH), to obtain the benzyl trityl derivative **126**. Finally, a simple methanolysis, carried out in weakly basic conditions, converted compound **126** into the free phenol **127** in quantitative yield. The structures of all intermediates and products were confirmed by NMR, and the data were in perfect agreement with those previously reported. The ^1H NMR and ^{13}C NMR spectra of compound **127** are reported in **Figures 102S** and **103S**, respectively (see **Appendix D**).

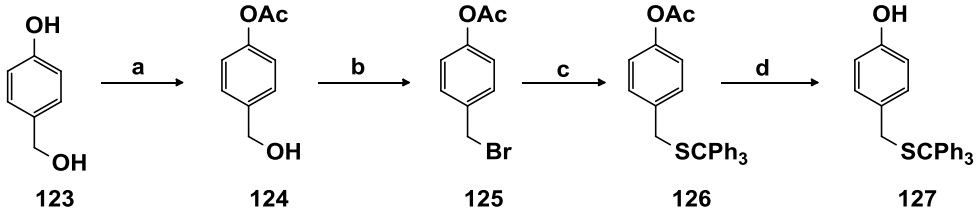

Scheme 34: (**a**) K_2CO_3 (1 eq), Ac_2O (1 eq), acetone, reflux, 6 h; (**b**) PPh_3 (1.1 eq), CBr_4 (1.3 eq), CH_2Cl_2, rt, 20 h; (**c**) K_2CO_3 (1.5 eq), TrSH (1.1 eq), acetone, reflux, 20 h; (**d**) K_2CO_3, MeOH, rt, 30 min.

2.4.2.3 Synthesis of the linker precursor

The key step, but also the most crytical one, was the *O*-glycosidation between **122** and **127** as reported in **Scheme 35**. The Koenigs-Knorr reaction conditions were selected to perform the fucosylation reaction to obtain the linker **128**, because this reaction reported in 1901 is still one of the most useful reactions for preparing a wide variety of *O*-glycosides.[190] This methodology requires silver compounds as catalyst and silver oxide as well as carbonate, nitrate, or triflate silver salts are the most commonly employed. Also a drying agent such as calcium sulfate (drierite), calcium chloride, or molecular sieves is recommended. Improved yields are obtained with iodide, vigorous stirring, and light protection during the course of the reaction. On this basis, I performed some experiments of *o*-fucosylation employing different Koenigs-Knorr reaction conditions: reagent, solvent and equivalents were varied as reported in the **Table 10**. All reactions were followed by TLC and NMR, and in each experiment the complete conversion of both **122** and **127** reagents was observed, but the expected product **128** was not obtained; it was observed only the formation of degradation products of **122** and **127**.

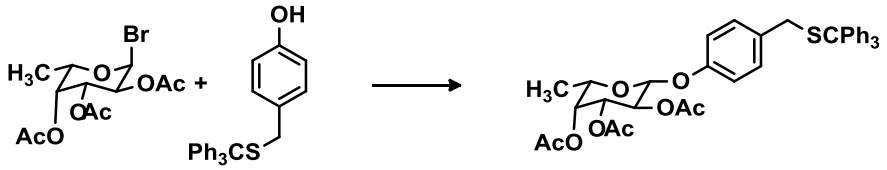

122 **127** **128**

Scheme 35

Table 10: different Koenigs-Knorr reaction conditions used

Entry	127	catalyst (equiv.)	solvent	*T* (°C)	time	conversion(%)	128 (%)
1	1.2 eq	Ag_2CO_3 (3.0)	CH_2Cl_2	rt	24 h	100	0
2	1.2 eq.	Ag_2CO_3 (3.0)	CH_2Cl_2	rt	24 h	100	0
3	2.2 eq	Ag_2CO_3 (5.0)	CH_2Cl_2	rt	24 h	100	0
4	2.2 eq	Ag_2CO_3 (4.0)	CH_2Cl_2	rt	24 h	100	0
5	1.0 eq	K_2CO_3 (3.0)	acetone	rt	24 h	100	0
6	1.0 eq	DIPEA (4.0)	CH_3CN	rt→reflux	24 h	100	0

To better understand what had happened during these reactions, I tried to purify one of these crude mixtures, namely the entry n. 6 In **Table 10**. After the purification, 4-hydroxy benzyl alcohol, 2-hydroxyacetotofucose and the reagent TrSH were isolated. These observations suggested an incompatibility of the Koenigs-Knorr reaction conditions with the pattern of substitution of our starting materials **122** and **127**. Thus, we decided to carry out the reaction according to the Mitsunobu conditions,[191] previously applied to several different phenols, where the acidity of the phenols was varied using electron donating or withdrawing substituents. In this reaction the hemiacetals can be activated *in situ*. Hence, the reaction was performed directly on fucose (**120**) in the conditions reported in **Table 11**. Unfortunately, also in this case the expected product was not obtained, and it is worth of noting here that no conversion of substrate was observed.

Table 11: different Mitsunobu reaction conditions used

Entry	120	reagent 1 (equiv.)	reagent 2 (equiv.)	Solvent	*T* (°C)	Time	Conversion (%)	128 (%)
1	3.0 eq	PPh_3 (3.0)	DIAD	dioxane	rt→reflux	48 h	0	0
2	3.0 eq.	PPh_3 (3.0)	DEAD	dioxane	rt→reflux	48 h	0	0

In conclusion, the attempts to perform *o*-glycosilation both on fucose (**120**) and acetobromofucose (**121**) in the above reported conditions did not succeed; furthermore, the *o*-glycosilation with Lewis acids was ruled out to avoid the deprotection of the trityl group of

compound **127**. Based on the unsuccessful experiments it was decided to modify the synthetic approach.

2.4.2.4 New synthetic approach to obtain a vescalagin-fucose conjugate

In the new target molecule (**129**) the connection between fucose and the aromatic linker was designed through an amidic bond. The retrosynthetic analysis indicated as starting materials 4-tritylthiomethylaniline (**130**) and the fucose derivative **131** in which the hydroxyl group at the anomeric carbon was substituted by an acetate group (**Scheme 37**). Thus, I planned all the steps to obtain the desired product **129** according to **Schemes 37**, **38** and **39**.

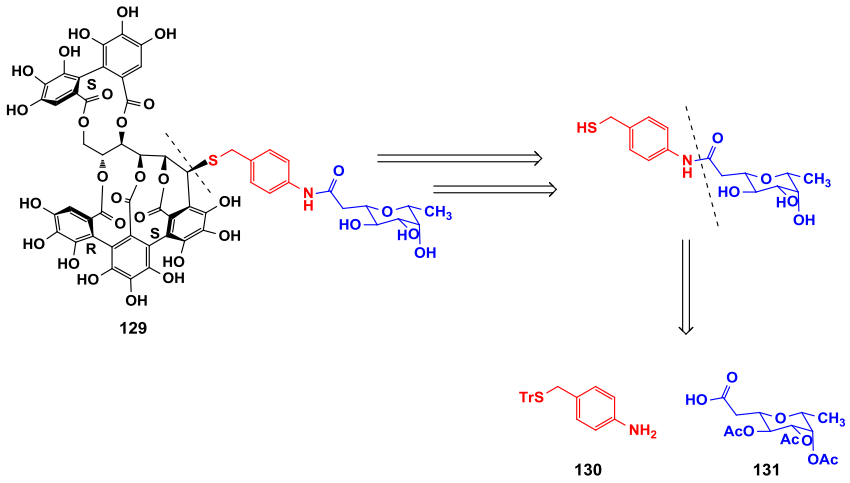

Scheme 36: retrosynthetic pathway

To obtain the intermediate **131** I used the reaction sequence reported in **Scheme 37**; namely, compound **120** was used as starting material and subjected to a standard peracetylation; the peracetate **121** in the presence of allyltrimethylsilane, boron trifluoride diethyl etherate ($BF_3 \bullet Et_2O$) and trimethylsilyl trifluoromethanesulfonate (TMSOTf)

afforded the intermediate **132**. Then, **132** was employed to obtain **131** using $NaIO_4$ and $RuCl_3$.

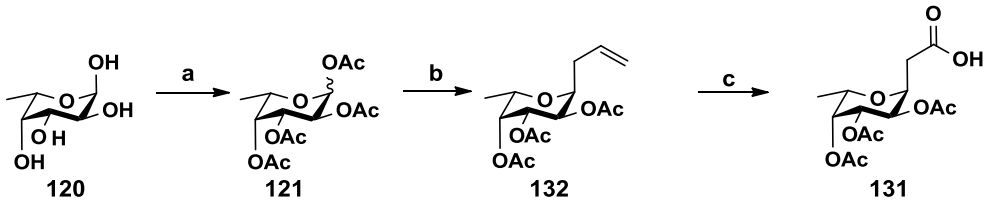

Scheme 37: (**a**) 1:1 pyridine-Ac_2O, reflux, 24 h; (**b**) allyltrimethylsilane (2.0 eq.), $BF_3.Et_2O$, TMSOTf (0.2 eq), *dry* CH_3CN, 0 °C, 8 h; (**c**) $NaIO_4$ (4 eq.), $RuCl_3$ (0.04 eq.), H_2O/ CH_3CN /CCl_4, rt, 4 h.

As usual, all the structures of compounds prepared in this section were confermed by NMR, and all data acquired were in perfect agreement with those previously reported in literature. In conclusion, also in this part of my work it was reached an important point along the synthesis of the complex vescalagin-fucose conjugate **129**, by providing access to the intermediate **131**, suitable for the synthesis of different fucose conjugates. In **Schemes 38** and **39** the other steps for the synthesis of the target molecule (**129**) are summarized.

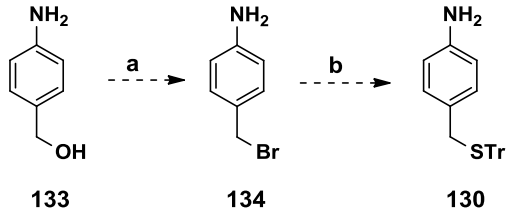

Scheme 38:(**a**) PPh_3 (1.1 eq), CBr_4 (1.3 eq), CH_2Cl_2, rt, 20 h; (**b**) K_2CO_3 (1.5 eq), TrSH (1.1 eq), acetone, reflux, 20 h;

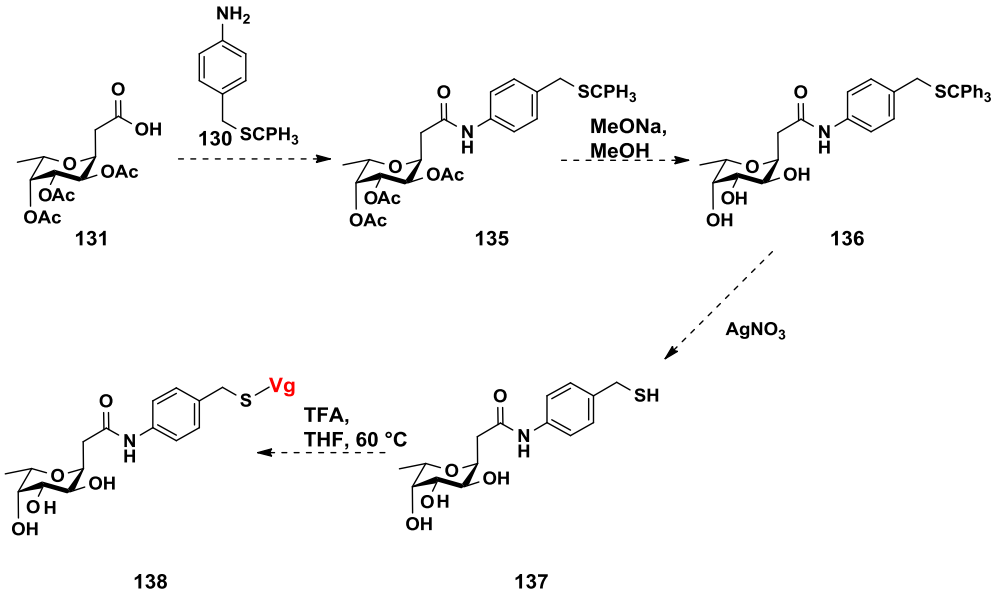

Scheme 39

CHAPTER 3

3. CONCLUSIONS AND PERSPECTIVES

For centuries, natural products have been considered a source of bioactive agents, capable to play a functional role in biological systems; traditional medicine is largely based on the use of natural products as chemotherapeutic or chemopreventive agents in the treatment of different diseases. In recent years a renewed attention towards bioactive natural products allowed to develop new effective drugs through synthetic modification of a natural 'lead' or total synthesis of new bioinspired compounds. My research project was planned in this scenario, with the aim to obtain new potential chemotherapeutic agents starting from natural or bio-inspired polyphenols.

Hence, during my PhD research activity, two polyphenol groups were studied, namely benzoxanthene lignans and bisphenol neolignans; during the synthesis of magnolol-inspired neolignans, an unexpected dihydrobenzofuran neolignan was also obtained and characterized. In addition, the last part of my work was carried out at the University of Bordeaux, under the guidance of Prof. Stéphane Quideau, and was devoted to synthetic work on ellagitannins, an important subgroup of tannin family.

3.1 Benzo[*k,l*]xanthene lignans

Benzok[k,l]xanthene lignans (BXLs) represent a small group of polyphenols very rarely encountered in Nature, possessing an extensively conjugated and fluorescent core; their biological properties are consequently scarcely explored, although a number of studies, including DNA interaction and antitumor properties, have been carried out by Prof. Tringali's team in recent years. We planned to study the possible interaction of BXLs with G-Quadruplex DNA, a target involved in the

research of new selective anti-cancer drugs; this study was carried out in collaboration with Prof. G. Piccialli (University of Naples, see section 2.1.7). I have synthetized some previously reported BXLs (**36**, **38**, **39** and **61**) and new benzoxanthene-related phenazines (**69**, **71**, **73**, **74** and **75**) with an extended planar moiety. Unfortunately, the phenazines were not able to effectively recognize G-Q DNA, whereas the BXLs, and in particular **36**, showed recognition of GQ-DNA: this confirmed the essential role of the catechol groups in BXL structure. A possible continuation of this study could be the synthesis of a new library of BXLs, modifying the flexible pendants at C1' and C1'' with more appropriate functional groups for G-Q specific recognition.

Further studies on BXLs were carried out in collaboration with other laboratories; namely, in collaboration with Prof. A. Zampella (University of Naples) and Prof. G. Fiorucci (University of Perugia, see Section 2.1.8), the BXLs **36**, **61**, **67** and the BXL-related phenazines **69**, **71** and **73** were studied as agonist/antagonist of the Bile X receptors FXR and LXRα/β. This preliminary study showed that the phenazine **73** was an effective antagonist of FXR/RXR and also the phenazine **71** showed a moderate activity. Both these phenazines are related to the most lipophilic BXLs **61** and **38**. These first data are encouraging, and we have already planned to test further compounds; in particular, the assay on BXL **38** should confirm that the phenazine portion is an important structural determinant for the antagonist action.

We also studied BXLs and their related phenazines as antimicrobial agents in collaboration with Prof. G. Tempera (University of Catania). Preliminary antibacterial assays on compounds **61, 67**, and **69** showed a low activity, showing MIC values higher than 85.5 μM (**61**), 94.3 μM (**67**), and 42.4 μM (**69**); thus, BXLs were not further evaluated

as antibacterial agents. The data on antimycotic activity were more encouraging and were carried out on a larger set of compounds (**38**, **43**, **61**, **63**, **65**, **67** and **69**); the results showed that BXLs are a promising class of new antimycotic agents, showing a strain growth inhibition in the range of μM and better than the fluconazole; for example BXLs **38**, **63**, **65** and **69** were better antymicotic than the used reference (13.0 μM) against the 3 strain, with inhibition values of 9.5, 5.8, 2.8 and 1.3 μM. Indeed they could be used to develop new chemotherapeutic against resistant strains of *Candida* spp.; in fact, BXLs **38** and **63** are significantly active against fluconazole resistent *Candida* non *albicans* strains 2, 3 and 4 (MIC = 11.7 μM and 19.2 μM, respectively). Furthermore, it is worth noting that the catechol moiety is important for growth inhibition of *Candida*, because **43**, the methylated analogue of **38**, is not active towards all strain of *Candida* evaluated in this context. Considering the difficulty to find new and effective antimycotic agents, these results are promising and suggest to continue this study on BXLs.

3.2 Magnolol-inspired neolignans

The second group of polyphenols included in this study is related to the neolignan magnolol (**44**); this bisphenol, originally found in *Magnolia* species, is largely cited in the literature for a variety of biological activities, although some aspects, such as its potential antidiabetic properties, were not properly studied. Thus, I firstly tried to modify magnolol employing the environmental benign reagent IBX; subsequently, I developed a simple chemo-enzymatic approach to obtain a small library of magnolol-inspired compounds employing both the peroxidase enzyme HPR and IBX. This work afforded compounds **81**, **82** and **84** – **93**, that we evaluated as yeast α-glucosidase inhibitors. The α-

Glucosidase inhibition is a chemotherapeutic strategy used to lower blood glucose level, so this biochemical assay is the first step to discover new potential antidiabetic agents. A number of synthetic bisphenols, and specially compounds **81** (IC_{50} =0.49 μM), **85** IC_{50} = 0.50 μM) and **86** (IC_{50} = 0.86 μM) showed IC_{50} values lower than the natural bisphenols magnolol (**44**) and honokiol (**45**), as well as of the reference compound quercetin; these compounds resulted by far more potent than acarbose (**46**), a carbohydrate-related drug based on α-glucosidase inhibition (See Section 2.2.2). To gain some insight about the mode of action of these neolignans, a kinetic study of the inhibitory effect of the most potent compound **88** on yeast α-glucosidase was carried out. The results indicated that **88** acts as a competitive inhibitor, with a *Ki* value of 0.86 μM. In conclusion, this study highlighted a new class of magnolol-related neolignans with potent yeast α-glucosidase inhibitory activity, which is a promising property in view of their possible optimization as new antidiabetic drugs.

It is worth of mention here that, during the above study, an unexpected product was obtained by reaction of isoeugenol (**97**) with IBX. This compound was isolated and its structure was established by spectral analysis as that of a new dihydrobenzofuran neolignan, demethylicarin A (**99**), related to the bioactive natural product licarin A. I proposed here a possible mechanism of formation for **99**. As a continuation of this work, further dihydrobenzofuran neolignans will be synthetized through this reaction, for a future evaluation of their biological properties.

It is well-known that polyphenols bearing a catechol moiety display enhanced antioxidant properties. Considering that some of the above cited magnolol-inspired compounds have one or two catechols, we

started a collaboration with Prof. R. Amorati (University of Bologna) to study the chain-breaking antioxidant activity of some hydroxylated and methoxylated magnolol derivatives, namely compounds **81**, **82**, **84** and **85.** The rate constant of the reaction with ROO• radicals of these compounds was determined (see **Table 6** in Section 2.2.3); in addition Infrared spectroscopy and DFT calculations were used to rationalize the results: this study pointed out the role of the H-bond network. These results confirmed that the introduction of *ortho*-hydroxyl groups in the magnolol scaffold is a good strategy to obtain new and more potent chain-breaking antioxidants. The recognized importance of antioxidant properties in contrasting degenerative diseases suggests that this results may help the discovery of novel pharmacologically active bisphenol neolignans.

The availability of compounds **81**, **82**, **84 - 96** related to magnolol prompted us to try to find new biological targets for this group of neolignans. So we asked to the group of Prof. G. Bifulco (University of Salerno) to carry out in collaboration an inverse virtual screening study, and to that of Prof. G. Valdameri (Federal University of Paraná, Brazil) to evaluate some magnolol analogues as ABCG2 inhibitors.

To perform the inverse virtual screening, I make a short internship at the laboratory of Prof. Bifulco in Salerno. The screening was carried out on a panel of 307 biological targets involved in the occurrence of cancer. The results showed the affinity of magnolol analogues with four proteins, namely: tankyrase 2, two different bromodomain-containig protein 4 and casein kinase II. The pertinent biochemical assays were carried out on selected candidates in collaboration with Prof. Panagis Filippakopoulos (Oxford University, UK) and with Prof. Ines Bruno (University of Salerno). The theoretical assumptions were confirmed only

for tankyrase 2: three compounds (**85**, **87** and **89**) showed a K_D in the low nanomolar range (7 – 21.9 nM), whereas other two and the natural 'lead' magnolol (**44**) resulted inactive. These results are very encouraging and indicate that the chemical modification of magnolol is a structural determinant for the interaction with tankyrase 2.

The study on ABCG2 inhibitors is still in progress. This protein is involved in the observed 'Multi Drug Resistance' (MDR), so find a new inhibitor could result useful to contrast resistance to many anticancer drugs. A first set of compounds has already been examined, and promising positive results were obtained for compounds **91** and **95** that are goog inhibitors in the range of μM. Considering this promising result we wanted to extend this evaluation also on the compounds **81**, **85**, **86**, **88**, **89**, **90** and **96**. The experiments are in progress.

3.3 Contribution to the total synthesis of vescalin

Many biological evaluation of ellagitannins has also showed their potent antiviral- and antitumor-related activities. From a structural point of view, ellagitannins have an unique structural characteristic, featured by an open-chain glucose core linked through a C-C bond to one of their galloyl-derived units.

However until today, there are conflitting data in literature about the stereochemistry of the NHTP unit of this class of compounds. For the above cited reasons is rasoneable to face up to the challange of total synthesis of ellagitannins, or to plan other stratetegies allowing to clarify this kind of issues. In this context my intership in the lab of Prof. Quideau has beeb inserted. In fact my activity was focused giving an important contribut to the total synthesis of vescalin (**54**) according to **Schemes 28 - 31** (see section 2.5.1), for which I achieved an important point along the

synthesis by supplying access to the intermediate **114**, which features the presence of synthetically challenging [2,3] biaryl bonds and orthogonally protected phenol rings. Furthermore, given the importance solving the stereochemistry issue of ellagitannins, I was also involved in a project in which a different strategy was used; the main goal of this project was to obtain a vescalagin fucose derivative to use it as substrate for the complexation with Lec-A, with the final objective to study by XRay this complex.

For this aim, I planned all the synthetic steps to obtain the vescalagine derivative **119**, and I reached a good point along this synthetic challange by supplying the access to the important intermediates **122** and **127**. The unsuccessful experiments to obtain the key intermediate **128** (see **Scheme 35**) prompted us to change the synthetic approach according to **Schemes 36 - 39**. For this last point, I achieved an important point planning the total synthesis of the new amidic vescalagine fucose derivative **139**, and I supplied the compound **132**, which is one of the building blocks.

3.4 Final comment

In conclusion the above reported results about synthesis and biological evaluation of bioinspired polyphenols confirm that natural products may be considered ‘lead compounds’ or ‘privileged structures’ and their optimization may afford new potential chemotherapeutic agents. On the basis of the available data at the moment of these conclusions, benzoxanthene lignans, already identified as DNA-interactive and antiproliferative, appear promising antimicotic agents, whereas the related phenazines are worth of further evaluation as FXR/RXR antagonists. Magnolol-related neolignans are very promising as potential anti-diabetic

agents and chain-breaking antioxidants, and further results are expected on inhibition of tankyrase 2 and ABCG2, two biological targets of special interest in cancer chemotherapy.

CHAPTER 4

4. EXPERIMENTAL SECTION

4.1 General Experimental Procedures

NMR spectra were run on a Varian Unity Inova spectrometer operating at 499.86 (^{1}H), and 125.70 MHz (^{13}C), and equipped with a gradient-enhanced, reverse-detection probe. Chemical shifts (δ) are indirectly referred to TMS using residual solvent signals. The 2D gHSQCAD experiments were performed with matched adiabatic sweeps for coherence transfer, corresponding to a central ^{13}C-^{1}H *J*-value of 146 Hz. gHMBCAD experiments were optimized for a long-range ^{13}C-^{1}H coupling constant of 8.0 Hz. All NMR experiments, including 2D spectra, i.e., gCOSY, gHSQCAD, and gHMBCAD, were performed using software supplied by the manufacturers, and acquired at constant temperature (300 K). Chloroform-d_1, methanol-d_4, acetone-d_6 were used as solvents. Mass spectra were acquired with an Agilent 6410 Triple Quadrupole (1200 Series) mass spectrometer equipped with a Multimodal Ionization Source operating in MMI-ESI, in positive or negative mode. Samples infused were eluted on a cartridge, (ZORBAX Eclipse XDB-C18; 4.6 x 30 mm, 3.5 µm; Agilent) with MeOH:H_2O:HCOOH (98:2:0.1). The following parameters were used for sample ionization: gas temperature 300 °C; vaporizer temperature 250 °C; gas flow 10 L/min; nebulizer 60 psi; capillary voltage 3500 V; charging 2000 V. Other mass spectra were acquired with a Thermo Scientific LCQ-DECA ion trap mass spectrometer equipped with an ESI ion source operating in negative ion mode. Samples were dissolved in methanol and directly infused; electrospray mass spectra were acquired from *m/z* 150 to 2000 using the following electrospray ion source parameters: capillary temperature

220 °C; capillary voltage -18 V; spray voltage 3.5 kV; gas flow rate 30 a.u.

High-performance liquid chromatography (HPLC) was carried out using an Agilent Series G1354A pump, and an Agilent UV G1315D as diode array detector (DAD). An auto-sampler Agilent Series 1100 G1313A was used for sample injection; an analytic reverse phase column (Luna C18, 5 μm; 4.6 × 250 mm; Phenomenex) was employed to monitor the course of the enzymatic and chemical reactions, eluting with different solvent systems, DAD was set at 254, 280 and 330 nm. PLC was performed on LiChroprep DIOL Silica-gel (40 – 63 μm; Merck) using different solvent systems.TLC was carried out using pre-coated silica gel F254 plates (Merck); visualization of reaction components was achieved under UV light at a wavelength of 254, and 366 nm, or by staining with a solution of cerium sulfate, and phosphomolybdic acid followed by heating.

All chemicals were of reagent grade, and were used without further purification. All enzymes, namely *Trametes versicolor* Laccase (TvL, 10.0 U/mg), *Pleurotus ostreatus* Laccase (PoL, 11.8 U/mg), *Agaricus bisporus* Laccase (AbL, 6.8 U/mg), horseradish peroxidase (HRP, Type I), α-Glucosidase from *Saccharomyces cerevisiae* (Type I, lyophilized powder, 10 units/mg protein) and the substrate *p*-nitrophenyl-α-D-glucopyranoside (*p*NP-α-G) were purchased from Sigma Aldrich. *Candida antarctica* Lipase (Chyralzyme, L-2, c.-f. C2, lyo) was purchased from Rosche. IBX was prepared in laboratory as described in the literature.[94]

4.2 Biomimetic synthesis of benzo[*k,l*]xanthene lignans 36, 38, 39, 41, 60, 63, 65 and 67

*Synthesis of benzo[k,l]xanthene **36**:* caffeic acid (**57**, 315.5 mg, 1.75 mmol), was dissolved in 75 mL of methanol and 1.2 mL of H_2SO_4 was added. The mixture was stirred at reflux temperature (67° C) for 4 h, and was monitored by TLC. The mixture was evaporated under vacuo; the residue was diluted with ethyl acetate and was extracted with 1 N $NaHCO_3$ (3 X 25 mL). The organic layer was washed with H_2O (2 X 25 mL), dried on Na_2SO_4, filtered and evaporated under reduced pressure. The methyl caffeate (**58**, 328.6 mg, 1.69 mmol) was obtained with of 97.1% of yield. R_f (TLC) = 0.5 (8% MeOH-$CHCl_3$). The acquired NMR and MS data are in agreement with those reported in literature.[114] Then, to a stirred suspension of $Mn(OAc)_3$ (512 mg, 1.91 mmol) in 40 mL $CHCl_3$, methyl caffeate (**58**, 89.5 mg, 0.46 mmol) was added. The mixture was stirred at room temperature for 20 h and was monitored by TLC. The mixture was treated with a saturated solution of ascorbic acid in methanol. After filtration, the solvent was removed under reduced pressure and the organic residue was purified by column chromatography on DIOL silica-gel in a gradient of MeOH in CH_2Cl_2 (from 0 to 6%) and 47.1 mg of pure benzo[*k,l*]xanthene **36** was recovered (yield: 27%). R_f (TLC) = 0.5, (6% MeOH-$CHCl_3$). The acquired NMR and MS data are in agreement with those reported in literature.[47]

*Synthesis of benzo[k,l]xanthene **38**:* to a stirred suspension of $Mn(OAc)_3$ (1100.0 mg, 4.2 mmol) in 90 mL of CH_2Cl_2, CAPE (**12**, 300 mg, 1.05 mmol) was added. The mixture was stirred at room temperature for 6 h and was monitored by TLC. The mixture was treated with a saturated solution of ascorbic acid in methanol. After filtration, the solvent was removed under reduced pressure and the organic residue was purified by

column chromatography on DIOL silica-gel in a gradient of MeOH in CH_2Cl_2 (from 0 to 4%) and 250 mg of pure benzo[*k,l*]xanthene **38** was recovered (yield: 84%). R_f (TLC) = 0.3, (6% MeOH-$CHCl_3$). The acquired NMR and MS data are in agreement with those reported in literature.[47]

*Synthesis of benzo[k,l]xanthene **39**:* Caffeic acid (**57**, 315 mg, 1.75 mmol), was dissolved in 90 mL of butanol, and 1.2 mL of H_2SO_4 was added. The mixture was stirred at reflux temperature (118 °C) for 5 h, and was monitored by TLC. The mixture was evaporated *in vacuo*; the residue was dissolved with ethyl acetate and was extracted with a saturated solution of $NaHCO_3$ (3 X 25 mL). The organic layer was washed with H_2O (2 X 25 mL), dried on Na_2SO_4, filtered and evaporated *in vacuo*. The butyl caffeate (**59**, 400 mg, 1.69 mmol) was obtained with a yield of 96.8%. R_f (TLC) = 0.5 (3% MeOH-$CHCl_3$). The acquired NMR and MS data are in agreement with those reported in literature.[115] Then, to a stirred suspension of $Mn(OAc)_3$ (455.6 mg, 1.70 mmol) in 150 mL of $CHCl_3$, butyl caffeate (**59**, 400 mg, 1.69 mmol) was added. The mixture was stirred at room temperature for 7 h and was monitored by TLC. The mixture was treated with a saturated solution of ascorbic acid in methanol. After filtration, the solvent was removed under reduced pressure and the organic residue was purified by column chromatography on DIOL silica-gel in a gradient of MeOH in CH_2Cl_2 (from 0 to 6%) and 200 mg of pure benzo[*k,l*]xanthene **39** was recovered (yield: 50.5 %). R_f (TLC) = 0.4, (6% MeOH-$CHCl_3$). The acquired NMR and MS data are in agreement with those reported in literature.[67]

*Synthesis of benzo[k,l]xanthene **43**:* Compound **38** (60.6 mg, 0.158 mmol) was placed into a boiling flask and dispersed in 10 mL of acetone and 25 mg of anhydrous potassium carbonate. To this suspension 20 ml of

dimethyl sulfate; The resulting mixture was heated for 18 h at reflux, then acetone was removed to afford a residue which was purified by LC (silica gel, 70% CHCl3 in n-hexane) so as to obtain 62.5 mg (93.3% yield) of **43**. Yellow amorphous powder: Rf (TLC) = 0.42 (100% $CHCl_3$). The NMR data are in perfect agreement with those previously reported in literature.[65]

*Synthesis of benzo[k,l]xanthene **61**:* caffeic acid (**57**, 311 mg, 1.72 mmol), was dissolved in 100 mL of ethanol, and 1.2 mL of H_2SO_4 was added. The mixture was stirred at reflux temperature (77° C) for 20 h, and was monitored by TLC. The mixture was evaporated under *vacuo*. The residue was diluted with ethyl acetate and was washed with a saturated solution of $NaHCO_3$ (3 X 25 mL) and H_2O (2 X 25 mL), dried on Na_2SO_4, filtered and evaporated under reduced pressure. The ethyl caffeate (**60**, 340 mg, 1.63 mmol) was obtained with 94% of yield. R_f (TLC) = 0.4 (6% MeOH-$CHCl_3$). The acquired NMR and MS data are in agreement with those reported in literature.[66] Then, to a stirred suspension of $Mn(OAc)_3$ (455.6 mg, 1.70 mmol) in 150 mL $CHCl_3$, ethyl caffeate (**60**, 340 mg, 1.63 mmol) was added. The mixture was stirred at room temperature for 10 h and was monitored by TLC. The mixture was treated with a saturated solution of ascorbic acid in methanol. After filtration, the solvent was removed under reduced pressure and the organic residue was purified by column chromatography on DIOL silica-gel in a gradient of MeOH in CH_2Cl_2 (from 0 to 2%) and 249 mg of pure benzo[*k,l*]xanthene **61** was recovered (yield: 71%). R_f (TLC) = 0.4, (10% MeOH-$CHCl_3$). The acquired NMR and MS data are in agreement with those reported in literature.[66]

*Synthesis of benzo[k,l]xanthene **63**:* caffeic acid (**57**, 300 mg, 1.65 mmol), was dissolved in 15 mL of dry THF; then DCC (412.6 mg, 1.9 mmol) and

4-methoxybenzyl alcohol (0.25 ml, 1.98 mmol) were added. The mixture was stirred at reflux temperature (70 °C) for 8 h. Then, the mixture was filtered and evaporated *in vacuo*. The 4-methoxybenzyl caffeate (**62**, 64 mg, 0.21 mmol) was obtained with a yield of 11%. R_f (TLC) = 0.6 (60% EP-EtOAc). The acquired NMR and MS data are in agreement with those reported in literature.[116] Then, to a stirred suspension of $Mn(OAc)_3$ (192.0 mg, 0.71 mmol) in 64 mL of CH_2Cl_2, 4-methoxybenzyl caffeate (**62**, 64 mg, 0.21 mmol) was added. The mixture was stirred at room temperature for 2 h. The mixture was treated with a saturated solution of ascorbic acid in methanol. After filtration, the solvent was removed under reduced pressure and the organic residue was purified by column chromatography on DIOL silica-gel in a gradient of MeOH in CH_2Cl_2 (from 0 to 3%) and 10.7 mg of pure benzo[*k,l*]xanthene **63** was recovered (yield: 16.0 %). R_f (TLC) = 0.4, (6% MeOH-$CHCl_3$). ^{1}H NMR (500 MHz, acetone-d_6) δ 8.17 (s, 1H, H-3), 7.49 (d, J = 8.7 Hz, 1H, H-4), 7.44 (d, J = 8.7 Hz, 2H,H^{IV}-2/6), 7.34 (s, 1H, H-8), 7.32 (d, J = 8.7 Hz, 2H, H^{V}-2/6), 7.30 (d, J = 8.7 Hz, 1H, H-5), 6.96 (d, J = 8.7 Hz, 2H, H^{IV}-3/5), 6.88 (d, J = 8.7 Hz, 2H, H^{V}-3/5), 6.70 (s, 1H, H-11), 5.27 (s, 2H, CH_2-1''), 5.26 (s, 2H, CH_2-1''), 3.81 (s, 3H, $CH_3{}^{IV}$-4), 3.77 (s, 2H, $CH_3{}^{V}$-4) ppm. ^{13}C NMR (125 MHz, acetone-d_6) δ 170.7 (C-1'), 166.7 (C, C-2'), 160.8 (C-4^{IV}), 160.7 (C-4^{V}), 149.2 (C-9), 147.8 (C-10), 142.8 (C-6), 142.6(C, C-7a), 137.6 (C-6a), 131.27 (C^{IV}-2/6), 131.22 (C^{V}-2/6), 129.8 (C-3), 129.1 (C^{IV}-1), 128.4 (C^{V}-1), 127.6 (C-3a), 126.1 (C-11b), 125.1 (C-11c), 124.2 (C-2), 122.3 (C-4), 121.7 (C-1), 120.7 (C-5), 114.8 (C^{IV}-3/5), 114.7 (C^{V}-3/5), 112.4 (C-8), 110.9 (C-11a), 104.9 (C-11), 68.3 (C-1'''), 67.5 (C-1''), 55.6 (-$OMe^{I\ V}$-4), 55.5 ((-OMe^{V}-4) ppm.

*Synthesis of benzo[k,l]xanthene **65**:* Caffeic acid (**57**, 392 mg, 2.17 mmol), was dissolved in 20 mL of dry THF; then DCC (495.0 mg, 2.38

mmol) and benzyl alcohol (0.28 ml, 2.60 mmol) were added. The mixture was stirred at reflux temperature (70 °C) for 3 h. Then, the mixture was filtered and evaporated *in vacuo*. The benzyl caffeate (**64**, 195.2 mg, 0.72 mmol) was obtained with a yield of 33.2%. R_f (TLC) = 0.4 (95% CH_2Cl_2-MeOH). The acquired NMR and MS data are in agreement with those reported in literature.[117] Then, to a stirred suspension of $Mn(OAc)_3$ (399.5 mg, 1.49 mmol) in 65 mL of CH_2Cl_2, benzyl caffeate (**64**, 100.6 mg, 0.37 mmol) was added. The mixture was stirred at room temperature for 2 h. The mixture was treated with a saturated solution of ascorbic acid in methanol. After filtration, the solvent was removed under reduced pressure and the organic residue was purified by column chromatography on DIOL silica-gel in a gradient of EtOAc in EP (from 30 to 60%) and 17.1 mg of pure benzo[*k,l*]xanthene **65** was recovered (yield: 17.0 %). R_f (TLC) = 0.4, (6% MeOH-$CHCl_3$). ^{1}H NMR (500 MHz, acetone-d_6) δ 8.22 (s, 1H, H-3), 7.51*(d, J = 8.7 Hz, 1H, H-4), 7.50* (dd, J = 8.5 Hz, 2.5 Hz, 2H,H^{IV}-3/5), 7.41 (m, 4H, H^{IV}-4, H^{V}-4, H H^{V}-3/5), 7.36 (s, 1H, H-8), 7.34° (m, 2H, H^{V}-2/6) 7.33° (d, J = 8.5 Hz, 2H, H^{IV}-2/6), 7.31° (d, J = 8.7 Hz, 1H, H-5), 6.71 (s, 1H, H-11), 5.35 (s, 2H, CH_2-1''), 5.34 (s, 2H, CH_2-1'')ppm. ^{13}C NMR (125 MHz, acetone-d_6) δ 170.7 (C-1'), 166.7 (C, C-2'), 149.2 (C-9), 147.8 (C-10), 142.9 (C-6), 142.7(C, C-7a), 137.6 (C-6a), 137.2 (C^{IV}-1), 136.5 (C^{V}-1), 129.9 (C-3), 129.5 (C^{IV}-3/5, C^{V}-3/5), 129.4 (C^{IV}-4), 129.3 (C^{IV}-2/6, C^{V}-2/6), 129.2 (C^{V}-4), 127.6 (C-3a), 125.9 (C-11b), 125.2 (C-11c), 124.2 (C-2), 122.3 (C-4), 121.6 (C-1), 120.7 (C-5), 112.2, (C-8), 110.9 (C-11a), 104.8 (C-11), 68.5 (C-1'''), 67.7(C-1'')ppm.

*Synthesis of benzo[k,l]xanthene **67**:* Caffeic acid (**57**; 415.8 mg; 2.31 mmol) was solved in butanediol (7.2 mL, 81.26 mmol) and in concentrated H_2SO_4 (0.4 mL). The solution was heated at 50 °C for 24 h.

(*E*)-4-hydroxybutyl 3-(3,4-dihydroxyphenyl)acrylate (**66**) was recovered by extraction with EtOAc (100 mL) and $NaHCO_3$ saturated solution (2 x 50 mL). The organic layer was washed with water, dried over Na_2SO_4 and concentrated *in vacuo*. Yellow powder (551.8 mg; 95% yield). R_f (TLC): 0.44 (92:8 CH_2Cl_2:MeOH). The NMR data of the recovered compound are in perfect agreement with trose previously reported in literature.[118] Then, the oxidant agent $Mn(OAc)_3$ (2.4665 g, 9.2 mmol) was suspended in CH_2Cl_2 (260 mL) and it was stirred. A solution of **66** (518.3 mg, 2.06 mmol) was added to the suspension and the mixture was heated at reflux for 3 h. The reaction was quenched by addition of ascorbic acid saturated solution (100 mL) and it was extracted with CH_2Cl_2 (6 x 50 mL). The combined organic layer was dried over Na_2SO_4, filtered and took to dry. The crude mixture was purified by flash chromatography on Silica Diol with a gradient of EtOH in CH_2Cl_2 (from 5 to 15%). Compound **67** (235.8 mg) was recovered with 46% yield as yellow oil: R_f (TLC): 0.57 (82:18 CH_2Cl_2:EtOH). The NMR data of the recovered compound are in perfect agreement with trose previously reported in literature.[118]

4.3 Synthesis of benzo[*k,l*]xanthene phenazine derivatives 69, 71, 73, 74 and 75

Preliminary screening: compound **39** was used as substrate for the optimization of benzo[*k,l*]xanthene oxidation method. Initially both chemical both enzymatic methods were carried out.

Enzymatic method: three samples of **39** (1.5 mg, 0.0032 mmol, C_{sub}/v_{tot} = 2.66 mg/mL, t_R = 8.9 min) were dissolved in EtOAc (0.5 mL), the following enzymes: **a**) TvL + 39 (1.0 mg), **b**) PoL + 39 (1.0 mg), **c**) AbL + 39(1.0 mg), previously solved in acetate buffer (pH= 4.7, 0.3 mL), were added. All three reactions were stirred at room temperature in vials

without caps; each experiment was reproduced in the same conditions without enzyme asblank. The reactions were monitored both by TLC (6% MeOH-CH_2Cl_2) and by HPLC on reverse phase column (RP-18), with a gradient of CH_3CN/H^+ (namely B) in H_2O/H^+ (namely A) at 1 mL/min: $t_{0\ min}$ B = 50 %, $t_{10\ min}$ B = 90 %, $t_{25\ min}$ 100 % B. the diode array detector was set at 254, 280, 360, 390 nm.

Chemical methods: two samples of **39** (1.5 mg, 0.003 mmol) were solved in CH_2Cl_2; $Mn(OAc)_3$ (vial 1: 3.4 mg, 0.012 mmol) and Ag_2O (vial 2: 2.77 mg, 0.012 mmol) were added. The reactions were stirred at room temperature and were monitored both by TLC (6% MeOH - CH_2Cl_2) and by HPLC at regular time intervals.

*Synthesis of benzo[k,l]xanthene phenazine **69**:* compound **39** (71.0 mg, 0.15 mmol) was dissolved in CH_2Cl_2 (23 mL); Ag_2O (128 mg, 0.55 mmol) was added a this solution. The reaction mixture was stirred at room temperature and was monitored by TLC (6% MeOH - CH_2Cl_2) for 6 h. The reaction mixture was filtered and evaporated *in vacuo*. 170 mg of crude benzo[*k,l*]xanthene quinone **68** were recovered. Then the crude of benzo[*k,l*]xanthene quinone **68** (160 mg, 0.34 mmol) was dissolved in dry CH_3CN (32 mL); *o*-phenylenediamine (111.0 mg, 1.02 mmol) and acetic acid (3.5 mL) were added. The reaction mixture was stirred at room temperature and was monitored by TLC (3% MeOH-CH_2Cl_2) for 24 h. The solution was concentrated *in vacuo*; the mixture was diluted with ethyl acetate and was extracted with 1 N $NaHCO_3$ solution (3 X 25 mL) and the recovered organic layer was washed with H_2O (2 X 25 mL), dried on Na_2SO_4, filtered and evaporated under reduced pressure. The organic residue was purified by column chromatography on DIOL silica-gel in a gradient of CH_2Cl_2 in hexane (from 60 to 100%) and MeOH in CH_2Cl_2 (from 0 to 25%) and 15.3 mg of pure benzo[*k,l*]xanthene phenazine **69**

were recovered (yield: 19%) as red residue. R_f (TLC) = 0.4 (3% MeOH-$CHCl_3$). UV (MeOH): λmax (ε) = 271.6 (63267), 511.4 (11719 M–1 cm–1) MS: [M+1] = 537.5 m/z, $C_{32}H_{28}N_2O_6$. ^{1}H NMR (500 MHz, $CDCl_3$) δ = 0.94 (t, *J* = 7.5 Hz, 3 H, H-4''),1.04 (t, J = 7.5 Hz, 3 H, H-4'''), 1.46 (sextet, *J* = 7.5 Hz, 2 H, H-3''), 1.54 (t, *J* = 7.5 Hz, 2 H, H-3'''), 1.84 (pent, *J* = 7.5 Hz, 2 H, H-2'''), 1.89 (pent, *J* = 7.5 Hz, 2 H, H-2''), 4.40 (t, *J* = 6.5 Hz, 2 H, H-1'''), 4.70 (t, *J* = 6.5 Hz, 2 H, H-1''), 7.28 (d, *J* = 8.7 Hz, 1 H, H-5), 7.44 (d, *J* = 8.7 Hz, 1 H, H-4), 7.65 (s, 1 H, H-8), 7.72 (dd, *J* = 6.7, 3.2 Hz, 2 H, H-11/12), 7.97 (d, *J* = 6.5, 3.4 Hz, 1 H, H-10), 8.36 (s, 1 H, H-3), 8.66 (s, 1 H, H-15); ^{13}C NMR (125 MHz) δ = 13.75 (C-4''), 13.79 (C-4'''), 19.2 (C-3''-3'''), 30.26 (C-2''), 30.76 (C-2'''), 65.65 (C-1'''), 66.70 (C-1''), 111.72 (C-8), 120.08 (C-5), 121.21 (C-15b), 122.13 (C-3a), 123.04 (C-4), 124.83 (C-15c), 125.49 (C-15a), 126.82 (C-2), 127.45 (C-1), 127.75 (C-15),128.87 (C-10), 129.63 (C-11), 130.05 (C-13), 131.10 (C-12), 132.35 (C-3), 134.63 (C-6a),141.52 (C-8a), 141.95 (C-6), 143.63 (C-9a), 143.77 (C-13a), 144.11 (C-14a), 152.72 (C-7a), 170.4 (C-1'), 165.5 (C-2').

*Synthesis of benzo[k,l]xanthene phenazine **71**:* a solution of benzo[*k,l*]xanthene (**60**, 81.4 mg, 0.19 mmol) in CH_2Cl_2 (26.2 mL), was stirred with Ag_2O (176.1 mg, 0.75 mmol). The mixture was retained at room temperature and monitored by TLC (5% MeOH-CH_2Cl_2) for 7 h. The reaction mixture was filtered and evaporated *in vacuo*. The organic residue (66.9 mg) containing the benzo[*k,l*]xanthene quinone **70** was recovered. Then the crude of benzo[*k,l*]xanthene quinone (**70**, 66.3 mg, 0.16 mmol) was solved in 20 mL of dry CH_3CN, to follow *o*-phenylenediamine (51.5 mg, 0.47 mmol) and acetic acid were added. The mixture was stirred at 37 °C and monitored by TLC (5% MeOH-CH_2Cl_2) for 7 h. The reaction mixture was filtered and evaporated under reduced

pressure and the organic residue was purified by column chromatography on DIOL silica-gel in a gradient of acetone in hexane (from 10 to 50%). 15.6 mg of pure benzo[*k,l*]xanthene phenazine **71** were recovered (yield: 19%) as a red residue. R_f (TLC) = 0.6 (6% MeOH - $CHCl_3$). MS: [M+1] = 481.3 m/z, $C_{28}H_{20}N_2O_6$. ^{1}H NMR (500 MHz, $CDCl_3$) δ = 1.39 (t, *J* = 7.0 Hz, 2 H, H-2''/2'''), 4.36 (t, *J* = 7.0 Hz, 2 H, H-1'''), 4.65 (t, *J* = 7.0 Hz, 2 H, H-1''), 7.32 (d, *J* = 9.0 Hz, 1 H, H-5), 7.50 (d, *J* = 9.0 Hz, 1 H, H-4), 7.82 (s, 1 H, H-8), 7.73 (t, *J* = 8.0 Hz, 1 H, H-11), 7.779 (t, J = 8.0 Hz, 1 H, H-12), 8.07 (d, *J* = 8.5 Hz, 1 H, H-10), 8.15 (d, *J* = 8.5 Hz, 1 H, H-13), 8.39 (s, 1 H, H-3), 8.361 (s, 1 H, H-15); ^{13}C NMR (125 MHz) δ = 14.09 (C-2'''), 60.09 (C-1'''), 62.92 (C-1''), 110.0 (C-8), 121.57 (C-5), 123.08 (C-3a), 123.89 (C-4), 124.83 (C-15c), 125.05 (C-6a), 125.32 (C-2), 126.96 (C-15b), 127.34 (C-10), 127.96 (C-1), 128.03 (C-15a), 130.16 (C-15), 130.39 (C-11), 131.28 (C-6), 132.67 (C-13), 133.23 (C-12), 135.27 (C-3), 142.34 (C-8a), 142.80 (C-13a), 144.90 (C-9a), 143.78 (C-14a), 155.33 (C-7a), 170.6 (C-1'), 165.0 (C-2').

Synthesis of benzo[k,l]xanthene phenazine 73: compound **38** (55.5 mg, 0.093 mmol) was dissolved in 17 mL of $CH_2Cl_2$and the solution was stirred with Ag_2O (100 mg, 0.32 mmol)at room temperature and the mixture was monitored by TLC (3% MeOH-CH_2Cl_2) for 16 h. The mixture was filtered and evaporated *in vacuo* and 52.4 mg of organic residue containing benzo[*k,l*]xanthene quinone **72** were recovered. Then the crude of benzo[*k,l*]xanthene quinone (**72**, 52.4 mg, 0.093 mmol) was dissolved in 11 mL of dry CH_3CN, *o*-phenylenediamine (12.6 mg, 0.11 mmol), and acetic acid were added. The mixture reaction was stirred at room temperature; the mixture was monitored by TLC (3% MeOH-CH_2Cl_2) and it was stopped at 24 h. The CH_3CN was concentrated under reduced pressure ; the mixture was diluted with CH_2Cl_2 and the organic

solution was extracted with 1 N $NaHCO_3$ solution (3 X 25 mL) and finally with H_2O (2 X 25 mL). The recovered organic layer was dried on Na_2SO_4, evaporated *in vacuo* and the organic residue was purified by column chromatography on DIOL silica-gel in isocratic (10-90 Ep-CH_2Cl_2). Pure benzo[*k,l*]xanthene phenazine **73** (22.7 mg) were recovered (yield: 38.5%) like red pigment. R_f (TLC) = 0.6 (6% MeOH-$CHCl_3$). MS: [M+1] = 633.4 m/z, $C_{40}H_{28}N_2O_6$. ^{1}H NMR (500 MHz, $CDCl_3$) δ = 3.11 (m, 4 H, H-2''/2'''), 4.55 (t, *J* = 6.5 Hz, 2 H, H-1'''), 4.84 (t, *J* = 6.5 Hz, 2 H, H-1'''), 6.86 (t, *J* = 7.5 Hz, 1 H, H-4^v), 6.95 (t, *J* = 6.5 Hz, 2 H, H-3^v/5^v), 7.18 (d, *J* = 7.0 Hz, 2 H, H-2^v/6^v), from 7.28 to 7.38 (m, 6 H, H-5, 2^{iv}/6^{iv}, 3/5^{iv}, 4^{iv}), 7.41 (d, *J* = 9.0 Hz, 1 H, H-4), 7.69 (s, 1 H, H-8), 7.72 (m, 2 H, H-11/12), 8.01 (dd, *J* = 6.7, 2.0 Hz, 1 H, H-10), 8.12 (dd, *J* = 6.7, 2.0 Hz, 1 H, H-13), 8.27 (s, 1 H, H-13) 8.54 (s, 1 H, H-15); ^{13}C NMR (125 MHz) δ = 35.17 (C-2''/2'''), 65.32 (C-1'''), 66.84 (C-1''), 110.59 (C-8), 118.14 (C-5), 121.38 (C-15b), 122.17 (C-3a), 122.22 (C-4), 122.27 (C-15c), 123.71 (C-15a), 126.25 (C-2), 126.81 (C-15), 126.87 (C-4^{iv}), 126.96 (C-4^v), 127.91 (C-2^v/6^v, 3^v/5^v), 127.97 (C-3^{iv}/5^{iv}), 128.07 (C-1), 128.72 (C-11/12), 128.88 (C-10), 128.96 (C-13), 129.84 (C-2^{iv}/6^{iv}), 130.42 (C-13a), 130.63 (C-9a), 131.48 (C-3), 135.93 (C-6a), 136.63 (C-1^v), 138.48 (C-1^{iv}), 140.39 (C-8a), 142.92 (C-6), 144.155 (C-14a), 151.79 (C-7a), 171.17 (C-1'), 165.55 (C-2').

*Synthesis of benzo[k,l]xanthene phenazine **74** and **75**:* The benzo[*k,l*]xanthene quinone (**68**, 82.0 mg, 0.177 mmol) was dissolved in dry CH_3CN (20 mL), 3,3′-diaminobenzidine (45.5 mg, 0.3 mmol) and acetic acid as catalyst were added. The mixture was stirred at room temperature for 6 h, under nitrogen atmosphere. After 6 hours, the mixture was concentrated *in vacuo* and the crude residue was diluted with CH_2Cl_2 and extracted with 1 N $NaHCO_3$ solution(3 X 25 mL). The

recovered organic layer was washed with H_2O (2 X 25 mL), dried on Na_2SO_4, and evaporated *in vacuo*; the organic residue was DIOL silica-gel with 20% PE-CH_2Cl_2 as eluent . Two isomers were obtained: **74** and **75** were recovered with 10.6 and 7.8% yield respectively. R_f (TLC) = 0.3 and 0.4 respectively (6% MeOH - $CHCl_3$). MS: [M+1] = 643.3 m/z, $C_{38}H_{34}N_4O_6$. ^{1}H NMR (500 MHz, $CDCl_3$) δ = 0.87 (t, *J* = 7.5 Hz, 3 H, H-4’’),1.02 (t, J = 7.5 Hz, 3 H, H-4’’’), 1.42 (m, 2 H, H-3’’), 1.51 (m, 2 H, H-3’’’), 1.80 (m, , 4 H, H-2’’2’’’), 4.35 (t, *J* = 6.5 Hz, 2 H, H-1’’’), 4.64 (t, *J* = 6.5 Hz, 2 H, H-1’’), 6.69 (d, *J* = 9.0 Hz, 1 H, H-5^{IV}), 7.10 (d, *J* = 9.0 Hz, 1 H, H-6^{IV}), 7.17 (s, 1 H, H-2^{IV}) 7.32 (d, *J* = 9.0 Hz, 1 H, H-5), 7.51 (d, *J* = 9.0 Hz, 1 H, H-4), 7.71 (s, 1 H, H-8), 7.82 (d, *J* = 6.7, 3.2 Hz, 2 H, H-11/12), 7.93 (d, *J* = 9.0 Hz, 1 H, H-10), 8.10 (s, 1 H, H-13), 8.34 (s, 1 H, H-3), 8.44 (s, 1 H, H-15); ^{13}C NMR (125 MHz) δ = 14.0 (C-4’’/4’’’), 31.0 (C-3’’), 31.5 (C-3’’’), 23.0 (C-2’’/2’’’), 66.3 (C-1’’’), 67.4 (C-1’’), 111.8 (C-8), 115.8 (C-2^{IV}), 117.3 (C-5^{IV}), 118.3 (C-6^{IV}), 119.9 (C-4), 121.3 (C-15b), 121.7 (C-3a), 122.2 (C-15a), 122.9 (C-5), 123.7 (C-15c), 124.03 (C-13), 126.25 (C-2), 126.1 (C-15), 127.1 (C-11), 128.0 (C-1), 128.6 (C-10), 129.62 (C-12), 130.2 (C-1^{IV}), 130.4 (C-13a), 133.3 (C-3), 135.4 (C-4^{IV}), 135.71 (C-6a), 137.2 (C-3^{IV}), 140.3 (C-8a), 142.2 (C-6), 143.6 (C-9a), 144.5 (C-14a), 156.9 (C-7a), 171.7 (C-1’), 167.0 (C-2’).

4.4 Chemoenzymatic synthesis of bis-phenol neolignans 81, 82 and 84 - 96

Preliminary Screening. Aliquots of the magnolol (**44**) were dissolved in three different solvents, namely DMSO, DMF and MeOH. The three different solutions were treated with the IBX, finally the reaction was quenched with $Na_2S_2O_4$. All experiments were carried out in different reaction conditions.

Experiments in DMSO: a) **44** (5.0 mg, 0.018 mmol, 0.1 M) was solubilized in DMSO (0.180 mL) and treated with 1.2 equiv. of IBX (6.0 mg, 0.021 mmol); the reaction was stirred at rt in a vial for 2h and then $Na_2S_2O_4$ solution was added (3.1 mg, 0.017 mmol in 0.180 mL of H_2O). b) **44** (5.0 mg, 0.018 mmol) was solubilized in DMSO (0.180 mL, 0.1 M) and then treated with 1.5 equiv of IBX (7.5 mg, 0.027 mmol) ; the reaction was stirred at rt in a vial for 4h and then $Na_2S_2O_4$ solution was added (3.1 mg, 0.017 mmol in 0.180 mL of H_2O). c) **44** (5.0 mg, 0.018 mmol) was solubilized in DMSO (0.180 mL, 0.1 M) and then treated with 2.1 equiv of IBX (10.5 mg, 0.037 mmol); the reaction was stirred at rt in a vial for 2 h and then $Na_2S_2O_4$ water solution was added (3.1 mg, 0.017 mmol in 0.180 mL of H_2O). d) **44** (5.0 mg, 0.018 mmol) was solubilized in DMSO (0.180 mL, 0.1 M) and then was treated with 1.5 equiv of IBX (7.5 mg, 0.027 mmol); the reaction was stirred at 80 °C in a vial for 4 h and then $Na_2S_2O_4$ solution was added (3.1 mg, 0.017 mmol in 0.180 mL of H_2O).

Experiments in DMF: a) **44** (5.0 mg, 0.018 mmol) was solubilized in DMF (0.180 mL, 0.1 M) and then treated with 1.5 equiv of IBX (7.5 mg, 0.027 mmol); the reaction was stirred at rt in a vial for 4 h and then $Na_2S_2O_4$ solution was added (3.1 mg, 0.017 mmol in 0.180 mL of H_2O). b) **44** (5.0 mg, 0.018 mmol) was solubilized in DMF (0.180 mL, 0.1 M)

and then was treated with 2.1 equiv of IBX (10.5 mg, 0.037 mmol); the reaction was stirred at rt in a vial for 2 h and then $Na_2S_2O_4$ solution was added (3.1 mg, 0.017 mmol in 0.180 mL of H_2O).

Experiments in MeOH: a) two aliquots of **44** (10.0 mg, 0.037 mmol) were solubilized in MeOH (0.180 mL, 0.2 M) and then treated with 1.2 equiv of IBX (12.59 mg, 0.0045 mmol); the reactions were stirred at rt and 0 °C respectively in two vials for 40 min and then $Na_2S_2O_4$ solution was added (6.44 mg, 0.037 mmol in 0.180 mL of H_2O). Both the experiments were monitored for 1h. b) **44** (10.0 mg, 0.037 mmol) was solubilized in MeOH (0.180 mL, 0.2 M) and then treated with 2.1 equiv of IBX (12.59 mg, 0.0045 mmol); the reaction was stirred at 0 °C in a vial for 40 min and then $Na_2S_2O_4$ solution was added (3.1 mg, 0.017 mmol in 0.180 mL of H_2O). All reactions were monitored at regular time intervals by HPLC with reverse phase column (RP-18) with the following gradient of CH_3CN/HCOOH (99:1v/v; B) in H_2O/HCOOH (99:1v/v; A) at 1 mL/min: t_0 min B = 40%, t_{10} min B = 100%, t_{15} min B = 60%. The best results in term both of substrate conversion, and formation of main products were obtained using MeOH as solvent with a concentration of substrate (**44**) of 0.2 M at 0 °C, wit 1.2 equiv of IBX.

*Synthesis 5,5'-diallyl-[1,1'-biphenyl]-2,2',3-triol (**81**) and 5,5'-diallyl-[1,1'-biphenyl]-2,2',3,3'-tetraol (**82**)*: Magnolol (**44**, 100 mg, 0.37 mmol) was dissolved in CH_3OH (1.8 mL, 0.2 M), and then IBX (123.1 mg, 0.44 mmol) was added. The solution was stirred at 0 °C until disappearance of the substrate (40 min). At the end, $Na_2S_2O_4$ solution (76.6 mg, 0.43 mmol in 1.8 mL of H_2O) was added, and the solution was stirred for 5 min at rt. After evaporation of the solvent under vacuum, the residue was solubilized with ethyl acetate and treated with a saturated $NaHCO_3$ solution. The aqueous phase was extracted with ethyl acetate. The organic

phases were washed with a saturated NaCl solution and dried over Na_2SO_4. After filtration, the solvent was evaporated under vacuum. The flash chromatography with DIOL silica-gel, eluted with *n*-hexane-$CHCl_3$ (30:70 → 0:100) and $CHCl_3$− AcOEt (99:1 → 80:20) gave the biphenyl neolignans **81** and **82**. The compound **81** was recovered with 36.5%yield (38.1 mg): R_f (TLC) 0.46 (*n*-hexane−acetone, 60:40); ESIMS *m/z* 281.1 $[M-H]^-$ (calcd for $C_{18}H_{18}O_3$); ^{1}H-NMR (500 MHz,$CDCl_3$): δ = 7.13 (d, 2.0 Hz 1 H, H-6'), 7.10 (dd, 8.5, 2.0 Hz, 1 H, H-/4'), 6.91 (d, 8.5 Hz, 1H, H-3'), 6.80 (d, 2.0 Hz, 1 H, H-4), 6.66 (d, 2.0 Hz, 1 H, H-6), 6.17 (bs,1 H, -OH), 5.96 (m, from 5.99 to 5.92, 2 H, H-8/8'), 5.85 (bs, 1 H, OH), 5.06 (m, from 5.11 to 5.05, 4 H, H_2-9/9'), 3.37 (d, 6.5 Hz, 2 H, H_2-7'), 3.32 (d, 7.0 Hz, 2 H, H_2-7). ^{13}C-NMR (125 MHz): δ = 150.4 (C-2'), 145.2 (C-3), 138.8 (C-2), 137.6 (C-8), 137.5 (C-8'), 134.0 (C-5'), 133.6 (C-5), 131.4 (C-6'), 129.8 (C-4'), 125.1 (C-1), 124.5 (C-1'), 122.3 (C-6), 116.6 (C-3'), 115.9 (C-9), 115.9 (C-9'), 115.1 (C-4), 39.7 (C-8), 39.4 (C-8'). The compound **82** was recovered with 28.9% of yield (32.1 mg): R_f (TLC) 0.36 (*n*-hexane−acetone, 60:40); ESIMS *m/z* 297.3 $[M-H]^-$ (calcd for $C_{18}H_{18}O_4$); ^{1}H-NMR (500 MHz,$CDCl_3$): δ = 6.79 (s, 2 H, H-4/4'), 6.70 (s,2 H, H-6/6'), 6.15 (bs,2 H,-OH), 5.95 (m, from 5.98 to 5.92, 2 H, H-8/8'), 5.07 (m, from 5.11 to 5.05, 4 H, H_2-9/9'), 3.33 (d, 6.5 Hz, 4 H, H_2-7/7'). ^{13}C-NMR (125 MHz): δ = 144.8 (C-3/3'), 138.5 (C-2/2'), 137.4 (C-8/8'), 134.0 (C-5/5'), 125.0 (C-1/1'), 122.4 (C-6/6'), 116.0 (C-4/4'), 115.0 (C-9/9'), 39.7 (C-7/7').

*4-allylbenzene-1,2-diol (**83**)*: eugenol (**76**, 600 mg, 3.6 mmol) was dissolved in THF (71.4 mL, 0.06 M), and then IBX (1550 mg, 5.4 mmol) was added. The solution was stirred at rt until disappearance of the substrate (16 h). At the end, $Na_2S_2O_4$ solution (630 mg, 3.61 mmol in 20.0 mL of H_2O) was added, and the solution was stirred for 5 min at rt.

After evaporation of the solvent under vacuum, the residue was solubilized with ethyl acetate and treated with a saturated $NaHCO_3$ solution. The aqueous phase was extracted with ethyl acetate. The organic phases were washed with a saturated solution of NaCl and dried over Na_2SO_4. After filtration, the solvent was evaporated under vacuum. The flash chromatography with DIOL Silica-gel, eluted with *n*-hexane-acetone (100:0 → 70:30) and gave the compound **83**; ESIMS and NMR data were identical to those previously reported in literature for the same compound.[153]

Preliminary experiments: Aliquots (1.0 mg) of the compound **83**, was dissolved in four different solvents (0.2 mL), namely acetone, MeOH, AcOEt and CH_2Cl_2. The four different solutions of compound were treated with the following enzymes: TvL (26 U/mL), PoL (26 U/mL), AbL (26 U/mL) and HRP (26 U/mL), previously dissolved in acetate buffer (0.2 mL, 0.1 M, pH = 4.5). The reactions were stirred at rt in vials without caps except for HRP-mediated reactions; in these latter a 30% (v/v) H_2O_2 solution (10 µL) was added to mixture and the reactions were carried out in capped vials. For each experiment a blank was carried out in the same conditions, without enzyme. The reactions were monitored at regular time intervals by TLC (5% MeOH-CH_2Cl_2) and HPLC-UV. Each experiment shows satisfactory results.

*5,5'-diallyl-3,3'-dimethoxy-[1,1'-biphenyl]-2,2'-diol (**84**)*: eugenol **76** (300.0 mg, 1.82 mmol) was solubilised in 12 mL of MeOH. The solution was stirred at rt with the enzyme solution (3.1 mg of HRP in 12 mL of acetate buffer) and three aliquots of hydrogen peroxide (0.3%, 0.1 mL) were added in 2 h intervals; after 4 h the total organic phase was finally washed with water, dried and evaporated under vacuum. The flash chromatography with DIOL Silica-gel, eluted with *n*-hexane −acetone

(100:0 → 50:50) gave the biphenyl neolignan **84** with 44.5% of yield (131.6 mg): Rf (TLC) 0.36 (*n*-hexane -acetone, 60:40); spectroscopic data were in agreement with those reported in literature.[88]

Preliminary experiments: Aliquots of the dieugenol (**84**) were dissolved in THF in two different concentrations. The two different solutions of each compound were treated with the IBX/$Na_2S_2O_4$. All experiments were monitored at regular reaction times by HPLC-UV. a) **84** (10.0 mg, 0.03 mmol, 0.06 M) was solubilized in THF (0.5 mL) and then was treated with 1.5 equiv. of IBX (12.59 mg, 0.045 mmol); the reaction was stirred at rt in a vial for 3 h and then $Na_2S_2O_4$ solution was added (7.8 mg, 0.045 mmol in 0.5 mL of H_2O). b) **84** (10.0 mg, 0.03 mmol) was solubilized in DMSO (0.15 mL, 0.2 M) and then was treated with 1.5 equiv. of IBX (7.5 mg, 0.027 mmol); the reaction was stirred at rt in a vial for 3 h and then $Na_2S_2O_4$ solution was added (7.8 mg, 0.045 mmol in 0.15 mL of H_2O).

*5,5'-diallyl-3'-methoxy-[1,1'-biphenyl]-2,2',3-triol (**85**)*: dieugenol (**84**, 180 mg, 0.55 mmol) was dissolved in THF (8.2 mL, 0.06 M), and then IBX (229.5 mg, 0.82 mmol) was added. The solution was stirred at rt until disappearance of the substrate (1 h). At the end, $Na_2S_2O_4$ solution (142.7 mg, 0.81 mmol in 8.2 mL of H_2O) was added, and the solution was stirred for 5 min. at rt. After evaporation of the solvent under vacuum, the residue was solubilized with ethyl acetate and treated with a saturated $NaHCO_3$ solution. The aqueous phase was extracted with ethyl acetate. The organic phases were washed with a saturated NaCl solution and dried over Na_2SO_4. After filtration, the solvent was evaporated under vacuum. The flash chromatography with DIOL Silica-gel, eluted with *n*-hexane - $CHCl_3$ (30:70 → 0:100) and $CHCl_3$− AcOEt (99:1 → 70:30) gave the biphenyl neolignans **85** and also a more polar product that showed ESIMS

and NMR data identical to those of 3,3'-dihydroxymagnolol (**82**). The compound **85** was recovered with 18.2% of yield (30.0 mg): R_f (TLC) 0.46 (CH_2Cl_2–MeOH, 94:6); ESIMS *m/z* 311.1 $[M-H]^-$ (calcd for $C_{20}H_{22}O_4$); ^{1}H-NMR (500 MHz,$CDCl_3$): δ = 6.83 (s, 2 H, H-3 and H-6'), 6.75 (d, 1.5 Hz, 1 H, H-/4'), 6.69 (d, 1.5 Hz, 1 H, H-6), 5.79 (m, from 6.10 to 5.95, 2 H, H-8/8'), 5.09 (m, from 5.14 to 5.05, 4 H, H_2-9/9'), 3.94 (s, 3 H, -OMe), 3.38 (d, 6.5 Hz, 2 H, H_2-7'), 3.34 (d, 6.5 Hz, 2 H, H_2-7). ^{13}C-NMR (125 MHz): δ = 146.6 (C-3), 146.4 (C-3'), 139.3 (C-2'), 138.9 (C-2), 137.7 (C-8), 137.5 (C-8'), 133.9 (C-5), 133.2 (C-5'), 126.09 (C-1), 124.3 (C-1'), 123.4 (C-6'), 121.6 (C-6), 116.0 (C-9'), 115.7 (C-9), 114.5 (C-4), 110.5 (C-4'), 56.3 (C3-OMe), 40.19 (C-7'), 39.91 (C-7).

*5,5'-bis(2-hydroxyethyl)-[1,1'-biphenyl]-2,2'-diol (**86**):* tyrosol **77**(100.0 mg, 0.64 mmol) was solubilised in 40 mL of acetone. The solution was stirred with the enzyme solution (5.2 mg of HRP in 20.0 mL of acetate buffer) at rt and three aliquots of H_2O_2 (0.3%, 0.1 mL) were added in 2 h intervals; after 4 h the total organic phase was finally washed with water, dried and evaporated under vacuum. The flash chromatography with DIOL Silica-gel, eluted with *n*-hexane –$CHCl_3$ (40:60 → 0:100) and $CHCl_3$–MeOH (99:1 → 94:6) gave the biphenyl neolignan **86** (20.1 mg, 19.1%) as yellow oil: Rf (TLC) 0.46 ($CHCl_3$–MeOH, 94:6); ESIMS *m/z* 273.1 $[M-H]^-$ (calcd for $C_{16}H_{18}O_4$); ^{1}H-NMR (500 MHz, Acetone-d_6, 298 K): δ = 7.13 (d, 1.5 Hz, 2H, H-6/6'), 7.06 (dd, 1.5, 7.5 Hz, 2 H, H-4/4'), 6.86 (d, 18.0 Hz, 2 H, H-3/3'), 3.70 (t, 7.0 Hz, 4 H, H_2-8/8'), 2.74 (t, 7.0 Hz, 4 H, H_2-7/7'). ^{13}C-NMR (125 MHz): δ = 153.0 (C-2/2'),132.9 (C-6/6'), 132.3 (C-5/5'), 130.0 (C-4/4'), 127.0 (C-1/1'), 117.3 (C-3/3'), 64.14 (C-8/8'), 39.54 (C-7/7').

*5,5'-bis(2-hydroxyethyl)-3,3'-dimethoxy-[1,1'-biphenyl]-2,2'-diol (**87**):* homovanillic alcohol **78** (80.0 mg, 0.47 mmol) was solubilized in 32 mL

of acetone. The solution was stirred at rt with the enzyme solution (4.16 mg of HRP in 16.0 mL of acetate buffer) and three aliquots of hydrogen peroxide (0.3%, 0.1 mL) were added in 2 h intervals; after 4 h the total organic phase was finally washed with water, dried and evaporated under vacuum. The flash chromatography with DIOL Silica-gel, eluted with *n*-hexane −CH_2Cl_2 (30:70 → 0:100) and CH_2Cl_2 − MeOH (99:1 → 94:6) gave the biphenyl neolignan **87** 43.5 % of yield (34.2 mg): R_f (TLC) 0.46 (CH_2Cl_2−MeOH, 94:6); ESIMS *m/z* 333.2 $[M-H]^-$ (calcd for $C_{16}H_{18}O_6$); ^{1}H-NMR (500 MHz, acetone-d_6): δ = 6.86 (d, 2.0 Hz, 2H, H-4/4'), 6.74 (d, 2.0 Hz, 2H, H-6/6'), 3.89 (s, 6H, 3/3'-OCH_3), 3.77 (t, 7.0 Hz, 4H, H_2-8/8'), 2.78 (t, 7.0 Hz, 4H, H_2-7/7'). ^{13}C-NMR (125 MHz): δ = 150.4 (C-3/3'), 144.5 (C-2/2'), 132.7 (C-5/5'), 128.2 (C-1/1'), 126.2 (C-6/6'), 113.9 (C-4/4'), 65.8 (C-8/8'), 58.0 (C-3/3'-OCH_3), 41.5 (C-7/7').

General procedure of enzymatic esterification: *Candida antarctica* Lipase (CAL, 300 mg) and the acyl donor (vinyl acetate) (42 mmol) were added to a solution of the substrate (**77** or **78**, 2.17 mmol) in *t*-butylmethyl ether (75 ml) and the mixture was shaken (400 rpm) at 40 °C for a convenient period of time, as reported below. The progress of each reaction was monitored, at regular time intervals, through TLC (2% MeOH-$CHCl_3$). The reactions were quenched through filtering off the enzyme and the filtrate was evaporated under vacum. The products were purified through flash chromatography on DIOL Silica-gel 40–63 lm (Merck). The elution system is reported below for each purified compound.

*4-hydroxyphenethyl acetate (**79**):* Compound **79** was prepared using tyrosol as starting material (**77**) through a 35 min. reaction, and purified on Diol Silica-gel using a gradient from 80% CH_2Cl_2 in *n*-hexane to 100% CH_2Cl_2; yield 95.0%. The spectroscopic data, compared with the

data previously obtained and reported in the literature,[155] confirmed the structure of the acetate derived of tyrosol.

*4-Hydroxy-3-methoxyphenetyl acetate (**80**)*: Compound **80** was prepared using homovanillyl alcohol as starting material (**78**) through a 60 min. reaction and purified on Diol Silica-gel using 70% CH_2Cl_2 in *n*-hexane; with a resulting yield of 96.8%. The spectroscopic data, compared with the data previously obtained and reported in the literature,[155] confirmed the structure of the acetate derived of homovanillyl alcohol.

(6,6'-dihydroxy-[1,1'-biphenyl]-3,3'-diyl)b*is(ethane-2,1-diyl) diacetate (**88**)*: tyrosol acetate **79** (382.3 mg, 2.14 mmol) was solubilised in 183.6 mL of acetone. The solution was stirred with the enzyme solution (12.3 mg of HRP in 47.6 mL of acetate buffer) at rt and three aliquots of H_2O_2 (0.3%, 0.1 mL) were added in 2 h intervals; after 4 h the total organic phase was finally washed with water, dried and evaporated under vacuum. The flash chromatography with DIOL Silica-gel, eluted with *n*-hexane−acetone (100:0 → 50:50) gave the biphenyl neolignan **88** with 19.9% of yield (20.1 mg): Rf (TLC) 0.46 (*n*-hexane −acetone, 70:30); ESIMS *m/z* 357.1 $[M-H]^-$ (calcd for $C_{20}H_{22}O_6$); ^{1}H-NMR (500 MHz, acetone-d_6): δ = 8.29 (bs, 1 H,-OH), 7.99 (s, 1 H, -OH), 7.21 (d, 2.5 Hz, 2 H, H-6/6'), 7.15 (dd, 2.5, 8.5 Hz, 2 H, H-4/4'), 6.95 (d, 8.5 Hz, 2 H, H-3/3'), 4.24 (t, 7.0 Hz, 4 H, H_2-8/8'), 2.91 (t, 7.0 Hz, 4 H, H_2-7/7'), 1.99 (s, 6 H, -CH3).^{13}C-NMR (125 MHz): δ = 170.9 (C-9/9'), 153.4 (C-2/2'), 132.9 (C-6/6'), 130.8 (C-5/5'), 130.06 (C-4/4'), 127.0 (C-1/1'), 117.4 (C-3/3'), 65.6 (C-8/8'), 34.9 (C-7/7'), 20.7 (C-10).

*(6,6'-dihydroxy-5,5'-dimethoxy-[1,1'-biphenyl]-3,3'-diyl)bis(ethane-2,1-diyl) diacetate (**89**)*: homovanillic alcohol acetate **80** (300.0 mg, 1.42 mmol) was solubilized in 142 mL of acetone. The solution was stirred at rt with the enzyme solution (9.3 mg of HRP in 35.8 mL of acetate buffer)

and three aliquots of H_2O_2 (0.3%, 0.1 mL) were added in 2 h intervals; after 4 h the total organic phase was finally washed with water, dried and evaporated under vacuum. The flash chromatography with DIOL Silica-gel, eluted with *n*-hexane −acetone (100:0 → 50:50) gave the biphenyl neolignan **89** with 49.3% of yield (146.5 mg): Rf (TLC) 0.36 (*n*-hexane-acetone, 70:30); ESIMS *m/z* 417.2 $[M-H]^-$ (calcd for $C_{22}H_{26}O_8$); ^{1}H-NMR (500 MHz, acetone-d_6): δ = 7.45 (bs, 2 H, -OH), 7.10 (d, 2.0 Hz, 2 H, H-4/4'), 6.83 (d, 2.0 Hz, 2 H, H-6/6'), 4.29 (t, 7.0 Hz, 4H, H_2-8/8'), 3.93 (s, 6H, 3/3'-OCH_3), 2.93 (t, 7.0 Hz, 2 H, H_2-7/7'), 2.05 (s, 6 H, -CH_3). ^{13}C-NMR (125 MHz): δ = 170.0 (C-9/9'), 147.8 (C-3/3'), 142.3 (C-2/2'), 128.8 (C-5/5'), 125.4 (C-1/1'), 123.7 (C-6/6'), 111.2 (C-4/4'), 64.8 (C-8/8'), 55.5 (C-3/3' OCH3), 34.56(C-7/7'),19.98 (C-10).

*(5,5',6,6'-tetrahydroxy-[1,1'-biphenyl]-3,3'-diyl)bis(ethane-2,1-diyl) diacetate (**90**)*: dityrosol diacetate (**88**, 175 mg, 0.48 mmol) was dissolved in MeOH (8.9 mL, 0.1 M), and then IBX (205.2 mg, 0.73 mmol) was added. The solution was stirred at 0 °C until disappearance of the substrate (50 min.). At the end, $Na_2S_2O_4$ solution (83.5 mg, 0.81 mmol in 8.9 mL of H_2O) was added, and the solution was stirred for 5 min. at rt. After evaporation of the solvent under vacuum, the residue was solubilized with ethyl acetate and treated with a saturated $NaHCO_3$ solution. The aqueous phase was extracted with ethyl acetate. The organic phases were washed with a saturated NaCl solution and dried over Na_2SO_4. After filtration, the solvent was evaporated under vacuum. The flash chromatography with DIOL Silica-gel, eluted with *n*-hexane -$CHCl_3$ (30:70 → 0:100) and $CHCl_3$− MeOH (99:1 → 97:3) gave the biphenyl neolignans **90.** The compound **90** was recovered 11.6 % of yield (22.6 mg): R_f (TLC) 0.46 (CH_2Cl_2−MeOH, 93:7); ESIMS *m/z* 389.1 $[M-H]^-$ (calcd for $C_{20}H_{22}O_8$); ^{1}H-NMR (500 MHz,$CDCl_3$): δ = 8.00 (s, OH), 6.81

(d, 2.0 Hz, 2 H, H-6/6'), 6.73 (d, 2.0 Hz, 2 H, H-4/4'), 4.22 (t, 7.0 Hz, 4 H, H_2-8/8'), 2.83 (t, 7.0 Hz, 4 H, H_2-7/7'), 1.98 (s, 6 H, H_3-10/10'). ^{13}C-NMR (125 MHz): δ = 171.0 (C-9/9'), 146.8 (C-3/3'), 141.1 (C-2/2'), 131.5 (C-5/5'), 127.4 (C-1/1'), 122.5 (C-4/4'), 115.2 (C-6/6'), 65.7 (C-8/8'), 35.3 (C-7/7'), 20.9 (C-10/10').

*(5,6,6'-trihydroxy-5'-methoxy-[1,1'-biphenyl]-3,3'-diyl)bis(ethane-2,1-diyl) diacetate (**91**)*: dihomovanillic alchol diacetate (**89**, 171.6 mg, 0.41 mmol) was dissolved in THF (5.82 mL, 0.06 M), and then IBX (172.5 mg, 0.61 mmol) was added. The solution was stirred at rt until disappearance of the substrate (1 h). At the end, $Na_2S_2O_4$ solution (107.0 mg, 0.61 mmol in 5.0 mL of H_2O) was added, and the solution was stirred for 5 min. at rt. After evaporation of the solvent under vacuum, the residue was solubilized with ethyl acetate and treated with a saturated $NaHCO_3$ solution. The aqueous phase was extracted with ethyl acetate. The organic phases were washed with a saturated NaCl solution and dried over Na_2SO_4. The organic phase was dried on Na_2SO_4. After filtration, the solvent was evaporated under vacuum. The flash chromatography with DIOL Silica-gel, eluted with *n*-hexane-$CHCl_3$ (15:85 → 0:100) and $CHCl_3$− MeOH (99:1 → 93:7) gave the biphenyl neolignan **91** and also a more polar product that shows ESIMS and NMR data identical to those of compound **90**. The compound **91** was recovered with 18.3 % of yield (30.3 mg): R_f (TLC) 0.46 (CH_2Cl_2−MeOH, 95:5); ESIMS *m/z* 403.1 $[M-H]^-$ (calcd for $C_{21}H_{24}O_8$); ^{1}H-NMR (500 MHz,$CDCl_3$): δ = 8.00 (s, OH), 6.94 (d, 1.5 Hz, 1 H, H-4), 6.83 (d, 1.5 Hz, 1 H, H-6), 6.78 (d, 1.5 Hz, 1 H, H-4'), 6.70 (d, 1.5 Hz, 1 H, H-6'), 4.23 (q, 7.0 Hz, 4 H, H_2-8/8'), 3.90 (s, 3 H, H_3-OMe), 2.91 (t, 7.0 Hz, 2 H, H_2-7), 2.83 (t, 7.0 Hz, 2 H, H_2-7'), 2.00 (s, 3 H, H_3-10), 1.99 (s, 3 H, H_3-10'). ^{13}C-NMR (125 MHz): δ = 171.0 (C-9/9'), 148.5 (C-3), 147.4 (C-2'), 142.1 (C-2), 141.4 (C-3'),

131.2 (C-5'), 131.1 (C-5), 127.5 (C-1'), 126.3 (C-1), 124.5 (C-6), 122.9 (C-6'), 115.6 (C-4'), 112.2 (C-4), 65.8 (C-8/8'), 56.6 (C-OMe), 35.5 (C-7), 35.3 (C-7'), 20.9 (C-10/10').

*Enzymatic Butanolysis of **90** and **91***: Candida antarctica lipase (10.0 mg) and n-butyl alcohol (0.05 mL) were added to a solution of a substrate (**90** and **91**, 10.0 mg) in MTBE (1.20 mL). The resulting mixture was stirred (400 rpm) at 40 °C, and the progress of each reaction was monitored by TLC (CH2Cl2−MeOH, 90:10). After the completion of each reaction, the enzyme was filtered off and the filtrate was evaporated in vacuo. The crude mixtures were purified by flash chromatography on Diol silica gel (CH2Cl2−MeOH, 98:2 → 90:10).

*5,5'-Bis(2-hydroxyethyl)-[1,1'-biphenyl]-2,2',3,3'-tetraol (**92**):* yellow oil (6.5 mg, 82.7%); Rf (TLC) 0.25 (CH_2Cl_2−MeOH, 90:10); ^{1}H NMR (acetone-d_6, 500 MHz) δ 6.76 (2H, s, H-6), 6.70 (2H, s, H-4), 3.73 (4H, t, *J* = 7.5 Hz, H2-8), 2.71 (4H, t, *J* = 7.5 Hz, H2-7); ^{13}C NMR (acetone-d_6, 125 MHz) δ 146.7 (C, C-3), 140.8 (C, C-2), 132.7 (C, C-5), 127.4 (C, C-1), 123.1 (CH, C-4), 115.7 (CH, C-6), 64.2 (CH2, C-8), 39.9 (CH2, C-7); ESIMS m/z 305.2 $[M - H]^-$ (calcd for $C_{16}H_{17}O_6$, 305.1); anal. C 62.76, H 5.95%, calcd for $C_{16}H_{18}O_6$, C 62.74, H 5.92%.

*5,5'-Bis(2-hydroxyethyl)-3'-methoxy-[1,1'-biphenyl]-2,2',3-triol (**93**):* yellow oil (6.6 mg, 82.4%); Rf (TLC) 0.30 (CH_2Cl_2−MeOH, 90:10); ^{1}H NMR (acetone-d_6, 500 MHz) δ 6.90 (1H, s, H-4), 6.79 (1H, s, H-6), 6.74 (1H, d, *J* = 1.5, H-4′), 6.66 (1H, d, *J* = 1.5 Hz, H-6′), 3.89 (3H, s, OCH3-3), 3.75 (2H, t, *J* = 7.1 Hz, H2-8), 3.71 (2H, t, *J* = 7.1 Hz, H2-8′), 2.75 (2H, t, *J* = 7.1 Hz, H2-7), 2.71 (2H, t, *J* = 7.1 Hz, H2-7′); ^{13}C NMR (acetone-d_6, 125 MHz) δ 147.4 (C, C-3), 147.3 (C, C-2′), 141.5 (C, C-2), 140.9 (C, C-3′), 132.7 (C, C-5′), 132.5 (C, C-5), 127.4 (C, C-1′), 126.3 (C, C-1), 124.5 (CH, C-6), 122.2 (CH, C-6′), 115.7 (CH, C-4′), 112.3 (CH, C-

4), 64.2 (CH2, C-8), 64.1 (CH2, C-8′), 56.5 (CH3, OCH3-3), 40.1 (CH2, C-7), 39.9 (CH2, C-7′); ESIMS m/z 319.1 $[M - H]^-$ (calcd for $C_{17}H_{19}O_6$, 319.1); anal. C 63.71, H 6.32%, calcd for $C_{17}H_{20}O_6$, C 63.74, H 6.29%.

*5,5'-diallyl-2'-methoxy-[1,1'-biphenyl]-2-ol (**94**) and 5,5'-diallyl-2,2'-dimethoxy-1,1'-biphenyl (**95**):* magnolol (**44**, 20.0 mg, 0.075 mmol) was dissolved in *dry* acetone (7.7 mL) and then was added K_2CO_3 (20.7 mg, 0.15 mol) and CH_3I (7.6 µL, 0.15 mmol); The solution was stirred at reflux for 48 h and then was quenched. After evaporation of the solvent under vacuum the residue was submitted to flash chromatography with DIOL Silica-gel, eluted with *n*-hexane -$CHCl_3$ (100:0 → 30:60) gave the monomethylated **94** and the permethylated **95**. The NMR data are in agreement with those previously reported in literature.[156]

*5,5'-diallyl-2'-methoxy-[1,1'-biphenyl]-2,3-diol (**96**):* Compound **94** (171.6 mg, 0.61 mmol) was dissolved in MeOH (3.0 mL, 0.2 M), and then IBX (205.2 mg, 0.73 mmol) was added. The solution was stirred at 0 °C until disappearance of the substrate (30 min.). At the end, $Na_2S_2O_4$ solution (83.5 mg, 0.81 mmol in 8.9 mL of H_2O) was added, and the solution was stirred for 5 min. at rt. After evaporation of the solvent under vacuum, the residue was solubilized with ethyl acetate and treated with a saturated $NaHCO_3$ solution. The aqueous phase was extracted with ethyl acetate. The organic phases were washed with a saturated NaCl solution and dried over Na_2SO_4. After filtration, the solvent was evaporated under vacuum. The flash chromatography with DIOL Silica-gel, eluted with *n*-hexane -$CHCl_3$ (30:70 → 0:100) and $CHCl_3$– MeOH (99:1 → 97:3) gave the biphenyl neolignans **96.** The compound **96** was recovered with 11.6 % of yield (22.6 mg): R_f (TLC) 0.46 (100% CH_2Cl_2); ^{1}H-NMR (500 MHz,$CDCl_3$): δ = 7.21 (m, from 7.21 to 7.19, 1 H, H-6'), 7.20 (m, from 7.21 to 7.19, 1 H, H-/4'), 6.99 (d, 8.5 Hz, 1H, H-3'), 6.82 (d, 2.0 Hz, 1 H,

H-4), 6.70 (s, 1 H, OH), 6.65 (d, 2.0 Hz, 1 H, H-6), 5.97 (m, from 5.95 to 6.0, 2 H, H-8/8'), 5.85 (s, 1 H, OH), 5.06 (m, from 5.12 to 5.04, 4 H, H_2-9/9'), 3.91 (s, 3 H, OMe), 3.31 (d, 7.0Hz, 2 H, H_2-7'), 3.34 (d, 7.0 Hz, 2 H, H_2-7). ^{13}C-NMR (125 MHz): δ = 153.5 (C-2'), 146.3 (C-3), 139.0 (C-2), 137.7 (C-8), 137.4 (C-8'), 134.4 (C-5'), 133.8 (C-5), 132.5 (C-6'), 129.3 (C-4'), 127.4 (C-1), 126.8 (C-1'), 121.9 (C-6), 116.0 (C-3'), 115.8 (C-9), 114.4 (C-9'), 112.3 (C-4), 56.9 (OMe), 39.9 (C-8), 39.4 (C-8').

*(±)-5-((E)-2-(4-Methylbenzylcarbamoyl)vinyl)-N-(4-methylbenzyl)-2,3-dihydro-2-(4-hydroxyphenyl)benzofuran-3-carboxamide [(±) -**99**]:* isoeugenol **97** (400.0 mg, 2.4 mmol) was dissolved in 12. 0 mL of *dry* THF and then IBX (806.0 mg, 2.88 mmol) was added. The solution was stirred at rt until disappearance of the substrate (1 h). At the end, $Na_2S_2O_4$ solution (500.0 mg, 2.87 mmol in 6.0 mL of H_2O) was added, and the solution was stirred for 5 min. at rt. After evaporation of the solvent under vacuum, the residue was solubilized with ethyl acetate and treated with a saturated $NaHCO_3$ solution. The aqueous phase was extracted with ethyl acetate. The organic phases were washed with a saturated NaCl solution and dried over Na_2SO_4. The organic phase was dried on Na_2SO_4. After filtration, the solvent was evaporated under vacuum. The flash chromatography with DIOL Silica-gel, eluted with *n*-hexane-$CHCl_3$ (30:60 → 0:100) and $CHCl_3$− MeOH (99:1 → 97:3) gave the dihydrbenzofuran neolignan **99**. The compound **99** was recovered with 15.0 % of yield (63.4 mg): R_f (TLC) 0.46 (CH_2Cl_2−MeOH, 97:3); ESIMS *m/z* 313.1 $[M-H]^+$ (calcd for $C_{19}H_{20}O_4$); ^{1}H NMR (acetone-d_6, 500 MHz) *δ* 1.35 (3H, d, *J* = 7.0 Hz, C-3-Me), 1.81 (3H, dd, *J* = 2.0, 6.0 Hz, H-9′), 3.41 (1H, m, *J* = 9.45 Hz, H-3), 3.85 (3H, s, OMe), 5.07 (1H, d, *J* = 9.5 Hz, H-2), 6.07 (1H, m, *J* = 6.55, 16.0Hz, H8′), 6.31 (1H, dd, *J* = 2.0, 16.0 Hz, H-7′), 6.73 (1H, bs, H-4), 6.77 (1H, bs, H-6), 6.86 (1H, d, *J* = 8.0 Hz,

H-5’), 6.93 (1H, dd, *J* = 2.0, 8.0 Hz, H-6’), 6.93 (1H, d, *J* = 2.0 Hz, H-2’), 7.64 (1H, bs, OH), 7.86 (1H, bs, OH); ^{13}C NMR (acetone-d_6, 125 MHz) δ 22.1 (C-3 Me), 22.8 (C-9′), 50.7 (C-3), 60.6 (OMe), 98.3 (C-2), 115.1 (C-2’), 117.4 (C-4), 118.5 (C-6), 119.5 (C-5’), 124.8 (C-6′), 127.3 (C-8′), 136.4 (C-7′), 137.1 (C-7), 137.2 (C-3a), 138.8 (C-5), 146.1 (C-1′), 150.8 (C-7a), 151.9 (C-3′), 152.7 (C-4’).

4.5 α-Glucosidase inhibition assay

The inhibitory activity on yeast a-glucosidase was assessed through a slight modification of a previously reported method *Kurihara et al.*,[103] employing *p*-nitrophenyl-α-D-glucopyranoside (*p*-NP-a-Glc) as substrate. Stock solutions at different concentration of the compounds **81**, **82**, **84** – **93** were prepared in MeOH (in the range 40 – 0.5 µM). For each assay, with the order, different aliquots (10, 20, 30, 40, 60 µL) of each sample were added to α-glucosidase from Saccharomyces cerevisiae (10 U/mL; 50 µL) in 5 mL volumetric flask and finally a 6.0 10^{-3} M *p*NP-α-G solution (buffer Na_2HPO_4/KH_2PO_4 0.05 M, pH = 7.2; 30 µL).The final concentration of MeOH did not exceed 1.5%. The solutions were incubated at 37 °C for 30 min and stopped by adding 1 M Na_2CO_3 solution (200 µL). Enzymatic activity was quantified by measuring absorbance at 405 nm. The assay was performed in triplicate with five different concentrations and quercetin was used as positive control. The inhibition percentage was calculated by the equation: Inhibition % = $[(A_{control} - A_{sample})/A_{control}]$ x 100. The IC_{50} value (µg/mL) was defined as the concentration that inhibited 50% of α-glucosidase activity.

4.6 Vescalin total synthesis

(2*R*,3*R*,5*R*,6*R*)-2-(acetoxymethyl)-6-((2-nitrobenzyl) oxy)tetrahydro-2H-pyran-3,4,5-triyl triacetate (**106**): according to the procedure described in the literature,[175] to a solution of commercially available 2-nitrobenzyl alcohol (**105**, 4.6 g , 30.3 mmol, 5 eq) in dry CH_2Cl_2 (24.8 mL) were added Ag_2CO_3 (5.01 g, 18.18 mmol, 3 eq), and one crystals of iodine. The reaction was stirred over 4Å molecular sieves for 15 minutes. A solution of commercially available 2,3,4,6-tetra-*O*-acetyl-α-*D*-glucopyranosyl bromide (**104**, 2.5 g, 6.06 mmol, 1 eq) in dry CH_2Cl_2 (12.5 mL) (also stirred over 4 Å molecular sieves for 15 minutes) was then added dropwise. The reaction flask was shielded from light and stirred at room temperature under nitrogen for 16 hours. The reaction mixture was diluted with EtOAc, filtered through celite, and concentrated in vacuo. Crude material (6.3 g) was purified by column chromatography (EtOAc/cyclohexane 0:100 → 80:20) to afford **105** as white crystals (0.838 g, 1.73 mmol, 28%). Rf = 0.20 (30:70 AcOEt/cyclohexane). ^{1}H-NMR (300 MHz, $CDCl_3$) δ (ppm): 2.02 (s, 3H, OAc), 2.04 (s, 3H, OAc), 2.06 (s, 3H, OAc), 2.09 (s, 3H, OAc), 3.73-3.79 (m, 1H, H5),4.15 (dd, *J* = 2.2, 12.3 Hz, 1H, H6), 4.30 (dd, *J* = 4.8, 12.4 Hz, 1H, H6), 4.68 (d, *J* = 7.9 Hz, 1H, H1), 5.06 and 5.26 (AB, *JAB* = 14.5 Hz, 2H, H7), 5.10-5.25 (m, 3H, H2/H3/H4), 7.46 (t, *J* = 7.6 Hz, 1H, H11), 7.63 (d, *J* = 7.6 Hz, 1H, H9), 7.70 (t, *J* = 7.7 Hz, 1H, H10), 8.09 (dd, *J* = 8.1 Hz, 1H, H12).

(2*R*,3*S*,4*S*,5*R*,6*R*)-2-(hydroxymethyl)-6-((2-nitrobenzyl) oxy)tetrahydro-2H-pyran-3,4,5-triol (**107**): According to the procedure described in the literature,[179] 1.0 equivalent of NaOMe (2.5 mL) was added to a stirred solution of nitrobenzylacetoglucose **106** (5.32 g, 11 mmol) in 22 mL of MeOH (0.5 M). After 30' TLC analysis showed a complete conversion of substrate in a more polar compound (5% acetone-AcOEt). The solution

was then neutralized on dowex (50 X 8 – 400 ion-exchange resin H^+) and concentrated in vacuo. Then the product **107** was recovered as white crystals (3.35 g, 11.9 mmol, 96%). R*f* = 0.15 (5:95 acetone/AcOEt); ^{1}H-NMR (300 MHz, methanol-*d4*) δ (ppm): 3.32-3.43 (m, 4H, H2/H3/H4/H5), 3.69 (dd, *J* = 4.9, 11.9 Hz, 1H, H6), 3.88 (dd, *J* = 2.0, 11.1 Hz, 1H, H6), 4.43 (d, *J* = 7.6 Hz, 1H, H1), 5.08 and 5.29 (AB, *J*AB = 15.3 Hz, 2H, H7), 7.51 (td, J = 1.3, 7.7 Hz, 1H, H10), 7.71 (td, *J* = 1.3, 7.2 Hz, 1H, H11), 8.02 (dd, *J* = 1.3, 8.1 Hz, 1H, H9).

2*R*,4*R*,6*R*,7*R*,8*R*,8*S*)-6-((2-nitrobenzyl)oxy)-2-phenylhexahydropyrano[3,2-d][1,3]dioxine-7,8-diol (**108**): $ZnCl_2$ (7.7 g, 56.3 mmol) was added under argon to a suspension of deacetyl glucose derivative (**107**, 3.35 g, 10.6 mmol) in 35.3 mL of benzaldehyde (0.3 M), then the mixture was stirred at room temperature for 24 h. The reaction solution was poured into ice and the crude product was extracted with EtOAc (3 X 30 mL). The combined organic layers were washed with brine, dried on Na2SO4 and concentrated in vacuo. Crude material (6.3 g) was purified by column chromatography (EtOAc/cyclohexane 10:90 → 50:50) to afford **108** as white crystals (2.9 g, 7.1 mmol, 70%). Rf = 0.10 (40:60 AcOEt/cyclohexane); ^{1}H-NMR (300 MHz, $CDCl_3$) δ (ppm): 3.42-3.66 (m, 3H, H2/H4/H5), 3.74-3.87 (m, 2H, H3/H6), 4.36 (dd, *J* = 4.8, 10.5 Hz, 1H, H6), 4.57 (d, *J* = 7.6 Hz, 1H, H1), 5.11 and 5.28 (AB, *J*AB = 14.7 Hz, 2H, H7), 5.53 (s, 1H, H14), 7.33-7.53 (m, 6H, H16/H17/H18/H10), 7.66 (t, *J* = 7.6 Hz, 1H, H11), 7.84 (d, *J* = 7.7 Hz, 1H, H12), 8.08 (d, *J* = 8.1 Hz, 1H, H9).

*4-(benzyloxy)-3,5-dihydroxybenzoic acid (**110**):* according to the procedure described in the literature,[184] to a stirred solution of the galloyl derivative (**109**, 9.7 g, 35.39 mmol) in 352 mL of THF:MeOH:H_2O (3:3:1, 0.1 M) was added NaOH (4.6 g, 116.7 mmol). The mixture was

then stirred at room temperature for 24 h. The excess of MeOH was evaporated and 5 M aqueous solution of HCl was added to acidify the reaction mixture. The mixture was extracted with AcOEt (3 x 20 ml) and the organic layer was washed with brine, dried over Na_2SO_4 and evaporated *in vacuo* to give the saponified product **110** (7.4 g, 28.4 mmol, 80.4%) as an orange powder. R*f* = 0.5 (40:60 AcOEt/PET); ^{1}H-NMR (300 MHz, acetone-d_6) δ (ppm): 5.19 (s, 2H, H6), 7.13 (s, 2H, H3), 7.28-7.54 (m, 5H, H8/H9/H10), 8.35 (2H, OH).

*4-(benzyloxy)-3,5-bis((tert-butyldimethylsilyl)oxy)benzoic acid (**111**):* to a stirred solution of benzyloxydihydroxybenzoic acid (**110**, 7.4 g, 28.45 mmol) in 56 mL of DMF (0.5 M), imidazole (19.3 g, 284.5 mmol) and TBSCl (20.3 g, 134.6 mmol) were added. Then the mixture was stirred at room temperature, under argon for 24 h. After addition of EtOAc (150 mL), the organic layer was washed 8 times with a 1:1 mixture of H2O/brine (8 x 100 ml), dried over Na_2SO_4 and concentrated in vacuo to afford the trisilylated product as an orange oil. Crude material was dissolved in 40 ml of dry THF at room temperature. A 3:1 mixture of AcOH/H_2O (120 ml) was then added to the solution and the mixture was allowed to stir at room temperature for 18h. The reaction was quenched with slow addition of $NaHCO_3$ (10 g) and the mixture was stirred for 10 minutes. After addition with caution of water (100 ml), the resulting aqueous phase was extracted with EtOAc (3 x 150 ml). Combined organic layers were washed with water until aqueous layer turned to pH 5-6, then washed with brine (200 ml), dried over Na_2SO_4 and concentrated in vacuo to yield crude material as an orange oil. Recrystallization in MeOH (200 ml) gave **111** as white crystals (8.2 g, 17.2 mmol, 60%). R*f* = 0.49 (20:80 AcOEt/PET); ^{1}H-NMR (300 MHz, $CDCl_3$) δ (ppm): 0.18 (s, 12H, H6), 0.97 (s, 18H, H7), 5.07 (s, 2H, H9), 7.29-7.44 (m, 7H, H3/H11/H12/H13).

*2-nitrobenzyl-4,6-O-benzylidene-2,3-bis(4-(benzyloxy)-3,5-[di(tert butyldimethylsilyl)oxy])benzoyl-β-D-glucopyranoside (**112**):* to a solution of **108** (2.0 g, 7.9 mmol, 1 eq) and **111** (8.3 g, 19.9 mmol, 2.5 eq) in CH_2Cl_2 (335 ml) were added at O°C DMAP (6.8 g, 55.7 mmol, 7 eq) and EDC-HCl (9.1 g, 39.8 mmol, 5 eq). The solution was purged with argon and stirred at room temperature for 20 h. A 1 M aqueous solution of H_3PO_4 (200 ml) was then added to quench the reaction and the mixture was extracted with CH_2Cl_2 (3 x 150 ml). The organic layer was then washed with brine (2 x 150 ml), dried over Na_2SO_4 filtered and concentrated under reduced pressure. The resulting residue was purified by column chromatography with EtOAc:PET (1:99 → 20:80) to furnish **112** (4.3 g, 3.2 mmol, 40.5 %) as a white foam. ^{1}HNMR (300 MHz, $CDCl_3$) δ (ppm): 0.12 (s, 6H, H10), 0.12 (s, 6H, H10), 0.13 (s, 6H, H10), 0.14 (s, 6H, H10), 0.93 (s, 36H, H11), 3.75 (dt, J = 4.7, 9.5 Hz, 1H, H5), 3.86-3.97 (m, 2H, H4/H6), 4.48 (dd, J = 4.7, 10.2 Hz, 1H, H6), 4.92 (d, J = 7.7 Hz, 1H, H1), 4.96-5.06 (m, 4H, H8), 5.08 & 5.36 (2H, J_{AB} = 15.7 Hz, H7), 5.56 (s, 1H, H9) ,.56 (s, 1H, H2), 5.74 (t, J = 9.5Hz, 1H, H3), 7.17 (s,2H, H2'^{I}/H2'^{II}/H6'^{I}/H6'^{II}), 7.17 (s, 2H, H2'^{I}/H2'^{II}/H6'^{I}/H6'^{II}), 7.28/7.48 (m, 17H, H2'$^{III/}$H3'^{III}/H4'^{III}/H2'^{IV}/H3'^{IV}/H4'^{IV}/H3'^{V}/H4'^{V}), 7.73 (dd, J = 1.2, 7.6 Hz, 1H, H2'V), 8.08 (dd, J = 1.4, 8.0 Hz, 1H, H5'V). ^{13}C NMR (75 MHz, $CDCl_3$) δ (ppm) : 164.9 ($C_{I=O}$), 164.6 ($C_{II=O}$), 149.7/149.6 (C3'I/C3'II/C5'I/C5'II), 146.6/146.5 (C4'I/C4'II), 146.5 (C6'V), 124.2/124.0 (C1'I/ C1'II), 116.1 (C2'I/C2'II/C6'I/C6'II), 101.6 (C9), 101.5 (C1), 78.9 (C4), 74.1 (C8), 72.2 (C2), 71.7 (C3), 68.5 (C6), 68.2 (C7), 66.7 (C5), 25.7 (C11), 25.7 (C11), 18.3 (C12), -4.5 (C10), -4.5 (C10)

*2-nitrobenzyl-4,6-O-benzylidene-2,3-bis(4-(benzyloxy)-3,5-dihydroxyl)benzoyl-β-D- glucopyranoside (**113**):* to a solution of **112** (4.2

g, 3.2 mmol, 1 eq) in dry THF (106 ml) was added a 1 M solution of TBAF in THF (19.2 ml, 19.2 mmol, 6 eq) and acetic acid (2.9 ml, 51.2 mmol, 16 eq). The solution was stirred under argon at room temperature for 2 hours. The reaction mixture was then diluted with 1 M aqueous solution of H_3PO_4 (100 ml). The product was extracted with AcOEt and the organic layer was washed with brine (10 ml), dried over Na_2SO_4 and concentrated *in vacuo*. Crude material was purified by column chromatography (AcOEt:PET 1:9 → 4:6) to afford **113** as a pale orange foam (2.9 g, 3.2 mmol, quantitative yield). ^{1}HNMR (300 MHz, acetone-*d6*) δ (ppm) : 3.88 (dt, J = 4.3, 9.4 Hz, 1H, H5), 3.95 (t, J = 9.8 Hz, 1H, H6), 4.12 (t, J = 9.3 Hz, 1H, H4), 4.42 (dd, J = 4.0, 9.4 Hz, 1H, H6), 5.13-5.32 (m, 7H, H1/H7/H8), 5.52 (dd, J = 7.9, 9.4 Hz, 1H, H2), 5.71 (s, 1H, H9), 5.78 (t, J = 9.5 Hz, 1H, H3), 7.11 (s, 2H, H2'^{I}/H2'^{II}/H6'^{I}/H6'^{II}), 7.13 (s, 2H, H2'^{I}/H2'^{II}/H6'^{I}/H6'^{II}), 7.28-7.54 (m, 17H, /H2'^{III}/H3'^{III}/H4'^{III}/H2'^{IV}/H3'^{IV}/H3'^{V}/H4'^{V}), 7.70-7.73 (m, 1H, H2'^{V}), 8.05-8.08 (m, 1H, H5'^{V}), 8.69 (s, 1H, OH), 8.74 (s, 1H, OH). ^{13}C NMR (75 MHz, acetone-*d6*) δ (ppm) : 165.7 (CII=O), 165.4 (CI=O), 151.3/151.2 (C3'I/C3'II/C5'I/C5'II), 147.8 (C6'V), 139.3/139.2 (C4'I//C4'II), 138.4 (C1'III), 138.4 (C1'IV), 134.8 (C1'V), 134.5 (C4'V), 129.6 (CHAr), 129.2 (CHAr), 129.2 (CHAr), 129.1 (CHAr), 129.0 (CHAr), 128.9 (CHAr), 128.9 (CHAr), 128.8 (CHAr), 128.7 (CHAr), 128.7 (CHAr), 127.1 (C2'IV/C3'IV), 125.6/125.5 (C1'I/ C1'II), 125.4 (C5'V), 110.2 (C2'I/ C6'I), 110.1 (C2'II/C6'II), 102.0 (C9), 101.9 (C1), 79.4 (C4), 74.6 (C8), 74.5 (C8), 73.3 (C2), 72.8 (C3), 68.9 (C6), 68.3 (C7), 67.3 (C5).

2-nitrobenzyl-4,6-*O*-benzylidene-2,3-[4,4',6,6' tetrakis(hydroxyl)5,5'dibenzyloxy-1,1'-(*S*)-biphenyl-2,2'-dicarboxylate]-β-*D*-glucopyranoside (**114**): to a stirred solution of $CuCl_2$ (756 mg, 5.69

mmol, 5 eq) in dry methanol (15 ml), *n*-butylamine (2.7 ml, 28.0 mmol, 25 eq) was added at room temperature, and the mixture was stirred for 45 minutes. To this blue solution, a solution of **113** (1.0 g, 1.12 mmol, 1 eq) in dry methanol (15 ml) was added and the mixture was stirred for 20 minutes. The reaction mixture is then poured into a 1:1 mixture of saturated aqueous solution of NH_4Cl:ethyl acetate (250 ml) and stirred at room temperature for 15 min. The mixture was next extracted with AcOEt. Combined organic layer were washed with brine, dried over Na_2SO_4 and concentrated under reduced pressure. The resulting residue was purified by column chromatography with a mixture of acetone:CH_2Cl_2 (0:100 → 4:96) to give (*S*)-**114** as a brown powder (426 mg, 0.5 mmol, 43 %). ^{1}H NMR (300 MHz, acetone-*d6*) δ (ppm) : 3.82 (dt, J = 4.6, 9.6 Hz, 1H, H5), 3.94 (t, J = 10.1 Hz, 1H, H6), 4.05 (t, J = 9.2 Hz, 1H, H4), 4.40 (dd, 1H, J = 4.7, 10.1 Hz, H6) 5.00 (t, 1H, J = 8.4 Hz, H2), 5.12- 5.26 (m, 7H, H1/H7/H8), 5.35 (t, J = 8.2 Hz, 1H, H3), 5.76 (s, 1H, H9), 6.58 (s, 1H, H2'^{I}/H6'^{II}), 6.73 (s, 1H, H2'^{I}/H6'^{II}), 7.28-7.54 (m, 15H), 7.63 (td, 1H, 1.8, 7.4 Hz), 7.80-7.89 (m, 2H), 8.11 (dd, 1H, J = 0.9, 8.1 Hz, H5'V), 8.40 (s, 2H, OH). ^{13}C NMR (75 MHz, acetone-*d6*) δ (ppm): 168.9 (CII=O), 168.4 (CI=O), 150.5/150.5 (C3'I/C3'II/C5'I/C5'II), 150.2 (C6'V), 150.2 (CHAr), 148.8 (CHAr) 138.7/138.7 (C4'I/C4'II), 138.6 (C1'III), 138.5 (C1'IV), 134.6 (C1'V), 134.3 (C4'V), 131.1 (CHAr), 130.9 (CHAr), 129.9 (CHAr), 129.8 (CHAr), 129.7 (CHAr), 129.3 (CHAr), 129.3 (CHAr), 129.0 (CHAr), 128.9 (CHAr), 127.3 (C2'IV/C3'IV), 125.5 (C5'V), 114.2 (CQ,C2'II/C6'I), 113.9 (CQ, C2'II/C6'I), 107.1 (CH, C2'I/C6'II), 107.0 (CH, C2'I/C6'II), 102.3 (CH), 100.8 (CH), 78.2 (C4), 76.9 (C2), 76.4 (C3), 74.8 (C8), 69.0 (C6), 68.6 (C7), 67.8 (C5).

4.7 Vescalagin fucose synthesis

*Acetofucose (**121**):* according to the procedure described in the literature,[187] to a solution of L(-)-Fucose (**120**, 1.0 g, 6.0 mmol) in pyridine (10 mL) was added Ac_2O (5.0 mL). The mixture was stirred under argon for about 6 hours at rt, and then the reaction was diluted in toluene, to remove pyridine and acetic acid, and evaporated in vacuo. This step was repeated twice to yield **121** (1.8 g, 5.42 mmol, 89% yield). The NMR data are in agreement with the previously reported in literature.

*Acetobromofucose (**122**):* according to the procedure described in the literature,[188] to a solution of fucose acetate (**121**, 6.0 mmol, 1.9 g) in dry CH_2Cl_2 (12 mL) was added the solution of HBr/CH_3COOH 33% (0.3 mL) in ice bath, then was stirred under argon at *rt* for 24 hours. After that ice water was added and the water layer was washed with EtOAc (3 x 20 mL); the organic layers were washed with $NaHCO_3$ saturated solution (2 x 20 mL), brine (1 x 20 mL), dried with Na_2SO_4, and evaporated in vacuo. The crude product acetobromofucose (**122**) was obtained with 85% of yield without further purification. The ^1H NMR data are in agreement with the previously reported in literature.

*4-acetoxy benzyl alcohol (**124**):* to a solution of 4-hydroxy benzyl alcohol (**123**, 2.0 g, 16.1 mmol) in dry CH_2Cl_2 (160 mL) was added K_2CO_3 (2.2 g, 16.1 mmol) and then Ac_2O (1.5 mL, 16.1 mmol). The mixture was stirred under argon for about 6 hours, then the reaction was washed with water (3 x 100 ml), brine (100 ml), dried over Na_2SO_4 and concentrated in vacuo to give the correspondent acetylated derivative **124** (2.3 g, 13.7 mmol). R*f* = 0.2 (30:70 AcOEt/PET); ^1H-NMR (200 MHz, $CDCl_3$) δ (ppm): 2.30 (s, 3H, $-COCH_3$), 4.68 (s, 2H, H-7), 7.08 (d, 2H, H-3/5), 7.37 (d, 2H, H-2/6); ^{13}C-NMR (75 MHz, $CDCl_3$) δ (ppm): 169.8 (C-

1'), 149.9 (C-1), 138.6 (C-4), 128.0 (C-2/6), 121.5 (C-5/3), 64.4 (C-7), 21.1 (C-2').

*4-acetoxy benzyl bromine (**125**):* according to the procedure described in the literature,[189] to a solution of 4-hydroxy benzyl acetate (**124**, 2.2 g, 13.24 mmol) in dry CH_2Cl_2 (44 mL) was added CBr_4 (5.7 g, 17.2 mmol,) and then PPh_3 (3.8 g, 14.5 mmol). The mixture was stirred under argon for about 6 hours, then the reaction was washed with water (3 x 100 ml), brine (100 ml), dried over Na_2SO_4 and concentrated in vacuo. The resulting residue was purified by column chromatography with a mixture of EtOAc:cyclohexane (0:100 → 85:15) to give the correspondent derivative **125** (965 mg, 3.7 mmol). R*f* = 0.2 (10:90 AcOEt/PET); ^{1}H-NMR (300 MHz, $CDCl_3$) δ (ppm) : 7.40 (2H,d, J = 8.6 Hz, H-3); 7.07 (2H, d, J = 8.6 Hz, H-2) ; 4.48 (2H, s, H-5) ; 2.30 (3H, s, H-7).

*4-((tritylthio)methyl)phenyl acetate compound (**126**):* To a solution of **125** (965 mg, 3.7 mmol) in acetone (6.2 ml) was added potassium carbonate (775.3 mg, 5.6 mmol) followed by triphenylmethanethiol (1.13 g, 4.7 mmol). The mixture was stirred for 20 h at reflux. The excess potassium carbonate was filtered and the filtrate was concentrated in vacuo. The resultant residue was reconstituted with ethyl acetate. Combined organic phases were dried over Na_2SO_4, filtered and concentrated in vacuo. The resulting residue was purified by column chromatography with a mixture of EtOAc:PET (0:100 → 15:85) to give the correspondent derivative **126** (1.5 g, 3.53 mmol). Rf: 0.2 (10% EtOAc-PET). ^{1}HNMR (300 MHz, $CDCl_3$) δ (ppm): 7.56 (6H, d, Tr); 7.36 (9H, m ,Tr); 7.22 (2H, d, J = 8,7 Hz, H- 3); 7.04 (2H, d, J = 8,7 Hz, H-2); 3.40 (2H, s, H-5); 2.33 (3H, s, H-7).

*4-((tritylthio)methyl)phenol compound (**127**):* The coumpound **126** (1.5 g, 3.53 mmol) is solubilised in methanol (117 ml). Potassium carbonate (2.4 g , 17.65 mmol) was then added to the solution. The reaction mixture was stirred at rt during 30 min to observe a total conversion of the starting material. The mixture is quenched with citric acid 5% (200 ml). The aqueous phase is extracted with dichloromethane (300 ml). Organic phases are combined, dried over Na_2SO_4, filtered and concentrated to afford the crude mixture. The resulting residue was purified by column chromatography with a mixture of EtOAc:cyclohexane (20:80 → 40:60) to give the correspondent derivative **127** (770 mg, 2.01 mmol). Rf 0.3 (50% EtOAc-PET); ^{1}HMR (300 MHz, $CDCl_3$) δ (ppm): 7.45 (6H, d, Tr) 7.26 (9H, m, Tr); 7.11 (2H, d, *J* = 8,6 Hz, H- 3); 6.68 (2H, d, *J* = 8,6 Hz, H-2); 5.20 (1H, sb, OH); 3.35 (2H, s, H-5).

*(2S,3R,4R,5R,6S)-2-allyl-6-methyltetrahydro-2H-pyran-3,4,5-triyl triacetate (**132**):* **132** was synthesized according to reported procedure.[187] The tetraacetate (**121**, 1.8 g, 5.4 mmol) was dissolved in dry acetonitrile (10 ml) and allyltrimethylsilane (1.7 ml, 10.8 mmol) was added. The resulting mixture was cooled down to 0 °C, and then $BF_3 \cdot OEt_2$ (1.3 ml, 10.8 mmol) and TMSOTf (0.2 ml, 1.08 mmol) were added dropwise and simultaneously over a period of 10 minutes. The resulting orange mixture was stirred for 8 hours at 0 °C. The reaction was quenched with 10 ml of ice and extracted with diethyl ether (3 X 15 ml). The organic phase was washed with saturated $NaHCO_3$ (20 ml) and brine (20 ml), dried over Na_2SO_4 and solvent was evaporated in vacuo to give **132** as an orange oil.

*2-((2S,3R,4R,5R,6S)-3,4,5-triacetoxy-6-methyltetrahydro-2H-pyran-2-yl)acetic acid (**131**):* In according with the previously reported

procedure,[187] **131** was synthesized. **132** (67.0 mg, 0.21 mmol) was dissolved in H_2O/ CH_3CN /CCl_4 (2.9/1.5/1.5 ml) and then $NaIO_4$ (179.6 mg, 0.84 mmol) and $RuCl_3$ (1.8 mg, 0.084 mmol) were added. The resulting mixture was stirred for four hours at room temperature. The reaction was quenched with 10 ml of cold water and extracted with CH_2Cl_2 (2 X 10 ml). The organic phase was acidified with HCl until pH 2 and re-extracted again with CH_2Cl_2 (2 X 10 ml). Then the organic phase was wasched with brine (1 X 10 ml), dried over Na_2SO_4 and evaporated in vacuo to give **131**.

CHAPTER 5

5. SUPPORTING MATERIAL

5.1 Appendix A

In this section the NMR spectra of Benzoxanthenes **36**, **38**, **39**, **41**, **61**, **63**, **65** and **67**.

5.1.1 Compound 36

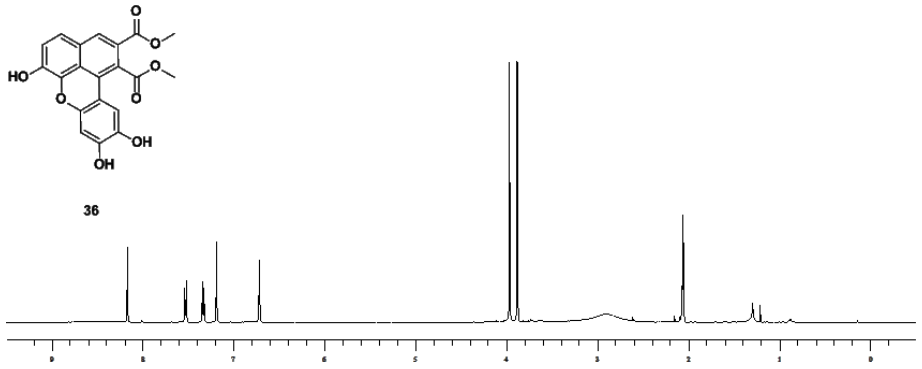

Figure 1S: ^{1}H-NMR spectrum (500 MHz, acetone-d_6) of compound **36**.

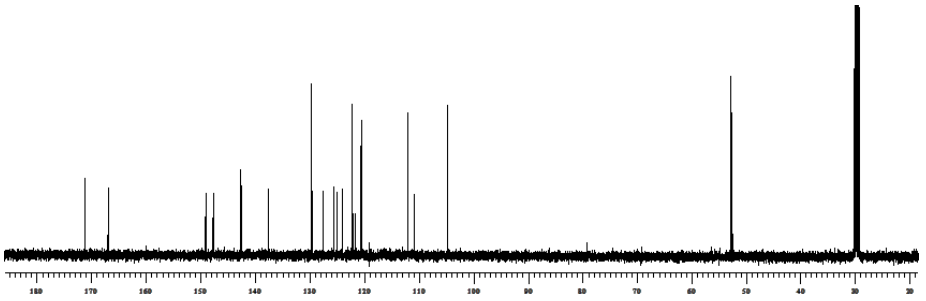

Figure 2S: ^{13}C-NMR spectrum (125 MHz, acetone-d_6) of compound **36**.

5.1.2 Compound 38

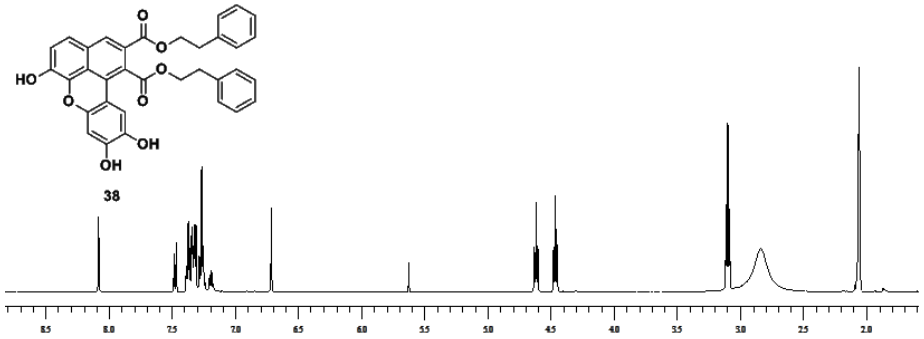

Figure 3S: ^{1}H-NMR spectrum (500 MHz, acetone-d_6) of compound **38**.

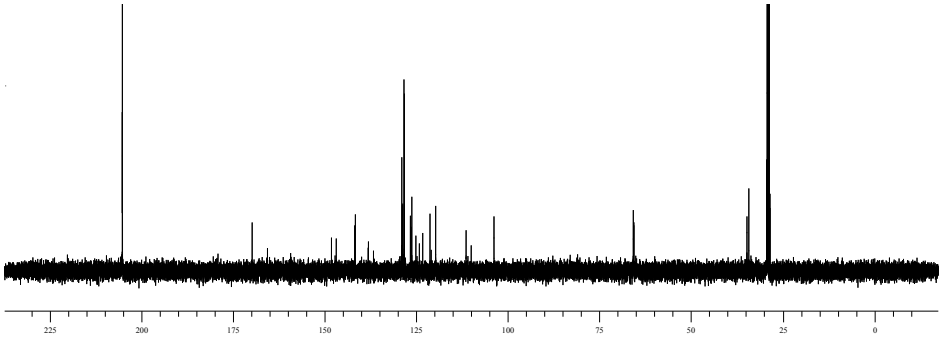

Figure 4S: ^{13}C-NMR spectrum (125 MHz, acetone-d_6) of compound **38**.

5.1.3 Compound 39

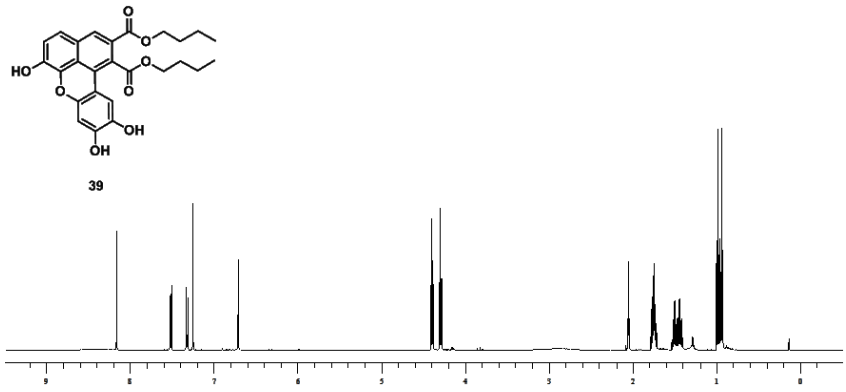

Figure 5S: ^{1}H-NMR spectrum (500 MHz, acetone-d_6) of compound **39**.

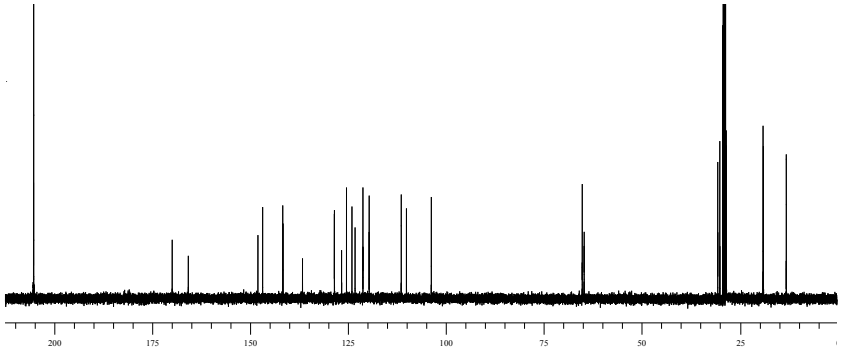

Figure 6S: ^{13}C-NMR spectrum (125 MHz, acetone-d_6) of compound **39**.

5.1.4 Compound 61

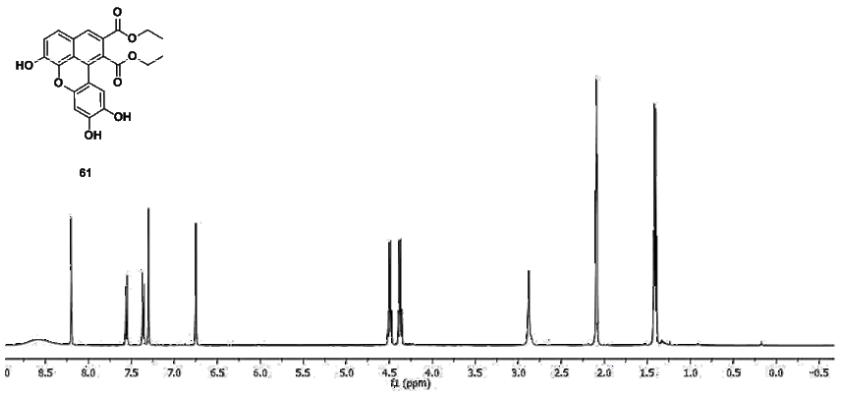

Figure 7S: ^{1}H-NMR spectrum (500 MHz, acetone-d_6) of compound **61**.

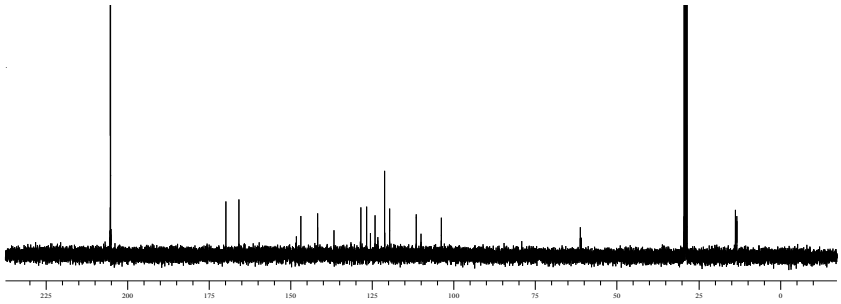

Figure 8S: ^{13}C-NMR spectrum (125 MHz, acetone-d_6) of compound **61**.

5.1.5 Compound 63

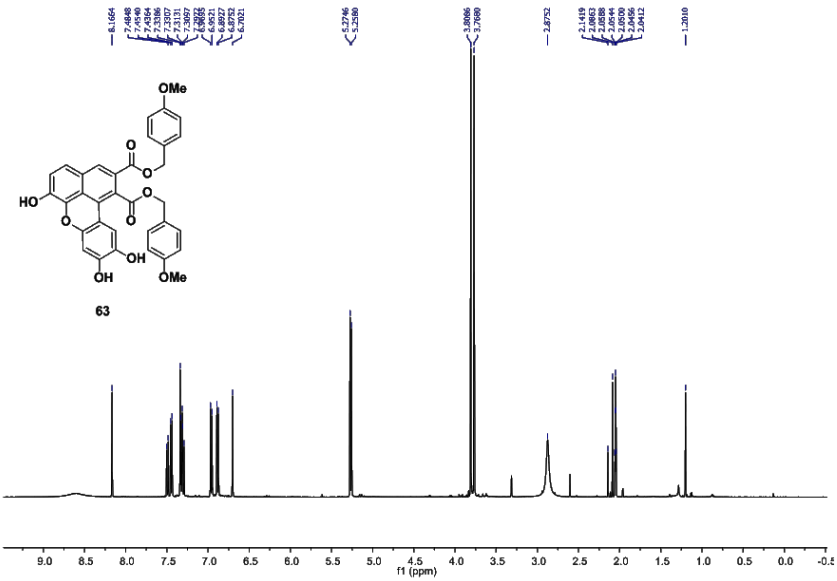

Figure 9S: ^{1}H-NMR spectrum (500 MHz, acetone-d_6) of compound **63**.

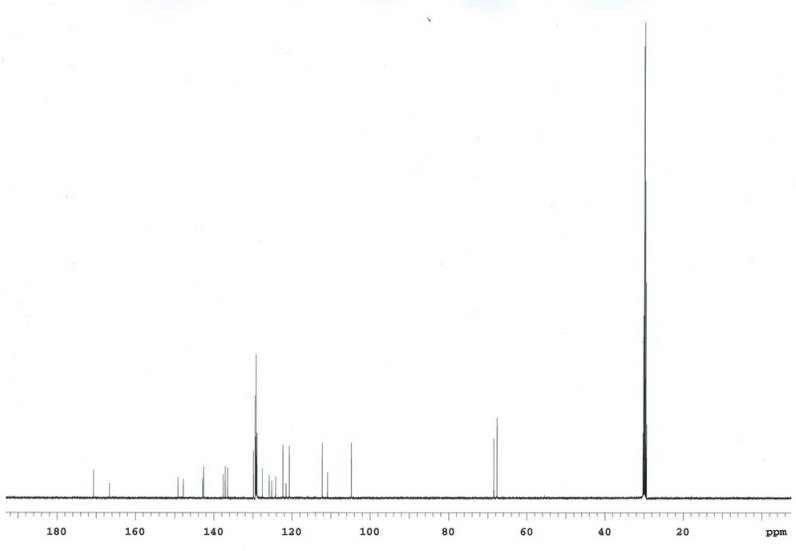

Figure 10S: ^{13}C-NMR spectrum (125 MHz, acetone-d_6) of compound **63**.

5.1.6 Compound 65

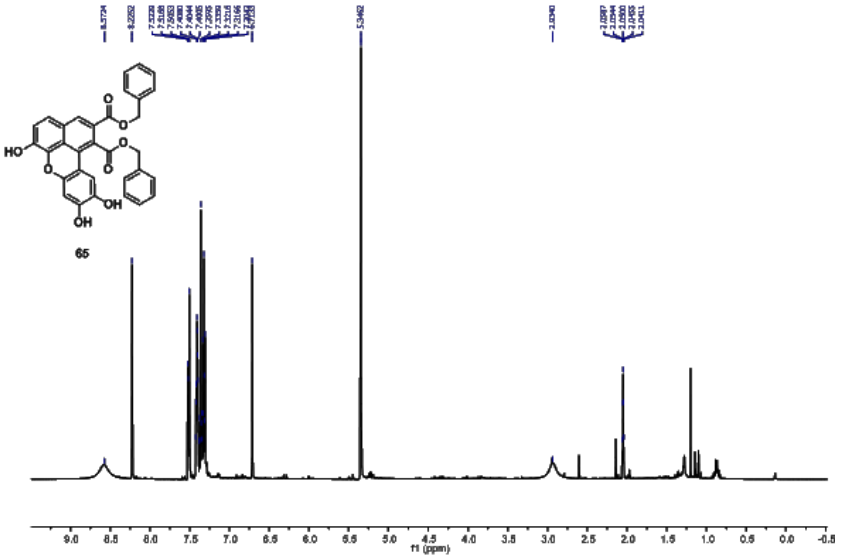

Figure 11S: ^{1}H-NMR spectrum (500 MHz, acetone-d_6) of compound **65**.

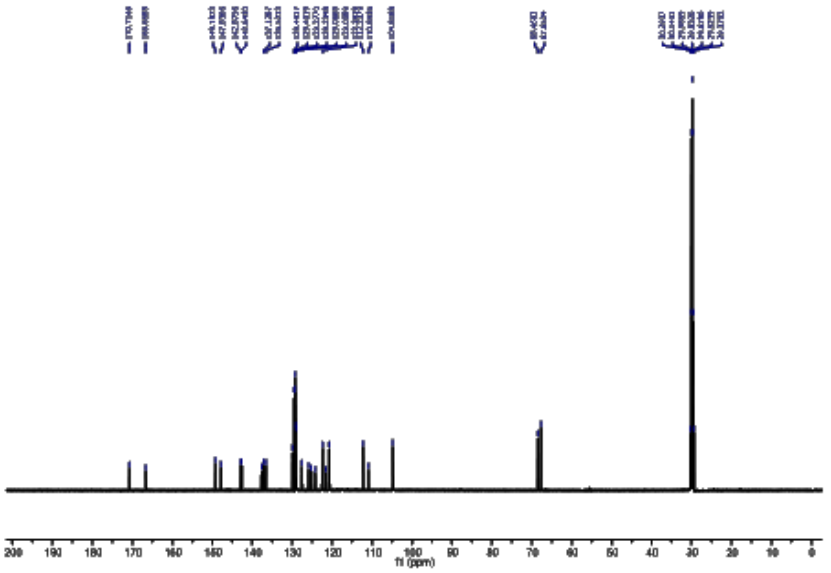

Figure 12S: ^{13}C-NMR spectrum (125 MHz, acetone-d_6) of compound **65**.

5.1.7 Compound 67

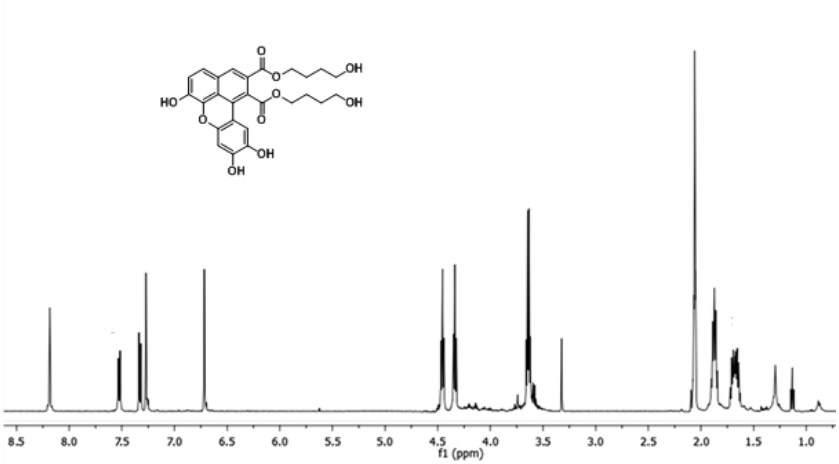

Figure 13S: ^{1}H-NMR spectrum (500 MHz, acetone-d_6) of compound **67**.

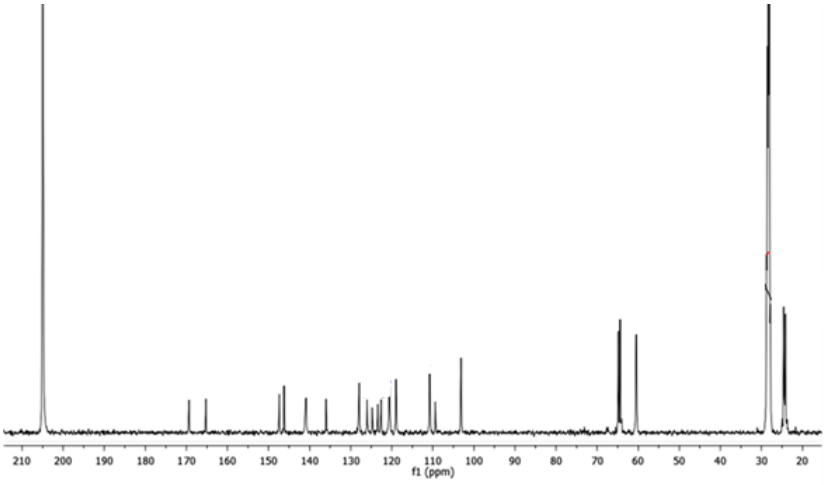

Figure 14S: ^{13}C-NMR spectrum (125 MHz, acetone-d_6) of compound **67**.

5.2 Appendix B

In this section the MS and NMR spectra of phenazines **69**, **71**, **73** and **74**/**75**

5.2.1 Compound 69

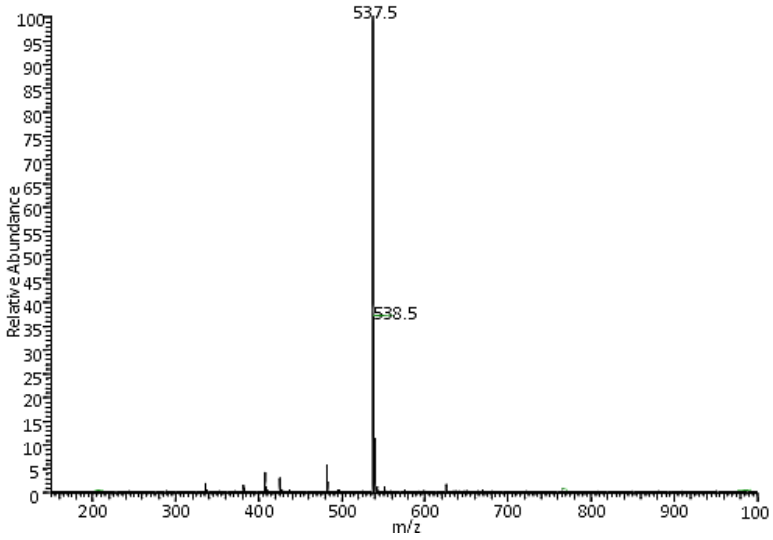

Figure 15S: ESI-Mass spectrum of **69**.

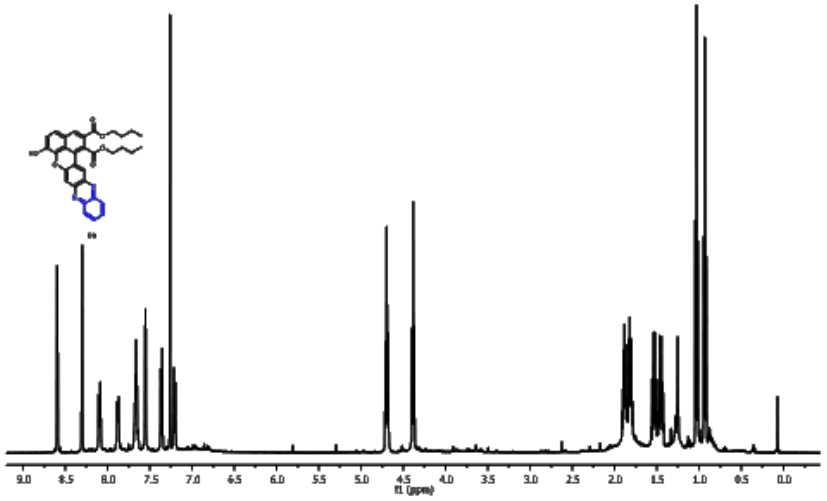

Figure 16S: ^{1}H-NMR spectrum (500 MHz,$CDCl_3$) of compound **69**.

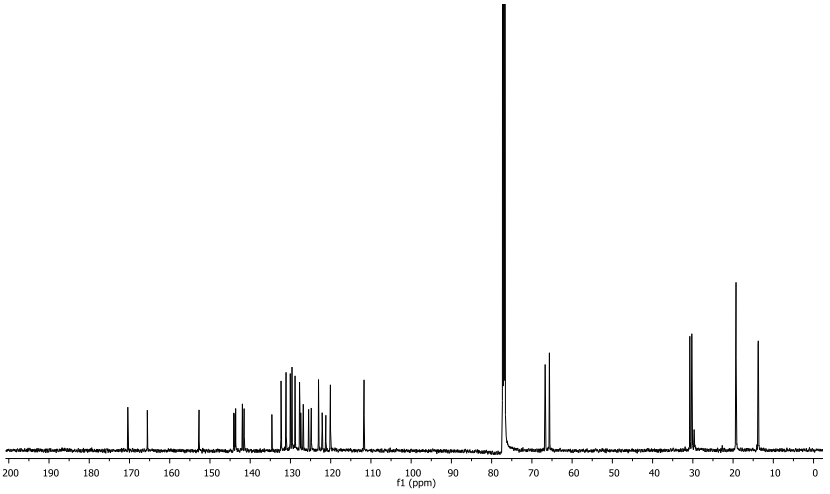

Figure 17S: ^{13}C-NMR spectrum (125 MHz,$CDCl_3$) of **69**.

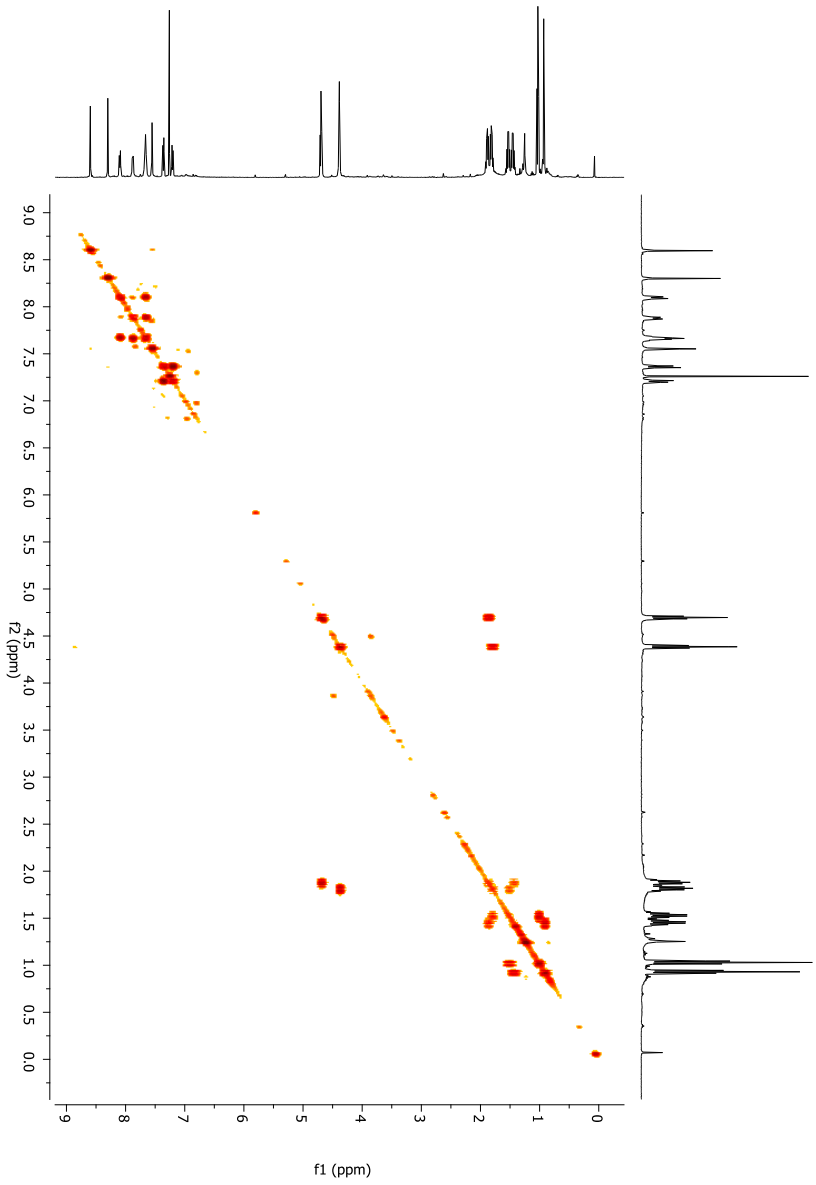

Figure 18S: gCOSY spectrum of compound of **69**.

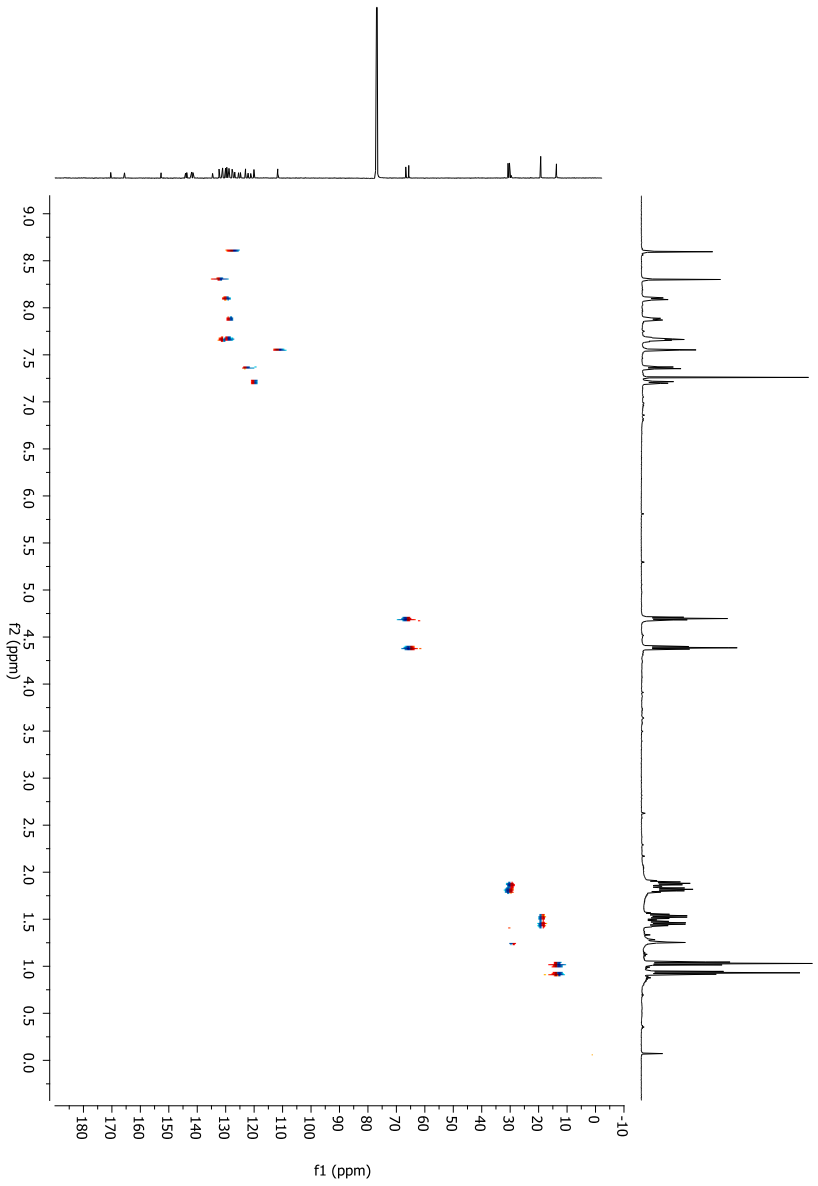

Figure 19S: gHSQCAD spectrum of compound of **69**.

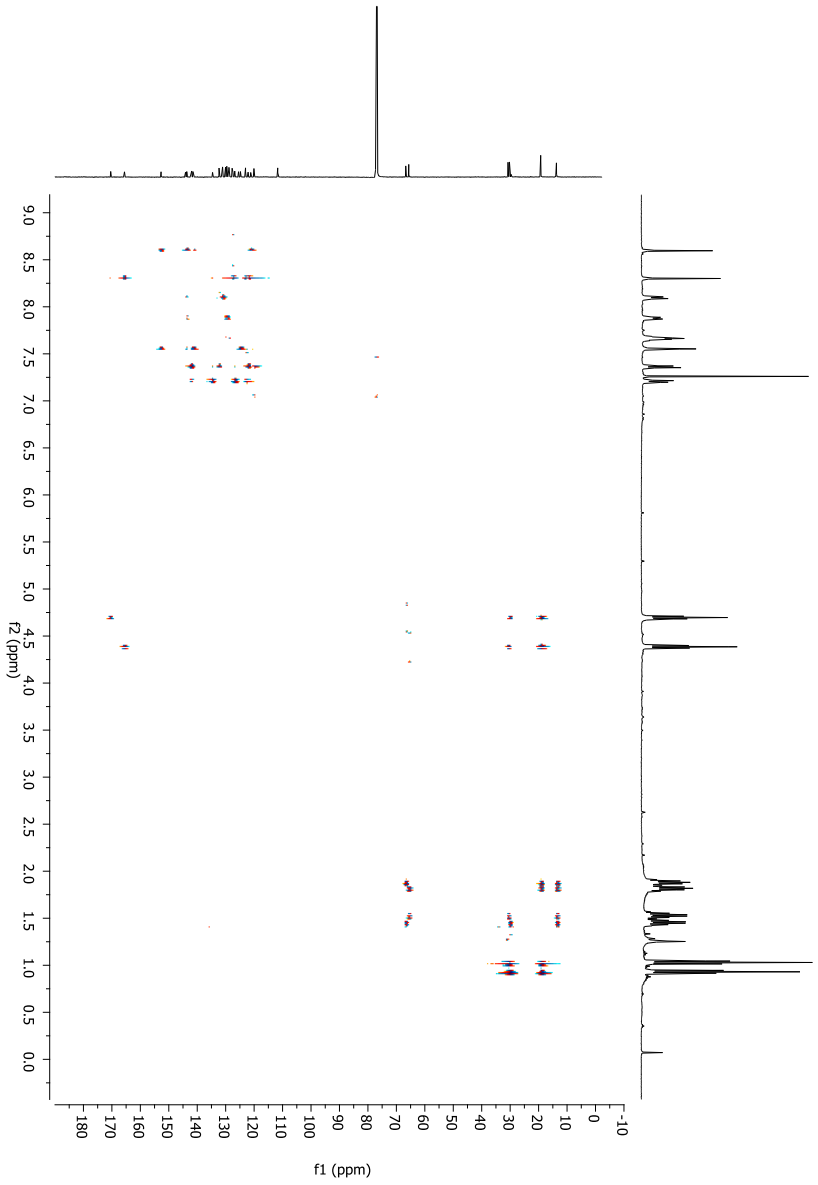

Figure 20S: gHMBCAD spectrum of compound of **69**.

5.2.2 Compound 71

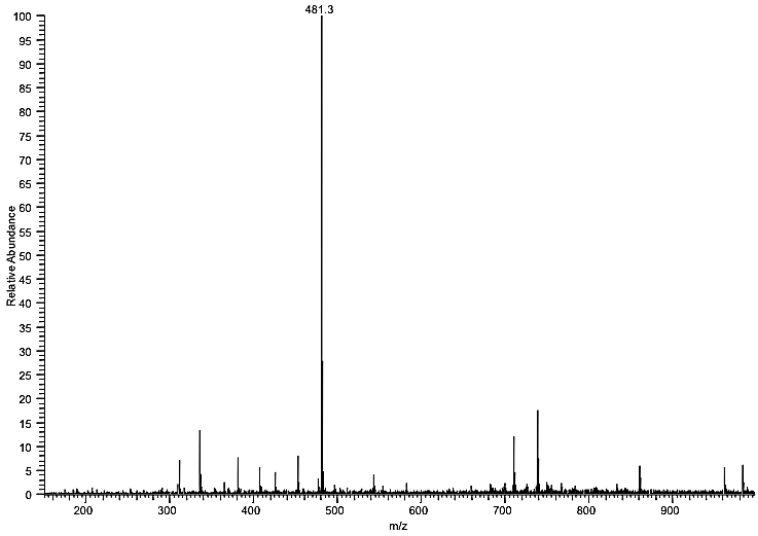

Figure 21S: ESI-MS spectrum of **71**.

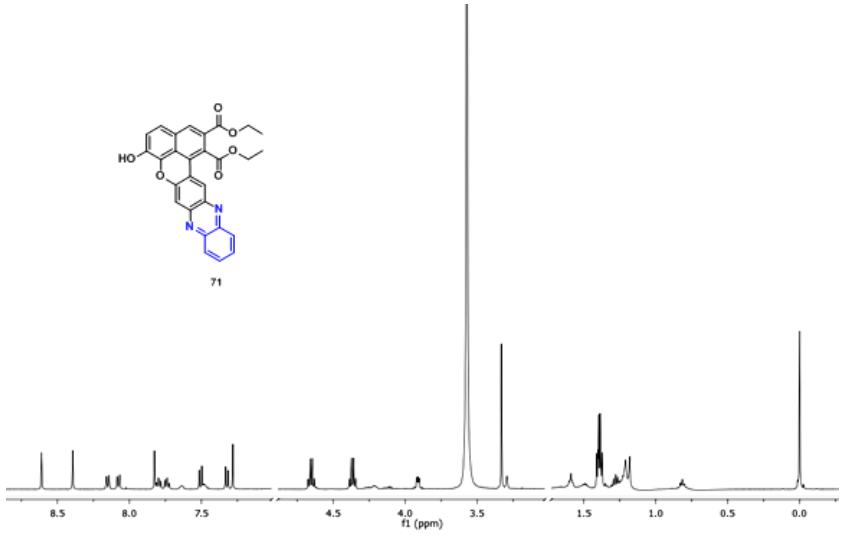

Figure 22S: ^{1}H-NMR spectrum (500 MHz,$CDCl_3$ and 1% of CD_3OD) of compound **71**.

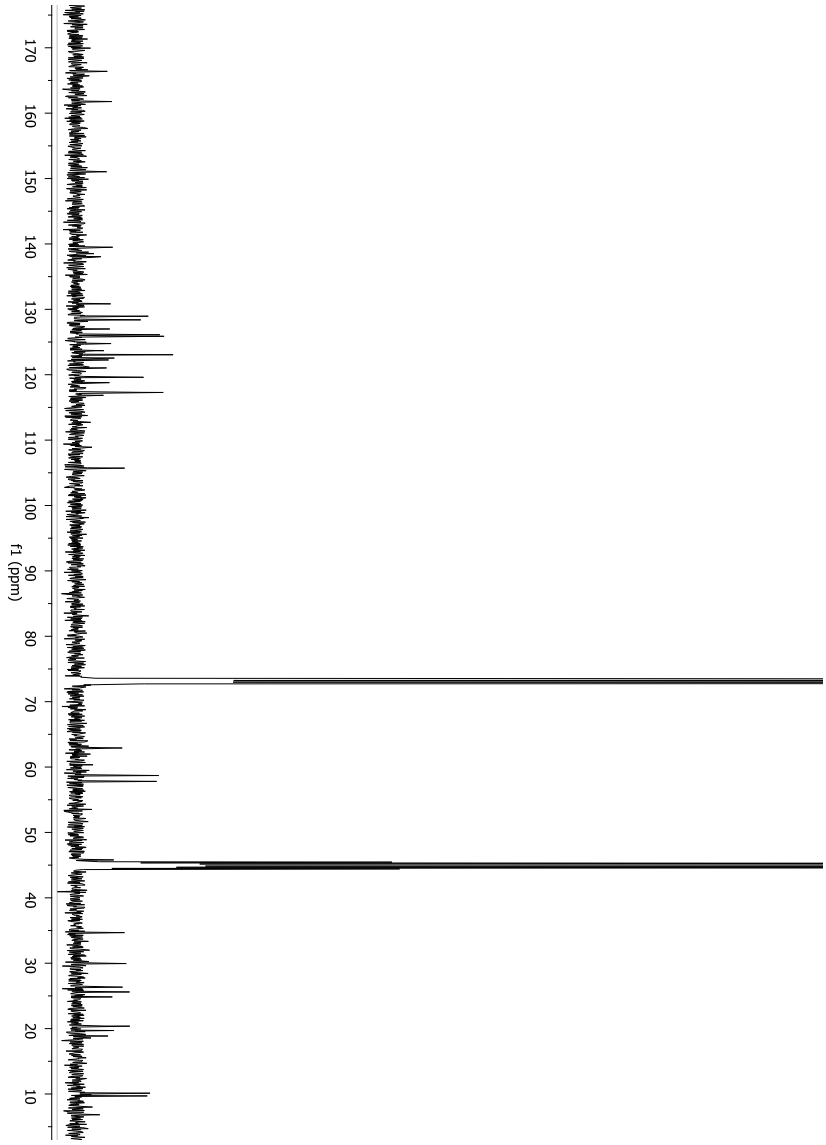

Figure 23S: ^{13}C-NMR spectrum (125 MHz, $CDCl_3$ and 1% of MeOD) of **71**.

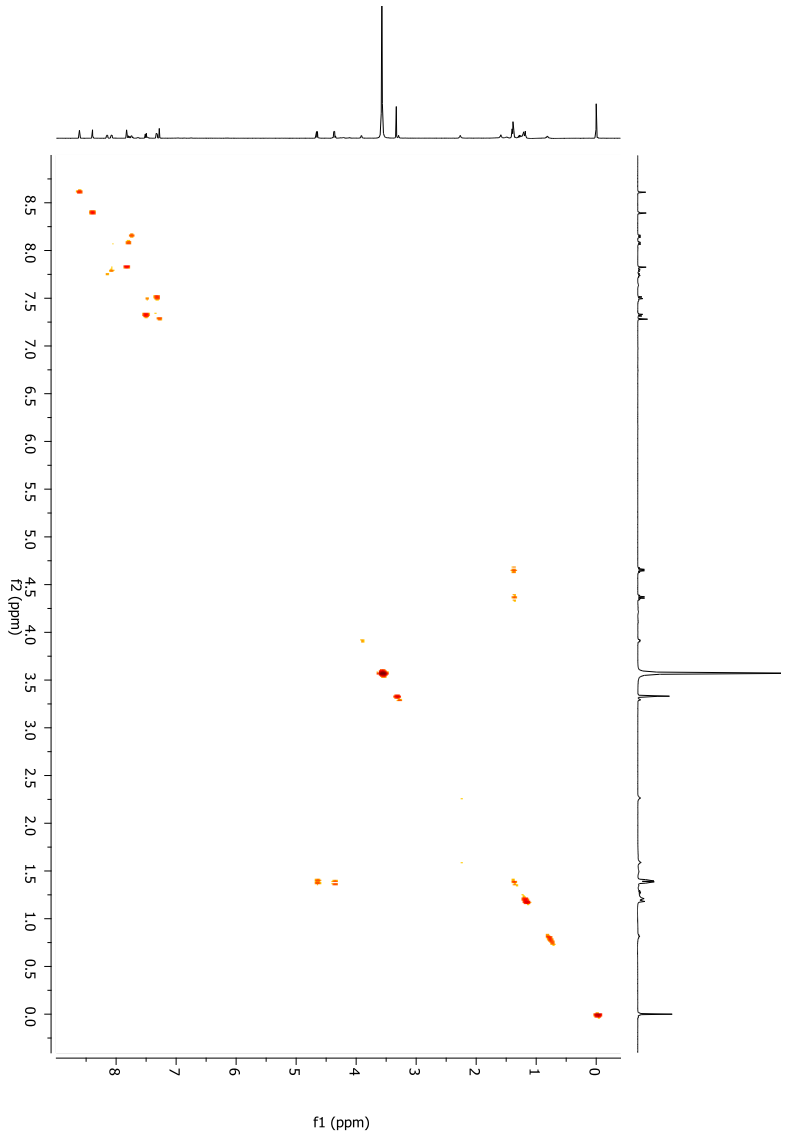

Figure 24S: gCOSY spectrum of compound of **71**.

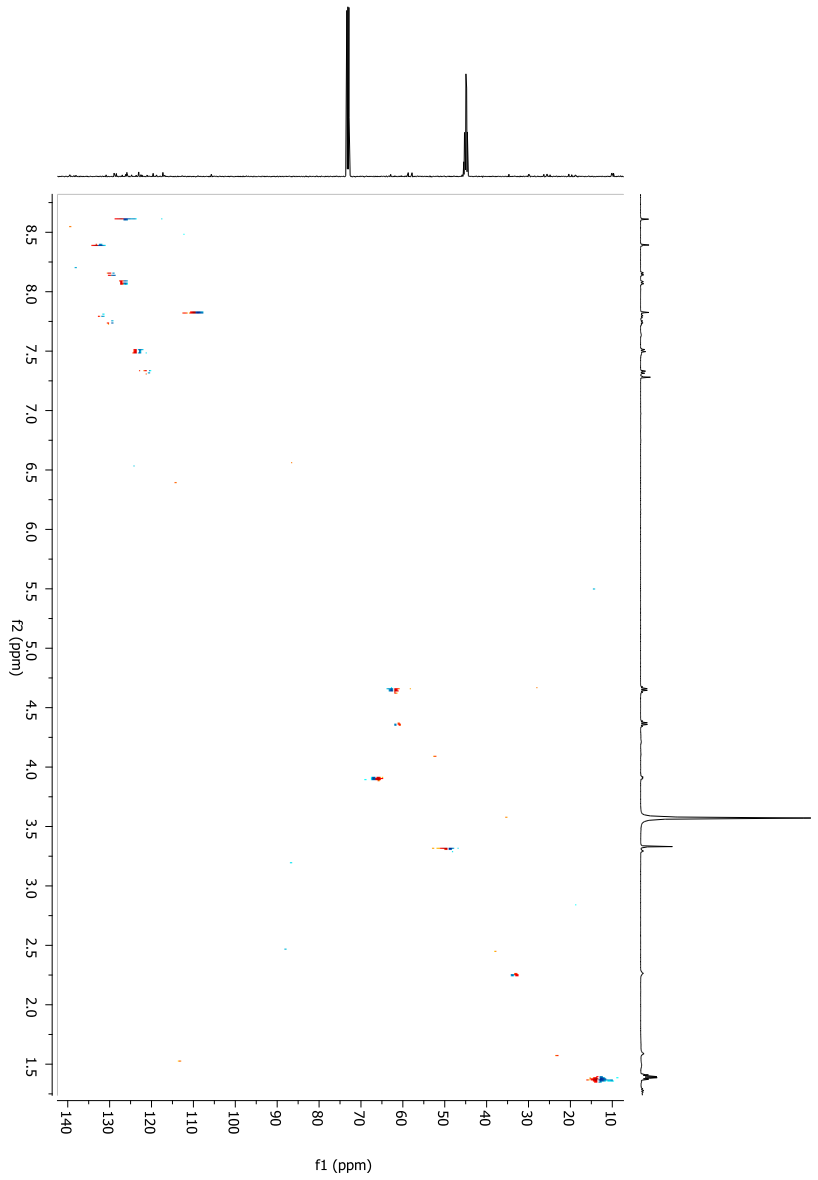

Figure 25S: gHSQCAD spectrum of compound of **71**.

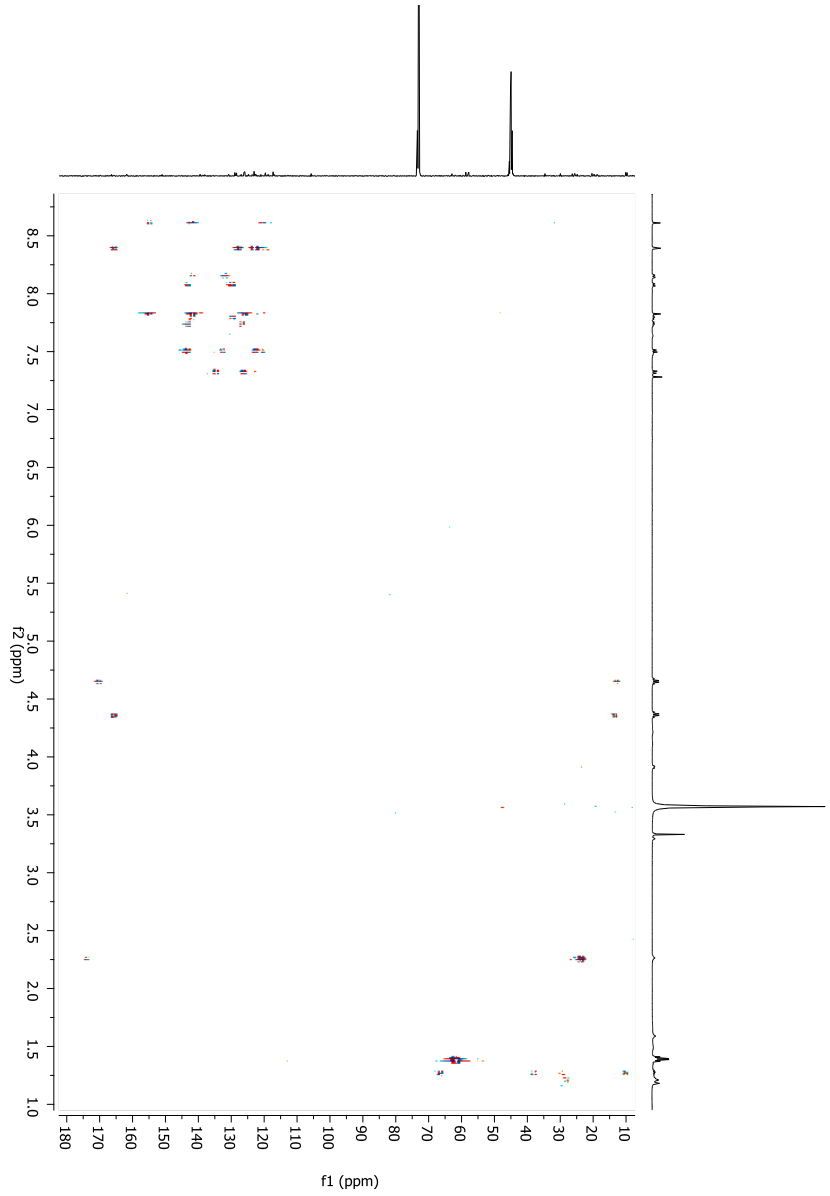

Figure 26S: gHMBCAD spectrum of compound of **71**.

5.2.3 Compound 71

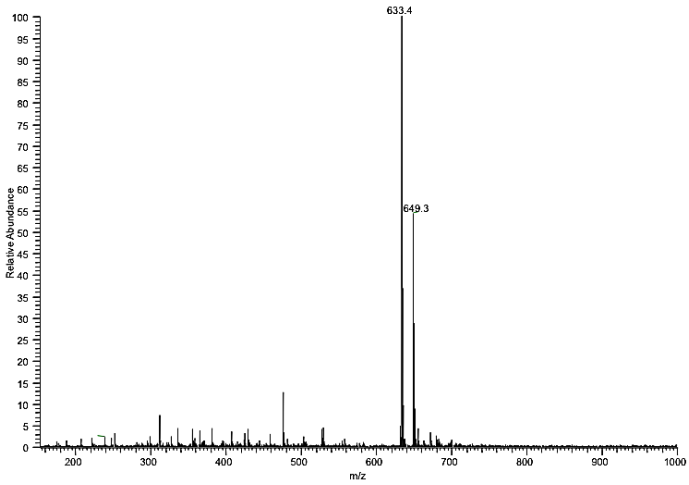

Figure 27S: ESI-MS spectrum of **73**.

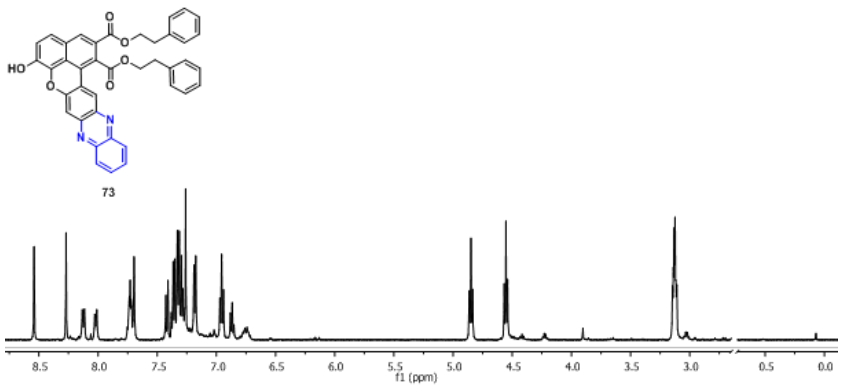

Figure 28S: ^{1}H-NMR spectrum (500 MHz,$CDCl_3$) of compound **73**.

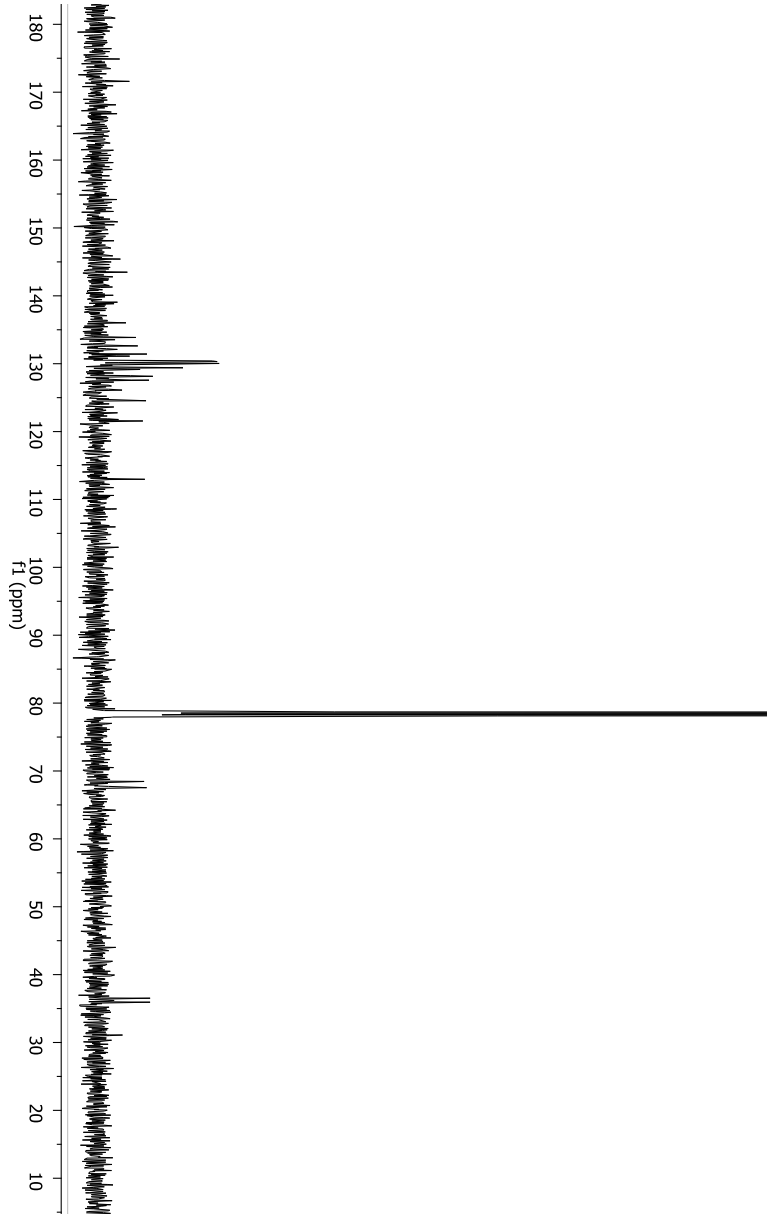

Figure 29S: ^{13}C-NMR spectrum (125 MHz,$CDCl_3$) of **73**.

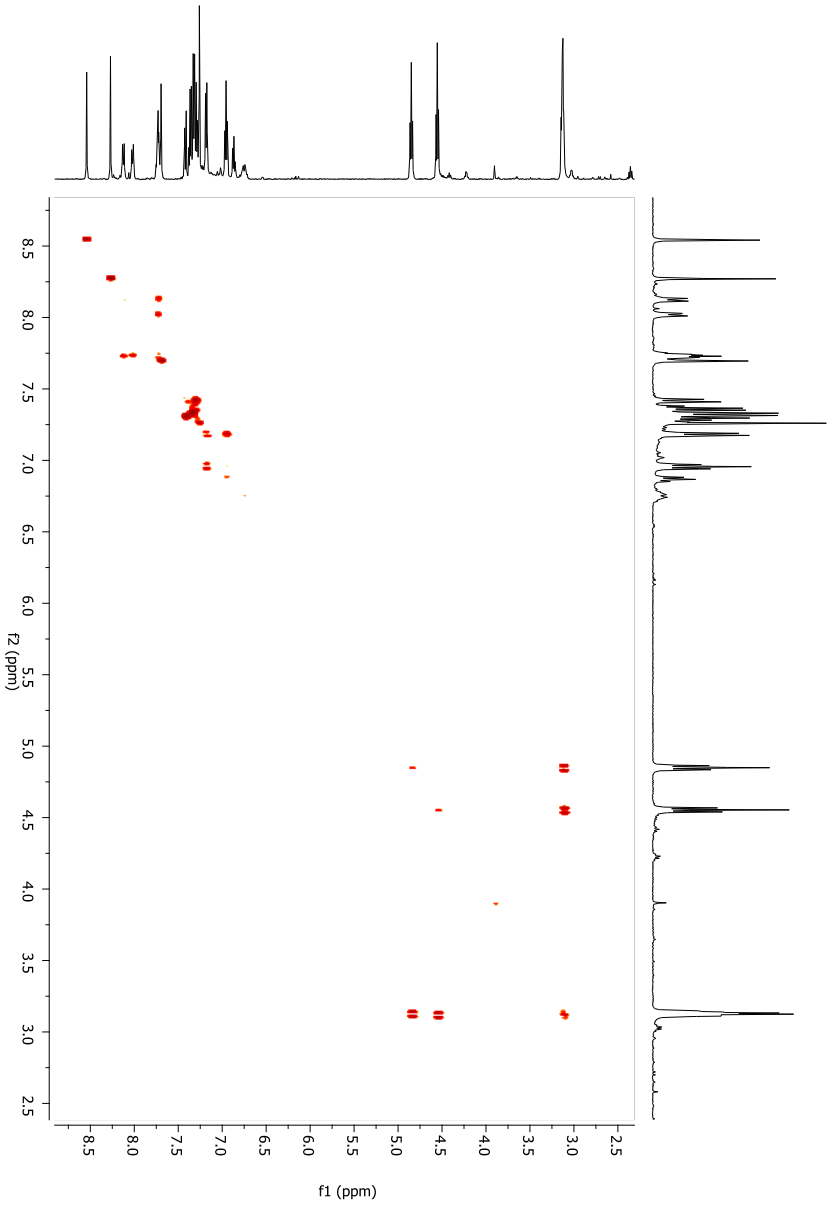

Figure 30S: gCOSY spectrum of compound of **73**

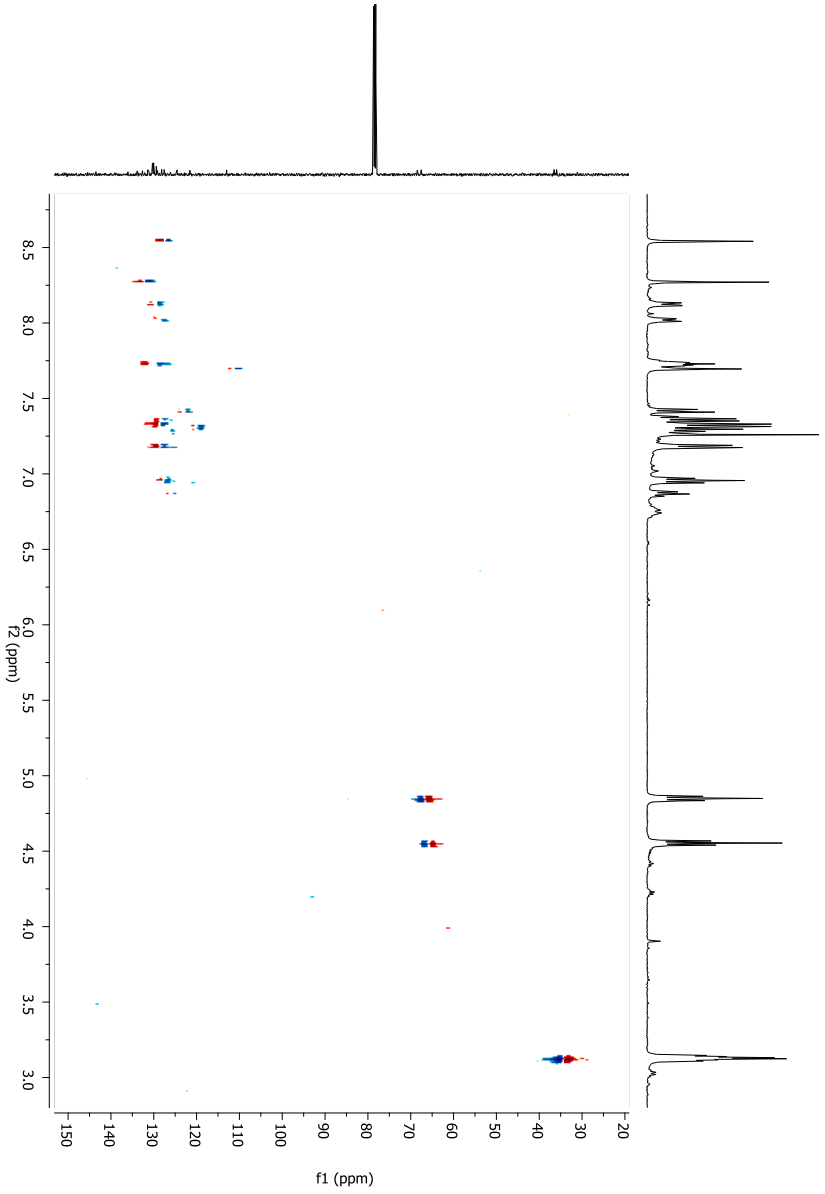

Figure 31S: gHSQCAD spectrum of compound of **73**.

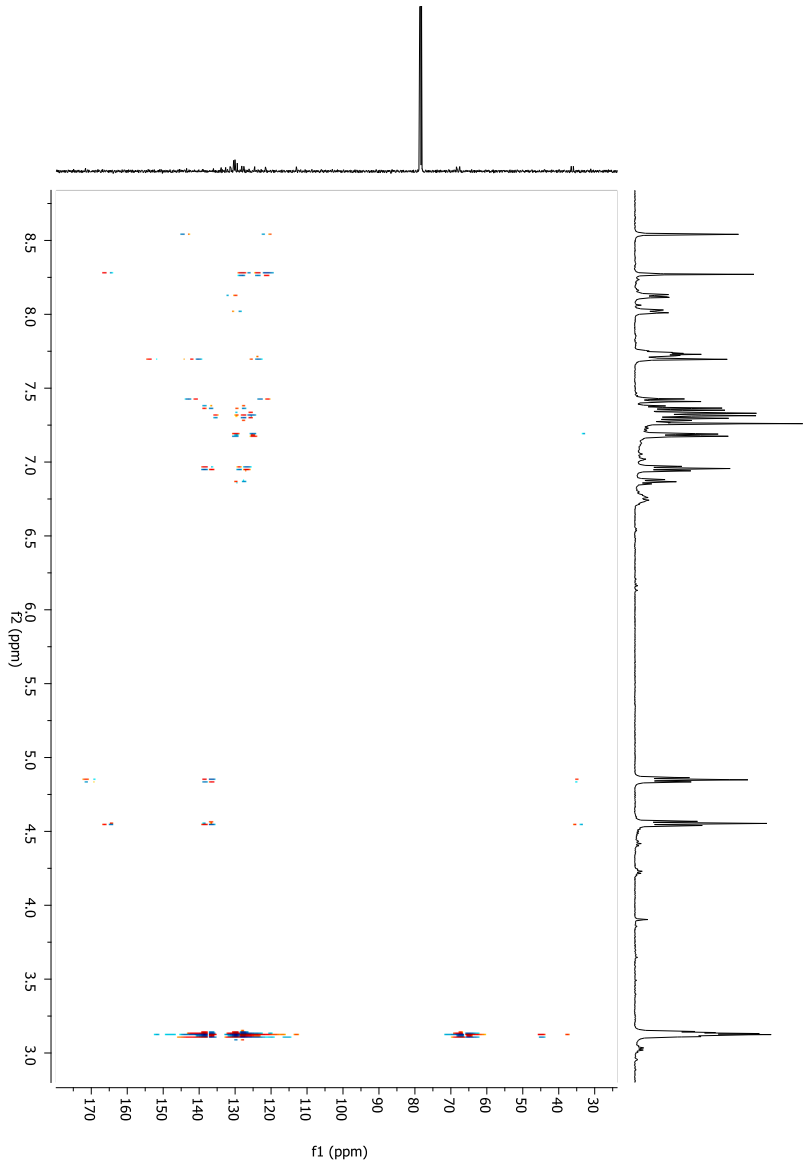

Figure 32S: gHMBCAD spectrum of compound of **73**.

5.2.4 Compound 74 and 75

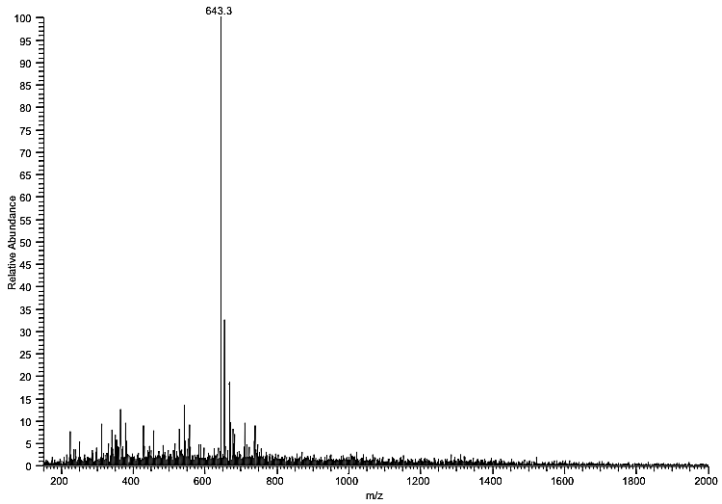

Figure 33S: ESI-MS spectrum of **74** or **75**.

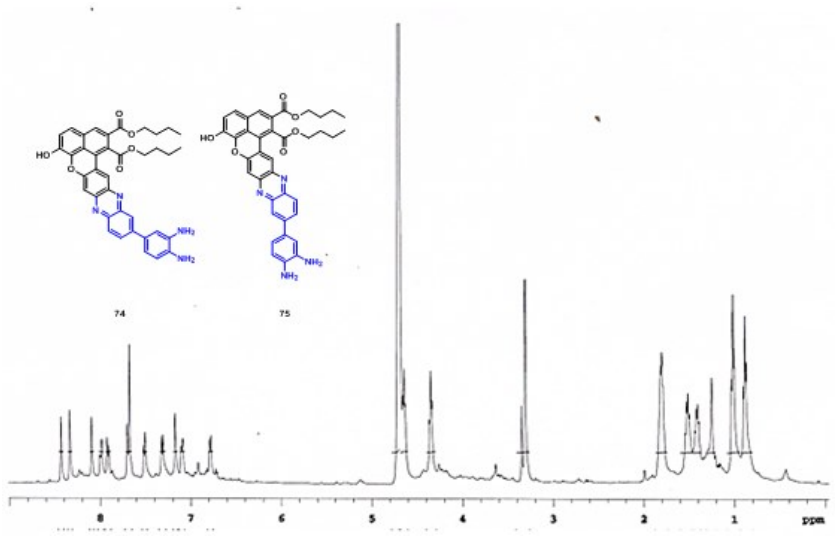

Figure 34S: ^{1}H-NMR spectrum (500 MHz, CD_3COD + $CDCl_3$) of **74** or **75**.

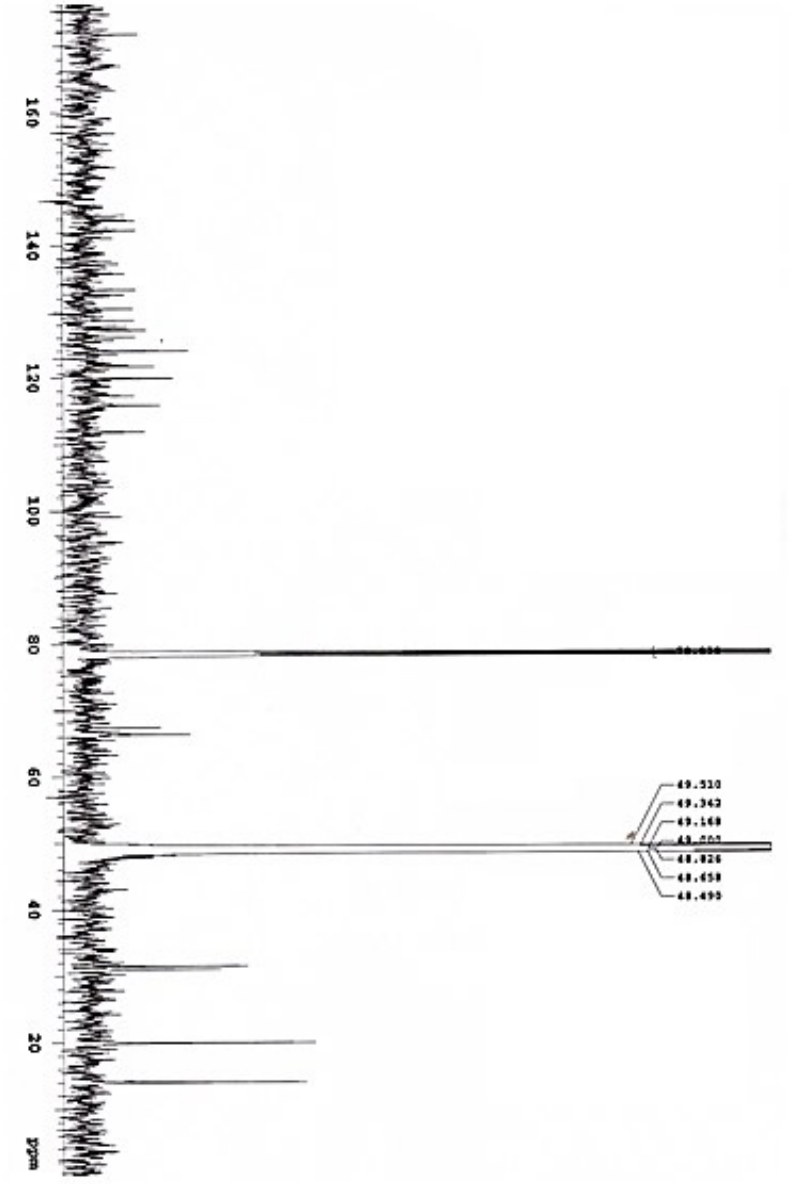

Figure 35S: ^{13}C-NMR spectrum (125 MHz, CD_3COD + $CDCl_3$) of **74** or **75**.

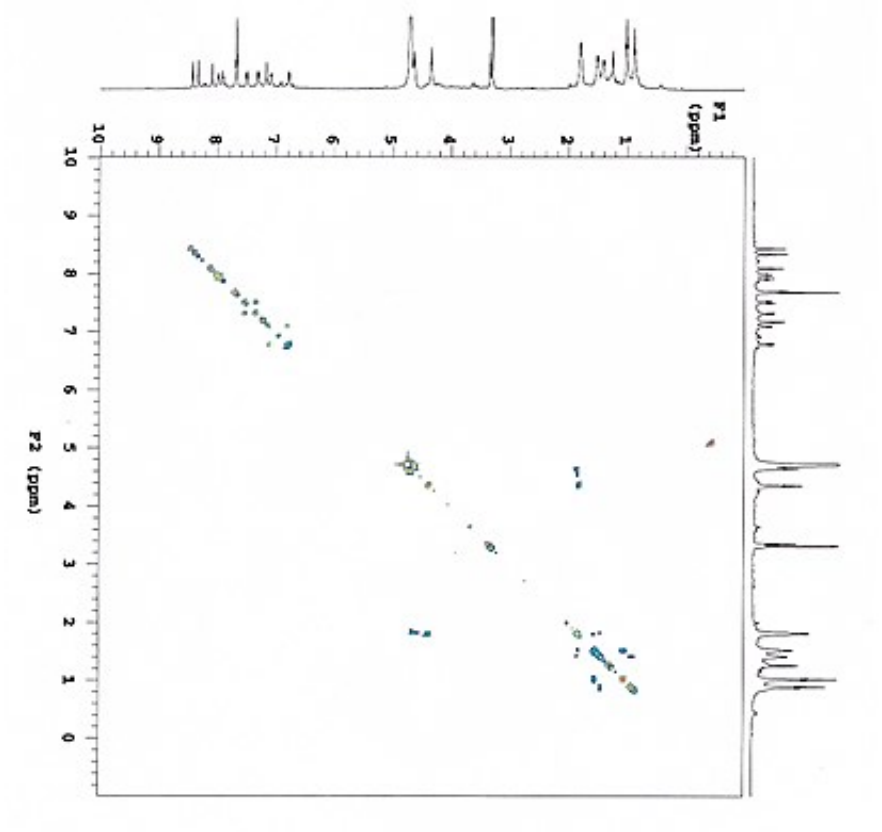

Figure 36S: gCOSY spectrum of compound of **74** or **75**.

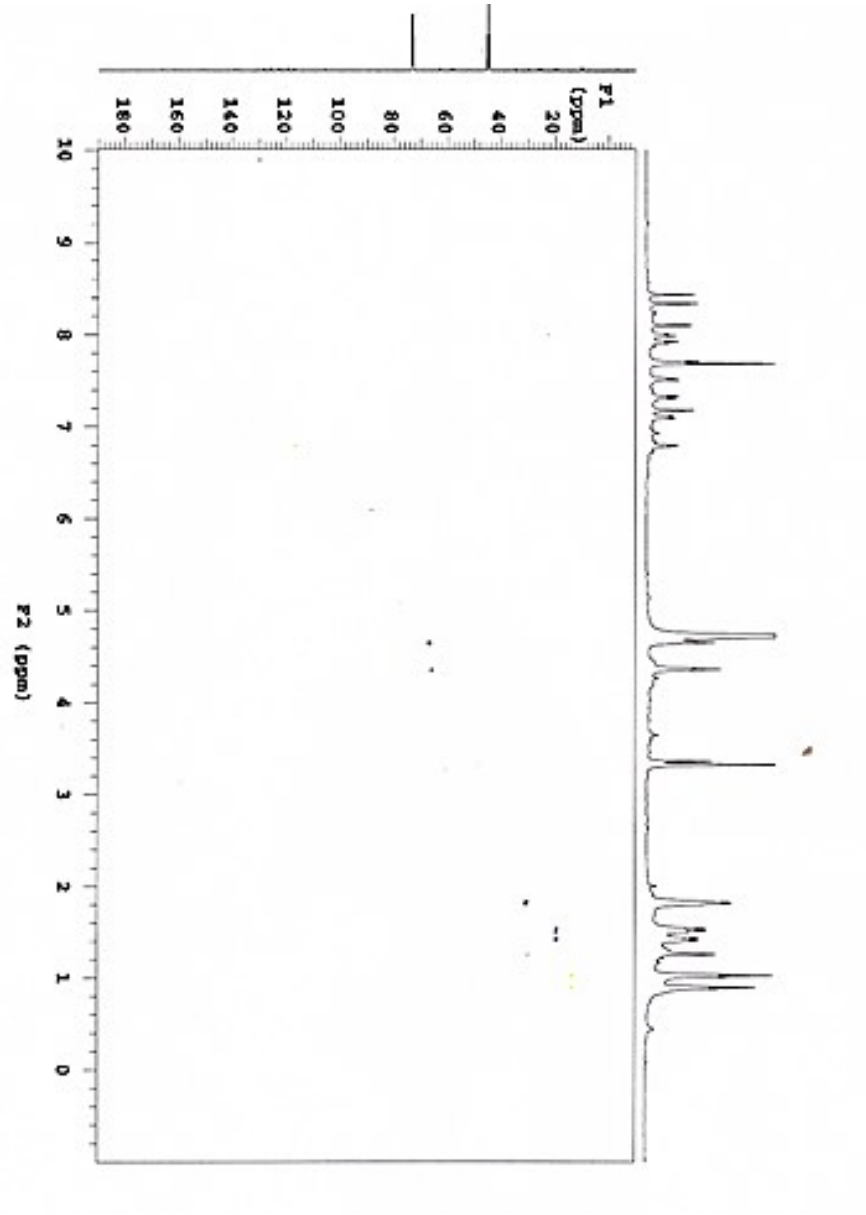

Figure 37S: gHSQCAD spectrum of compound of **74** or **75**.

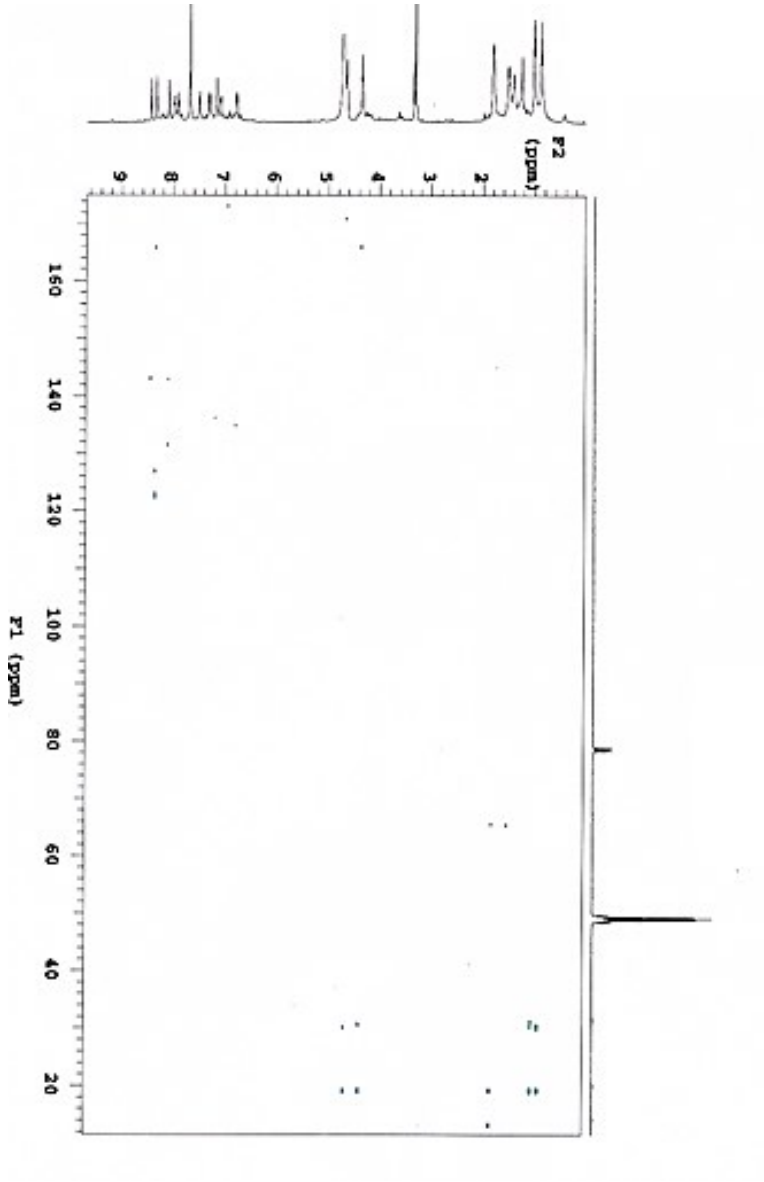

Figure 38S: gHMBCAD spectrum of compound of **74** or **75**.

5.3 Appendix C

In this section the MS and NMR spectra of magnolol related compounds **81**, **82**, **84** – **93** and **96**, **99**.

5.3.1 Compound 81

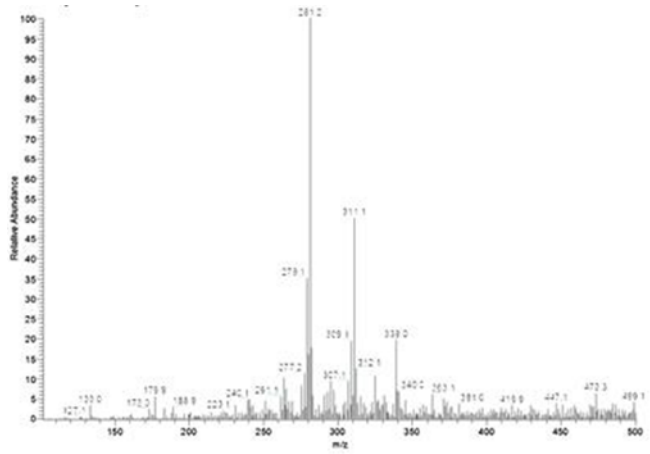

Figure 39S: ESIMS spectrum of compound **81**.

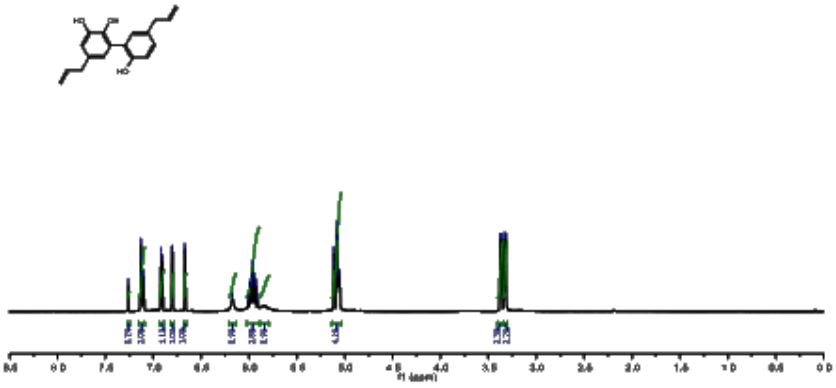

Figure 40S: ^{1}H NMR spectrum (500 MHz, $CDCl_3$) of compound **81**.

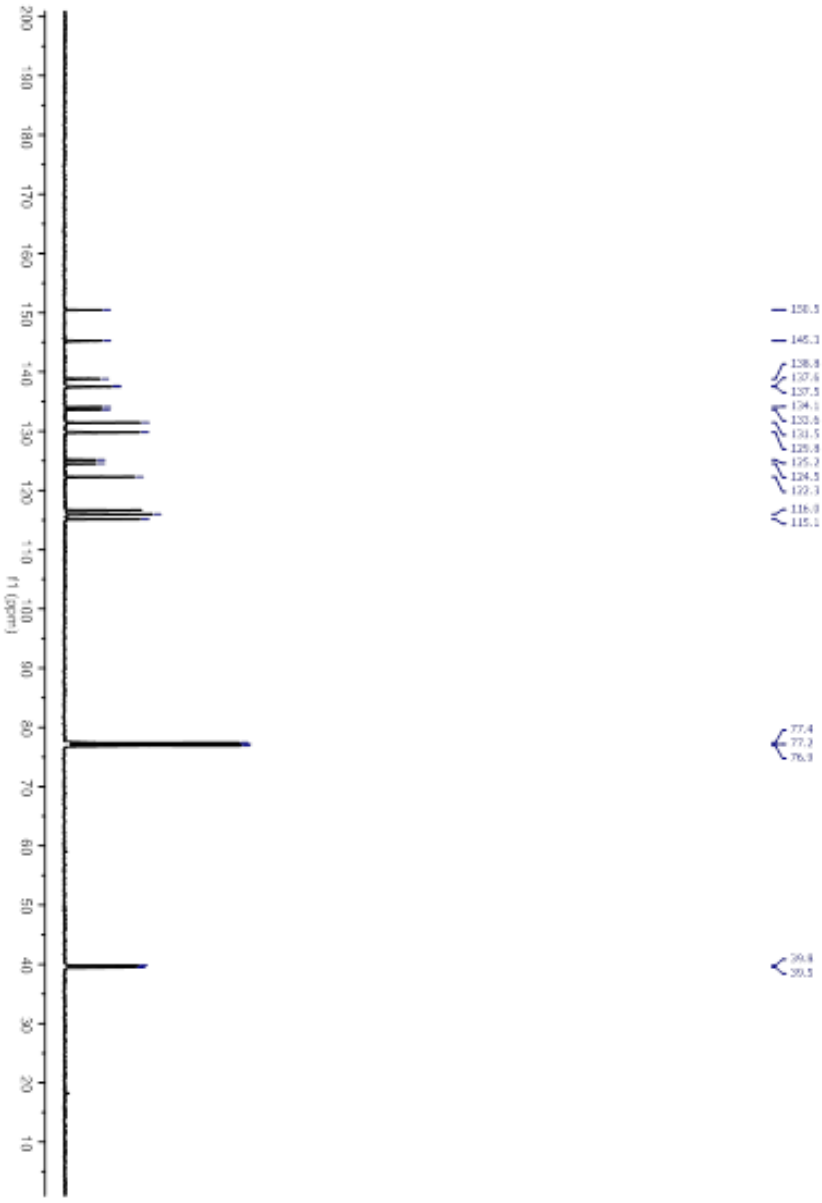

Figure 41S: ^{13}C NMR spectrum (125 MHz, $CDCl_3$) of compound **81**.

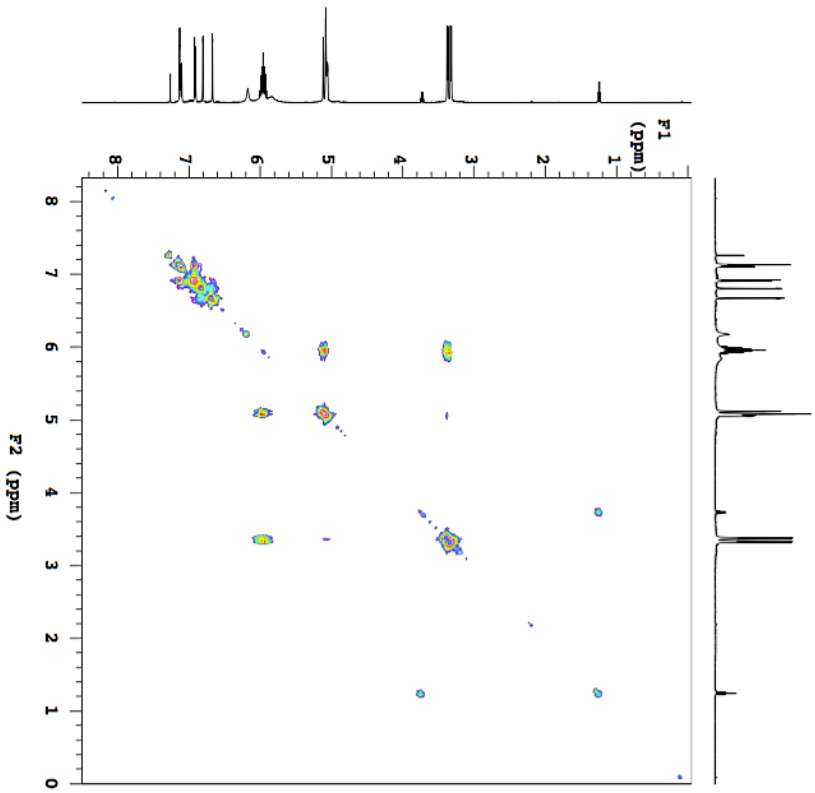

Figure 42S: gCOSY spectrum of compound **81**.

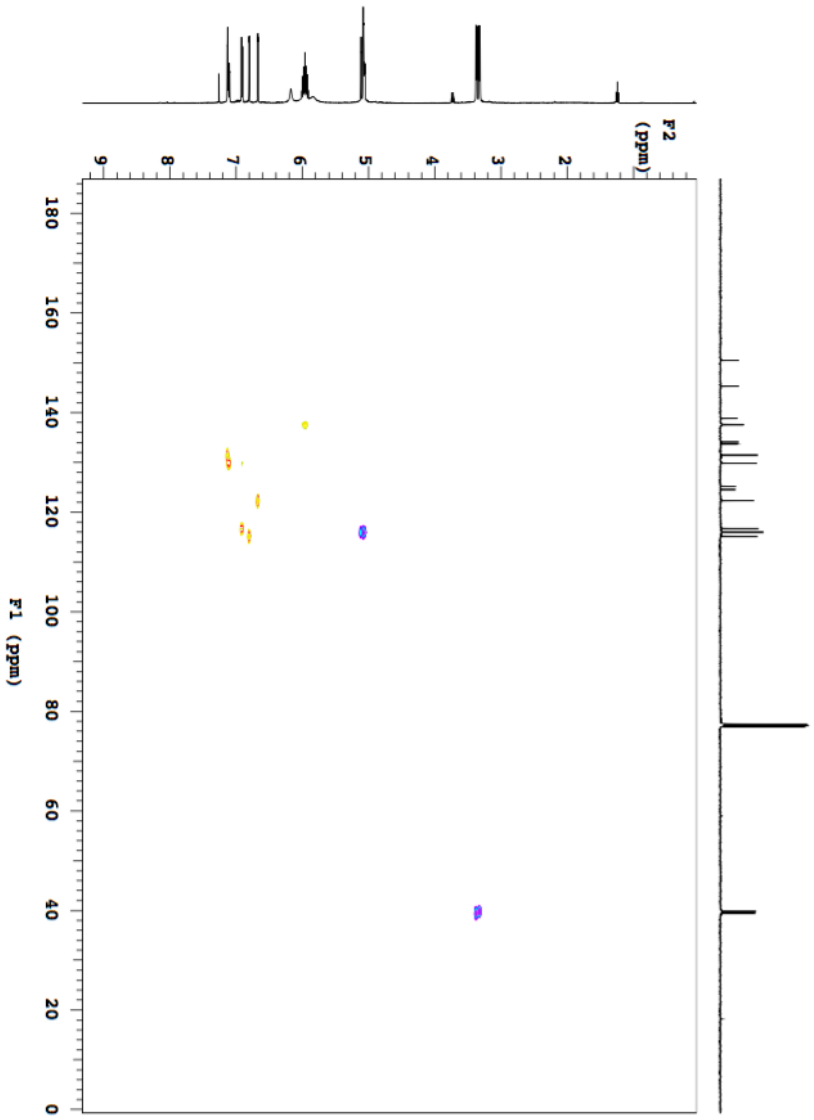

Figure 43S: gHSQCAD spectrum of compound **81**.

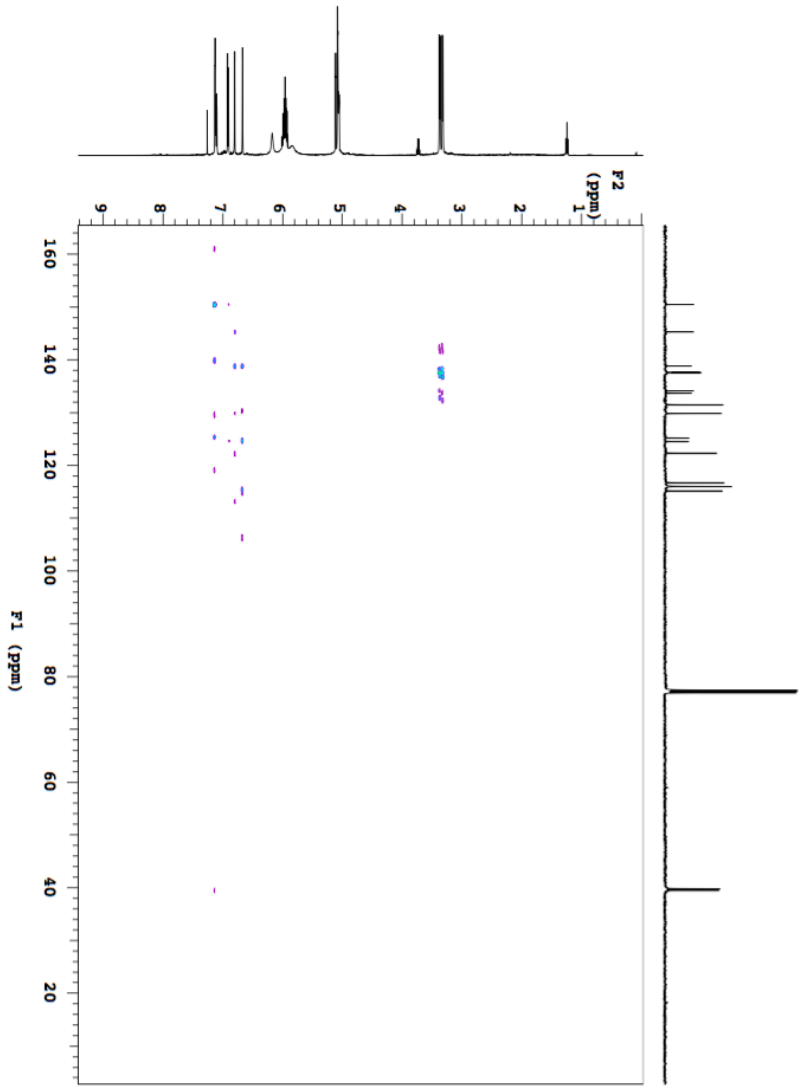

Figure 44S: gHMBCAD spectrum of compound **81**.

5.3.2 Compound 82

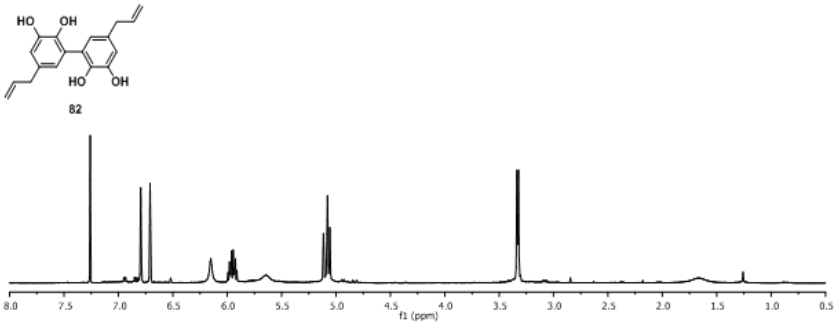

Figure 45S: ^{1}H NMR spectrum (500 MHz, $CDCl_3$) of **82**.

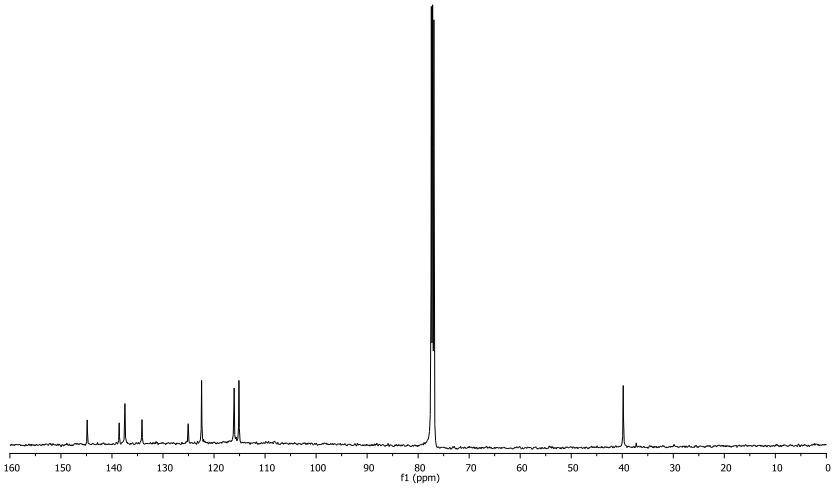

Figure 46S: ^{13}C NMR spectrum (125 MHz, $CDCl_3$) of **82**.

5.3.3 Compound 84

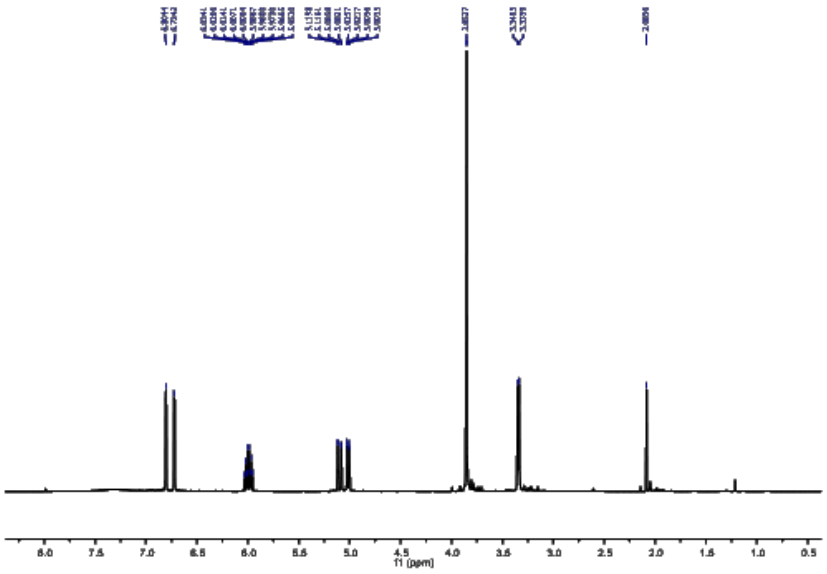

Figure 47S: ^{1}H NMR spectrum (500 MHz, $CDCl_3$) of **84**.

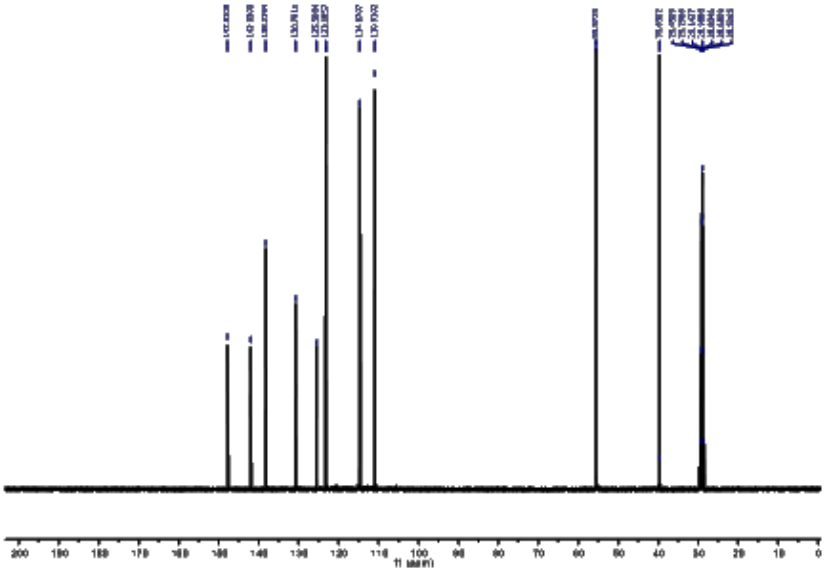

Figure 48S: ^{13}C NMR spectrum (125 MHz, $CDCl_3$) of **84**.

5.3.4 Compound 85

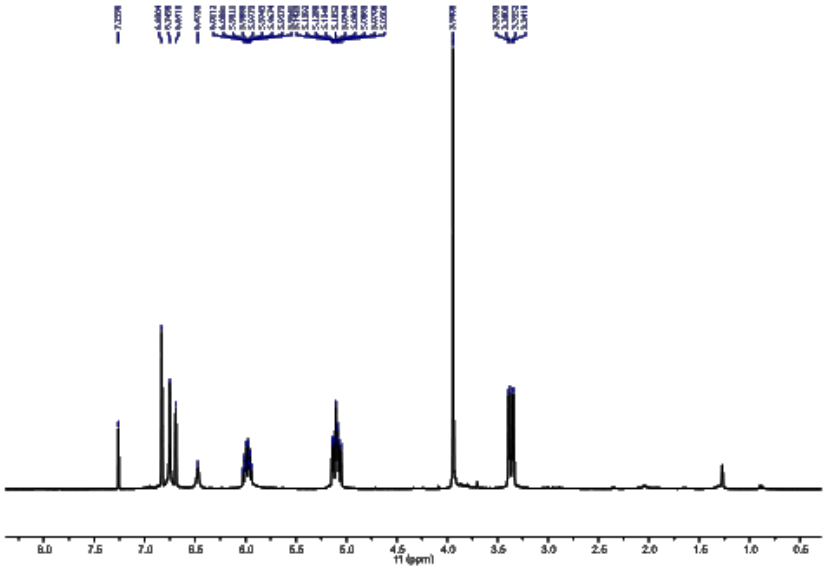

Figure 49S: ^{1}H NMR spectrum (500 MHz, $CDCl_3$) of **85**.

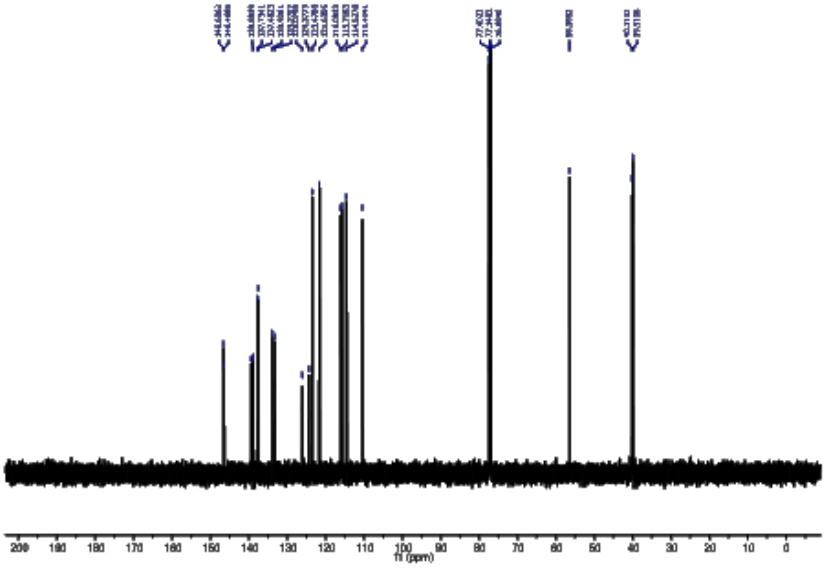

Figure 50S: ^{13}C NMR spectrum (125 MHz, $CDCl_3$) of **85**.

5.3.5 Compound 86

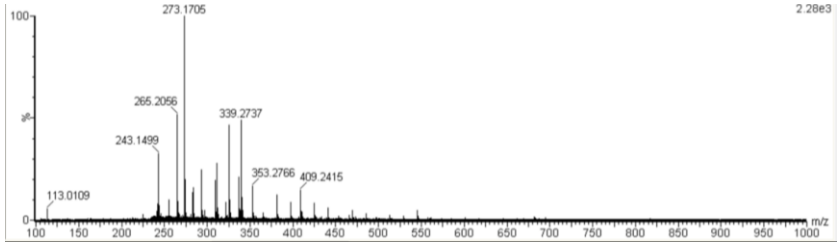

Figure 51S: HRMS spectrum of compound **86**.

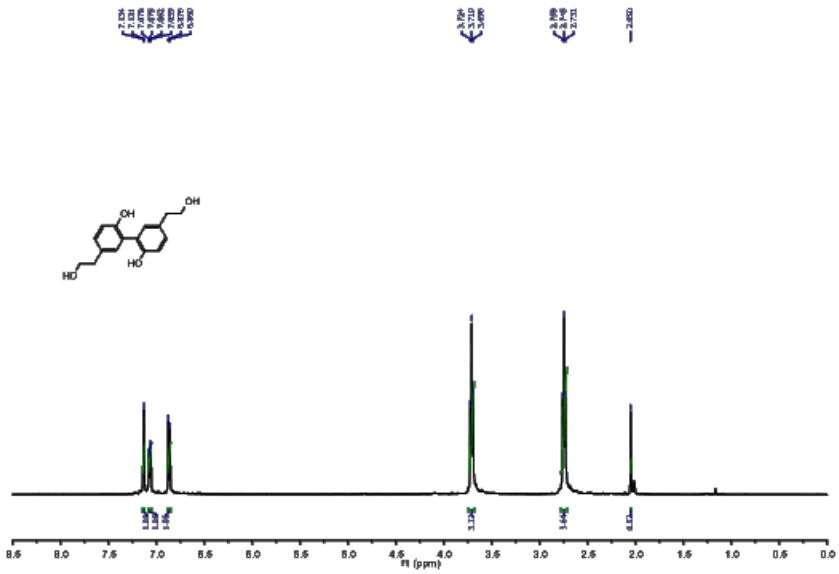

Figure 52S: ^{1}H NMR spectrum (500 MHz, acetone-d_6) of compound **86**.

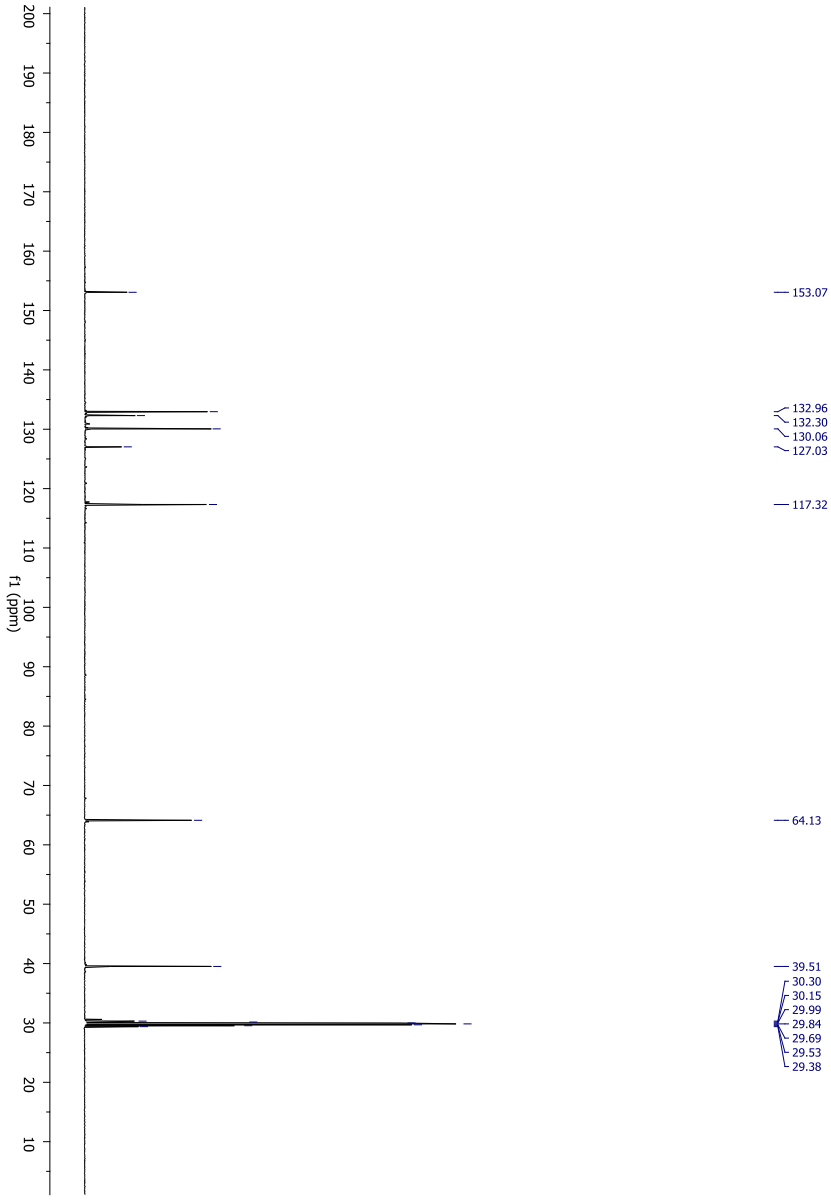

Figure 53S: ^{13}C NMR spectrum (125 MHz, acetone-d_6) of compound **86**.

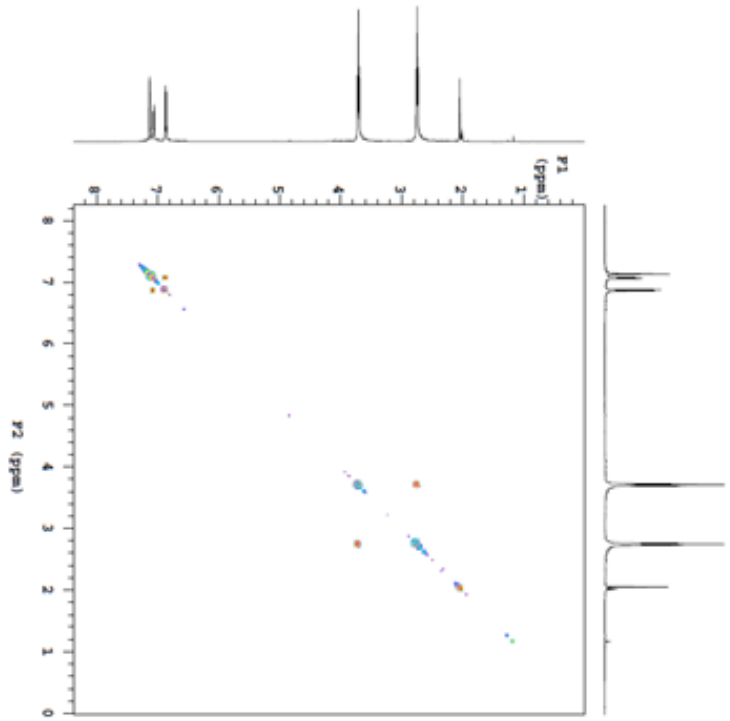

Figure 54S: gCOSY spectrum of compound **86**.

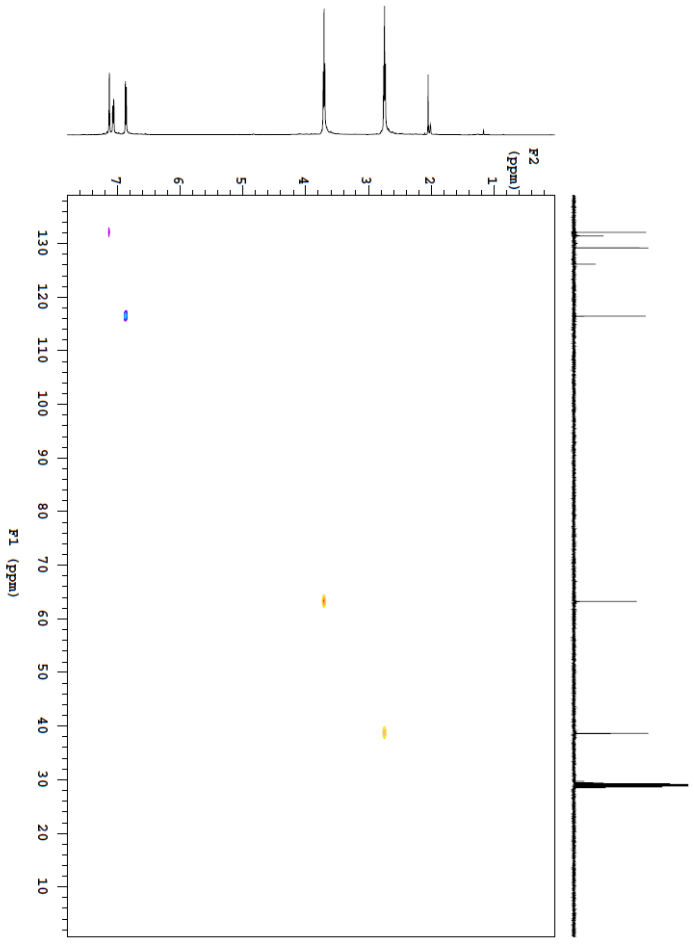

Figure 55S: gHSQCAD spectrum of compound **86**

5.3.6 Compound 87

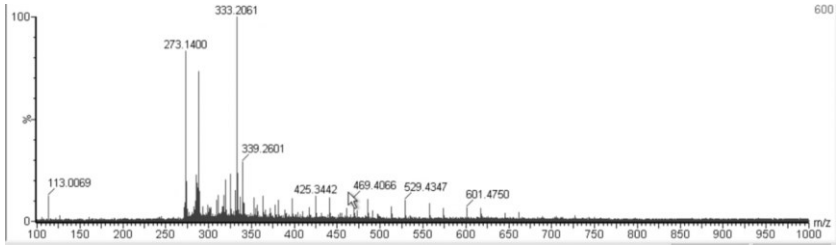

Figure 56S: HRMS spectrum of compound **87**.

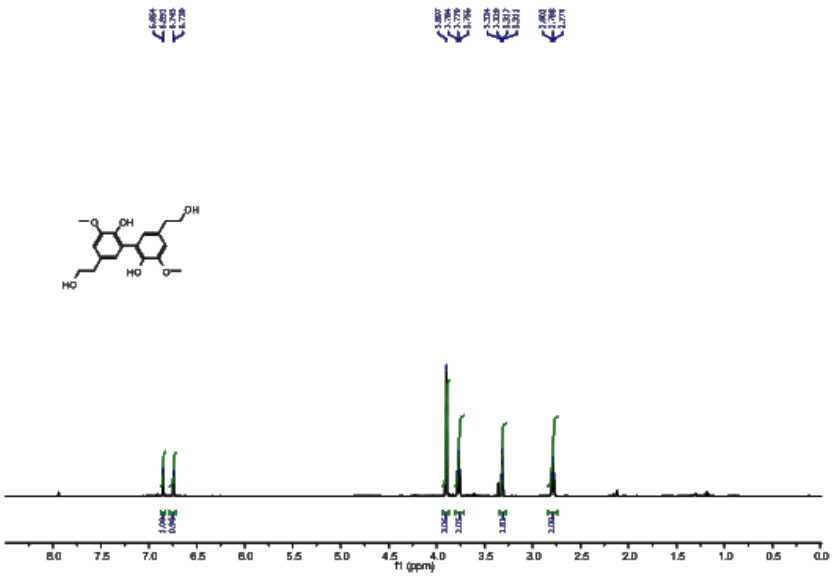

Figure 57S: ^{1}H NMR spectrum (500 MHz, acetone-d_6) of compound **87**.

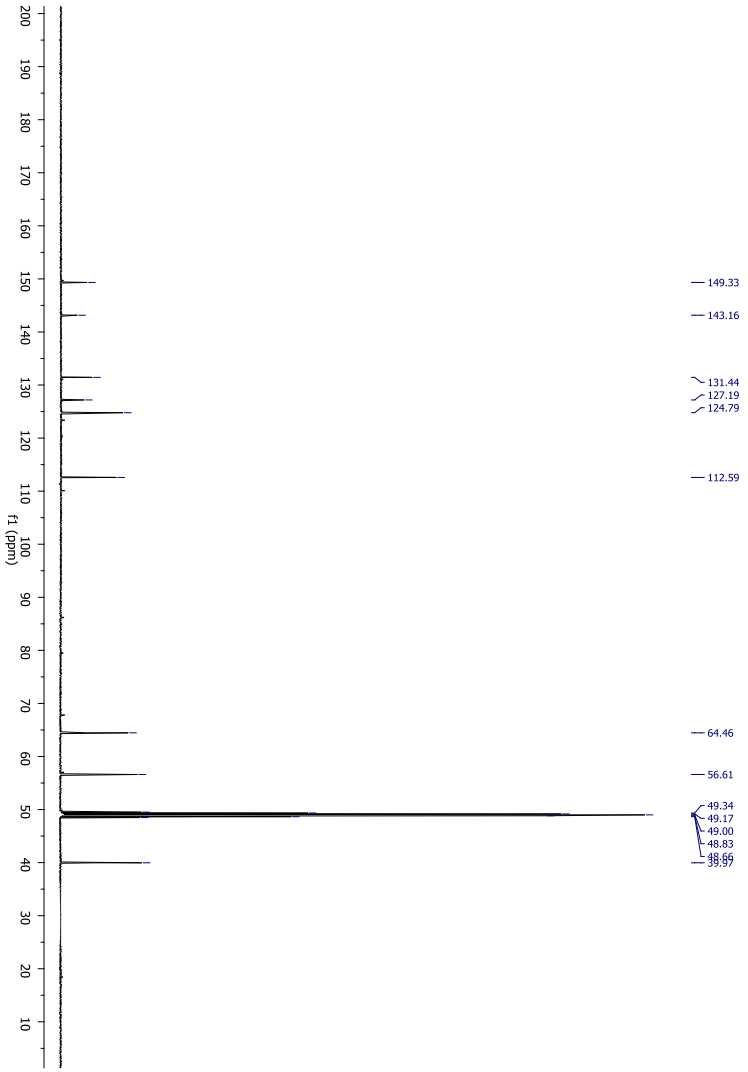

Figure 58S: ^{13}C NMR spectrum (125 MHz, acetone-d_6) of compound **87**.

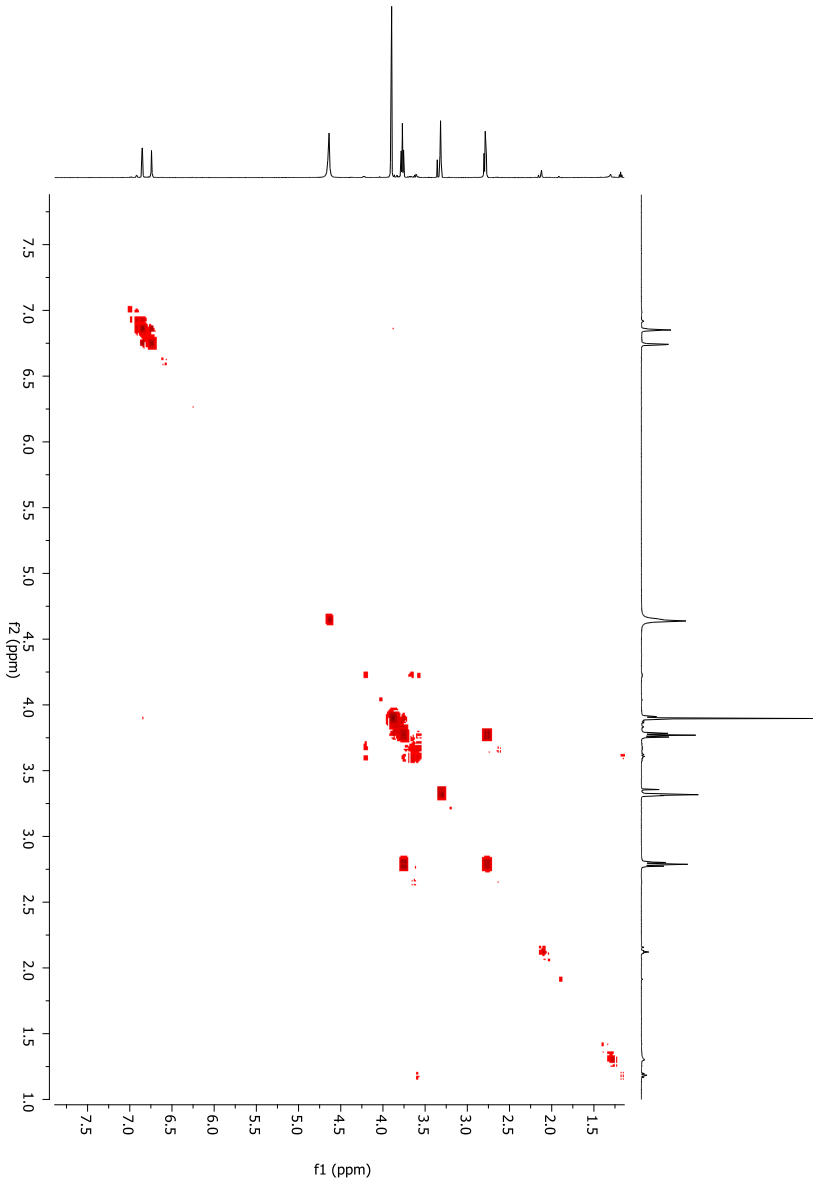

Figure 59S: gCOSY spectrum of compound **87**.

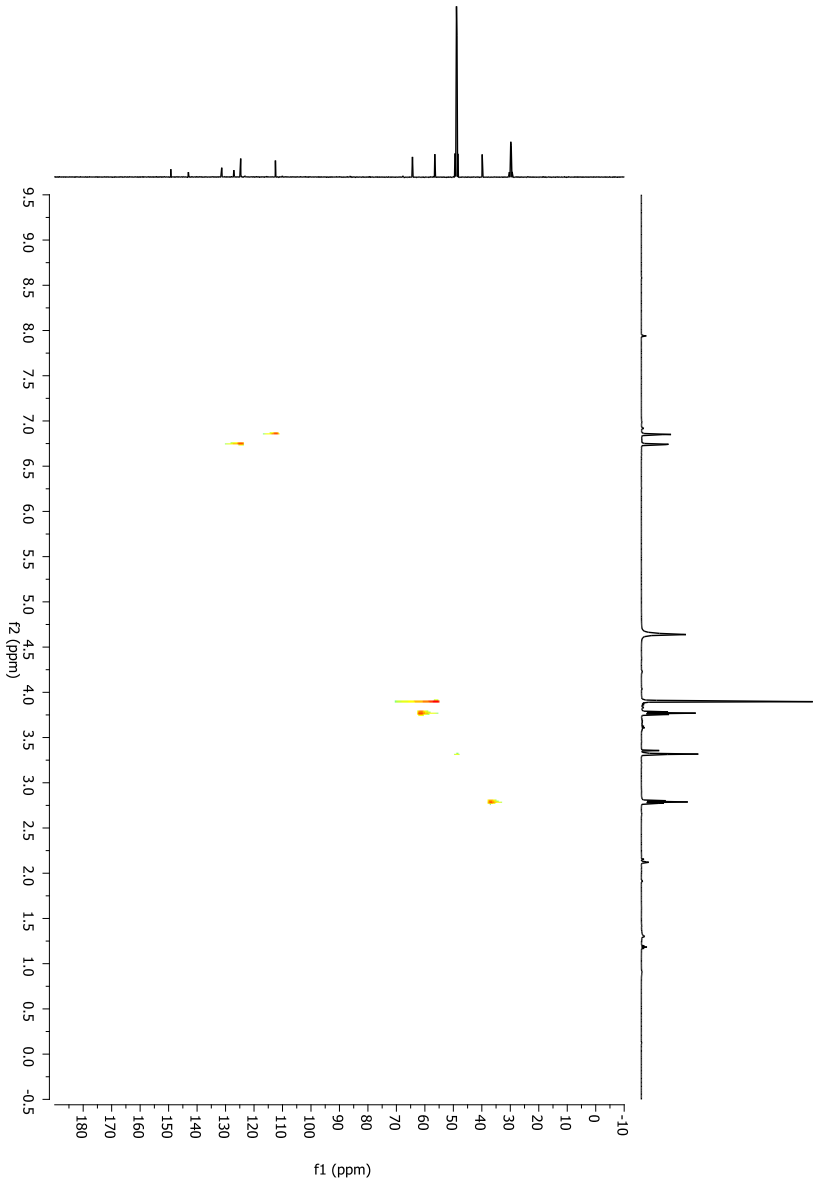

Figure 60S: gHSQCAD spectrum of compound **87**.

5.3.7 Compound 88

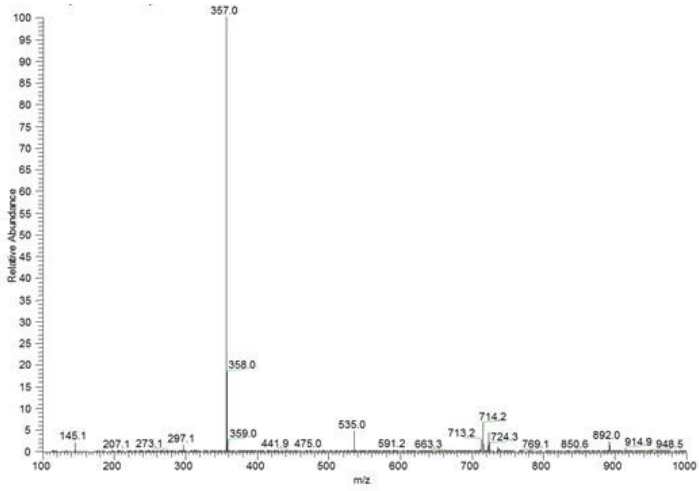

Figure 61S: ESIMS spectrum of compound **88**.

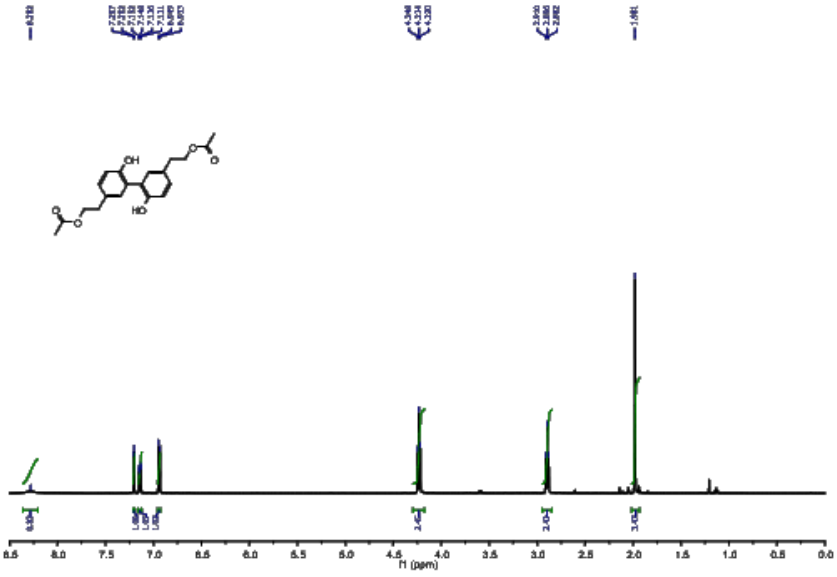

Figure 62S: ^{1}H NMR spectrum (500 MHz, acetone-d_6) of compound **88**.

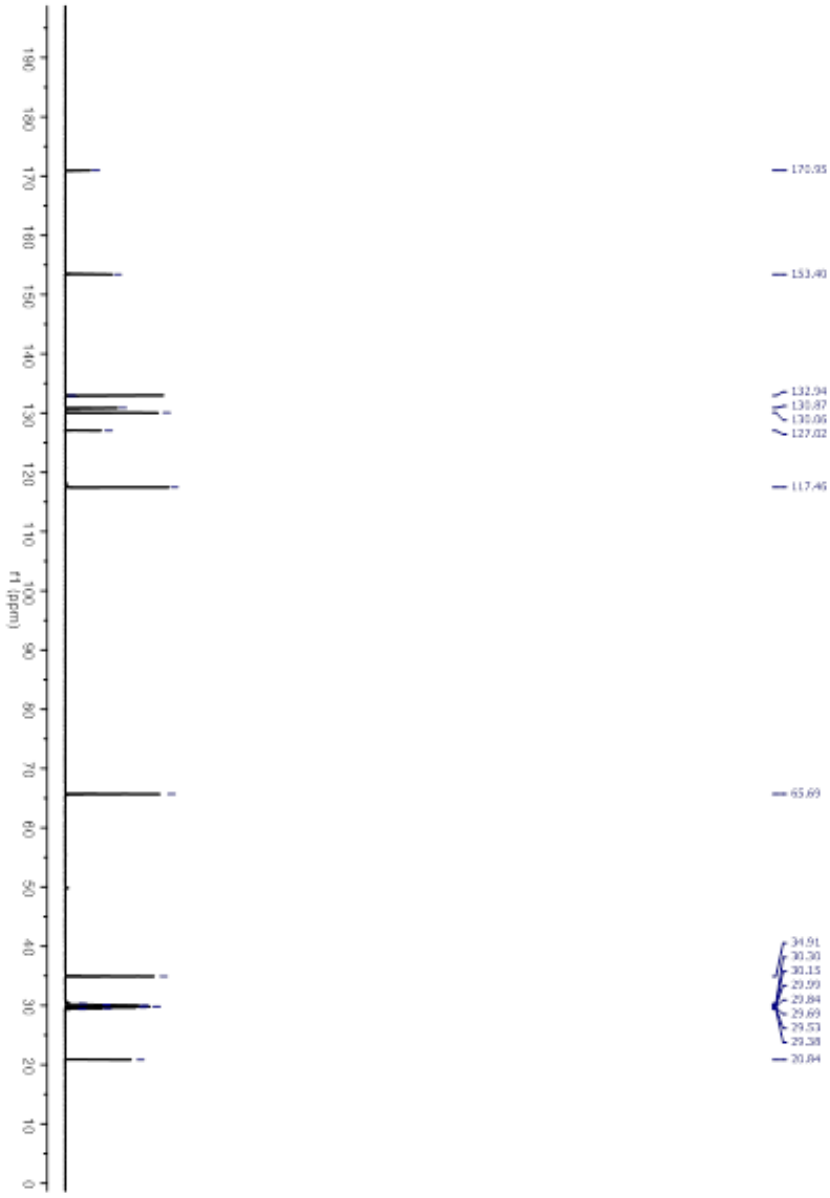

Figure 63S: ^{13}C NMR spectrum (125 MHz, acetone-d_6) of compound **88**.

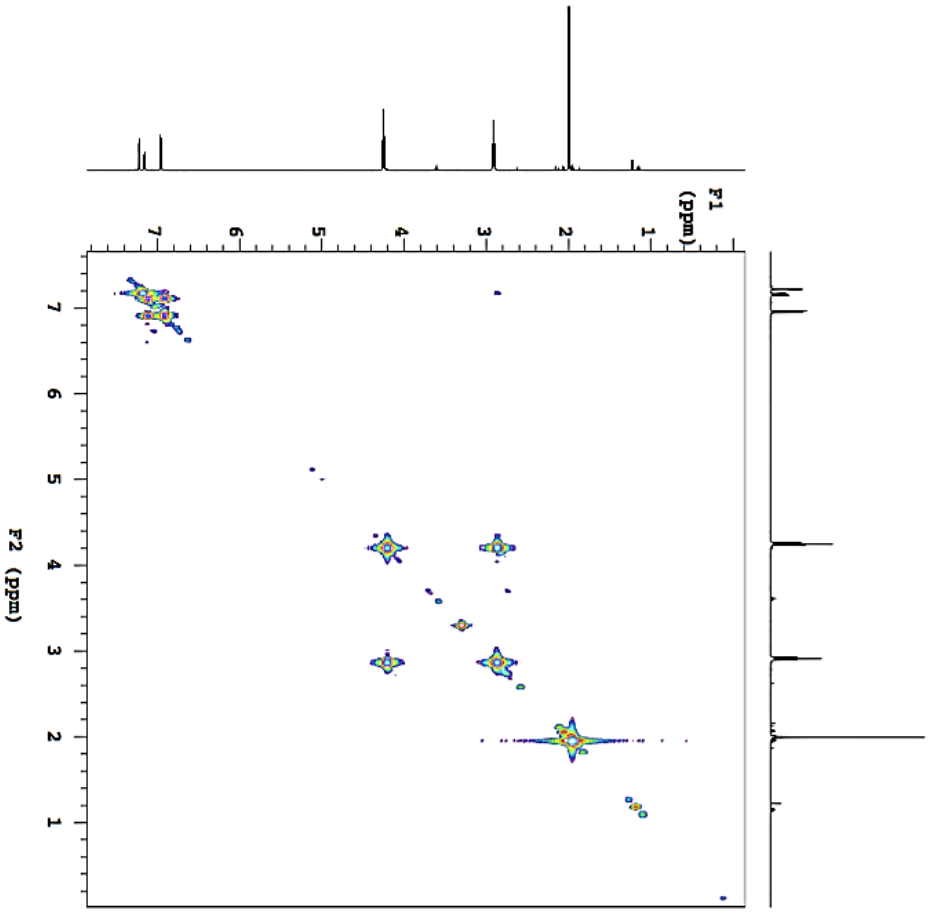

Figure 64S: gCOSY spectrum of compound **88**.

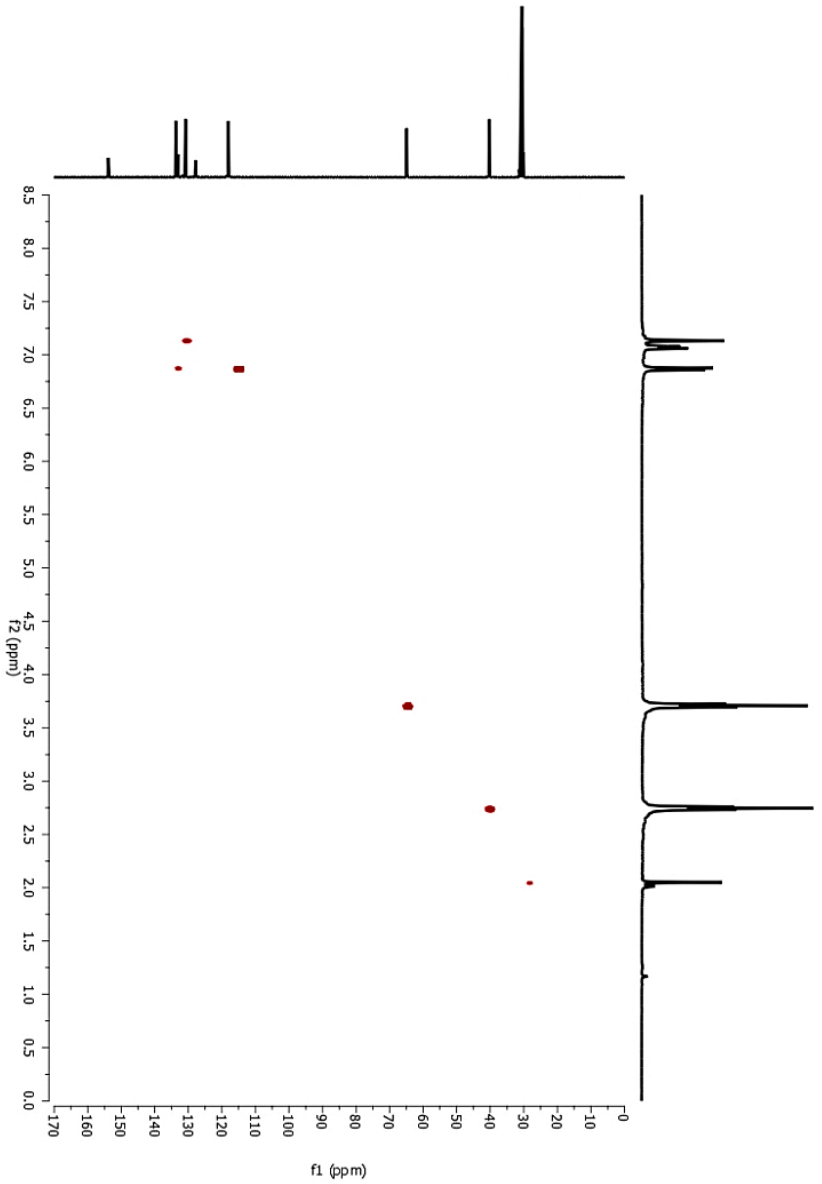

Figure 65S: gHSQCAD spectrum of compound **88**.

5.3.8 Compound 89

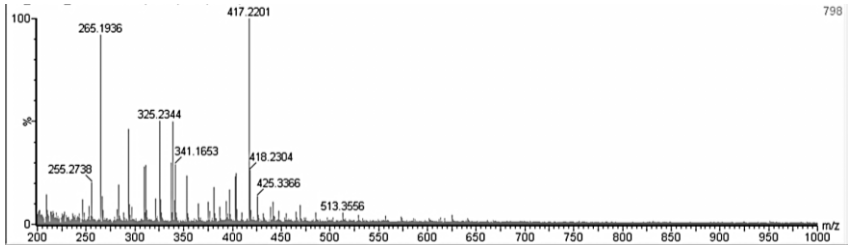

Figure 66S: ESIMS spectrum of compound **89**.

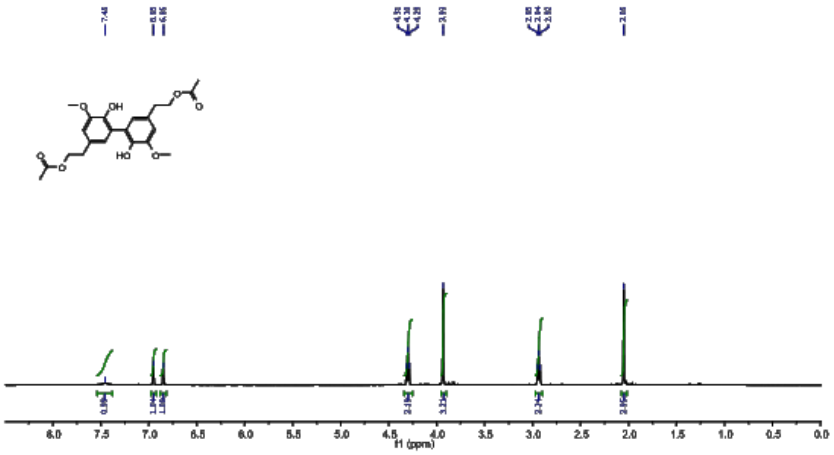

Figure 67S: ^{1}H NMR spectrum (500 MHz, acetone-d_6) of compound **89**.

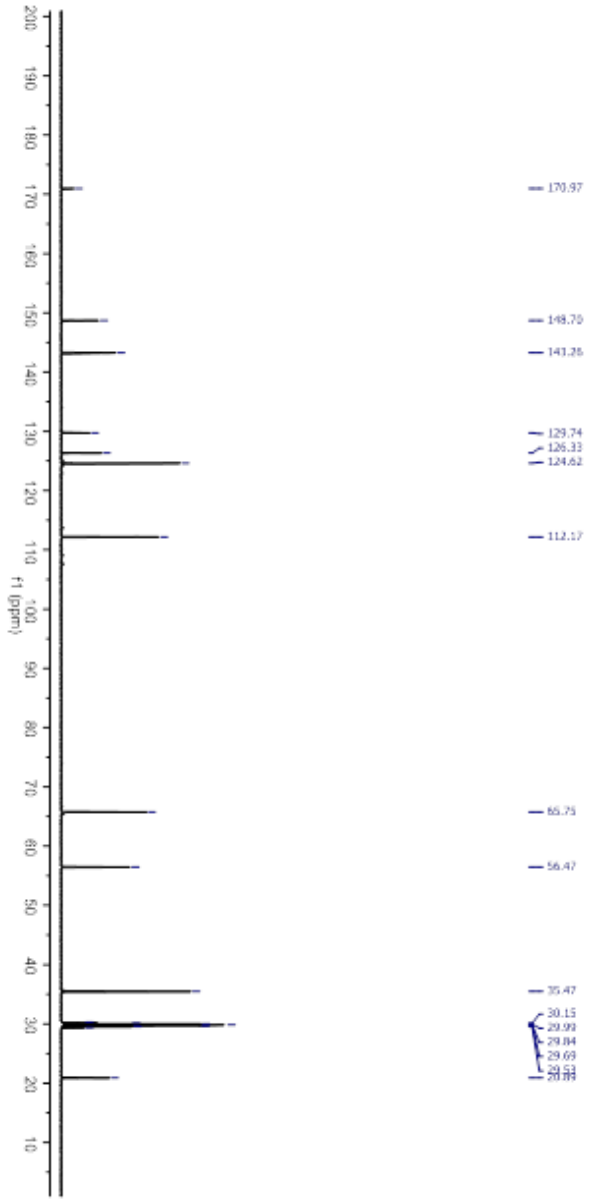

Figure 68S: ^{13}C NMR spectrum (125 MHz, acetone-d_6) of compound **89**.

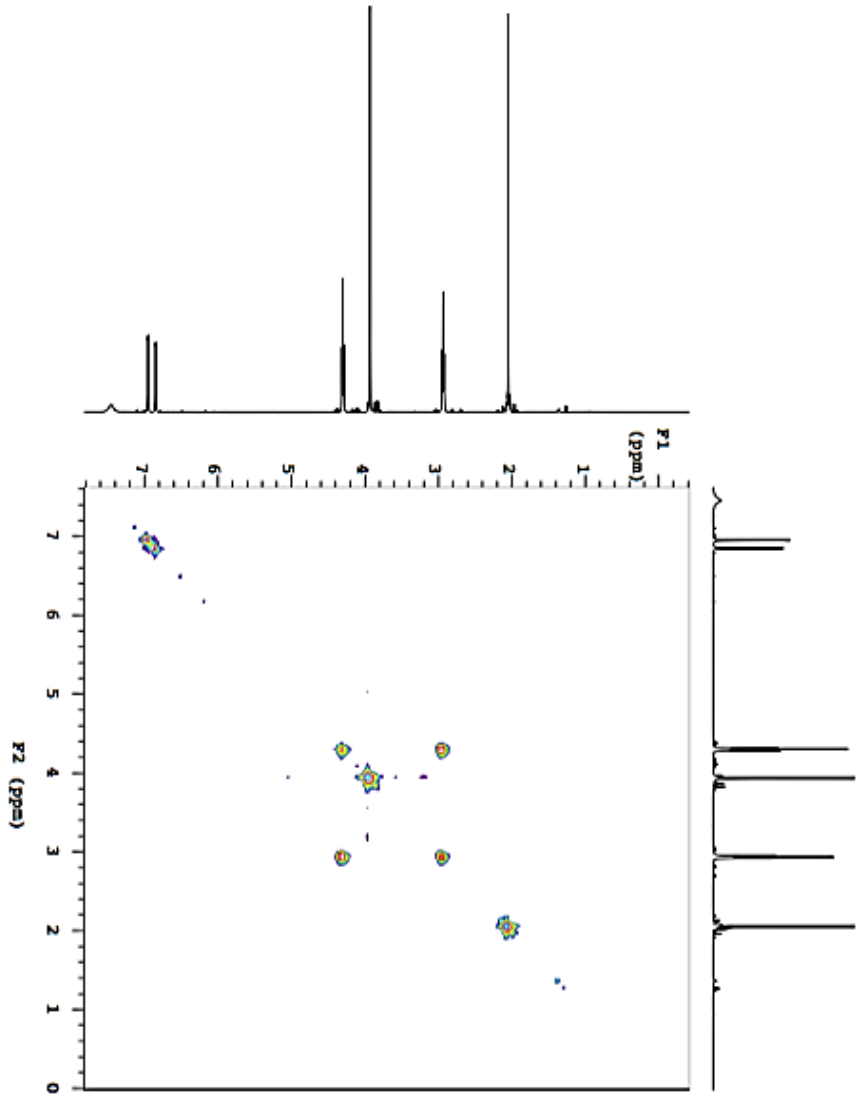

Figure 69S: gCOSY spectrum of **89**.

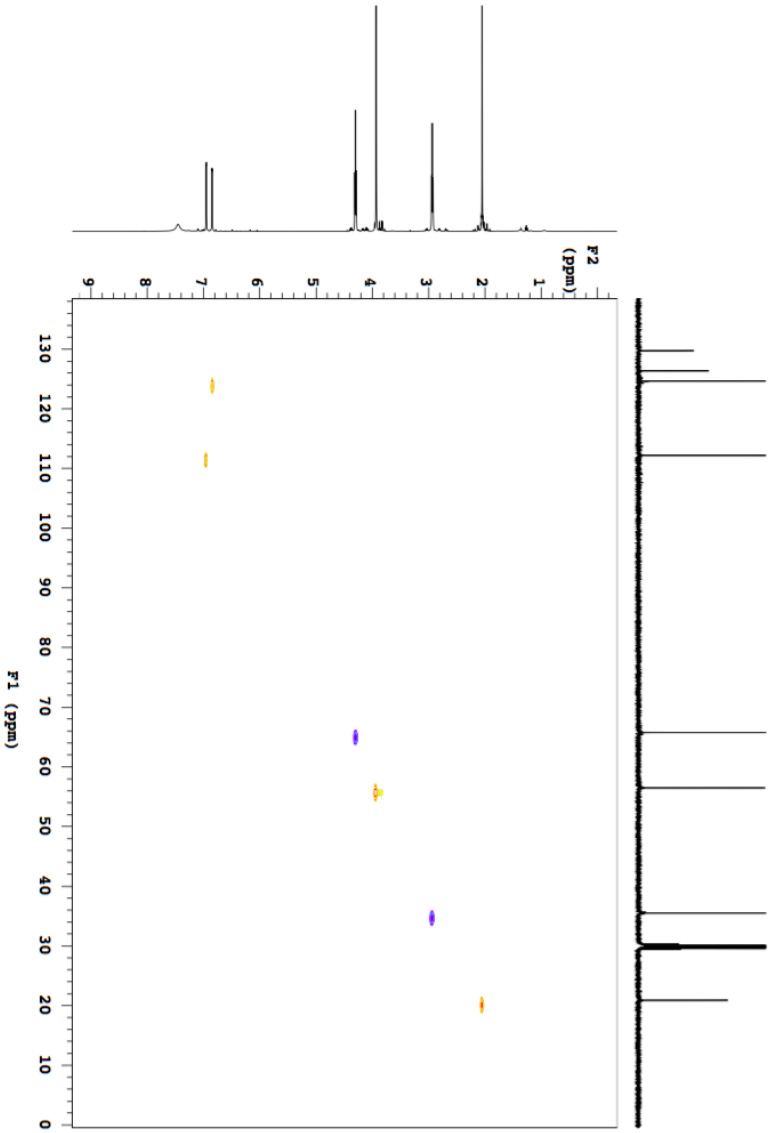

Figure 70S: gHSQCAD spectrum of **89**.

5.3.9 Compound 90

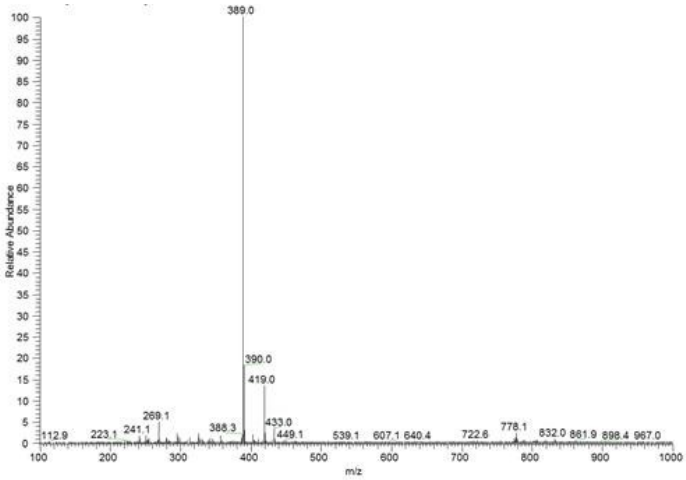

Figure 71S: ESIMS spectrum of compound **90**.

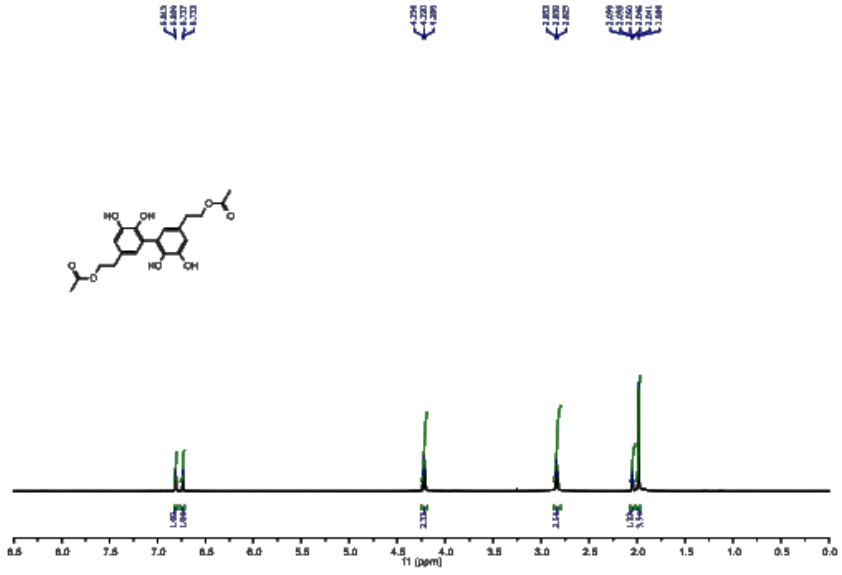

Figure 72S: ^{1}H NMR spectrum (500 MHz, acetone-d_6) of compound **90**.

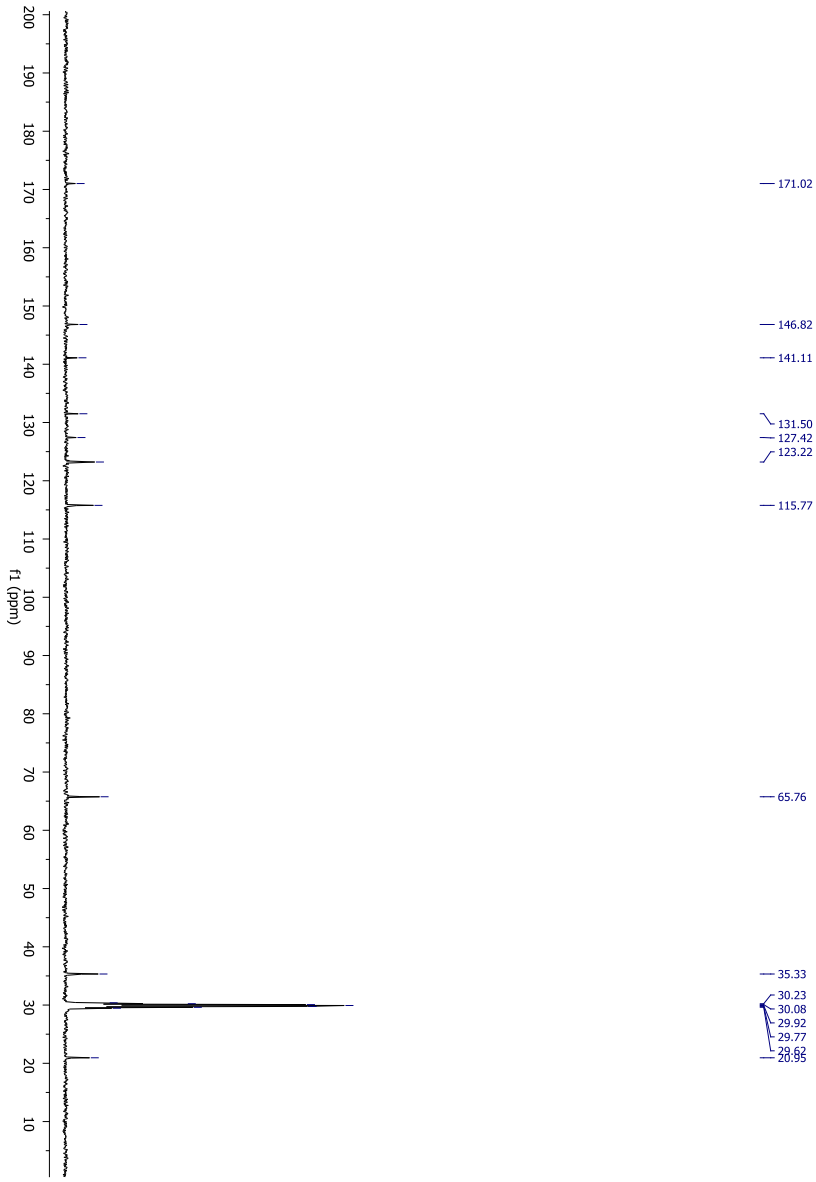

Figure 73S: ^{13}C NMR spectrum (125 MHz, acetone-d_6) of compound **90**.

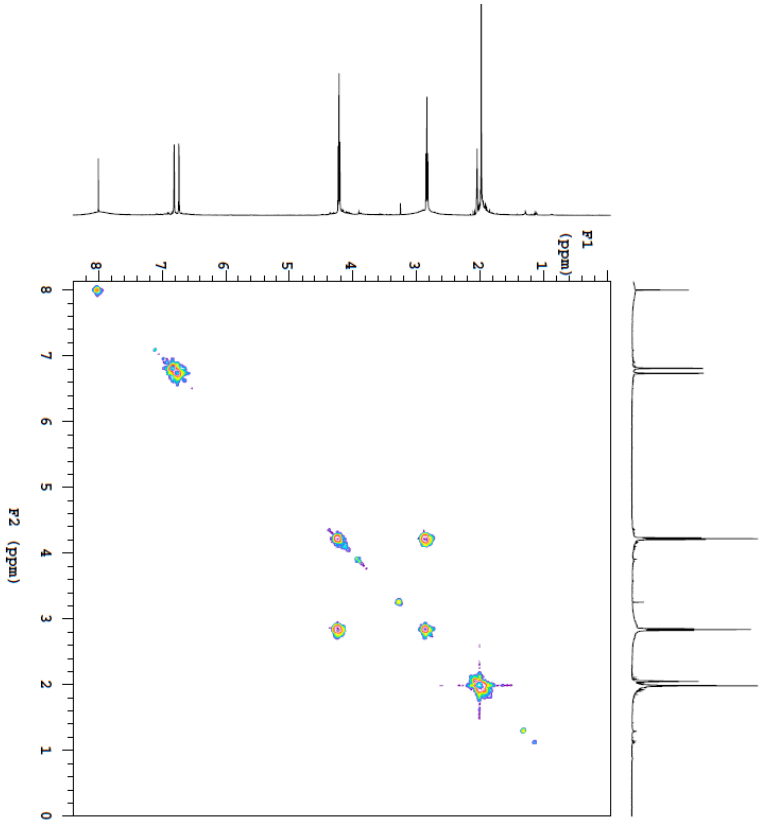

Figure 74S: gCOSY spectrum of **90**.

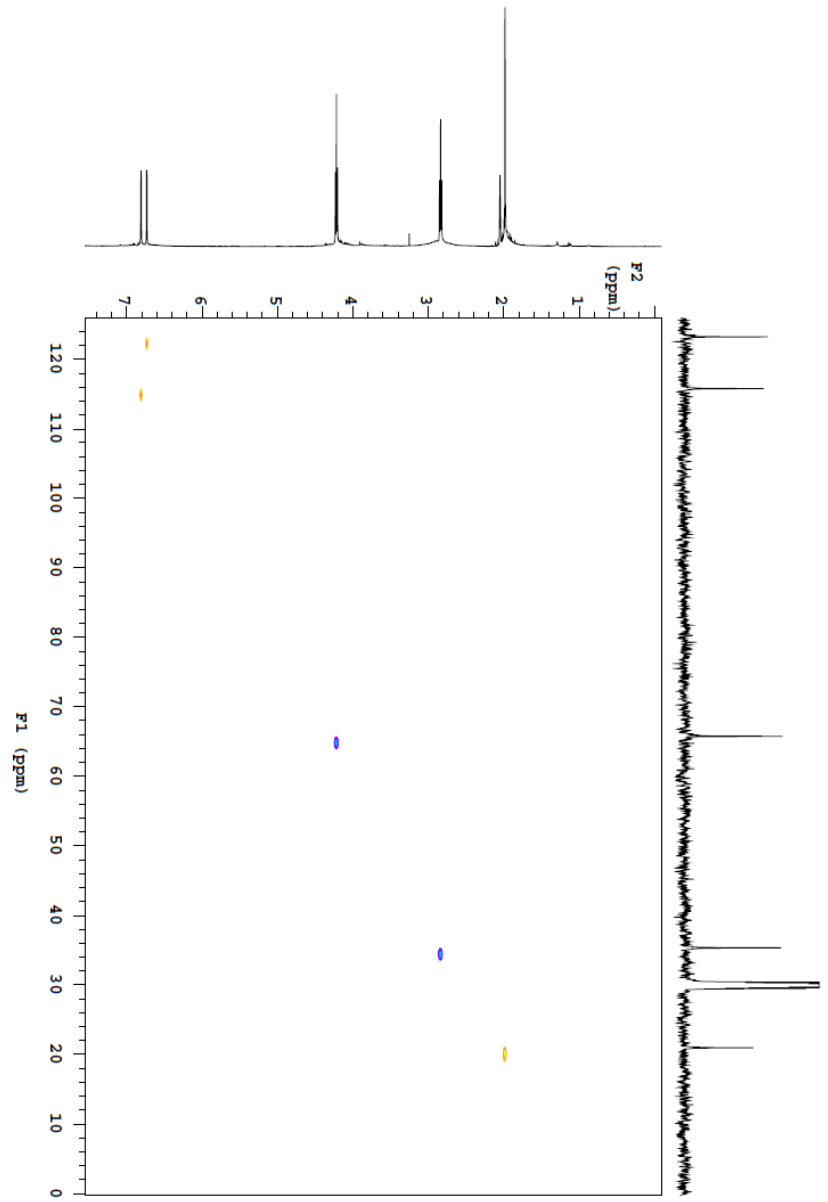

Figure 75S: gHSQCAD spectrum of **90**.

5.3.10 Compound 91

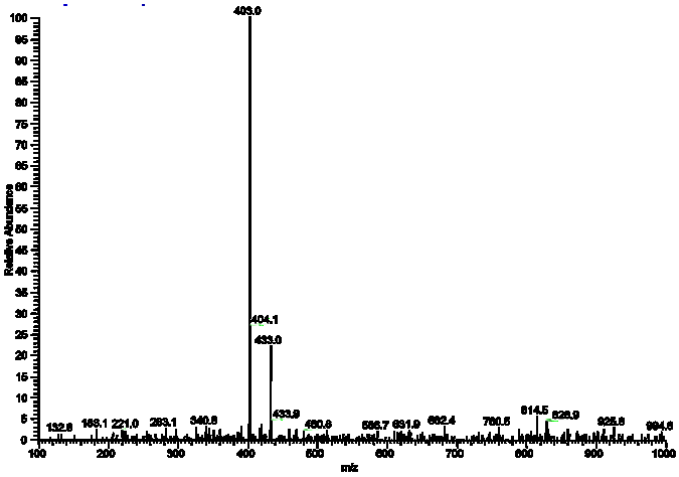

Figure 76S: ESIMS spectrum of compound **91**.

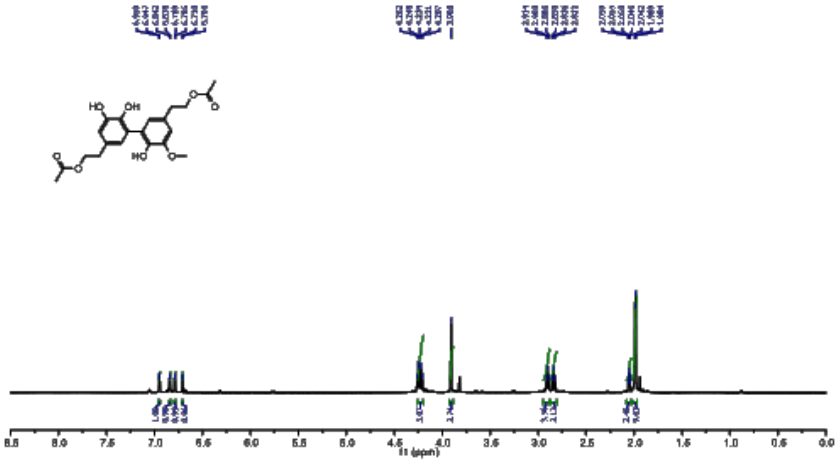

Figure 77S: ^{1}H NMR spectrum (500 MHz, acetone-d_6) of compound **91**.

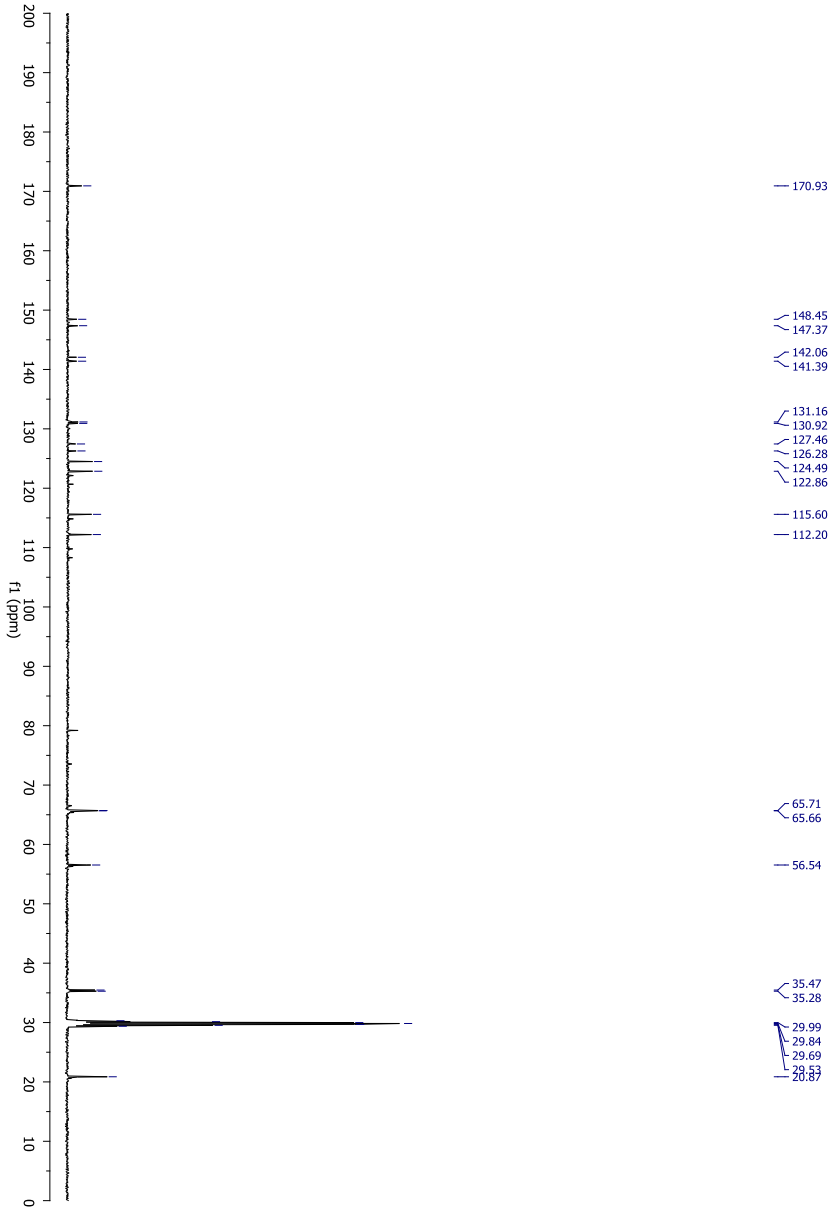

Figure 78S: ^{13}C NMR spectrum (125 MHz, acetone-d_6) of compound **91**.

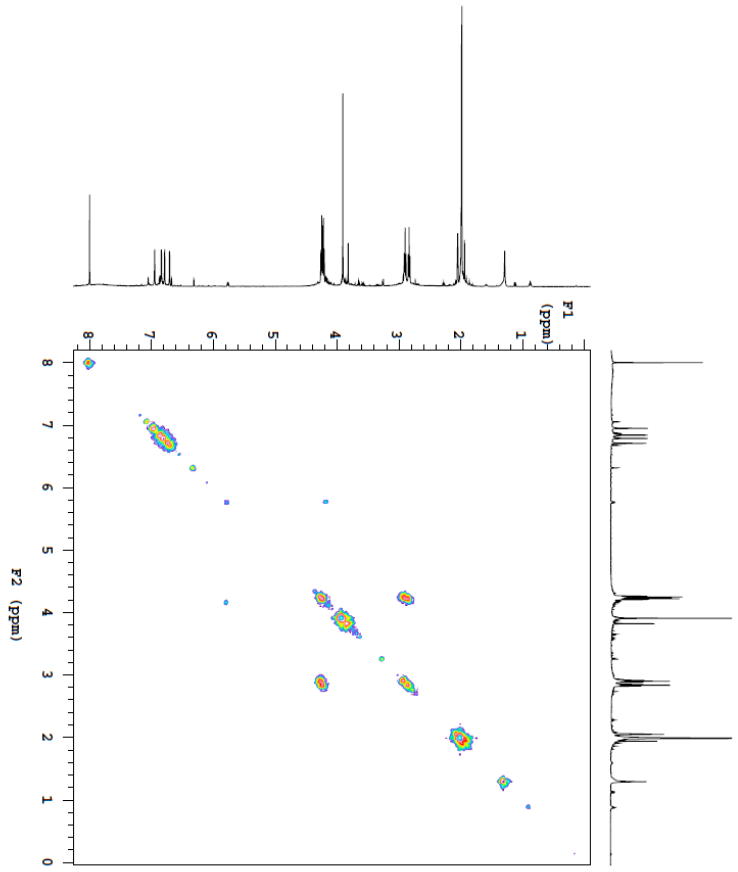

Figure 79S: gCOSY spectrum of **91**.

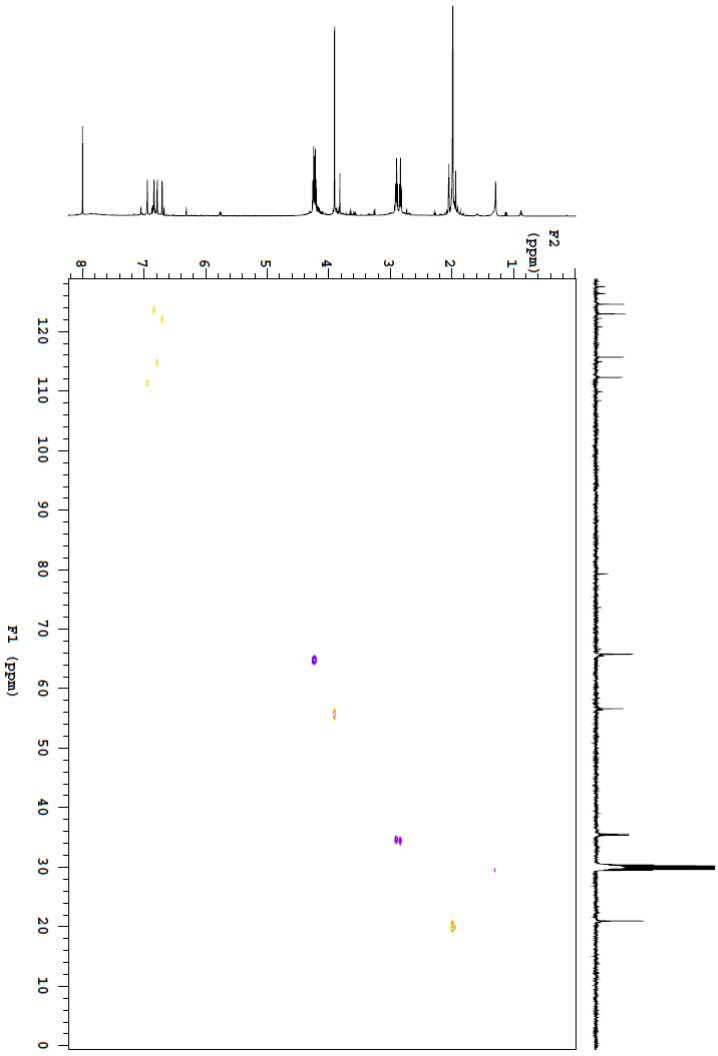

Figure 80S: gHSQCAD spectrum of **91**.

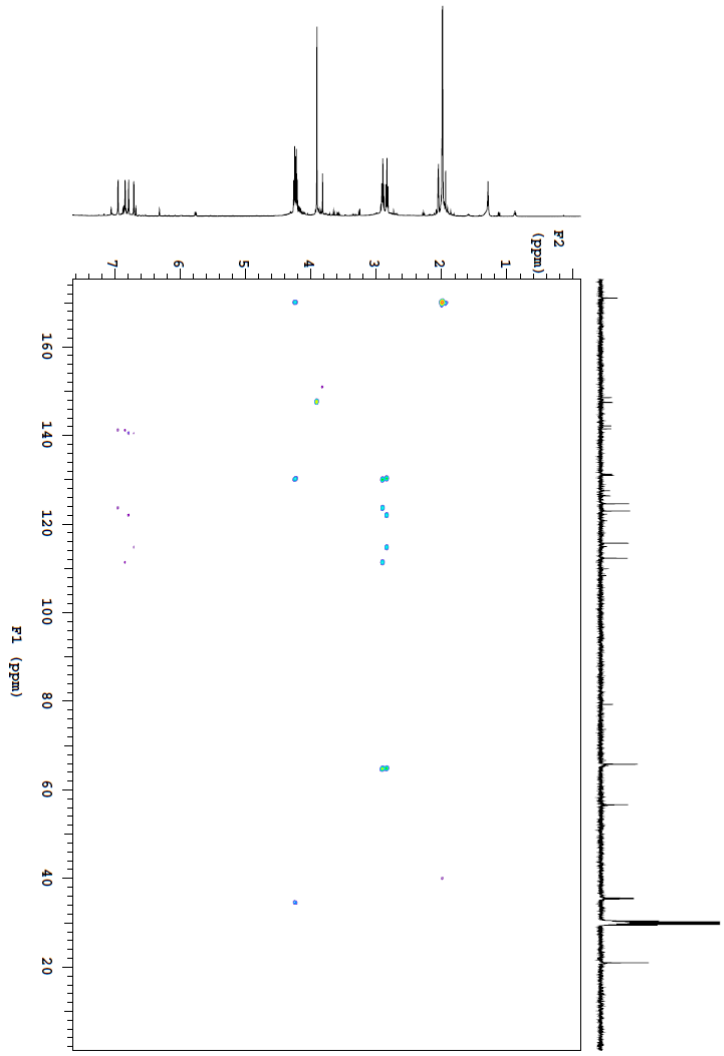

Figure 81S: gHMBCAD spectrum of **91**.

5.3.11 Compound 92

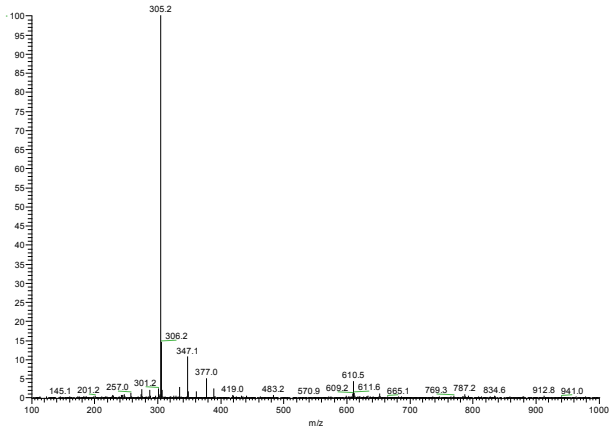

Figure 82S: ESIMS spectrum of compound **92**.

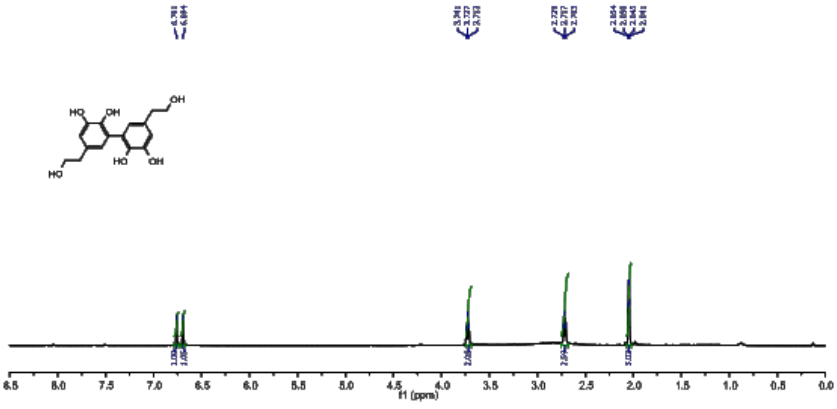

Figure 83S: ^{1}H NMR spectrum (500 MHz, acetone-d_6) of compound **92**.

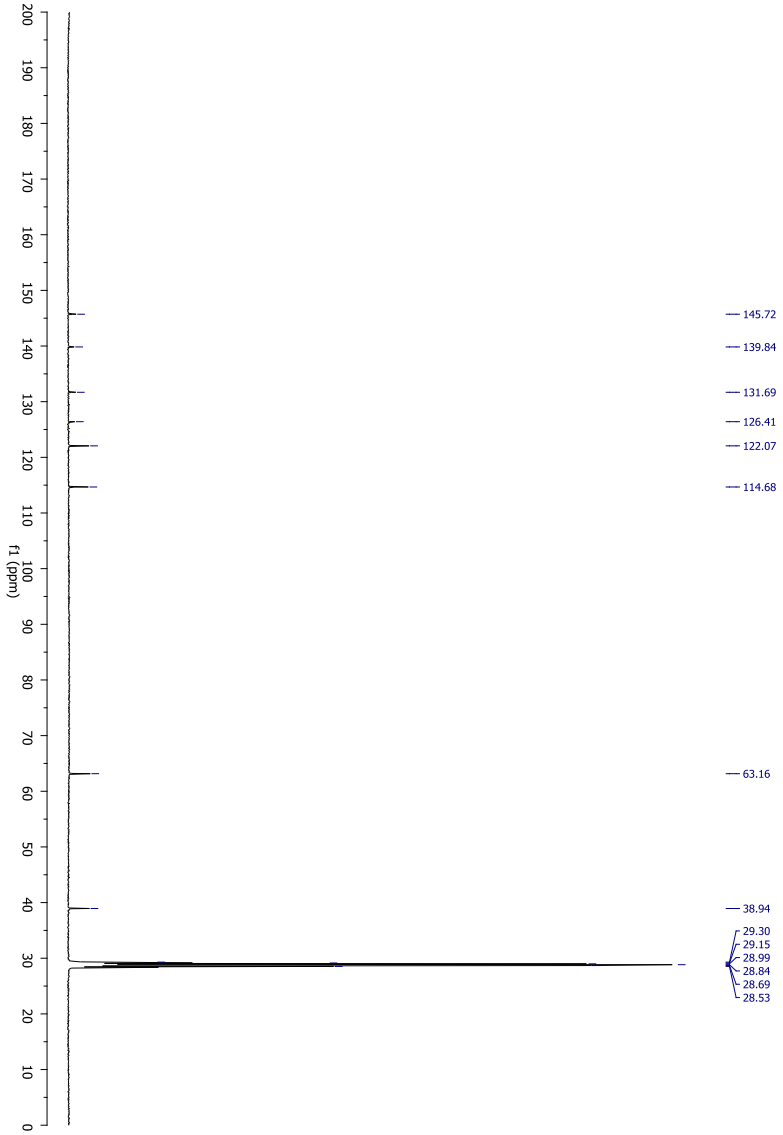

Figure 84S: ^{13}C NMR spectrum (125 MHz, acetone-d_6) of compound **92**.

5.3.12 Compound 93

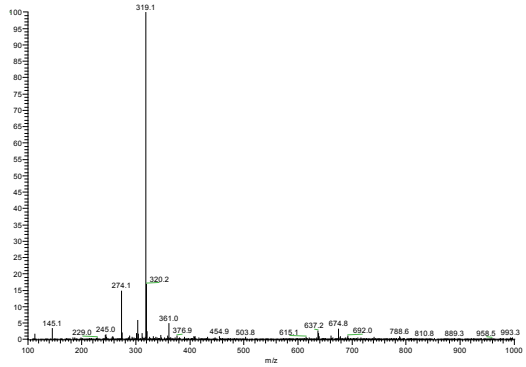

Figure 85S: ESIMS spectrum of compound **93**.

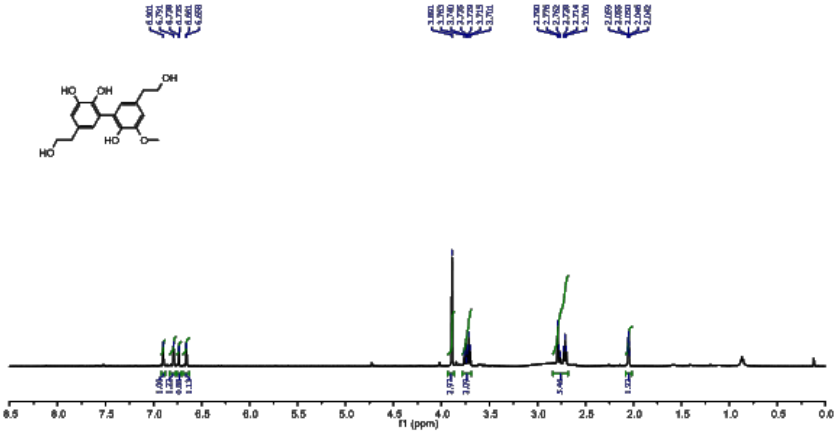

Figure 86S: ^{1}H NMR spectrum (500 MHz, acetone-d_6) of compound **93**.

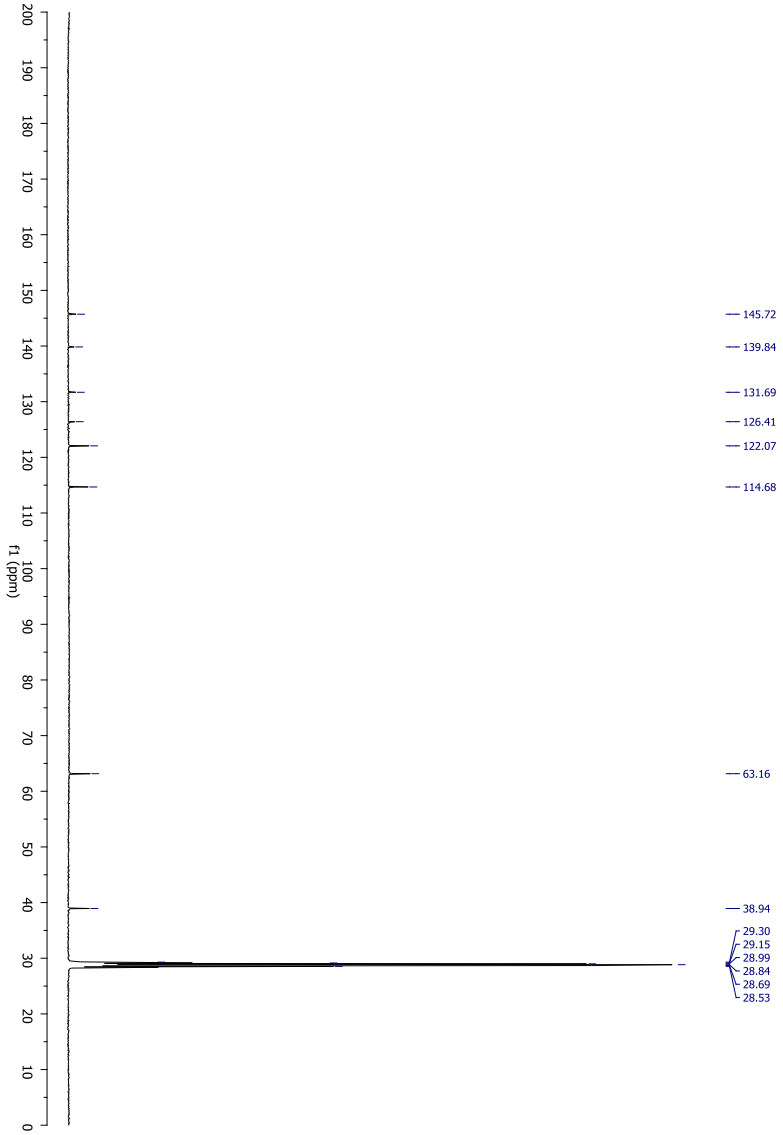

Figure 87S: ^{13}C NMR spectrum (125 MHz, acetone-d_6) of compound **93**.

5.3.12 Compound 96

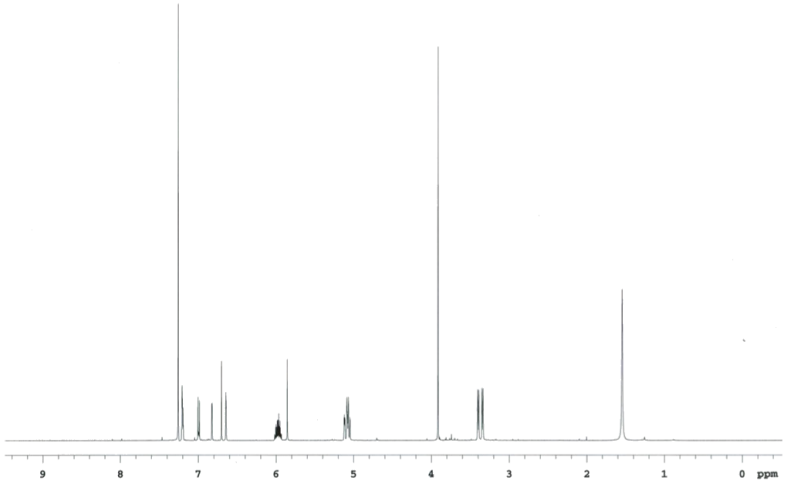

Figure 88S: ^{1}HNMR spectrum (500 MHz, in acetone-d_6) of **96.**

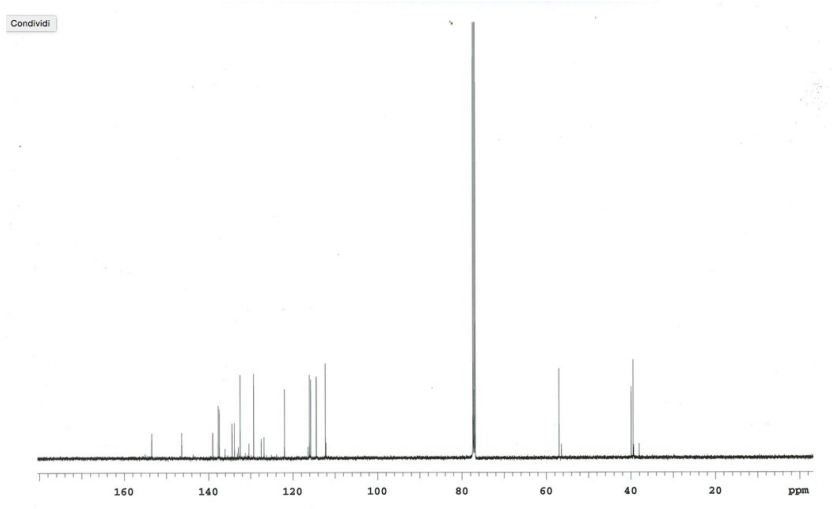

Figure 89S: ^{13}C NMR spectrum (125 MHz, in acetone-d_6) of **96.**

5.3.13 Compound 99

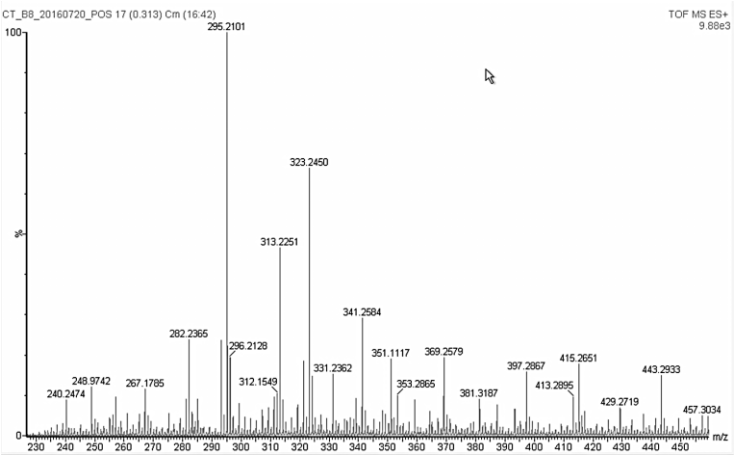

Figure 90S: ESIMS spectrum of **99**.

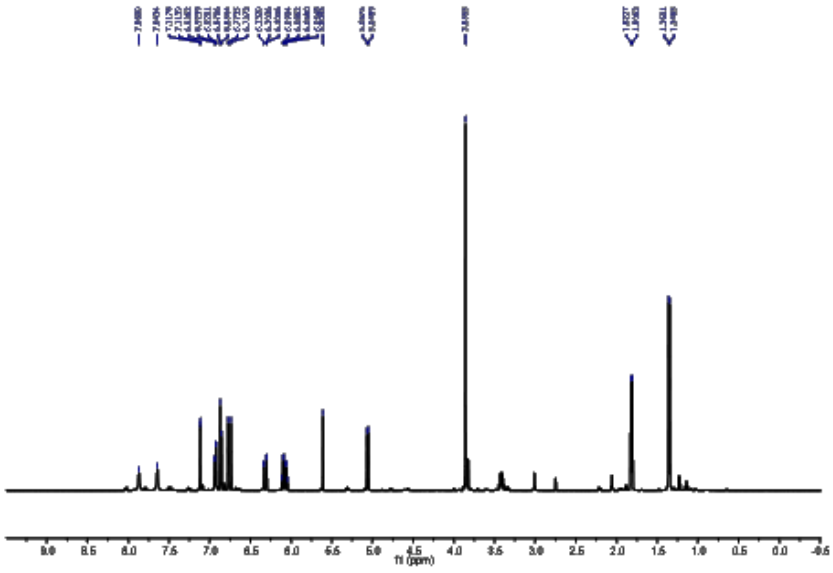

Figure 91S: ^{1}HNMR spectrum (500 MHz, in acetone-d_6) of **99.**

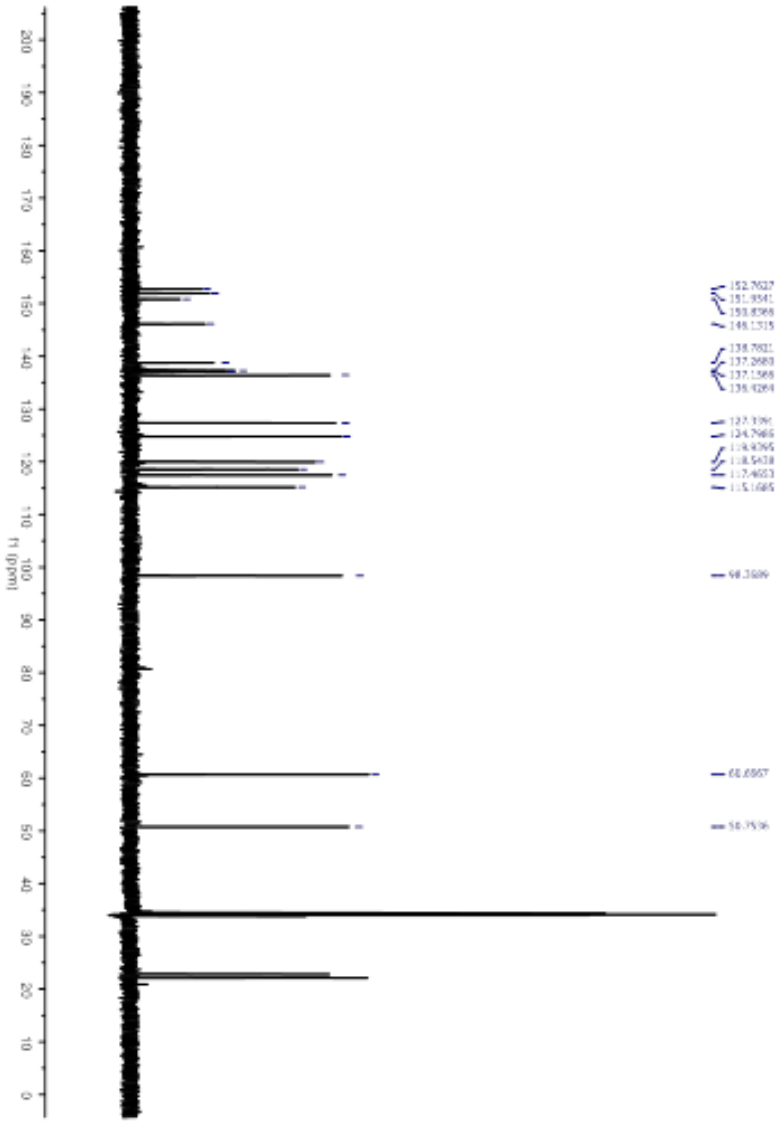

Figure 92S: ^{13}C NMR spectrum (125 MHz, in acetone-d_6) of **99.**

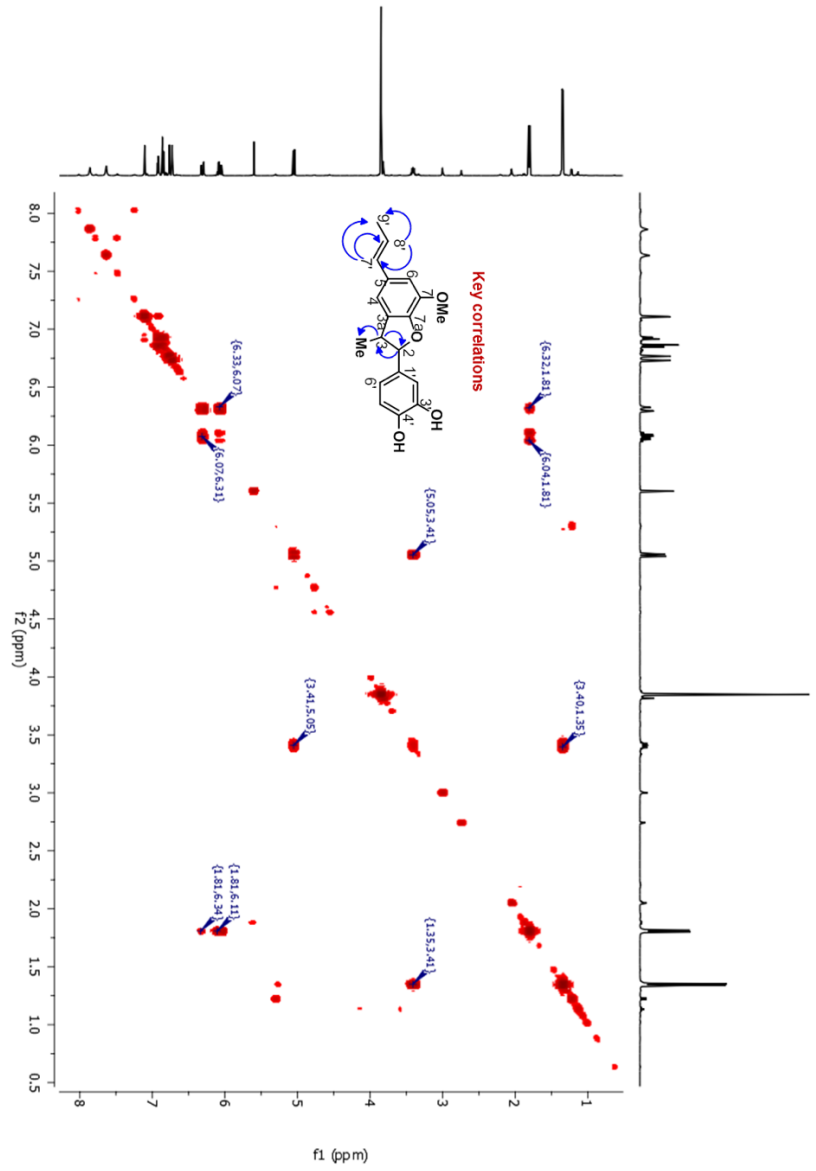

Figure 93S: gCosy spectrum of **99** and key correlations

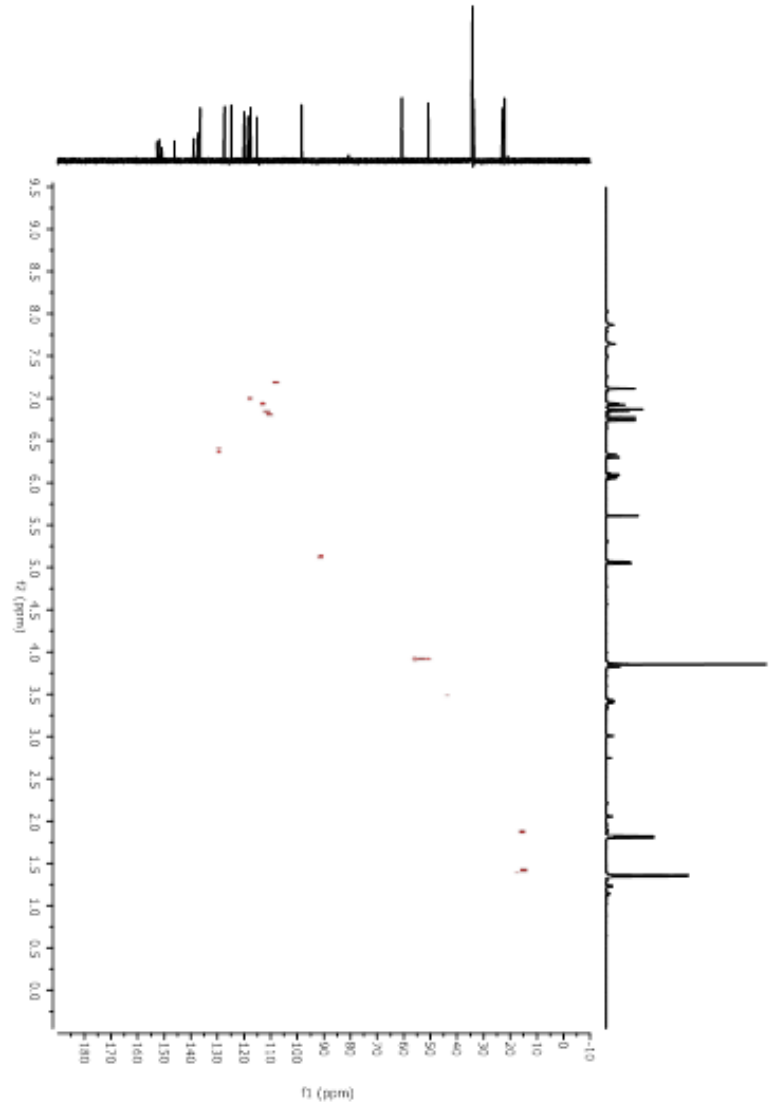

Figure 94S: gHSQCAD spectrum of **99**.

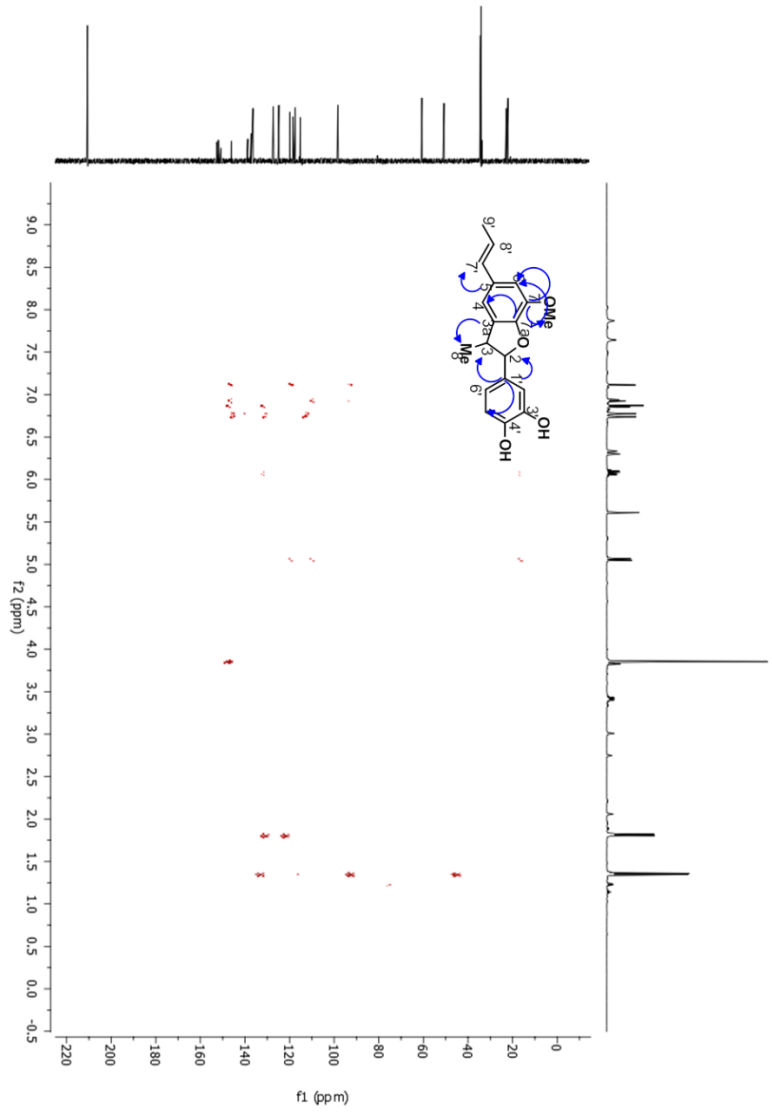

Figure S95: gHMBCAD spectrum of **99** and key correlations

5.3 Appendix D

In this section the NMR spectra of compounds **108**, **111**, **114**, and **127.**

5.3.1 Compound 108

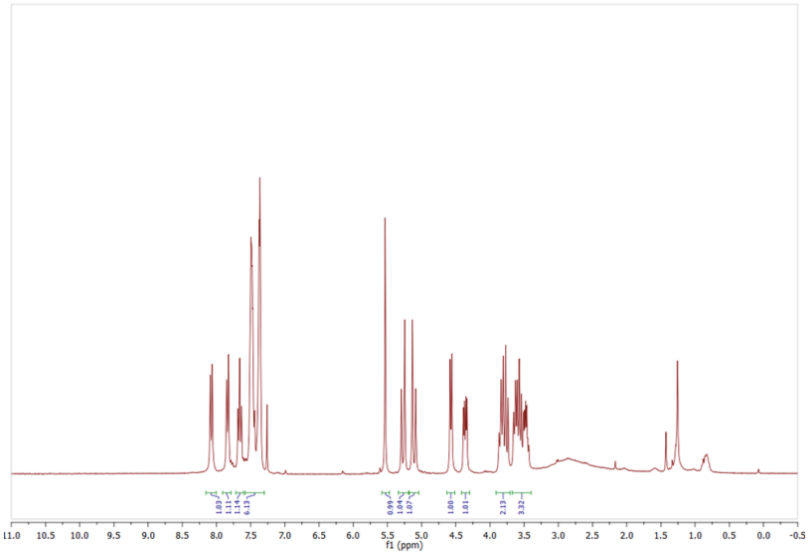

Figure 96S: ^{1}HNMR spectrum (300 MHz, in $CDCl_3$) of **108.**

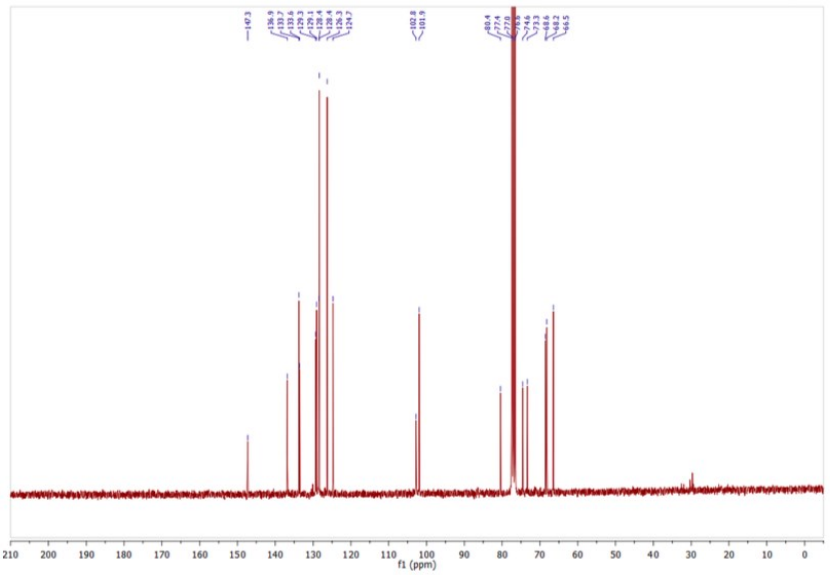

Figure 97S: ^{13}C NMR spectrum (75 MHz, in $CDCl_3$) of **108.**

5.3.2 Compound 111

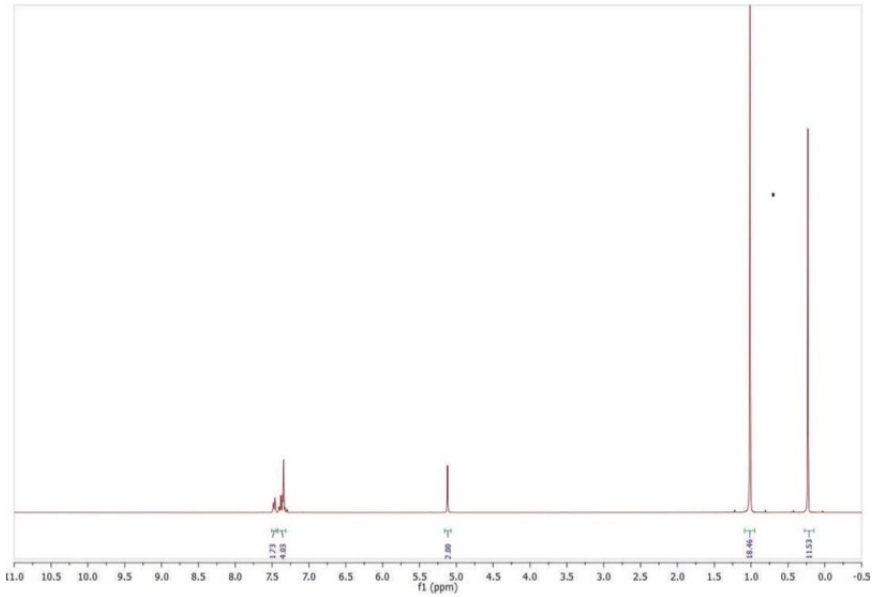

Figure 98S: $^{1}HNMR$ spectrum (300 MHz, in $CDCl_3$) of **111.**

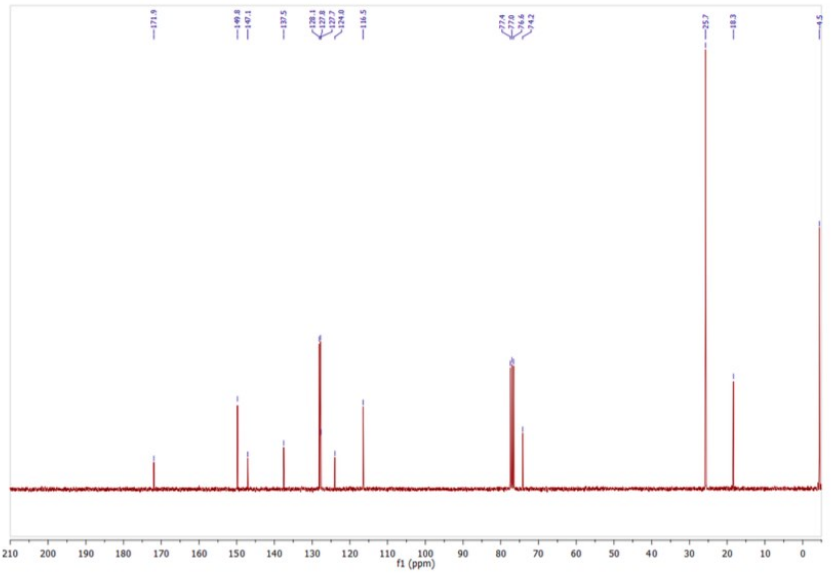

Figure 99S: ^{13}C NMR spectrum (75 MHz, in $CDCl_3$) of **111.**

5.3.2 Compound 114

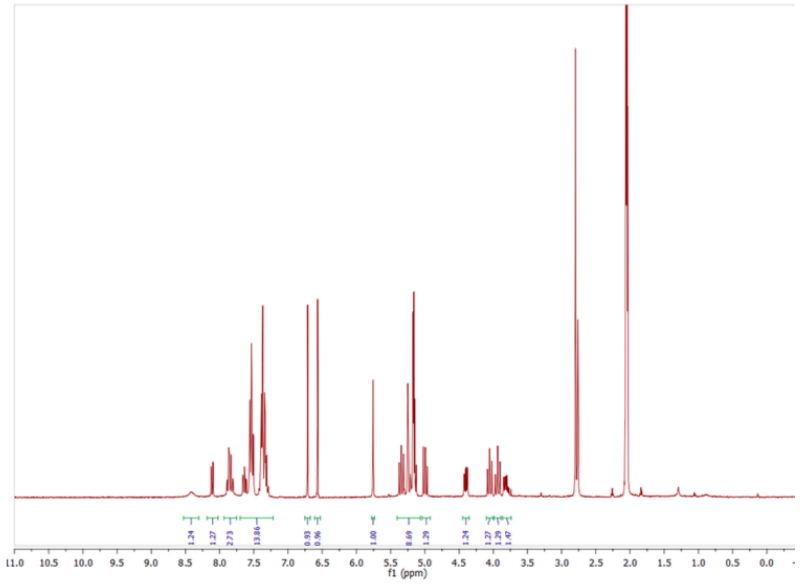

Figure 100S: ^{1}HNMR spectrum (300 MHz, in acetone-d_6) of **114.**

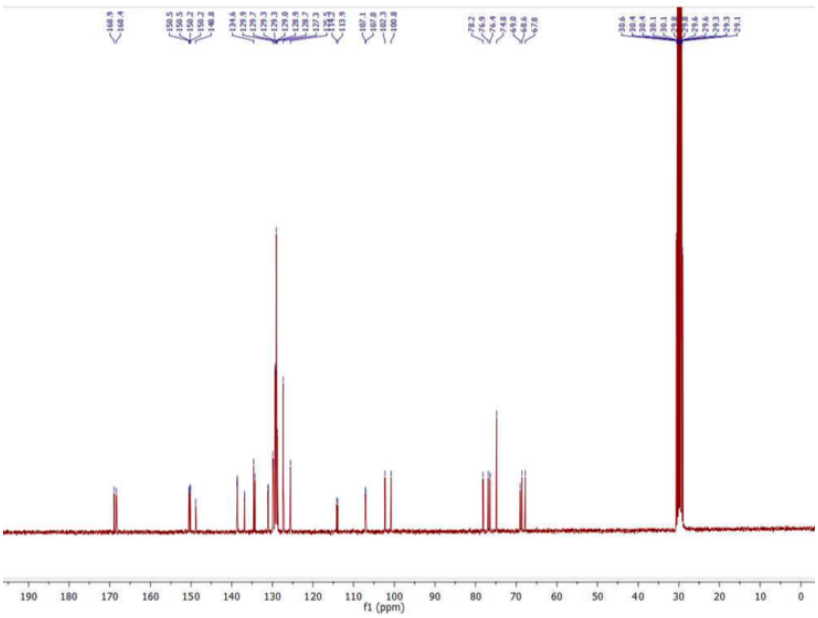

Figure 101S: ^{13}C NMR spectrum (75 MHz, in acetone-d_6) of **114.**

5.3.2 Compound 127

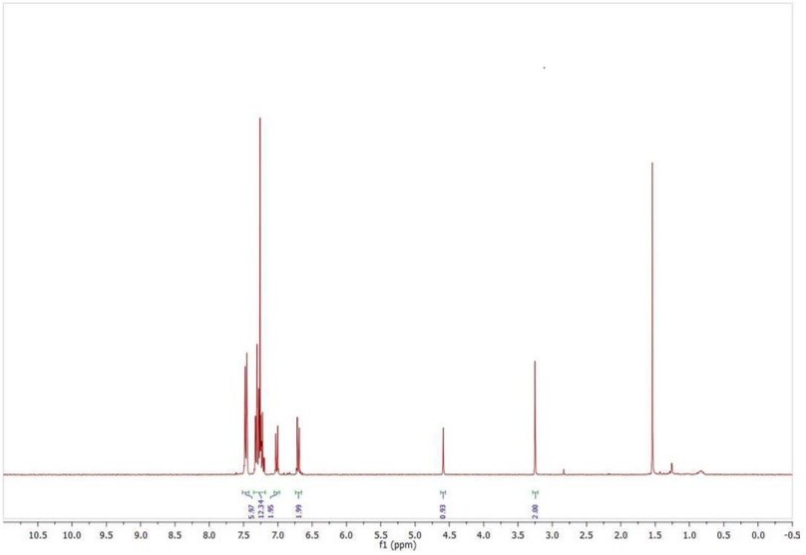

Figure 102S: ^{1}HNMR spectrum (300 MHz, in $CDCl_3$) of **127**.

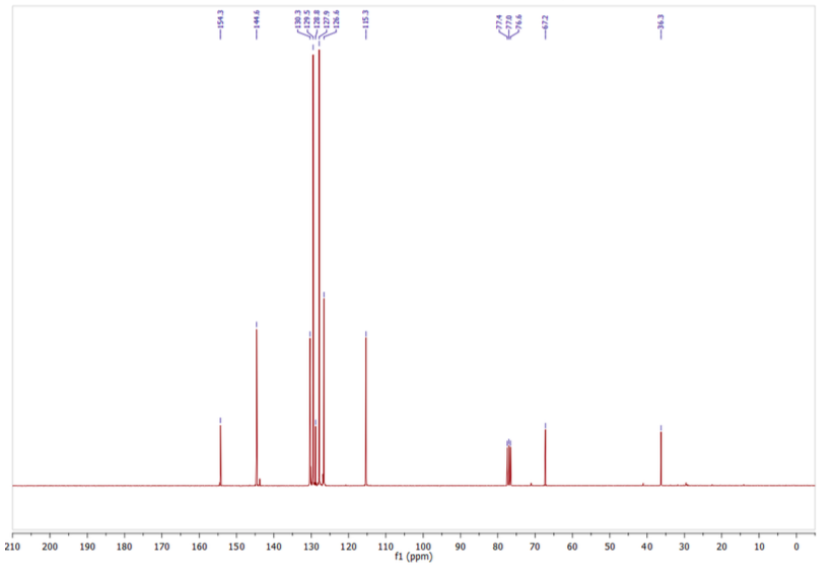

Figure 103S: ^{13}C NMR (75 MHz, in $CDCl_3$) of **127.**

➢ List of publications

N. Cardullo, L. Pulvirenti, C. Spatafora, N. Musso, V. Barresi, D.F. Condorelli, C. Tringali; Dihydrobenzofuran Neolignanamides: Laccase-Mediated Biomimetic Synthesis and Antiproliferative Activity*, J. Nat. Prod.,* 79, 2122-2134, **2016**.

L. Pulvirenti, V. Muccilli, N. Cardullo, C. Spadafora and C. Tringali; Chemo-enzymatic synthesis and α- glucosidase inhibitory activity of dimeric neolignans inspired by magnolol; *J. Nat. Prod.*, **2017**, *80* (5), pp 1648–1657.

A. Baschieri, L. Pulvirenti, V. Muccilli, R. Amorati, C. Tringali; Chain-breaking antioxidant activity of hydroxylated and methoxylated magnolol derivatives: the role of H-bonds; *Org. Biomol. Chem.*, **2017**, 15, 6177-6184

➢ List of communications

1. N. Cardullo, L. Pulvirenti, C. Spatafora, C. Tringali; Lignani e neolignani da ammidi dell'acido ferulico: sintesi biomimetica mediata da enzimi; Convegno congiunto delle Sezioni Calabria e Sicilia della Società Chimica Italiana, 2 - 3 Dicembre **2013**, Catania – poster comunication.
2. N. Cardullo, L. Pulvirenti, C. Spatafora, C. Tringali; Sintesi biomimetica mediata da enzimi di lignani da ammidi di acidi cinnamici; XXV Congresso Nazionale della Società Chimica Italiana, 7-12 Settembre **2014**, Rende (Cosenza) .
3. N. Cardullo, L. Pulvirenti, S. Di Micco, C. Spatafora, C. Tringali, O. Werz, R. Riccio , G. Bifulco Nature-derived phenolic amides as potential inhibitors of mPGES-1 - International Summer School of Natural Product – 6-10 Giugno **2015**, Napoli.
4. N. Cardullo, L. Pulvirenti, N. Musso, C. Spatafora, V. Barresi, D. Condorelli, C. Tringali; Biomimetic Synthesis And Biological Evaluation Of New Natural-Related Neolignanamides International Summer School of Natural Product – 6-10 Giugno **2015**, Napoli.
5. N. Cardullo, L. Pulvirenti, N. Musso, C. Spatafora, V. barresi, D. Condorelli, C. Tringali."Bioinspired neolignans: chemo-enzymatic synthesis and antiproliferative activity". - Convegno Nazionale della

Divisione di Chimica dei Sistemi Biologici, Siracusa, 24-25 Settembre **2015**.

6. N. Cardullo, V. Muccilli, L. Pulvirenti, C. Spatafora, C. Tringali; Chimica & Natura per uno sviluppo sostenibile: i composti naturali nella valorizzazione di matrici biologiche; Workshop PLANET GREEN CHEM for SICILIA, Palermo, 30 Giugno **2016**.

7. L. Pulvirenti, V. Muccilli, N. Cardullo, C. Spatafora, C. Tringali; Chemo-Enzymatic Synthesis and Selective Hydroxylation of Dimeric Neolignans Inspired by Magnolol; XXXVII Convenvegno della Divisione di Chimica Organica, 18-22 Settembre **2016**, Venezia – Mestre.

8. L. Pulvirenti, G. Oliviero, N. Borbone, F. Nici, C. Spatafora, G. Piccialli, C. Tringali; Preliminary Studies on New Selective G-Quadrulex Ligands Based on the Benzo[k,l]xanthene Scaffold; XXXVII Convenvegno della Divisione di Chimica Organica, 18-22 Settembre **2016**, Venezia – Mestre.

9. N. Cardullo, C. Spatafora, S. Di Micco, N. Musso, R. Riccio, K. Fischer, C. Pergola, A. Koeberle, O. Werz, L. Pulvirenti, V. Barresi, D. F. Condorelli, G. Bifulco, Corrado Tringali; Merck young chemists symposium – Rimini 25-27 ottobre **2016**.

10. L Pulvirenti, N. Cardullo, V. Muccilli, C. Tringali; Sintesi Chemo-emzimatica di neolignani correlati al magnololo e studio dell‟attività di inibizione dell‟ α-glucosidasi; Workshop delle sezioni Sicilia Calabria SCI – Messina **2017**.

11. A.Baschieri; L.Pulvirenti; V.Muccilli; R.Amorati; C.Tringali; Dimeric neolignans inspired by magnolol: chemo-enzymatic synthesis and chain-breaking antioxidant activity; Paris Redox 2017- 19th International Conference on Oxidative Stress Reduction, Redox Homeostasis and Antioxidants-26- 27/06/**2017**.

6. ACKNOWLEDGMENTS

I want to acknowledge my tutor, Prof. C. Tringali and his research collaborators Dott. Vera Muccilli and Dott. Nunzio Cardullo for the support shown to me during the period of my PhD.

Thanks are also for my lovely family (my mom, my father and my sisters) and Antonio who have always been there for me, and they will always be there for me.

7. REFERENCES

[1] M. Tulp, L. Bohlin, *Bioorganic & Medicinal Chemistry* **2005**, *13*.

[2] C. Tringali, *Bioactive Compounds from Natural sources, Isolation, characterization and biological properties*, Taylor & Francis, London, **2001**.

[3] M. Feher, J. M. Schmidt, *Journal of Chemical Information and Computer Sciences* **2003**, *43*, 218-227; A. M. Rouhi, *CHEMICAL & ENGINEERING NEWS* **2003**, *81*, 77-91; D. J. Newman, G. M. Cragg, *Journal of Natural Products* **2007**, *70*, 461-477.

[4] M. S. Butler, *Journal of Natural Products* **2006**, *69*, 172-172; O. Potterat, M. Hamburger in *Natural Compounds as Drugs Volume I, Vol. 65*, **2008**, pp. 45-118.

[5] R. Breinbauer, I. R. Vetter, H. Waldmann, *Angewandte Chemie-International Edition* **2002**, *41*, 2879-2890.

[6] P. M. DEWICK, *Chimica, biosintesi e bioattività delle sostanze naturali*, II ed., Piccin, **2012**.

[7] T. S. Lin, A. S. Ruppert, A. J. Johnson, B. Fischer, N. A. Heerema, L. A. Andritsos, K. A. Blum, J. M. Flynn, J. A. Jones, W. H. Hu, M. E. Moran, S. M. Mitchell, L. L. Smith, A. J. Wagner, C. A. Raymond, L. J. Schaaf, M. A. Phelps, M. A. Villalona-Calero, M. R. Grever, J. C. Byrd, *Journal of Clinical Oncology* **2009**, *27*, 6012-6018.

[8] Y. Q. Ma, S. B. Fang, H. H. Li, C. Han, Y. Lu, Y. L. Zhao, Y. Q. Liu, C. Y. Zhao, *Chemical Biology & Drug Design* **2013**, *82*, 12-21.

[9] S. U. Lule, W. S. Xia, *Food Reviews International* **2005**, *21*, 367-388.

[10] E. Haslam, Y. Cai, *Natural Product Reports* **1994**, *11*, 41-66.

[11] S. Quideau, D. Deffieux, C. Douat-Casassus, L. Pouysegu, *Angewandte Chemie-International Edition* **2011**, *50*, 586-621.

[12] A. Crozier, M. N. Clifford, H. Ashihara, *Plant secondary metabolites:occurrence, structure and role in the human diet*, wiley, **2007**; G. C. Fraga, *Plant phenolics and human health: Biochemistry, nutrition and pharmacology*, John Whiley & Sons: New Jersey, **2009**.

[13] J. M. Pezzuto, *Pharmaceutical Biology* **2008**, *46*, 443-573.

[14] C. L. Van Patten , I. A. Olivotto, G. K. Chambers, K. A. Gelmon, T. G. Hislop, E. Templeton, A. Wattie, J. C. Prior, *Journal Of Clinical Oncology* **2002**.

[15] C. Bell, S. Hawthorne, *Journal of Pharmacy and Pharmacology* **2008**, *60*, 139-144.

[16] A. Angelini, R. Di Pietro, L. Centurione, M. L. Castellani, P. Conti, E. Porreca, F. Cuccurullo, C. Di Ilio, *Journal of Biological Regulators e Homeostatic Agents* **2012**, *26*, 495-504.

[17] T. Dorai, B. B. Aggarwal, *Cancer Letters* **2004**, *215*, 129-140.

[18] H. Y. Lee, Y. I. Jeong, E. J. Kim, K. D. Lee, S. H. Choi, Y. J. Kim, D. H. Kim, K. C. Choi, *Journal of Pharmaceutical Sciences* **2015**, *104*, 144-154.

[19] L. Q. Wang, *Journal of Chromatography B-Analytical Technologies in the Biomedical and Life Sciences* **2002**, *777*, 289-309.

[20] C. Spatafora, C. Tringali, *Anti-Cancer Agents in Medicinal Chemistry* **2012**, *12*, 902-918.

[21] J. Vaya, M. Aviram, *Current Medicinal Chemistry - Immunology, Endocrine & Metabolic Agents* **2001**, *1*, 99 – 117,.

[22] H. U. Simon, A. Haj-Yehia, F. Levi-Schaffer, *Apoptosis* **2000**, *5*, 415 – 418.
[23] M. T. Lee, W. C. Lin, B. Yu, T. T. Lee, *Asian-Australasian Journal of Animal Sciences* **2017**, *30*, 299-308.
[24] P. Goupy, C. Dufour, M. Loonis, O. Dangles, *Journal of Agricultural and Food Chemistry* **2003**, *51*, 615-622.
[25] M. N. Clifford, *journal of the Science of Food and Agriculture* **1999**, *79*, 362 – 372.
[26] K. M. Wilson, E. Giovannucci, L. A. Mucci, *Journal of the National Cancer Institute* **2012**, *104*, 1686-1686.
[27] H. Piotrowska, M. Kucinska, M. Murias, *Mutation Research-Reviews in Mutation Research* **2012**, *750*, 60-82.
[28] Y. Q. Wei, X. Zhao, Y. Kariya, H. Fukata, K. Teshigawara, A. Uchida, *Cancer Research* **1994**, *54*, 4952-4957.
[29] A. Saija, D. Trombetta, A. Tomaino, R. Lo Cascio, P. Princi, N. Uccella, F. Bonina, F. Castelli, *International Journal of Pharmaceutics* **1998**, *166*, 123-133.
[30] C. Manna, P. Galletti, V. Cucciolla, G. Montedoro, V. Zappia, *Journal of Nutritional Biochemistry* **1999**, *10*, 159-165.
[31] C. Manna, P. Galletti, V. Cucciolla, O. Moltedo, A. Leone, V. Zappia, *Journal of Nutrition* **1997**, *127*, 286-292.
[32] R. Venkatesan, E. Ji, S. Y. Kim, *Biomed Research International* **2015**.
[33] A. Umeno, M. Horie, K. Murotomi, Y. Nakajima, Y. Yoshida, *Molecules* **2016**, *21*.
[34] J. S. Bose, V. Gangan, R. Prakash, S. K. Jain, S. K. Manna, *Journal of Medicinal Chemistry* **2013**, *56*, 1787-1787.
[35] S. Apers, D. Paper, J. Burgermeister, S. Baronikova, S. Van Dyck, G. Lemiere, A. Vlietinck, L. Pieters, *Journal of Natural Products* **2002**, *65*, 718-720.
[36] D. C. Ayres, J. D. Loike, *Lignans: chemical, biological and clinical properties*, Cambridge University Press: New York, USA,, **1990**; G. Topcu, O. Demirkiran, in *Bioactive Heterocycles V. Topics in Heterocyclic Chemistry., Vol. 11*, **2007** pp. 103-144, .
[37] G. P. Moss, *Pure and Applied Chemistry* **2000**, *72*, 1493-1523.
[38] G. E. Magoulas, D. Papaioannou, *Molecules* **2014**, *19*, 19769-19835.
[39] B. Pickel, A. Schaller, *Applied Microbiology and Biotechnology* **2013**, *97*, 8427-8438.
[40] M. Gordaliza, M. A. Castro, J. M. M. del Corral, A. San Feliciano, *Current Pharmaceutical Design* **2000**, *6*, 1811-1839; Y. Damayanthi, J. W. Lown, *Current Medicinal Chemistry* **1998**, *5*, 205-252.
[41] X. X. Huang, C. C. Zhou, L. Z. Li, Y. Peng, L. L. Lou, S. Liu, D. M. Li, T. Ikejima, S. J. Song, *Fitoterapia* **2013**, *91*, 217-223.
[42] S. Lee, I. H. Song, J. H. Lee, W. Y. Yang, K. B. Oh, J. Shin, *Bioorganic & Medicinal Chemistry Letters* **2014**, *24*, 44-48.
[43] J. Y. Cho, K. U. Baik, E. S. Yoo, K. Yoshikawa, M. H. Park, *Journal of Natural Products* **2000**, *63*, 1205-1209.
[44] E. L. Ghisalberti, *Phytomedicine* **1997**, *4*, 151-166.
[45] L. Pieters, S. Van Dyck, M. Gao, R. L. Bai, E. Hamel, A. Vlietinck, G. Lemiere, *Journal of Medicinal Chemistry* **1999**, *42*, 5475-5481.

[46] L. Moujir, A. M. L. Seca, A. M. S. Silva, M. R. Lopez, N. Padilla, J. A. S. Cavaleiro, C. P. Neto, *Fitoterapia* **2007**, *78*, 385-387.
[47] C. Daquino, A. Rescifina, C. Spatafora, C. Tringali, *European Journal of Organic Chemistry* **2009**, 6289-6300.
[48] O. E. Adelakun, T. Kudanga, A. Parker, I. R. Green, M. le Roes-Hill, S. G. Burton, *Journal of Molecular Catalysis B-Enzymatic* **2012**, *74*, 29-35.
[49] F. Saliu, E. L. Tolppa, L. Zoia, M. Orlandi, *Tetrahedron Letters* **2011**, *52*, 3856-3860.
[50] K. Piontek, M. Antorini, T. Choinowski, *Journal of Biological Chemistry* **2002**, *277*, 37663 – 37669.; U. Guzik, K. Hupert-Kocurek, D. Wojcieszynska, *Molecules* **2014**, *19*, 8995-9018.
[51] F. Van de Velde, F. Van Rantwijk, R. A. Sheldon, *Trends in Biotechnology* **2001**, *19*, 73 – 80.
[52] M. Mogharabi, M. A. Faramarzi, *Advanced Synthesis & Catalysis* **2014**, *356*, 897-927.
[53] A. P. M. Tavares, R. O. Cristovao, J. M. Loureiro, R. A. R. Boaventura, E. A. Macedo, *Journal of Hazardous Materials* **2009**, *162*, 1255-1260; R. O. Cristovao, A. P. M. Tavares, L. A. Ferreira, J. M. Loureiro, R. A. R. Boaventura, E. A. Macedo, *Bioresource Technology* **2009**, *100*, 1094-1099.
[54] J. F. Osma, J. L. Toca-Herrera, S. Rodriguez-Couto, *Enzyme Research* **2010**, 1-10; A. M. Mayer, R. C. Staples, *Phytochemistry* **2002**, *60*, 551-565.
[55] S. Van Miert, S. Van Dyck, T. J. Schmidt, R. Brun, A. Vlietinck, G. Lemiere, L. Pieters, *Bioorganic & Medicinal Chemistry* **2005**, *13*, 661-669.
[56] C. Spatafora, C. Tringali, in *Targets in Heterocyclic Systems. Chemistry and Properties Vol. 11* (Ed.: S. C. I. O. Attanasi e D. Spinelli Editori), **2007**, p. 284−312.
[57] S. Tranchimand, T. Tron, C. Gaudin, G. Iacazio, *Journal of Molecular Catalysis B-Enzymatic* **2006**, *42*, 27-31.
[58] S. Shi, Y. Zhang, K. Huang, S. Liu, Y. Zhao, *Food Chemistry* **2008**, *108*, 402-406.
[59] S. A. S. da Silvaa, A. L. Souto, M. D. Agra, E. V. L. da-Cunha, J. M. Barbosa, M. S. da Silva, R. Braz Filho, *Arkivoc* **2004**, 54-58.
[60] T. Tanaka, A. Nishimura, I. Kouno, G. Nonaka, C. R. Yang, *Chemical & Pharmaceutical Bulletin* **1997**, *45*, 1596-1600.
[61] Z. H. Jiang, T. Tanaka, I. Kouno, *Chemical & Pharmaceutical Bulletin* **1996**, *44*, 1669-1675.
[62] M. Kumar, P. Rawat, N. Rahuja, A. K. Srivastava, R. Maurya, *Phytochemistry* **2009**, *70*, 1448-1455.
[63] Z. Y. Qu, Y. W. Zhang, C. L. Yao, Y. P. Jin, P. H. Zheng, C. H. Sun, J. X. Liu, Y. S. Wang, Y. P. Wang, *Biochemical Systematics and Ecology* **2015**, *60*, 199-203.
[64] X. Li, S. Shi, Y. Xu, Q. Tao, J. Stockhit, Y. Zhao*, Vol. CN Pat., 101024640,* , **2007**.
[65] S. Di Micco, F. Mazue, C. Daquino, C. Spatafora, D. Delmas, N. Latruffe, C. Tringali, R. Riccio, G. Bifulco, *Organic & Biomolecular Chemistry* **2011**, *9*, 701-710.
[66] C. Spatafora, V. Barresi, V. M. Bhusainahalli, S. Di Micco, N. Musso, R. Riccio, G. Bifulco, D. Condorelli, C. Tringali, *Organic & Biomolecular Chemistry* **2014**, *12*, 2686-2701.
[67] V. Vijayakurup, C. Spatafora, C. Daquino, C. Tringali, P. Srinivas, S. Gopala, *Life Sciences* **2012**, *91*, 1336-1344.

[68] V. Vijayakurup, C. Spatafora, C. Tringali, P. C. Jayakrishnan, P. Srinivas, S. Gopala, *Molecular Biology Reports* **2014**, *41*, 85-94.
[69] C. Spatafora, C. Daquino, C. Tringali, R. Amorati, *Organic & Biomolecular Chemistry* **2013**, *11*, 4291-4294.
[70] E. N. Pitsinos, V. P. Vidali, E. A. Couladouros, *European Journal of Organic Chemistry* **2011**, 1207-1222.
[71] M. Fujita, H. Itokawa, S. Y., *Chemical and Pharmaceutical Bulletin* **1972**, *20*, 212-213.
[72] Y. J. Lee, Y. M. Lee, C. K. Lee, J. K. Jung, S. B. Han, J. T. Hong, *Pharmacology & Therapeutics* **2011**, *130*, 157-176.
[73] L. C. Chen, Y. C. Liu, Y. C. Liang, Y. S. Ho, W. S. Lee, *Journal of Agricultural and Food Chemistry* **2009**, *57*, 7331-7337; B. T. McKeown, R. A. R. Hurta, *Functional Foods in Health and Disease* **2015**, *5*, 17-33.
[74] B. Y. Yang, Y. Xu, S. S. Yu, Y. S. Huang, L. Lu, X. L. Liang, *Inflammation Research* **2016**, *65*, 81-93.
[75] L. E. Fried, J. L. Arbiser, *Antioxidants & Redox Signaling* **2009**, *11*, 1139-1148.
[76] K. Y. Ho, C. C. Tsai, C. P. Chen, J. S. Huang, C. C. Lin, *Phytotherapy Research* **2001**, *15*, 139-141; L. M. Sun, K. Liao, D. Y. Wang, *Plos One* **2015**, *10*.
[77] J. Li, A. P. Meng, X. L. Guan, Q. Wu, S. P. Deng, X. J. Su, R. Y. Yang, *Bioorganic & Medicinal Chemistry Letters* **2013**, *23*, 2238-2244.
[78] R. Amorati, J. Zotova, A. Baschieri, L. Valgimigli, *Journal of Organic Chemistry* **2015**, *80*, 10651-10659.
[79] D. H. Kuo, Y. S. Lai, C. Y. Lo, A. C. Cheng, H. Wu, M. H. Pan, *Journal of Agricultural and Food Chemistry* **2010**, *58*, 5777-5783.
[80] S. H. Lu, T. H. Chen, T. C. Chou, *Journal of Natural Products* **2015**, *78*, 61-68.
[81] H. K. Han, T. V. A. Luu, *Anticancer Research* **2012**, *32*, 4445-4452.
[82] C. P. Chang, Y. C. Hsu, M. T. Lin, *Clinical and Experimental Pharmacology and Physiology* **2003**, *30*, 387-392.
[83] S. Jada, M. R. Doma, P. P. Singh, S. Kumar, F. Malik, A. Sharma, I. A. Khan, G. N. Qazi, H. M. S. Kumar, *European Journal of Medicinal Chemistry* **2012**, *51*, 35-41.
[84] F. Amblard, B. Govindarajan, B. Lefkove, K. L. Rapp, M. Detorio, J. L. Arbiser, R. F. Schinazi, *Bioorganic & Medicinal Chemistry Letters* **2007**, *17*, 4428-4431.
[85] L. Yang, Z. H. Wang, H. Lei, R. D. Chen, X. L. Wang, Y. Peng, J. G. Dai, *Tetrahedron* **2014**, *70*, 8244-8251.
[86] W. Schuhly, A. Hufner, E. M. Pferschy-Wenzig, E. Prettner, M. Adams, A. Bodensieck, O. Kunert, A. Oluwemimo, E. Haslinger, R. Bauer, *Bioorganic & Medicinal Chemistry* **2009**, *17*, 4459-4465.
[87] J. M. Lin, A. S. P. Gowda, A. K. Sharma, S. Amin, *Bioorganic & Medicinal Chemistry* **2012**, *20*, 3202-3211.
[88] Z. L. Kong, S. C. Tzeng, Y. C. Liu, *Bioorganic & Medicinal Chemistry Letters* **2005**, *15*, 163-166.
[89] M. Alexeev, D. K. Grosenbaugh, D. D. Mott, J. L. Fisher, *Neuropharmacology* **2012**, *62*, 2507-2514.
[90] C. Yang, X. Y. Zhi, H. Xu, *Bioorganic & Medicinal Chemistry Letters* **2015**, *25*, 2217-2219.

[91] Y. He, X. B. Wang, B. Y. Fan, L.Y.Kong, *Bioorganic and Medicinal Chemistry* **2014**, *22*, 762-771.
[92] H. Y. Wang, J. S. Wang, S. M. Shan, X. B. Wang, J. Luo, M. H. Yang, L. Y. Kong, *Planta Medica* **2013**, *79*, 1767-1774.
[93] V. H. Lillelund, H. H. Jensen, X. F. Liang, M. Bols, *Chemical Reviews* **2002**, *102*, 515-553; N. Asano, *Glycobiology* **2003**, *13*, 93R-104R; I. Robina, A. J. Moreno-Vargas, A. T. Carmona, P. Vogel, *Current Drug Metabolism* **2004**, *5*, 329-361; T. Kajimoto, M. Node, *Current Topics in Medicinal Chemistry* **2009**, *9*, 13-33; A. E. Stutz, T. M. Wrodnigg, *Advances in Carbohydrate Chemistry and Biochemistry, Vol 66* **2011**, *66*, 187-298.
[94] K. C. Maki, *American Journal of Cardiology* **2004**, *93*, 12C-17C.
[95] H. Bischoff, *European Journal of Clinical Investigation* **1994**, *24*, 3-10.
[96] L. J. Scott, C. M. Spencer, *Drugs* **2000**, *59*, 521-549.
[97] Y. Yang, G. Y. Lian, B. Yu, *Israel Journal of Chemistry* **2015**, *55*, 268-284.
[98] N. Cardullo, C. Spatafora, N. Musso, V. Barresi, D. Condorelli, C. Tringali, *Journal of Natural Products* **2015**, *78*, 2675-2683.
[99] V. Muccilli, N. Cardullo, C. Spatafora, V. Cunsolo, C. Tringali, *Food Chemistry* **2017**, *215*, 50-60.
[100] B. Cerda, F. A. Tomas-Barberan, J. C. Espin, *Journal of Agricultural and Food Chemistry* **2005**, *53*, 227-235.
[101] J. P. Martinez, F. Sasse, M. Bronstrup, J. Diez, A. Meyerhans, *Natural Product Reports* **2015**, *32*, 29-48.
[102] S. Quideau, *Chemistry and Biology of Ellagitannins—An Underestimated Class of Bioactive Plant Polyphenols*, World Scientific, **2009**; P. Buzzini, P. Arapitsas, M. Goretti, E. Branda, B. Turchetti, P. Pinelli, F. Ieri, A. Romani, *Mini-Reviews in Medicinal Chemistry* **2008**, *8*, 1179-1187.
[103] S. Quideau, M. Jourdes, D. Lefeuvre, D. Montaudon, C. Saucier, Y. Glories, P. Pardon, P. Pourquier, *Chemistry-a European Journal* **2005**, *11*, 6503-6513; S. Quideau, M. Jourdes, C. Saucier, Y. Glories, P. Pardon, C. Baudry, *Angewandte Chemie-International Edition* **2003**, *42*, 6012-6014.
[104] S. Quideau, C. Douat-Casassus, D. M. D. Lopez, C. Di Primo, S. Chassaing, R. Jacquet, F. Saltel, E. Genot, *Angewandte Chemie-International Edition* **2011**, *50*, 5099-5104.
[105] L. Pouysegu, D. Deffieux, G. Malik, A. Natangelo, S. Quideau, *Natural Product Reports* **2011**, *28*, 853-874.
[106] S. Quideau, K. S. Feldman, *Chemical Reviews* **1996**, *96*, 475-503.
[107] O. T. Schmidt, in *Progress in the Chemistry of Organic Natural Products, Vol. 13*, Springer, Vienna, **1956**, pp. 70-136; O. T. M. Schmidt, W., *Angewandte Chemie* **1956**, *68*, 103-115.
[108] G. Bringmann, A. J. P. Mortimer, P. A. Keller, M. J. Gresser, J. Garner, M. Breuning, *Angewandte Chemie-International Edition* **2005**, *44*, 5384-5427.
[109] W. Mayer, W. Gabler, A. Riester, H. Korger, *European Journal of Organic Chemistry* **1967**, *707*, 177-181.
[110] G. Nonaka, K. Ishimaru, M. Watanabe, I. Nishioka, T. Yamauchi, A. S. C. Wan, *Chemical & Pharmaceutical Bulletin* **1987**, *35*, 217-220.

[111] J. P. Salminen, M. Karonen, J. Sinkkonen, *Chemistry-a European Journal* **2011**, *17*, 2806-2816; R. V. Barbehenn, C. P. Constabel, *Phytochemistry* **2011**, *72*, 1551-1565; T. Yoshida, Y. Amakura, M. Yoshimura, *International Journal of Molecular Sciences* **2010**, *11*, 79-106.
[112] N. Vivas, M. Laguerre, Y. Glories, G. Bourgeois, C. Vitry, *Phytochemistry* **1995**, *39*, 1193-1199; N. Vivas, M. Laguerre, I. P. De Boissel, N. V. De Gaijlejac, M. F. Nonier, *Journal of Agricultural and Food Chemistry* **2004**, *52*, 2073-2078.
[113] Y. Matsuo, H. Wakamatsu, M. Omar, T. Tanaka, *Organic Letters* **2015**, *17*, 46-49.
[114] M. C. Foti, C. Daquino, C. Geraci, *Journal of Organic Chemistry* **2004**, *69*, 2309-2314.
[115] B. Etzenhouser, C. Hansch, S. Kapur, C. D. Selassie, *Bioorganic & Medicinal Chemistry* **2001**, *9*, 199-209.
[116] J. Zhang, L. X. Xu, X. S. Xu, B. W. Li, R. Wang, J. J. Fu, *International Journal of Clinical and Experimental Medicine* **2014**, *7*, 1022-1027.
[117] T. Silva, T. Mohamed, A. Shakeri, P. P. N. Rao, L. Martinez-Gonzalez, D. I. Perez, A. Martinez, M. J. Valente, J. Garrido, E. Uriarte, P. Serrao, P. Soares-da-Silva, F. Remiao, F. Borges, *Journal of Medicinal Chemistry* **2016**, *59*, 7584-7597.
[118] A. Capolupo, A. Tosco, M. Mozzicafreddo, C. Tringali, N. Cardullo, M. C. Monti, A. Casapullo, *Chemistry-a European Journal* **2017**, *23*, 8371-8374.
[119] L. F. Fieser, M. Fieser, *Reagents for Organic Synthesis*, John Wiley and Sons, **1976**.
[120] Y. L. Zhang, Y. C. Shen, Z. Q. Wang, H. X. Chen, X. Guo, Y. C. Cheng, K. H. Lee, *Journal of Natural Products* **1992**, *55*, 1100-1111.
[121] M. Miyahara, Y. Kashiwada, X. Guo, H. X. Chen, Y. C. Cheng, Lee, K. H., *Heterocycles* **1994**, *39*, 361-369.
[122] Z. Q. Wang, H. Hu, H. X. Chen, Y. C. Cheng, Lee, K. H., *Journal of Medicinal Chemistry* **1992**, *35*, 871-877.
[123] V. Balogh, M. Fetizon, M. Golfier, *Journal of Organic Chemistry* **1971**, *36*, 1339-1341.
[124] H. Tazaki, D. Taguchi, T. Hayashida, K. Nabeta, *Bioscience Biotechnology and Biochemistry* **2001**, *65*, 2613-2621.
[125] W. I. Sundquist, A. Klug, *Nature* **1989**, *342*, 825-829.
[126] L. H. Hurley, D. D. Von Hoff, A. Siddiqui-Jain, D. Z. Yang, *Seminars in Oncology* **2006**, *33*, 498-512.
[127] V. Esposito, A. Virgilio, A. Pepe, G. Oliviero, L. Mayol, A. Galeone, *Bioorganic & Medicinal Chemistry* **2009**, *17*, 1997-2001.
[128] D. D. Le, M. Di Antonio, L. K. M. Chan, S. Balasubramanian, *Chemical Communications* **2015**, *51*, 8048-8050.
[129] T. M. Ou, Y. J. Lu, C. Zhang, Z. S. Huang, X. D. Wang, J. H. Tan, Y. Chen, D. L. Ma, K. Y. Wong, J. C. O. Tang, A. S. C. Chan, L. Q. Gu, *Journal of Medicinal Chemistry* **2007**, *50*, 1465-1474.
[130] N. L. Urizar, A. B. Liverman, D. T. Dodds, F. V. Silva, P. Ordentlich, Y. Z. Yan, F. J. Gonzalez, R. A. Heyman, D. J. Mangelsdorf, D. D. Moore, *Science* **2002**, *296*, 1703-1706.
[131] S. Fiorucci, G. Rizzo, A. Donini, E. Distrutti, L. Santucci, *Trends in Molecular Medicine* **2007**, *13*, 298-309.

[132] C. Festa, B. Renga, C. D'Amore, V. Sepe, C. Finamore, S. De Marino, A. Carino, S. Cipriani, M. C. Monti, A. Zampella, S. Fiorucci, *Journal of Medicinal Chemistry* **2014**, *57*, 8477-8495.
[133] S. Schwarz, A. Loeffler, K. Kadlec, *Veterinary Dermatology* **2017**, *28*, 82-+.
[134] T. Nurnberger, F. Brunner, B. Kemmerling, L. Piater, *Immunological Reviews* **2004**, *198*, 249-266.
[135] J. Kuc, *Annual Review of Phytopathology* **1995**, *33*, 275-297; P. Jeandet, C. Clement, E. Courot, S. Cordelier, *International Journal of Molecular Sciences* **2013**, *14*, 14136-14170.
[136] A. Seyoum, K. Asres, F. K. El-Fiky, *Phytochemistry* **2006**, *67*, 2058-2070.
[137] G. Anuj, S. Sanjay, **2010**, *2*, 108-120.
[138] J. Fernandez-Bolanos, B. Felizon, M. Brenes, R. Guillen, A. Heredia, *Journal of the American Oil Chemists Society* **1998**, *75*, 1643-1649.
[139] G. W. Lambert, G. Eisenhofer, G. L. Jennings, M. D. Esler, *Life Sciences* **1993**, *53*, 63-75.
[140] R. Bernini, E. Mincione, M. Barontini, F. Crisante, *Journal of Agricultural and Food Chemistry* **2008**, *56*, 8897-8904.
[141] V. M. Bhusainahalli, C. Spatafora, M. Chalal, D. Vervandier-Fasseur, P. Meunier, N. Latruffe, C. Tringali, *European Journal of Organic Chemistry* **2012**, 5217-5224.
[142] G. Basini, C. Spatafora, C. Tringali, S. Bussolati, F. Grasselli, *Journal of Biomolecular Screening* **2014**, *19*, 1282-1289.
[143] N. Cardullo, L. Pulvirenti, C. Spatafora, N. Musso, V. Barresi, D. F. Condorelli, C. Tringalii, *Journal of Natural Products* **2016**, *79*, 2122-2134.
[144] V. V. Zhdankin, *Journal of Organic Chemistry* **2011**, *76*, 1185-1197.
[145] A. Duschek, S. F. Kirsch, *Angewandte Chemie-International Edition* **2011**, *50*, 1524-1552.
[146] C. Hartmann, V. Mayer, *Chemische Berichte* **1893**, *26*, 1727-1732.
[147] M. Frigerio, M. Santagostino, S. Sputore, *Journal of Organic Chemistry* **1999**, *64*, 4537-4538.
[148] D. Magdziak, A. A. Rodriguez, R. W. Van De Water, T. R. R. Pettus, *Organic Letters* **2002**, *4*, 285-288; Y. D. Huang, J. S. Zhang, T. R. R. Pettus, *Organic Letters* **2005**, *7*, 5841-5844.
[149] R. Bernini, M. Barontini, P. Mosesso, G. Pepe, S. M. Willfor, R. E. Sjoholm, P. C. Eklund, R. Saladino, *Organic & Biomolecular Chemistry* **2009**, *7*, 2367-2377.
[150] L. Norena-Franco, I. Hernandez-Perez, P. Aguilar, A. Maubert-Franco, *Catalysis Today* **2002**, *75*, 189-195.
[151] R. K. Boeckman, Shao, P., Mullins, J. J., in *Organic Syntheses*, **2003**.
[152] L. Pouysegu, D. Deffieux, S. Quideau, *Tetrahedron* **2010**, *66*, 2235-2261.
[153] A. Ozanne, L. Pouysegu, D. Depernet, B. Francois, S. Quideau, *Organic Letters* **2003**, *5*, 2903-2906.
[154] A. Llevot, E. Grau, S. Carlotti, S. Grelier, H. Cramail, *Journal of Molecular Catalysis B-Enzymatic* **2016**, *125*, 34-41.
[155] S. Grasso, L. Siracusa, C. Spatafora, M. Renis, C. Tringali, *Bioorganic Chemistry* **2007**, *35*, 137-152.

[156] C. F. Lin, T. L. Hwang, S. A. Al-Suwayeh, Y. L. Huang, Y. Y. Hung, J. Y. Fang, *International Journal of Pharmaceutics* **2013**, *445*, 153-162.
[157] H. Kurihara, J. Ando, M. Hatano, J. Kawabata, *Bioorganic and Medicinal Chemistry Letter* **1995**, *5*, 1757.
[158] R. Z. Cer, U. Mudunuri, R. Stephens, F. J. Lebeda, *Nucleic Acids Research* **2009**, *37*, W441-W445.
[159] R. Amorati, A. Baschieri, L. Valgimigli, *Journal of Chemistry* **2017**.
[160] R. Amorati, L. Valgimigli, *Free Radical Research* **2015**, *49*, 633-649.
[161] L. Gavernet, A. Talevi, E. A. Castro, L. E. Bruno-Blanch, *Qsar & Combinatorial Science* **2008**, *27*, 1120-1129.
[162] G. Lauro, A. Romano, R. Riccio, G. Bifulco, *Journal of Natural Products* **2011**, *74*, 1401-1407.
[163] Y. Z. Chen, D. G. Zhi, *Proteins-Structure Function and Genetics* **2001**, *43*, 217-226; S. Zahler, S. Tietze, F. Totzke, M. Kubbutat, L. Meijer, A. M. Vollmar, J. Apostolakis, *Chemistry & Biology* **2007**, *14*, 1207-1214.
[164] O. Trott, A. J. Olson, *Journal of Computational Chemistry* **2010**, *31*, 455-461.
[165] J. A. Endicott, V. Ling, *Annual Review of Biochemistry* **1989**, *58*, 137-171.
[166] S. P. C. Cole, G. Bhardwaj, J. H. Gerlach, J. E. Mackie, C. E. Grant, K. C. Almquist, A. J. Stewart, E. U. Kurz, A. M. V. Duncan, R. G. Deeley, *Science* **1992**, *258*, 1650-1654.
[167] L. A. Doyle, W. D. Yang, L. V. Abruzzo, T. Krogmann, Y. M. Gao, A. K. Rishi, D. D. Ross, *Proceedings of the National Academy of Sciences of the United States of America* **1998**, *95*, 15665-15670.
[168] A. Ahmed-Belkacem, A. Pozza, S. Macalou, J. M. Perez-Victoria, A. Boumendjel, A. Di Pietro, *Anti-Cancer Drugs* **2006**, *17*, 239-243.
[169] G. Valdameri, C. Gauthier, R. Terreux, R. Kachadourian, B. J. Day, S. M. B. Winnischofer, M. E. M. Rocha, V. Frachet, X. Ronot, A. Di Pietro, A. Boumendjel, *Journal of Medicinal Chemistry* **2012**, *55*, 3193-3200.
[170] S. Y. Lin, H. H. Ko, S. J. Lee, H. S. Chang, C. H. Lin, I. S. Chen, *Chemistry & Biodiversity* **2015**, *12*, 1057-1067.
[171] K. Sawasdee, T. Chaowasku, V. Lipipun, T. H. Dufat, S. Michel, K. Likhitwitayawuid, *Tetrahedron Letters* **2013**, *54*, 4259-4263.
[172] C. J. Ma, S. R. Kim, J. Kim, Y. C. Kim, *British Journal of Pharmacology* **2005**, *146*, 752-759.
[173] L. Juhasz, L. Kurti, S. Antus, *Journal of Natural Products* **2000**, *63*, 866-870.
[174] A. Richieu, P. A. Peixoto, L. Pouységu, D. Deffieux, Q. S., **2017**, *56*.
[175] C. S. Rye, S. G. Withers, *Journal of the American Chemical Society* **2002**, *124*, 9756-9767.
[176] V. N. R. Pillai, *Synthesis* **1980**, *1*; U. Zehavi, in *Advances in Carbohydrate Chemistry and Biochemistry, Vol. 46*, Academic Press, **1988**, pp. 179-204.
[177] A. K. Sen, N. Banerji, *Indian Journal of Chemistry Section B-Organic Chemistry Including Medicinal Chemistry* **1989**, *28*, 818-823.
[178] J. J. Oltvoort, M. Kloosterman, J. H. Boom, *Recueil des Travaux Chimiques des Pays-Bas* **1983**, *102*, 501–505.
[179] U. Zehavi*, Vol. 37*, American Chemical Society, **1972**, p. 2285.

[180] K. S. Feldman, A. Sambandam, *Journal of Organic Chemistry* **1995**, *60*, 8171-8178.
[181] Y. Ikeda, K. Nagao, K. Tanigakiuchi, G. Tokumaru, H. Tsuchiya, H. Yamada, *Tetrahedron Letters* **2004**, *45*, 487-489.
[182] K. S. Feldman, S. M. Ensel, R. D. Minard, *Journal of the American Chemical Society* **1994**, *116*, 1742-1745.
[183] N. Michihata, Y. Kaneko, Y. Kasai, K. Tanigawa, T. Hirokane, S. Higasa, H. Yamada, *Journal of Organic Chemistry* **2013**, *78*, 4319-4328.
[184] A. J. Pearson, P. R. Bruhn, *Journal of Organic Chemistry* **1991**, *56*, 7092-7097.
[185] G. Malik, A. Natangelo, J. Charris, L. Pouysegu, S. Manfredini, D. Cavagnat, T. Buffeteau, D. Deffieux, S. Quideau, *Chemistry-a European Journal* **2012**, *18*, 9063-9074.
[186] H. Yamada, K. Nagao, K. Dokei, Y. Kasai, N. Michihata, *Journal of the American Chemical Society* **2008**, *130*, 7566-+.
[187] E. M. V. Johansson, S. A. Crusz, E. Kolomiets, L. Buts, R. U. Kadam, M. Cacciarini, K. M. Bartels, S. P. Diggle, M. Camara, P. Williams, R. Loris, C. Nativi, F. Rosenau, K. E. Jaeger, T. Darbre, J. L. Reymond, *Chemistry & Biology* **2008**, *15*, 1249-1257.
[188] T. H. Shie, Y. L. Chiang, J. J. Lin, Y. K. Li, L. C. Lo, *Carbohydrate Research* **2006**, *341*, 443-456.
[189] D. Stoermer, D. Vitharana, N. Hin, G. Delahanty, B. Duvall, D. V. Ferraris, B. S. Grella, R. Hoover, C. Rojas, M. K. Shanholtz, K. P. Smith, M. Stathis, Y. Wu, K. M. Wozniak, B. S. Slusher, T. Tsukamoto, *Journal of Medicinal Chemistry* **2012**, *55*, 5922-5932.
[190] W. Koenigs, E. Knorr, *Chem. Ber .,* **1901**, *34*, 957.
[191] M. Jacobsson, J. Malmberg, U. Ellervik, *Carbohydrate Research* **2006**, *341*, 1266-1281.